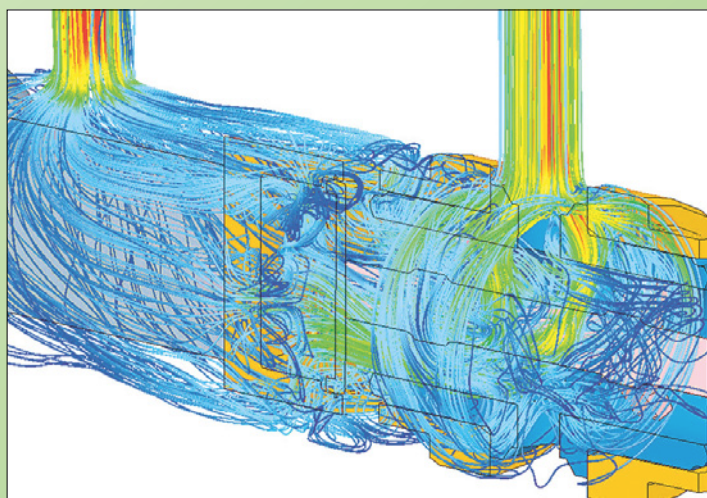
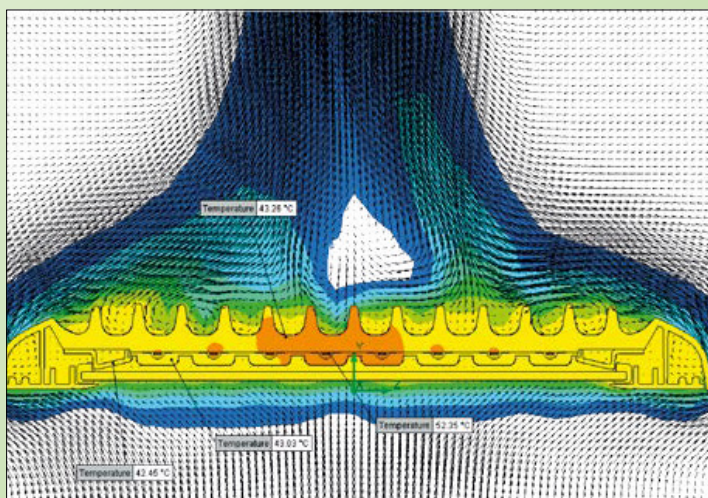
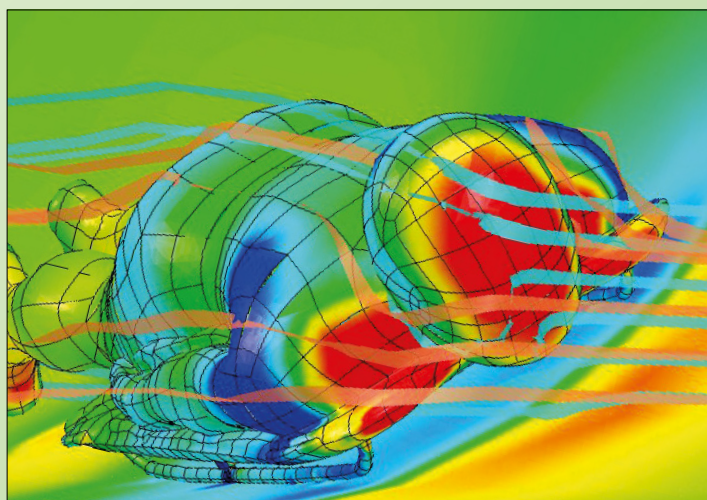
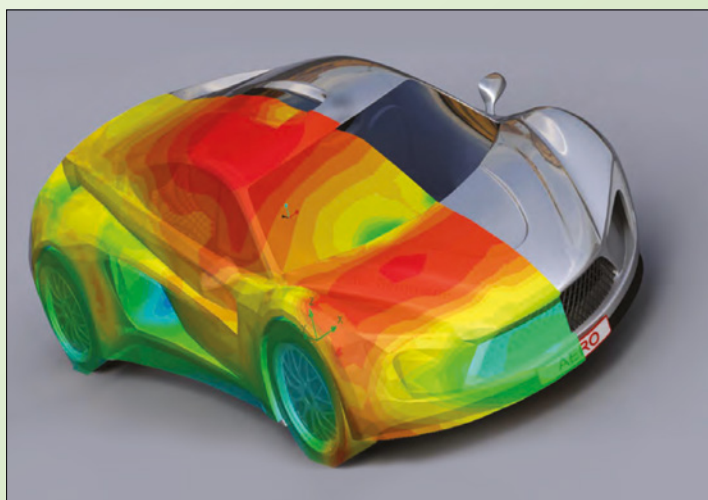


ENGINEERING EDGE

Accelerate Innovation
with CFD & Thermal
Characterization

FloEFD™ 3D CFD Analysis Software



This collection of **Engineering Edge** articles showcases our customers' success with FloEFD™ 3D CFD Analysis Software across a number of industries and disciplines including Automotive, Process, Power Generation, Electronic Cooling, Power Electronics, Aerospace, and Military. Test-drive the fully featured **FloEFD**, **FloTHERM XT**, or **Flowmaster** Virtual Lab.

- Fully operational software, hosted in Mentor Graphics virtual lab environment
- Immediate access from any current PC web browser
- Test at work, home or while traveling
- No IT department approval required
- No special equipment
- Evaluate **FloEFD**, **Flowmaster**, or **FloTHERM XT** at your own pace

Index

01 High School Students Fly with FloEFD™

The Real World Design Challenge (RWDC) is an annual high school competition in the USA run by a public-private partnership with the goal of assisting in the increase of the Science, Technology, Engineering and Mathematics (STEM) workforce in America.

03 Let there be more LED light!

Over the last decade, as the efficiencies of Light Emitting Diodes (LEDs) has increased to the point where they are a viable replacement for incandescent bulbs and compact fluorescent lamps (CFLs) the world has reached a tipping point in the usage of LED Lighting within automotive lighting, street lighting, back lighting (for consumer electronics) and now general lighting applications.

05 Small but Mighty Powerful

Micro-turbine jet engine simulation and structural analysis using FloEFD™ and Creo® Simulate

09 Athlete Engineered Technology Fine Tuned by CFD

The Science that could bring in Winter Olympic Gold Medals for Bob Skeleton Athletes

11 Dem Bones, Dem Bones, Dem Microgravity Cow Bones

Designing an experimental capsule environment to assess the effects of bone density in space

14 Improving 1D Data with 3D CFD

Improving 1D Thermo-Fluid System Automotive Engine Data with 3D Computational Fluid Dynamics

16 Megawatt Engines need Mega Cooling

18 Lights, Camera, Action!

Grass Valley Video Camera Modeling using FloEFD™

20 The Family Business: How to be a World Champion

Kristan Bromley relies heavily on the help and support of a number of people to keep him at the sharp end of a sport that affords little room for error

22 Understanding Plume Dispersion

Predicting the External Aerodynamics of Cooling Towers using CFD

25 Benchmarking takes off for NASA CRM & Tupolev Tu-214

FloEFD™ Simulation of External Aerodynamics

29 The A to Z of Breaking a World Water Speed Record

It's not every day that a World Record is broken and in speedsports it's indeed a very rare experience. To do it both safely and cost effectively requires meticulous planning, solid engineering design and quality manufacturing, plus a balance between taking calculated risks versus the accrued speed benefits to be gained.

32 Optimizing Air - to - Air Refueling Systems

A study of a complex aero air-to-air refueling system

36 Zero to 90 in 166,440 hours

It's what happens off stage that counts

38 Driving Flanders to Electric Powertrain Innovation

Voxdale BVBA and Flanders' DRIVE delivering on the demand for innovation in the Automotive Industry.

41 Upgrading a Biomass Furnace: A Simulation Driven Approach

43 More Power Please!

What do Tim, the Toolman, Taylor in the TV-Series "Home Improvement" and Raul Cano at Stanley Black & Decker have in common?
The need for "More power!!"

45 FloEFD™ for Cyclone Simulation

Air cyclones are a popular method for separating out particulates due to their simple design and low capital and running costs.

47 Saipem S.p.A moves FloEFD Offshore

Saipem S.p.A take advantage of FloEFD to support operations

49 Leaving on a Jet Plane

Simulation of a Jet Engine Thrust Reverser

51 Advanced Natural Convection Cooling Designs for LED Bulb Systems

55 Avoiding Hot Spots

Discom B.V. use FloEFD™ to ensure Temperatures are kept within Bounds

56 ShowerPower® Turbulator keeps IGBTs Cool

FloEFD™ Efficiently Cools IGBT Power Modules

59 The Three Waves of Commercial CFD

62 Engineering Techniques for a Helicopter Rotor Simulation

66 Lighting the Way

Development of the Bertrandt Full-LED Headlight Thermal Simulation and Design

71 Cost Optimization of LED Street Lighting

LED Lighting Technologies from Vestel Engineering

74 Up, Up and Away!

Using CFD tools to develop a Real-Time Flight Model

80 How to Gain 3 Seconds Per Lap

83 FloEFD™ Shines a Light on Automotive Lighting

Condensation and Radiation Modeling Technologies in Automotive CFD Simulation

87 JSAE Benchmark of Automotive Aerodynamic Test Measurements

Ahmed-Type Car Body Versus CFD Software Predictions

93 Making Light Work of Lifting

Liebherr-Werk Nenzing GmbH use FloEFD™ for Creo™ in their Mobile Harbor Crane Designs

95 Layer by Layer

battenfeld-cincinnati use FloEFD™ to Model High-spec Extrusion Pipes

97 Optimizing an Automotive Air Handling Unit for Uniform Temperatures using FloEFD™

100 Steering Towards Flow Optimization

FloEFD™ is an established part of the development process at Robert Bosch Automotive Steering GmbH

102 Innovation isn't Optional

Mercury Racing® use FloEFD™ in the design of their latest intercooler filter

104 Fluid Dynamics Simulation Of Aqueous Humor In A Hole Implantable Collamer Lens Ks-Aquaporttm

Concept and development history of the Hole Implantable Collamer Lens

108 Voxdale bvba

Optimizing a NASCAR Racing Machine

112 Tamturbo Oy

Air Dynamics Simulation of an Oil-Free Air Turbo Compressor

116 Interview

Dr. Uwe Lautenschlager, Continental

118 Mitsubishi Materials

Design of Liquid-Cooled Nozzles for Cutting Tools

122 Voxdale bvba

Building a Wind Tunnel with FloEFD

124 TsAGI & Irkut Corporation

Cleared for Landing

130 Geek Hub

Ever wondered if a LEGO Aero Hawk Helicopter could actually fly?

134 Team Velarde

Gears up for Red Bull Air Race

138 E-Cooling

Cooling Power Electronics at Room Level

140 Dr. Schneider Group

Shortening Product Development Time

143 Interview:

Paul-Henri Matha, Groupe Renault

144 Groupe Renault

Driving down Automotive Headlamp Costs

148 Koenigsegg Regera

Sports Car Brake Cooling Simulation

154 Irkut Corporation

Commercial Aircraft Wing High Lift Modeling

159 ZFW

Successfull Electrothermal Simulation Study with Powertester and FloEFD

163 Geek Hub:

Spiralled Skyline

High School Students Fly with FloEFD™

The Real World Design Challenge (RWDC) is an annual high school competition in the USA run by a public-private partnership with the goal of assisting in the increase of the Science, Technology, Engineering and Mathematics (STEM) workforce in America.



Dr. Ralph Coppola, PTC, Director of the Real World Design Challenge

EVERY year teams of three to seven high school students are asked to address a real challenge that confronts leading engineers.

Often students are asked to design an aeroplane or car looking at the forces of lift, weight, thrust and drag with the goal of either enhancing performance or fuel efficiency. It is free for high school teachers and students to participate. Indeed, each participating teacher gets access to \$1M worth of commercial professional engineering simulation software to use in the competition, as well as access to professional mentors. To date 45 State governors have supported the RWDC "Governor's Challenge" and following State level competitions, a national competition final is held each year in Washington, DC.

RWDC helps to address the critical need in the United States for the development of a replacement workforce in the STEM fields, especially as a large proportion of the American aerospace and automotive engineering workforce comes closer to retirement. It is estimated that there are not enough young students with the resources and the enthusiasm to replace the baby boomer generation in these industries. Moreover, throughout America many companies across all industry sectors are increasingly demanding new hires from universities with 21st century skills in engineering simulation allied with creativity, problem solving, collaboration and "real world" knowledge that is comparable to experience. RWDC is therefore an innovative and unique response to this emerging need in America.

It was the brainchild of Dr. Ralph Coppola from Parametric Technologies Corporation (PTC) in Needham, Massachusetts. The idea came to him five years ago, seeking to bridge the gap between high school students and modern engineering simulation technologies and tools with a view to giving school children an aerospace or automotive related challenge that the world is typically facing today. The ultimate goal of the challenge, from PTC's perspective, is to stimulate interest in engineering with

15 - 16 year olds and to illustrate that engineering is a mainstay of the American economy and an ongoing factor behind its GDP growth.

Softer goals for the RWDC were to inspire and engage students in science, technology, engineering and mathematics education and highlight the economic importance of having the world's most skilled and innovative workforce in these fields.

In 2007, Dr. Coppola piloted his RWDC program in 10 States ending the year with the winning teams from each of the participating States competing for national honors at the Smithsonian National Air and Space Museum. Dr. Coppola's vision has always been to create an educational initiative that infuses "real world" experiences, one-on-one communication with industry experts, professional tools and software donated by companies like PTC and Mentor Graphics which is free and accessible to all students in the United States. The Real World Design Challenge aims at being a high-quality national engineering competition that allows any school to participate, regardless of economic limitations or geographic location.

As of today, over 13,000 students in 45 States have participated in the program. Each year the national championship winning team is sponsored by the RWDC to participate in the President's White House Science Fair. In five years RWDC has grown from just 10 to over 700 high schools. Numerous engineers, designers, mentors and judges from across industry, government and academia have been key to the success of the program by donating their expertise, sharing their knowledge with the students and evaluating the students' work.

Executives from an impressive array of 55 governmental, defense and private companies including NASA, the Federal Aviation Authority, the US Department of Defense, Northrup Grumman, Rockwell Collins, Cessna-Textron, SpaceX, GKN Aerospace and Lockheed Martin participate



RWDC 2012 Blue Ribbon Judging Panel including Mentor's Dr. Erich Buergel as well as judges from Lockheed Martin Corporation, Honeywell Aerospace, Northrop Grumman Information Systems and Airbus Americas Engineering, Inc.



in the local and national finals as judges. This year, Dr. Erich Buergel from Mentor Graphics was one of the Blue Ribbon judges.

Boasting a 55% growth in participation last year, the RWDC has now become one of the fastest growing STEM education programs in America, with support from the Aerospace States Association and the National Lieutenant Governors Association. Dr. Coppola chose FloEFD™ from Mentor Graphics because it is a fully-embedded general purpose CFD tool within the popular Mechanical CAD Pro/Engineer and Creo productlines. In addition, FloEFD's unique push-button geometry and mesh generation pre-processing capabilities – the bane of traditional CFD tools – makes it ideal for

high school children to pick up and use with minimal supervision.

FloEFD's robustness, built-in convergence intelligence and parametric simulation methodologies make it relatively foolproof for the high school students to use. Its history and pedigree as a well-validated 3D external aerodynamics solver making it ideal for virtual "wind tunnel" simulations. Schools are also offered PTC's Mechanical structural analysis tool, Windchill for their PLM needs and MathCAD as their engineering calculation tool. Dr. Coppola has arguably created the most popular and dynamic engineering design contest in America if not the world. In 2013 schools will be able to compete to design an unmanned aerial

vehicle that has been proposed by Northrop Grumman. The true value of RWDC will be in the number of new young engineers it enthuses and stimulates into the profession in years to come.

Want to know more about RWDC or to encourage your high school to participate?

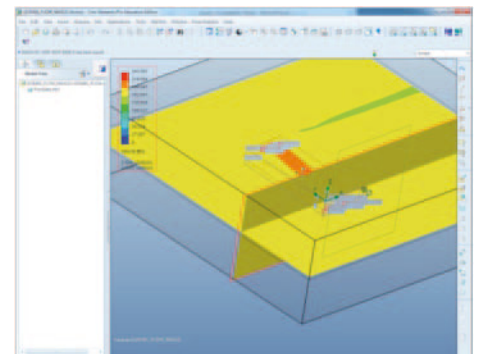
To get involved or for additional information, contact:

Dr. Ralph K. Coppola,
Real World Design Challenge Director
Phone: (1) 703-298-6630
email: rcoppola@ptc.com
or go to www.realworlddesignchallenge.org

Registration is open on the RWDC website.

"Real World Design Challenge has changed his life. I see so much happiness and satisfaction ahead of him and it came from a seed planted by RWDC." **Parent of a RWDC high school pupil**

A Connecticut School's RWDC 2012 Cessna-type Plan Design (in PTC Creo)



A Connecticut School's RWDC 2012 Cessna-type FloEFD for Creo Aerodynamic Analysis of the proposed aircraft wing

Let there be more LED light!

Over the last decade, as the efficiencies of Light Emitting Diodes (LEDs) has increased to the point where they are a viable replacement for incandescent bulbs and compact fluorescent lamps (CFLs) the world has reached a tipping point in the usage of LED Lighting within automotive lighting, street lighting, back lighting (for consumer electronics) and now general lighting applications.

By Dr. John Parry
Electronics Industry Manager
Mentor Graphics
Mechanical Analysis Division



Up to 95% of the electric input in traditional incandescent light sources becomes heat and is largely dissipated via radiation. LEDs however are significantly more efficient with up to 60% becoming heat and not all of it dissipated via radiation. The challenge for this rapidly growing industry is therefore effective thermal management of these Solid-State Lighting (SSL) products. Heat must be removed by conduction and convection in order to keep the LED cool for quality lighting outputs, reliability and product lifetime. Hence, the key technology barrier to LED adoption for general lighting applications is thermal.

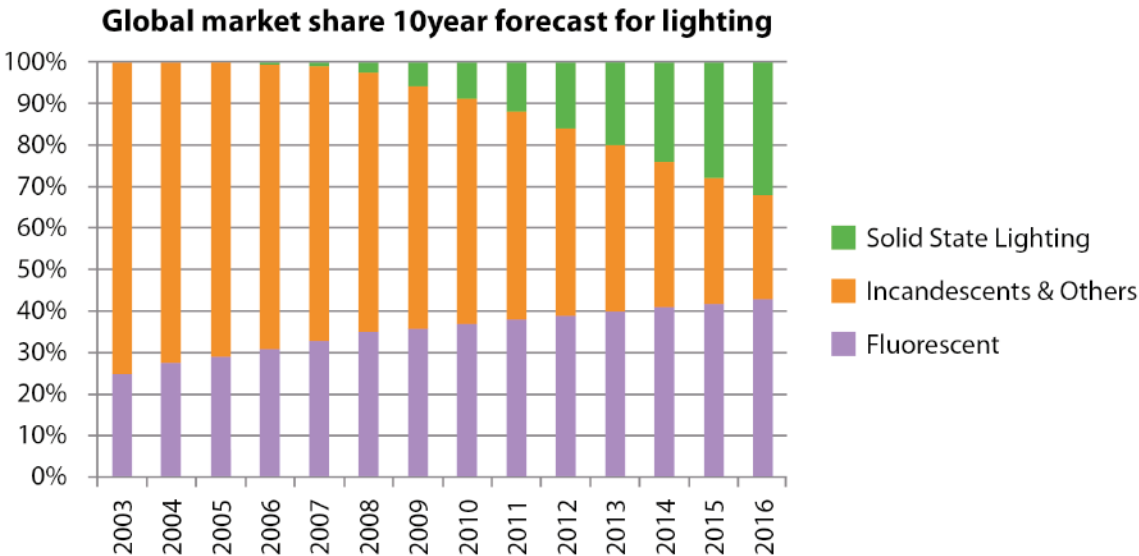
The LED lighting industry has also been hampered by a lack of standardization on data relating to the thermal performance of the LEDs themselves. As LEDs emit a substantial proportion of the power they consume as light, the power emitted as light has to be taken into account when calculating their real thermal resistance. It was for this purpose that the Mentor Graphics hardware product TeraLED™ was originally developed and released in 2005, and as LED light emission and lifetime strongly depends on temperature, proper thermal characterization of individual LED components is therefore very important. Accurate information on the real thermal

resistance of LEDs is critical for lighting system designers to develop proper thermal management solutions of their SSL products. Knowledge about temperature dependence of the light output characteristics (such as luminous flux or color coordinates) of LEDs is necessary for designing luminaires which provide light intensity and light distribution patterns as required by lighting standards. Unfortunately, due to lack of industry standards, LED vendors' data sheets hardly provide any useful information in this regard.

With these factors and trends in mind, Mentor Graphics has released two new productlines. These offer new capabilities for the LED supply chain from manufacturers through sub-assembly to end user SSL products; a larger TeraLED and an LED Module for the CAD-embedded CFD product, FloEFD:

Extended TeraLED Product Family

The market demand for bigger, brighter LEDs that dissipate more power has necessitated the development and release of a larger TeraLED sphere with greater heat sinking capability. Mentor is now offering both 30cm and 50cm integrating spheres and a range of cooling options up to 50W of cooling. T3Ster® measurement results can be converted into so-called compact thermal models (CTMs) suitable for CFD simulation.



Source: Optoelectronics Industry Development Association (OIDA) Lighting Technology forecast 2007 – 2017

These models have now been extended via TeraLED measurements to include temperature-dependent light output data. These provide SSL designers, for the first time, with the precise models of individual LEDs needed to calculate the 'hot lumens' of their luminaire designs.

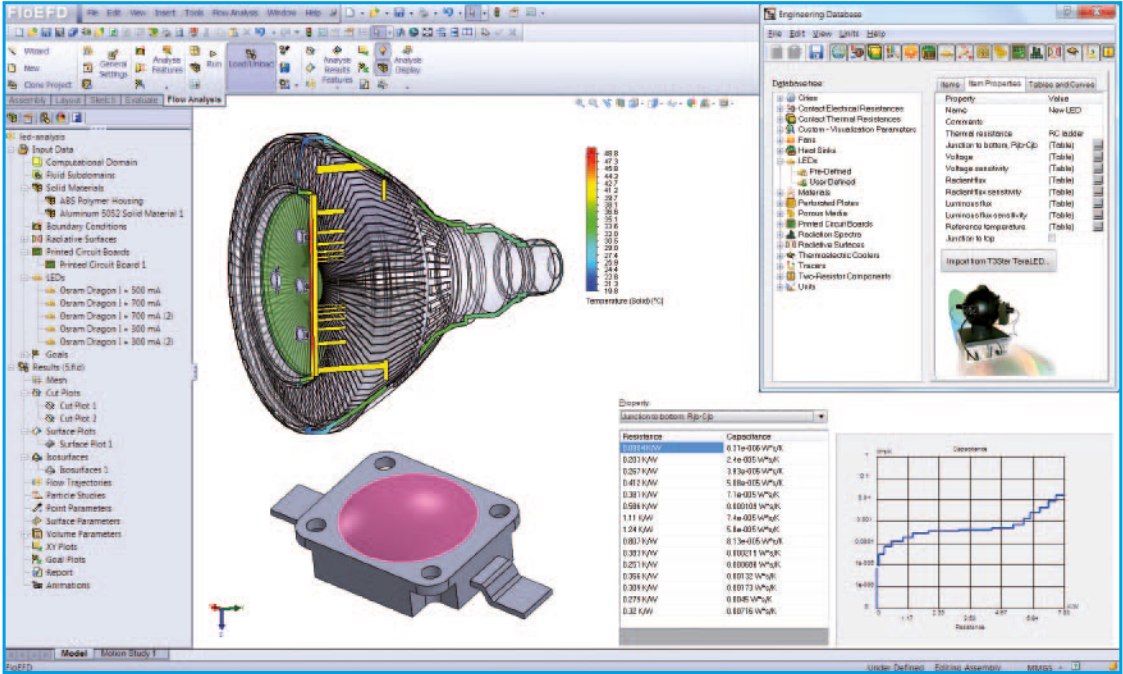
New CFD Module for LEDs

The FloEFD V12 release includes a unique CFD solution capability for designing Solid State Lighting. The innovative LED Module

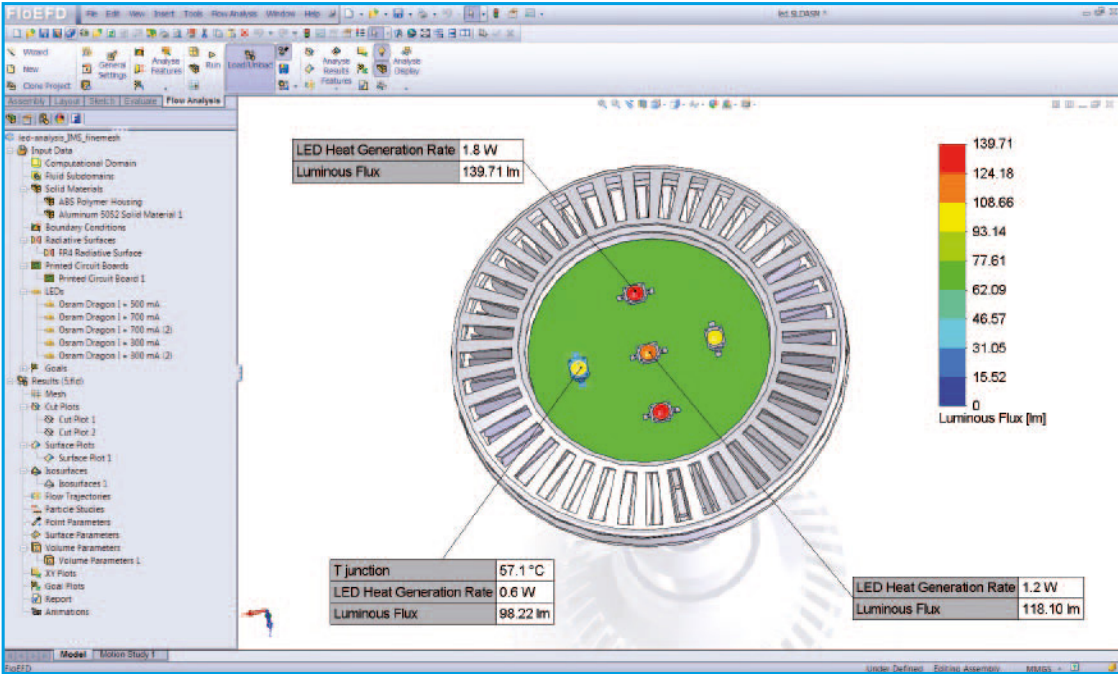
now allows designers to use accurate CTM and photometric models of LEDs obtained from T3Ster and TeraLED within a general purpose CFD simulation package. These models are uniquely driven at constant current as opposed to estimated power consumption inputs that yield less accurate predictions. This ensures correct accounting for power that is emitted as light when calculating the heat dissipation of the LED. Hence, the temperature, power consumption and light output (hot lumens)

of the LED are all predicted accurately by FloEFD. To enable this, a "starter pack" of thermally and photometrically characterized LED models is provided as part of the module. These are: CREE XT-E; Osram Golden Dragon; Seoul P4; and Philips Luxeon REBEL. The module also includes the ability to account for adsorption of radiation in semi-transparent solids such as a lens in front of the LED, and is able to represent a PCB as a compact model with orthotropic thermal conductivity.

New 50cm, 50W TeraLED



Typical LED Module interface panels illustrating the T3Ster-TeraLED workflow in FloEFD 12.0



Typical LED Module "Hot Lumens" prediction of a retrofit SSL bulb in FloEFD 12.0

Small but Mighty Powerful

Micro-turbine jet engine simulation and structural analysis using FloEFD™ and Creo® Simulate

by Tatiana Trebunskikh,
Andrey Ivanov, Gennady Dumnov

WHEN talking about jet engines in aerospace, visions of the enormous assemblies that propel passenger aircraft inevitably spring to mind. However just as notable and impressive are the much smaller micro-turbines which propel radio controlled model aircraft and Unmanned Aerial Vehicles (UAVs). Used primarily for military purposes, but also increasingly in civil applications such as firefighting and surveillance, UAVs or Drones are controlled either by computers in the craft or by remote control. In more recent years, jet engine development has been focused on fuel efficiency, reducing emissions and quieter engines.

These goals go hand-in-hand with the latest component designs, fuel types or utilization of flow behavior. The biggest influence

on the aforementioned parameters was achieved by a high-bypass ratio, developed in the mid-1960s as seen today in every passenger aircraft. Reaching up to 115,000 pound (514 kN) of thrust at a bypass ratio (BPR) of 10:1 with a mass flow rate of up to 1,300 kg/s, is enough to impress any engineer. Now of course so called smaller micro-turbine jet engines cannot compete with such numbers but it doesn't make them less impressive or complex. Whilst designers of micro-turbines must also achieve efficiency and power goals, they have an added challenge of doing so on a much smaller scale which poses more problems for materials and components. The best way to efficiently design such high performance engines is by using virtual prototyping such as Computational Fluid Dynamics (CFD) and structural analysis. This article explores how FloEFD is used to simulate the fluid flow, heat condition and combustion of a micro-turbine and how these simulation results apply to a structural analysis model.

Micro-turbine engines are developed for specific flight applications. They are used in UAVs which are designed for short flight duration. Today, lots of different UAVs are operating worldwide for all kinds of mission types. In general UAV missions range from reconnaissance, surveillance, target acquisition, signals intelligence (SIGINT) to scientific research. Another common use for small gas turbines is for auxiliary power units (APU), supplementing aircraft engines

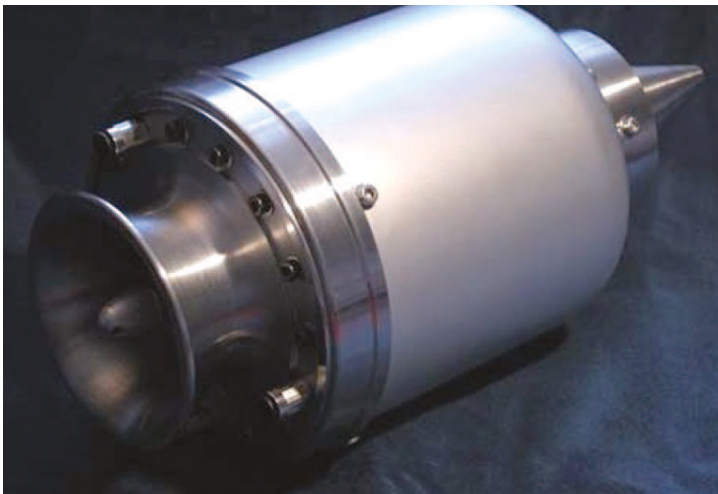


Figure 1. The model (left) and real prototype (above) of KJ 66 micro-turbine engine.

which provide additional power for non-propulsion functions when required. Their small size means, micro-turbine engines have small air mass flow rates and low pressure ratios, but very high rotational speeds of turbine and compressor stage.

For the purposes of this study a KJ 66 (Figure. 1) was chosen, as it is one of the more robust small engines with accessible design data.

Turbojet engines have complex geometries and physical processes. Understanding these processes is very important for designing such a high-performance product. The complex geometry and small size of this kind of engine limits the access of typical instruments used for the measurement of flow parameters as is required for a better understanding of the complex flow structure. As well as this, creating the optimal design for individual parts of an engine during testing can be an expensive procedure, making CFD analysis a very useful tool.

This article presents the CFD analysis of the KJ 66 micro-turbine engine, which is calculated as one unit without any transferred, symmetrical and periodical conditions between its parts. It takes into account the rotation of air in the compressor and turbine, conjugate heat transfer and air/kerosene combustion all within the multiCAD-embedded full-

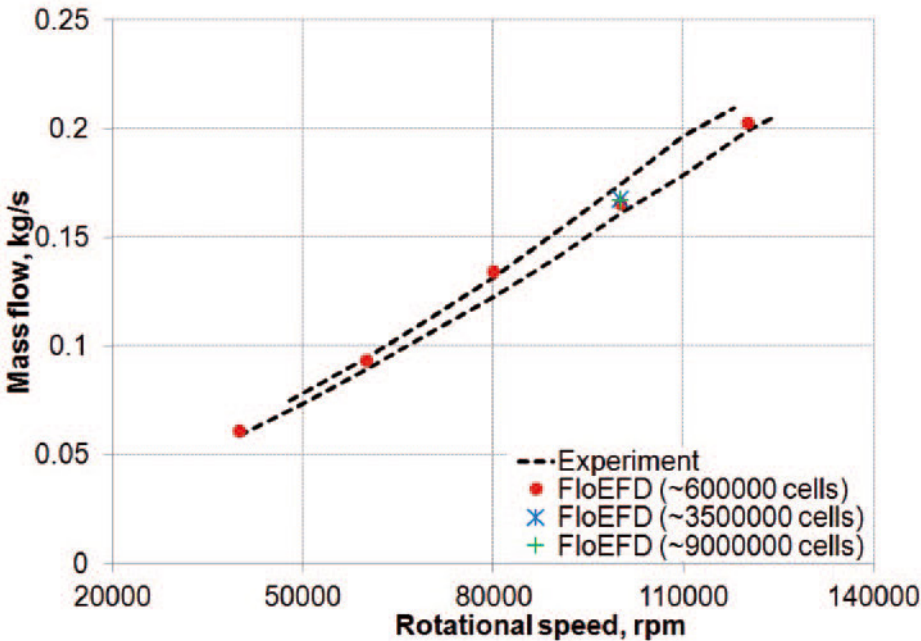


Figure 2. Air mass flow at the inlet of KJ 66 engine.

featured general purpose CFD tool FloEFD™. Thermal and structural analysis were conducted using PTC’s Creo Simulate together with thermal and pressure load results obtained from FloEFD.

Five cases of varying rotational speeds of 40000, 60000, 80000, 100000 (the normal mode) and 120000 rpm were considered for the compressor and turbine by specifying local rotational zones. The solid parts are specified as aluminum, steel and inonel for the consideration of conjugate heat transfer.

The air mass flow at the inlet of the engine at various rotational speeds of the compressor

can be seen in Figure 2. The FloEFD results are compared with the experimental data of Kamps [1], and show the values of mass flow match the experimental data very well with almost no dependence on the number of mesh cells.

The calculation results in Figure 3 show flow trajectories colored by velocity magnitude and pressure distribution with Line Integral Convolution (LIC) on the surfaces of the compressor and diffuser at the normal mode. The pressure on the compressor’s blades can be lower than 65000 Pa and can reach 180000 Pa on the diffuser’s blades.

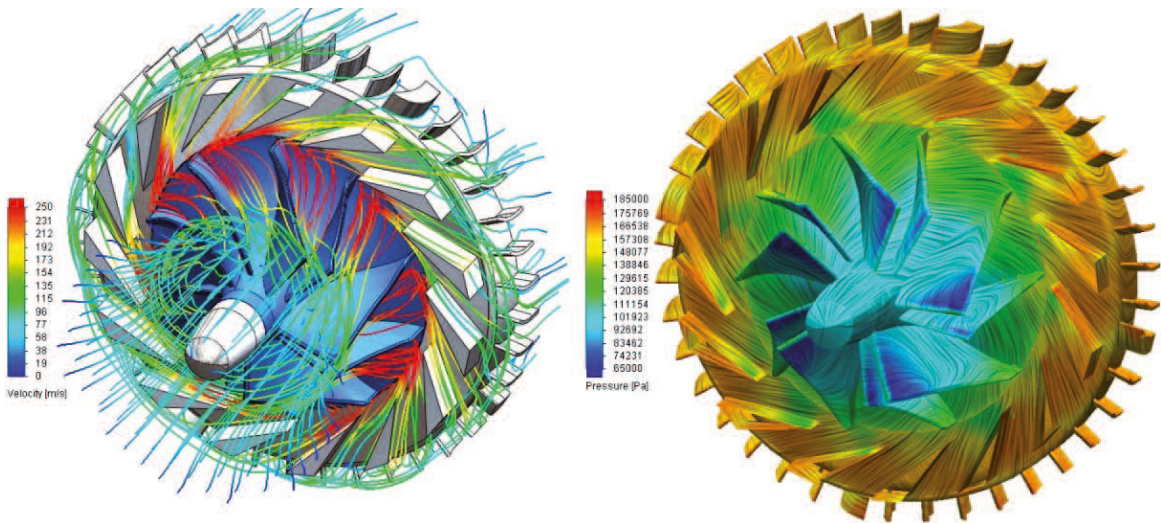


Figure 3. Flow trajectories colored by velocity magnitude (left) and pressure distribution with LIC on surfaces of the compressor and the diffuser (right) at normal mode.

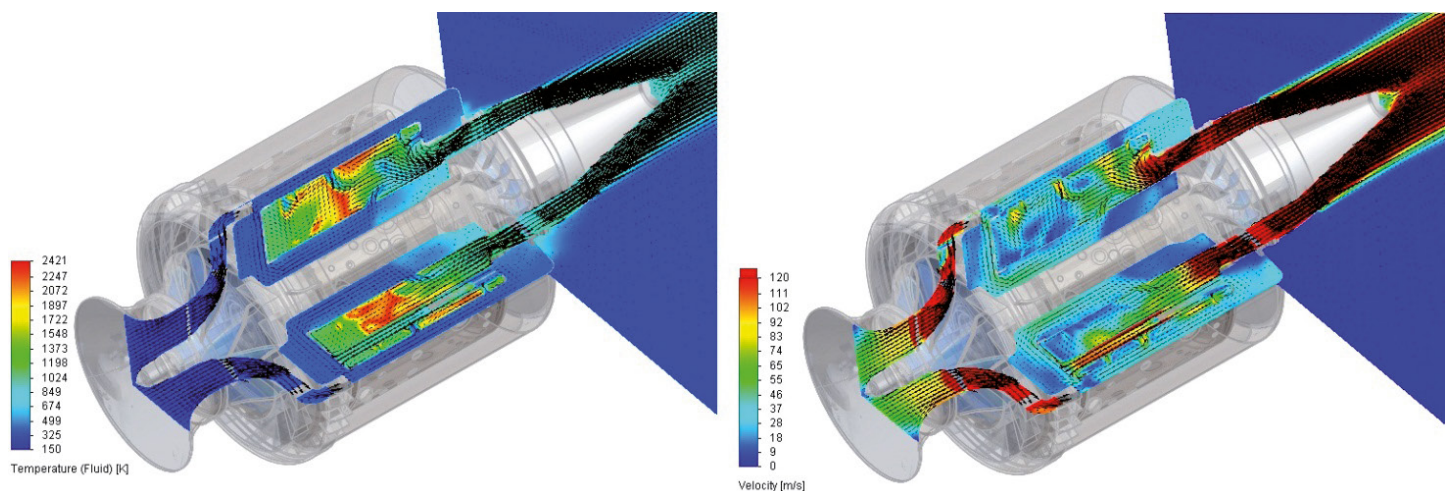


Figure 4. Fluid temperature (left) and velocity (right) distributions at two longitudinal sections of the combustion chamber with flow vectors at the normal mode.

The combustion chamber of the KJ 66 engine features direct fuel injection through six vaporizing sticks to ensure complete combustion inside the chamber. Figure 4 presents the fluid temperature and velocity distributions at two longitudinal sections of the combustion chamber with flow vectors at the normal mode. The temperature in the combustion chamber reaches approximately 2400 K. An increase of the velocity in the region of the openings of the combustion chamber can be clearly seen especially on the rear wall of the chamber.

Further evaluation of the results shows a direct comparison of the temperature distribution in the combustion chamber at 120000 rpm obtained with FloEFD (left) and a traditional CFD tool (right) presented by C.A. Gonzales, K.C. Wong and S. Armfield [2]. Both models have been simplified by not examining all parts of the engine, but all features of the combustion chamber have been taken into account. The symmetry conditions are not used in the FloEFD model as they were in that

of the traditional CFD model, resulting in some differences in the parameter's distribution which can be seen in Figure 5. Considering these factors, both FloEFD and the traditional CFD tool, show reasonable accordance in their results. It is clearly visible in Figure 5 that the primary combustion zone is located in the central part of the chamber.

Besides thermal simulation, FloEFD also allows some parameters to be exported as loads for structural and thermal analyses with Creo Simulation. In this case the surface temperature was exported from the CFD calculation to run the thermal calculation with Creo Simulation. Then the structural analysis was conducted using the temperature of the previous calculation and the pressure exported from FloEFD. The results in Figure 6 show the displacement distribution of the structural analysis. It can be clearly seen that the combustion chamber is deformed under the loads with the displacement reaching a maximum of 0.001 m.

A pressure and velocity distribution near the surfaces of the engine is presented in Figure 7 and the increase and decrease of the pressure at the compressor and turbine stage is shown respectively.

The overall performance of the engine is usually measured by thrust and Figure 8 shows the comparisons of measured and predicted values of thrust of the KJ 66 engine at different modes. Experimental and predicted values are similar up to 80000 rpm with some divergence at 100000 rpm.

Comparisons of measured and predicted values of the main integral parameters such as air mass flow at the inlet of the engine, thrust and temperatures at the outlet of the diffuser and combustion chamber are almost identical.

This study demonstrates that FloEFD can provide a series of "what-if" CFD analyses and export data values for structural and thermal analyses. With its CAD embedded approach it is very efficient should there be

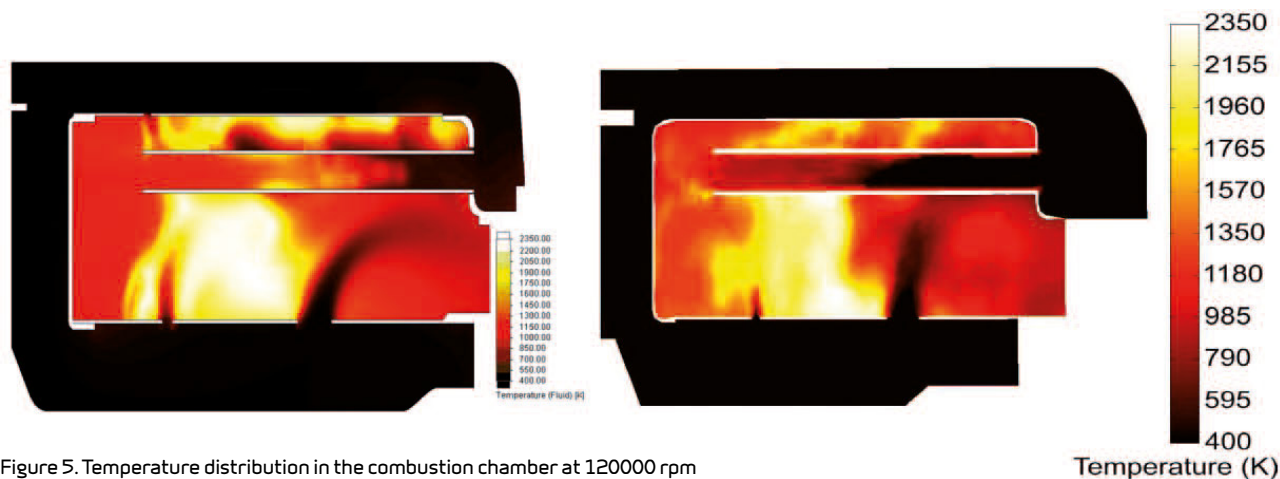


Figure 5. Temperature distribution in the combustion chamber at 120000 rpm obtained in FloEFD (left) and traditional CFD software [2] (right).

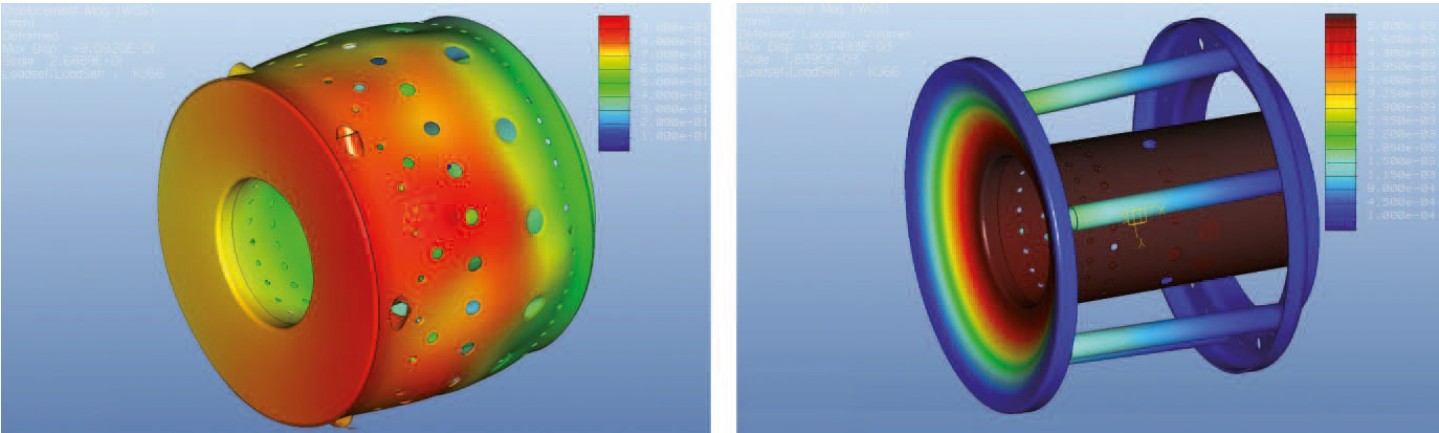


Figure 6. Displacement distribution on the surface of the combustion chamber in Creo Simulate (scaling 20%).

a need to experiment with different designs of any component in the model. By simply changing the CAD parameter of a parametric model, such as the opening diameter of the combustion chamber, multiple simulations can be created in little time, whilst at the same time changing any boundary conditions. The simulation project is always up-to-date with the CAD data.

FloEFD provides high accuracy in high-end applications such as demonstrated in this aerospace example. With its CAD embedded approach, FloEFD allows the user to set up and run simulations and design iterations quickly in order to determine the appropriate design modifications, saving time and money.

References

[1] Kamps, T. Model jet engines, UK, 2005.

[2] Gonzalez, C.A., Wong, K.C., Armfield S. Computational study of a micro-turbine engine combustor using large eddy simulation and Reynolds average turbulence models, Austral Mathematical Soc, Australia, 2008.

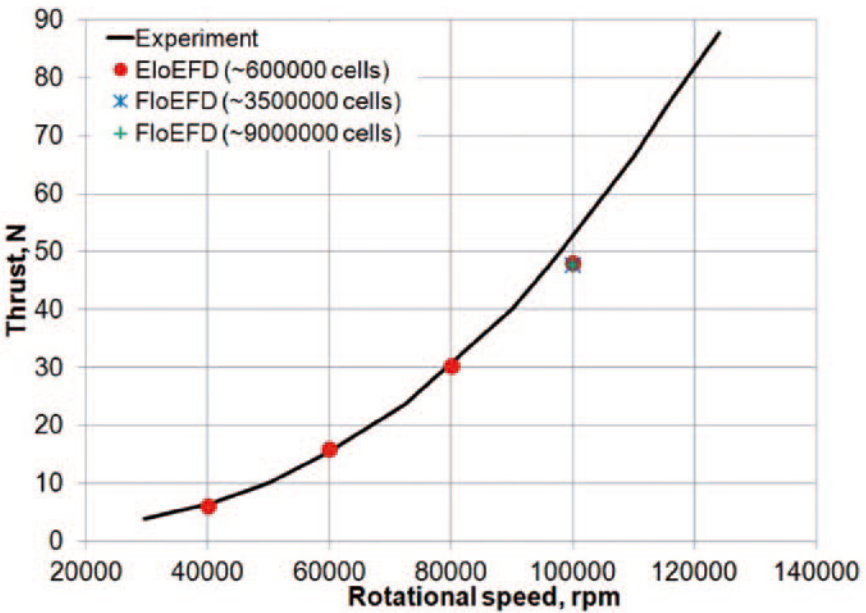


Figure 8. Thrust of KJ 66 engine.

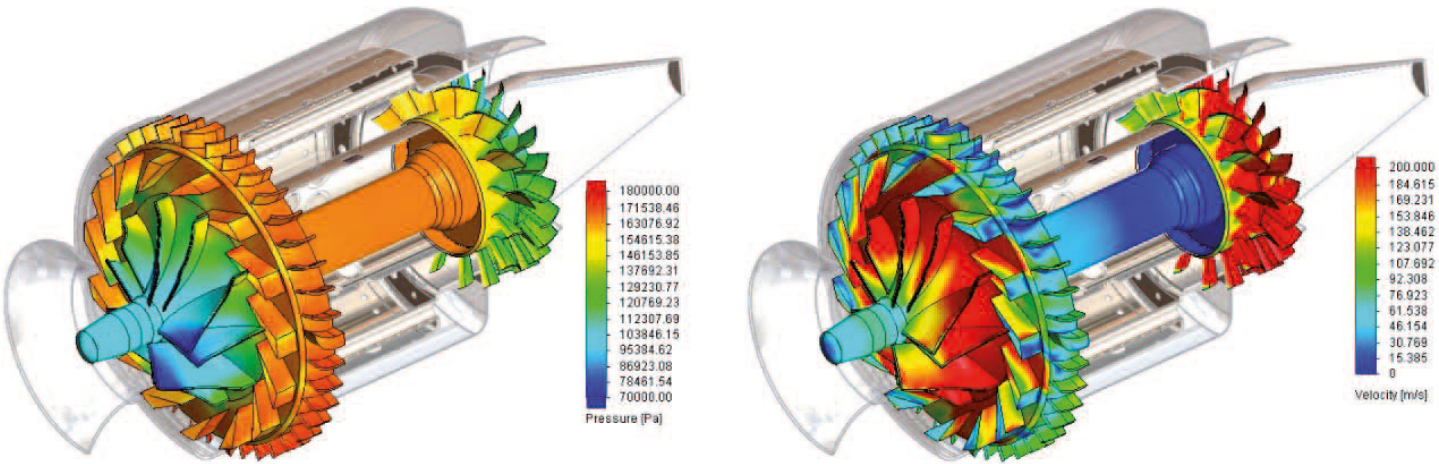


Figure 7. Pressure (left) and velocity (right) distributions.

Athlete Engineered Technology Fine Tuned by CFD

The Science that could bring in Winter Olympic Gold Medals for Bob Skeleton Athletes



Bromley Technologies Founders: CEO Kristan Bromley (right) & Structural Dynamics & Systems Director Richard Bromley (left).



Shelley Rudman, currently ranked #1 Skeleton athlete in the world

A GREAT skeleton ride combines athleticism and courage with the science of physics and meticulous engineering design, according to Professor Kristan Bromley. Over the past 18 years, Professor Bromley, aka Dr. Ice, has used this powerful combination to personally win the 2003-2004 World Cup and the 2008 World Championship titles and three European Championship titles. This winning streak was no fluke, when following the reinstatement of Skeleton at the Winter Olympics in Salt Lake City, Kristan's scientific approach went on to support consecutive medal winning performances as part of a winning streak for British athletes.

Kristan, with a doctorate in the science and engineering behind the Skeleton sport, is CEO of Bromley Technologies Ltd. which he founded with his brother Richard and supports fellow athlete and 2012 world number one Shelley Rudman. Their impressive offices are located on The Advanced Manufacturing Park in Sheffield, England, where they neighbor aerospace giants such as Rolls Royce and the AMRC Boeing. It is here that Kristan works on developing high-performance sports products with a small but dedicated group of engineers and world-class athletes. Their company focuses on developing and manufacturing cutting edge sports products and technology that give Olympic athletes and professional teams a competitive edge. Bromley has forged a world-leading position in Skeleton Sled sport, however their expertise also extends to projects in bobsleigh, luge, composite hockey sticks, sprint footwear and bobsleigh track simulation. More recently Bromley has been nominated to partner the International Skeleton & Bobsleigh Federation in developing the sport's first Paralympic sled designs.

It's the skeleton bobsleigh that has impassioned Professor Bromley. For those unfamiliar with the sport, to briefly describe it would be to say that is it a 90 mph head-first, face-down hurtle on a narrow one man sled down a 1,500 meter ice track against a roaring 5g-force. Runs are timed electronically to the nearest hundredth of a second, and athletes are continually striving to shave off time in pursuit of the perfect run and medal success.

It's a highly tuned performance, and each sled is customized to the athlete. The athlete must be in unison with the sled and the track physics to successfully complete the course. The track is negotiated by the athlete's body using only shoulders and knee pressure on the sled and the occasional 'toe on ice' to induce subtle steering effects. There are no brakes or active mechanical steering elements. Not only is this a great physical feat but also one of mental strength and courage, because there is no place for fear as athletes hurtle down the track at dangerously high speeds, one tiny mistake could be fatal.

In preparation for the 2014 Sochi Games, Kristan and the experts at Bromley Technologies are putting their sport, engineering, and design knowledge to work to create the fastest sleds on the planet. A meticulous approach to design and testing is being undertaken, consisting of four stages. Stage one, which took place this past summer, included a detailed analysis of the aerodynamics of the athlete-sled system. The focus was on developing equipment that worked optimally with each individual athlete's form. Stages two and three see the team trialing their findings and fine tuning the design and set-up before stage four, the final production ahead of the winter games.

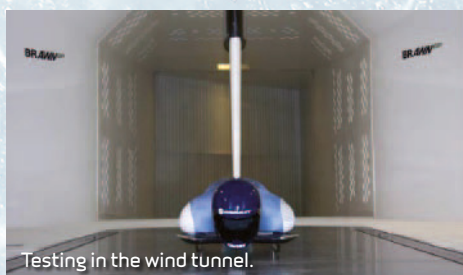


Kristan started his career as a graduate engineer for British Aerospace and is very familiar with Computational Fluid Dynamics (CFD) modeling and simulation techniques, having designed and tested his first sled some 17 years ago for the British Bob Skeleton Association. Kristan uses FloEFD™ modeling and simulation software to optimize the design of the skeletons. Doing the simulation himself, Kristan comments, "When I use a traditional CFD approach to do aerodynamic simulations, it can take weeks to get results back but now I can use engineering feedback within hours."

"An iterative approach is taken with new projects progressing from design to design. During a competitive season I can observe any new developments made by my competitors and combine these with our own ideas hot off the Bromley 'design board'. FloEFD enables me to quickly analyze these ideas to make an initial assessment before further detailed analysis is performed later in the program. It's an extremely efficient way to work in very unforgiving timescales."

For analysis, Kristan uses various flow visualization techniques, including flow lines, pressure contours and maps as well as other data gathered from testing. "I use a mix of visual and numeric outputs to inform me of what's actually happening with respect to air flow around the athlete and the sled. Visualization techniques are extremely powerful, allowing an intuitive approach to design innovation. Numerical outputs enable the direct impact of design changes to be assessed in relation to performance. Drag values from FloEFD are input into Bromley's own track simulation software in order to convert drag saving into time savings. A key part of working closely with athletes is in understanding how the changes made in one area affects other areas. For example, aerodynamic design improvements may have a secondary structural affect on the sled which would change its behavior. This means that design modifications must be made with consideration to how the change will ultimately affect the athlete."

A combination of FloEFD and Pro/ENGINEER Creo™ is used for aerodynamic analysis. In



Testing in the wind tunnel.



keeping with Kristan's "Athlete Engineered Technology" philosophy, he said "We're testing a variety of shapes that work with the geometry of the athlete. When we're talking about an athlete lying on a sled traveling at speeds close to 90 mph, the first part of the equation is the equipment, (the helmet and the sled), the other parts being the athlete and the track. Our goal is to bring all those components together into one system. We can't change the shape of the track or the athlete's body but we can change the shape of the other components to try and optimize the system. The sport is governed by very tight rules and regulations which limit large advancements. Our aim is to find multiple gains, each with a small percentage improvements that combine to make a tangible difference on the track."

The engineers at Bromley Technologies test their CFD predictions against wind-tunnel measurements to validate their results and be assured of accuracy. Reserving time in the same wind tunnel used by Formula One racing teams is expensive, so Kristan aims to use the FloEFD data, benchmarked in the wind tunnel with comparable results, to make multiple design changes within hours rather than days.

Over the past two years, Kristan and his team have worked to narrow down the optimal shape for the sled using simulation results in FloEFD. "We needed to combine aerodynamic design improvements with design modification made in other areas. This was one of our biggest challenges because any modification in one area must not negatively impact upon other areas of sled performance."

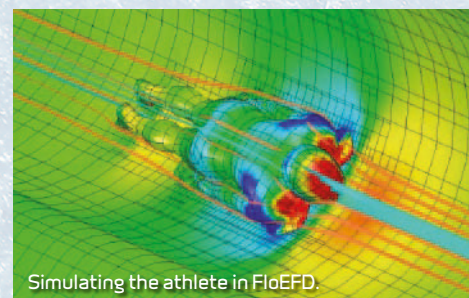
The Bromley team has been painstakingly working on numerous sled geometries over the last two years. This has resulted in a shortlist that was tested on ice at the 1994 Olympic Bobsleigh and Luge Track in Lillehammer, Norway in October. "Our aerodynamics program runs in parallel to other areas of development."

"This is a critical stage of the four year development program, where we find out if the virtual gains highlighted in FloEFD translates into real performance improvements on the track. "We need to get on the ice to test the sled. This is the only way we will know if the innovations result in performance gain."

Following testing in October the team will have a busy schedule in order to move into the final development stages in preparation for the Winter Games of 2014, which are less than 500 days away. We will be catching up with Kristan in the next issue and reporting on their results from the track testing.

For More Information...

Kristan Bromley: www.kristanbromley.com
Twitter: [@kristanbromley](https://twitter.com/kristanbromley)
Bromley Technologies:
www.bromleysports.com

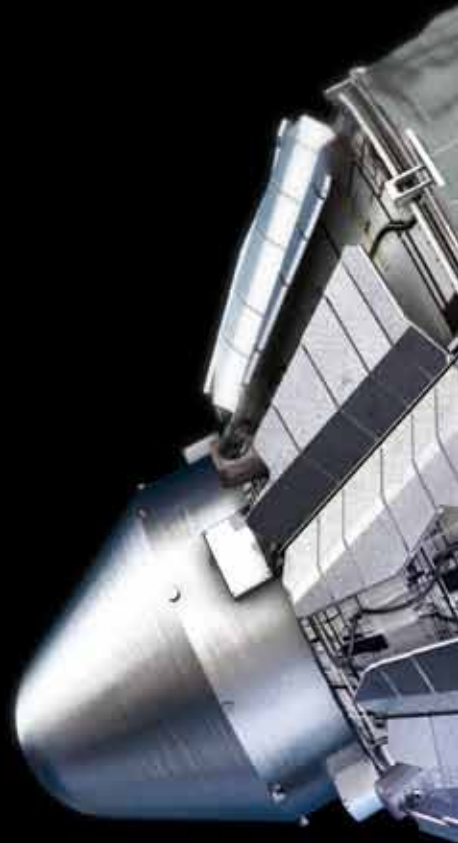


Simulating the athlete in FloEFD.

Dem Bones, Dem Bones, Dem Microgravity Cow Bones

Designing an
experimental
capsule
environment to
assess the effects
of bone density in
space

By Koen Beyers, Voxdale BVBA





The Flemish Space Cluster is a \$200M, 30 company manufacturing base dedicated to developing and commercializing Belgium's science and technology associated with space. Voxdale BVBA is a member of the cluster as well as providing other engineering services over a wide range of industries from their offices in Antwerp. One of the more interesting space projects they are working on is the possibility of three year long manned journeys to neighboring planets, such as Mars to address the problem of astronauts' bones becoming brittle and even suffering osteoporosis during long space flights in microgravity.

To gain a deeper understanding of this phenomenon, the 'FreqBone' bioreactor project was conceived by Jos Vander Sloten, Gerrit Van Lenthe and Geert Carmeliet of the Catholic University of Leuven, Division of Biomechanics and Engineering Design, in Belgium, and deployed in a European

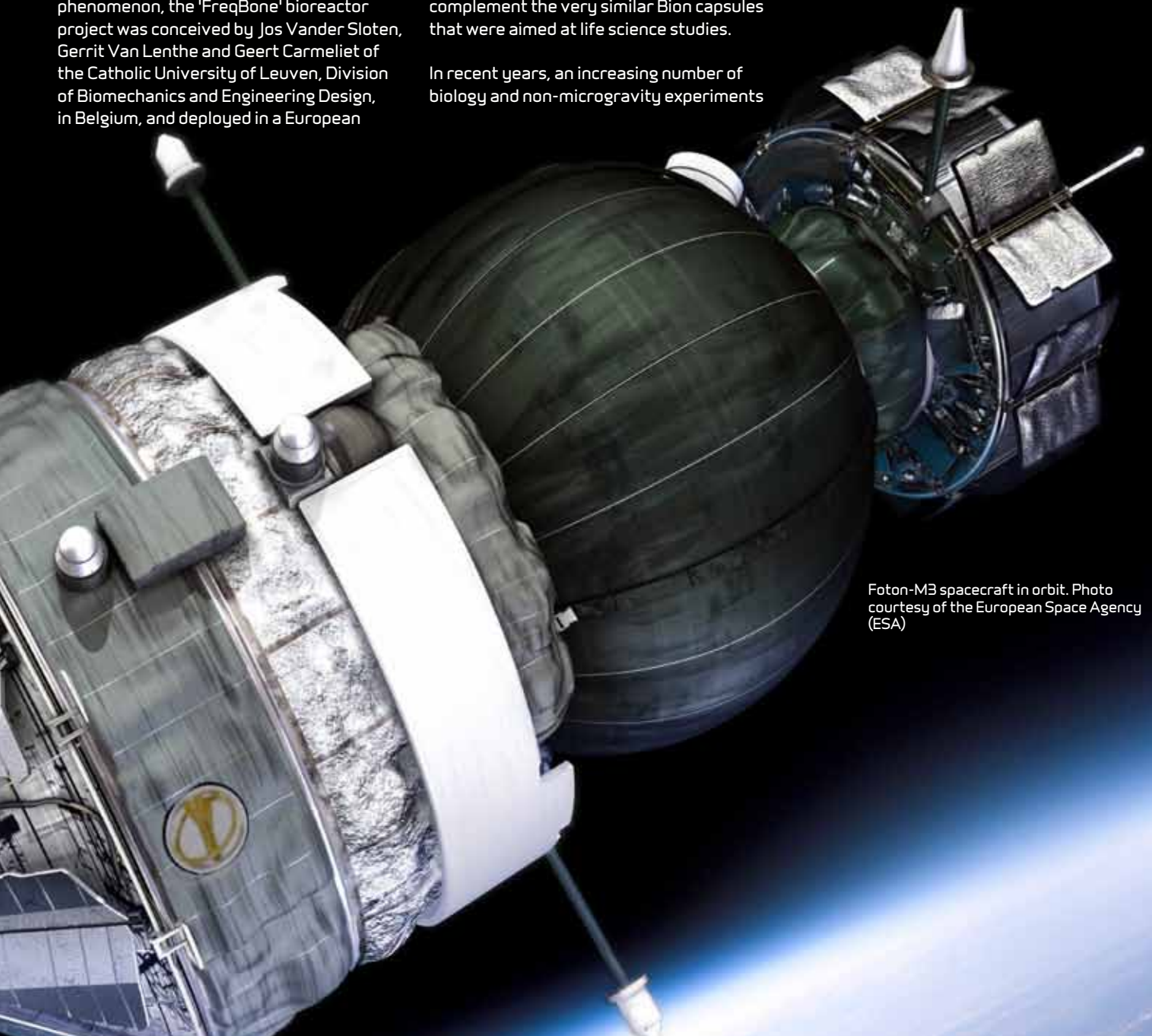
Space Agency (ESA) low-earth orbit mission. In essence their FreqBone experiment involved 12 pieces of living cowbone (that were constantly 'fed' during the flight to keep the bones alive) being exposed to a 12 day vibration experiment inside a satellite orbiting the earth under weightless conditions and exposed to cyclical solar loads due to it orbiting the earth 15 times a day at a speed of 28,000 km/h.

The Foton unmanned recoverable spacecraft series was first introduced by the former Soviet Union with an inaugural flight in 1985 after the successful Soviet Soyuz rockets and capsules from the 1960s. It was conceived as a microgravity platform for physicists and materials scientists to complement the very similar Bion capsules that were aimed at life science studies.

In recent years, an increasing number of biology and non-microgravity experiments

were transferred to Foton, while the Bion program was discontinued.

The Foton-M3 Russian spacecraft is designed to perform space experiments during a short mission life (generally up to two weeks). The Russian Space Agency, Roskosmos, is responsible for the spacecraft while ESA is responsible for its payload and experiments. The FreqBone project was completed and the experimental test done on the Russian Foton-M3 Rocket ESA, and indeed it was one of fourteen ESA experiments in the rocket payload bay including ones for fluid physics, biology, protein crystal growth, meteoritics, radiation dosimetry and exobiology.



Foton-M3 spacecraft in orbit. Photo courtesy of the European Space Agency (ESA)

It is well-known that mechanical loading is necessary in obtaining adequate bone strength; however, the specific details are still largely unknown. Hence, the FreqBone space flight experiment was designed to investigate how mechanical stresses and strains affect bone remodeling processes, and how this is affected by microgravity. In November 2007, FreqBone was flown successfully on board of the Foton-M3 mission. A total of 12 bovine trabecular bone specimens spent 14 days in microgravity. Half of them were biomechanically stimulated by high-frequency, low amplitude loads; the other half were kept unloaded in microgravity. The specific aim of the project was to analyze these samples with the goal of linking the local mechanical milieu in the bone samples to areas of bone resorption and bone apposition.

Each day, as part of the experiment, half of these cow bones were subjected to a 10 minute-long vibration (high frequency, low amplitude mechanical stimulation) and the effects monitored throughout the mission. In effect, trabecular bone cores were tested in a dedicated loaded and perfused bioreactor. Under microgravity conditions, the effect of mechanical stimulation was compared in loaded and perfused samples versus non-loaded (only perfused) samples. The scientists wanted to see what happened to the vibrated and non-vibrated bones when exposed to both radiation and microgravity while being in orbit. The actual FreqBone flight hardware and one ground control experimental model based on the requirements of the Leuven team were designed and built by Marc Dielissen at QinetiQ Space (a subsidiary of QINETIQ). The FreqBone rig had to be designed to fit within very tight physical size, weight and robustness constraints for operating within the satellite payload bay.

For the FreqBone project to be successful QinetiQ Aerospace engineers in Flanders had in essence to design a box that was under 10kg in weight with an internal temperature in the 'bonechamber' of exactly 37.2°C plus or minus 0.1°C. They turned to Voxdale to help them in the thermofluid design of the ducting and chamber in which the experiment needed to be kept at a uniform temperature during the repeated low-earth orbits. The real challenge to the experiment was in the transition periods when the satellite was exposed to full-sunlight and then full-darkness as it moved into the earth's shadow. These 25 second transitions proved to be the most critical in terms of thermal shock to the chamber and designing out these solar heating effects was the most difficult part of the equipment's design.

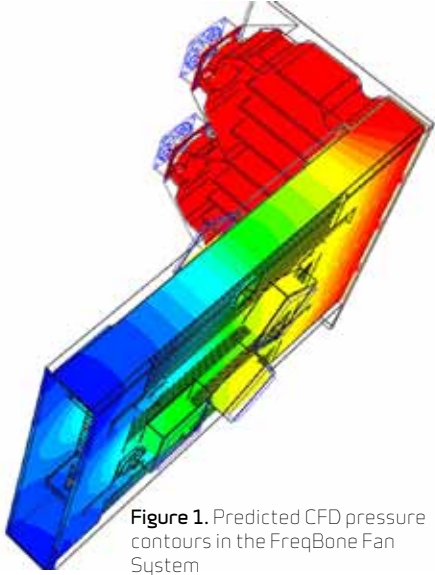


Figure 1. Predicted CFD pressure contours in the FreqBone Fan System

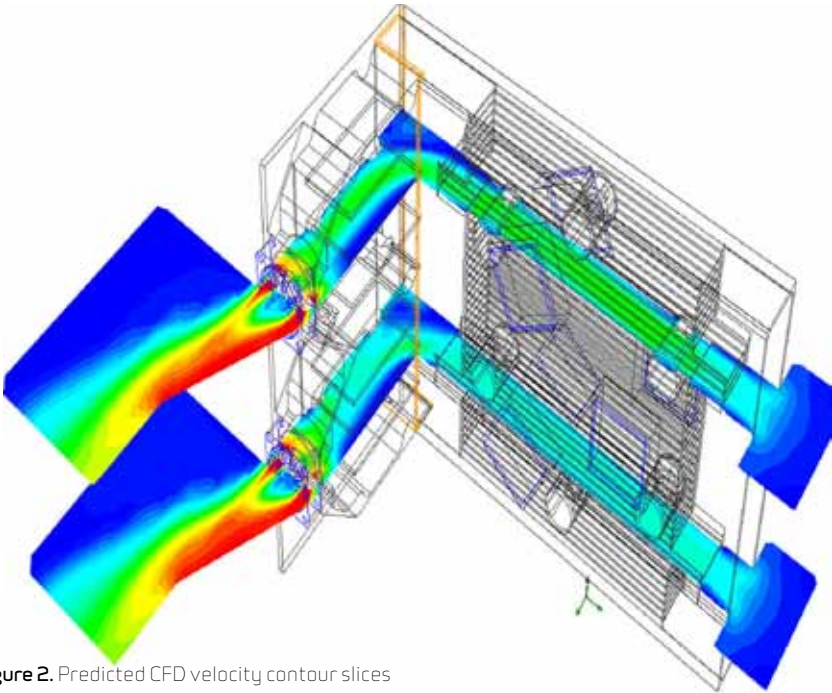


Figure 2. Predicted CFD velocity contour slices

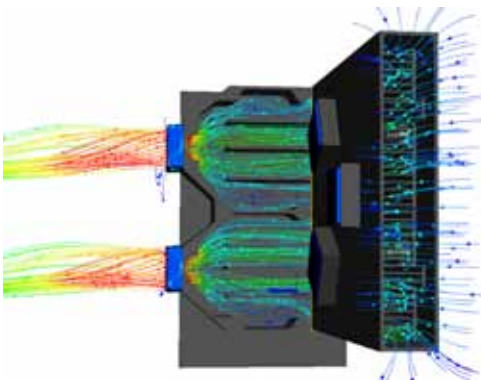


Figure 3. Predicted CFD flow streamlines in the FreqBone Fan System

Voxdale turned to the PTC Creo CAD-embedded CFD software, FloEFD, to assess multiple designs of the bonechamber fan system quickly and effectively in order to meet the design spec. A recommended design for the FreqBone fan system ducting, heat sinks, six peltier fans and two mechanical fans as well as internal conduction materials was duly made to compensate for the internal temperature fluctuations to be expected during the 15 daily orbits of the payload bay and the cycles of zero to full solar radiation in particular.

The FreqBone experiment worked perfectly during the mission and once the Foton-M3 capsule returned to earth the bioscientists

were able to compare the evolution of the bone structure in the loaded and unloaded cowbones to that on earth. Valuable insights were gained that will be employed in future long distance and inter-planetary manned space flights.

For more information:

- [1.] Flemish Space Cluster: www.vrind.be/en/
- [2.] Belgium in Space Website: www.belgiuminspace.be/nieuws/ruimtevaartbedrijven/verhaert-space-ontwikkeld-drie-instrumenten-voor-foton-m3-missie
- [3.] Foton-M3 Mission: www.eoportal.org/directory/pre_FotonM3MissionYES2andOWLSExperiment.html

Improving 1D Data with 3D CFD

Improving 1D Thermo-Fluid System Automotive Engine Data with 3D Computational Fluid Dynamics

By Joe Proulx, Mentor Graphics

When working with larger cooling systems that incorporate several components such as heat exchangers, thermostats, coolant pumps and different cooling cycles like oil and coolant, a 1D CFD simulation tool is the common choice for thermal analysis. However, when considering an automotive engine cooling system, which is rather more complex when you take into account their transient behaviors with corresponding drive cycles and system reactions with all components, it becomes even more complex on any changes in flow rates or temperatures.

Moreover, such systems can only be as accurate as the data that is supplied to them. One way to improve accuracy would be to get 3D component data and characteristics from measurements. If however components are still in the design stage, building a prototype and measuring them can be extremely expensive. To facilitate this, Mentor offers a direct interface by coupling CAD embedded CFD software FloEFD™ with system simulation software Flowmaster®, resulting in a CFD characterized model as a component in the Flowmaster system.

A recent paper for the SAE World Congress [1] demonstrates the use of coupled 1D-3D CFD simulation for an automotive engine block (see Figure 1).

The Problem

It is well known that bringing an automotive engine up to normal operating temperature quickly after starting is the best way to improve vehicle efficiency. The engine and complementary components, along with

the coolant and oil, all start out cold. By confining the heat to the engine during the warm up period, efficiencies during the startup cycle of a vehicle can be improved.

A combination of 1D and 3D CFD can be utilized to determine the optimal design of such an engine. Each type of simulation has its virtues, whilst 1D simulation can run long transient simulations quickly it can lack some detail. 3D CFD simulations on the other hand can accurately simulate details of solid components but it tends to be slower in regard to transients.

An engine system has many components and as a consequence when the design develops not all the pieces are ready at once. As well as this, obtaining vital data can take time, so an efficient design process incorporating engine cooling data obtained through testing can be supplied to the 1D simulation tool for analysis. Should the component require modifications through the design cycle, testing will need to be repeated. Conversely, if testing has not yet been performed and all that is available is empirical data to quantify the engine, then accuracy could come into question. The net effect is that these types of approaches can be time consuming or inaccurate. In this instance the engine block and head were available as CAD models and the majority of the details of the 1D model were already in place making a 1D-3D approach ideal.

How CFD was used

A CAD model of the engine block and head was used for the 3D simulation. Figure 2. shows the coolant and oil flow paths in the engine (in blue). When setting up the

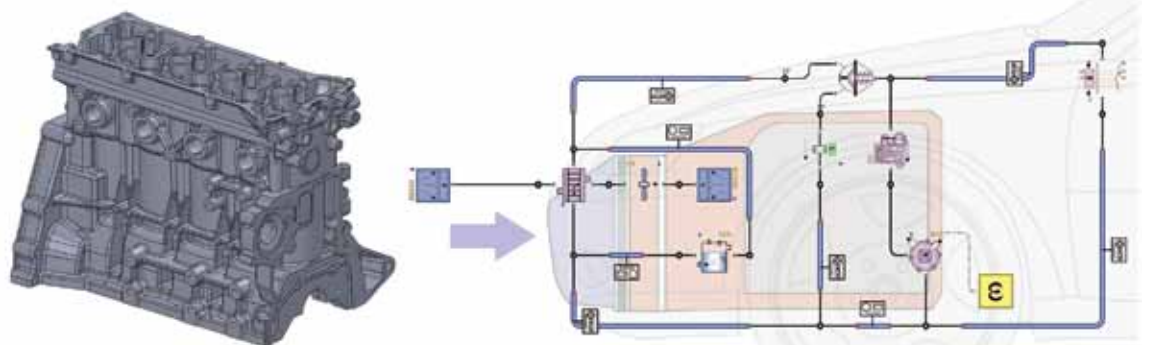


Figure 1. 3D engine CAD model and 1D design of a cooling system

power boundary conditions in the model, the portion of heat that is dissipated from the combustion into the cylinder walls was applied as a constant. The value of heat used for this dissipation was developed from earlier experimental data and the imposed drive cycle. Goals were set in the model to automatically capture flow versus heat transfer coefficients for each fluid. Air around the engine and head also contributed to the engine cooling through natural convection. Once the base case was setup, an array of nine models was run using a parametric study in FloEFD. The model was created to vary coolant and oil flow. Heat dissipations in the motor were also varied. Once the array of nine CFD models was run, the data was then compared to empirical data according to Dittus-Boelter correlations.

Solution & Results

The 3D CFD simulation was setup in a short time and the results from the parametric study were imported as a new component into Flowmaster for the overall system simulation of the transient drive cycle. The graph in Figure 3 below shows a significant difference in the methods used to quantify the heat transfer from the engine to the coolant. Heat transfer coefficients from the engine to the coolant had differences as high as 20% between hand calculation and 3D CFD simulations. This shows that the overall accuracy when using 3D CFD simulation data is far more accurate than hand calculations. The overall process of characterizing a component for a range of working parameters as shown here enables the system designer to evaluate any changes in the system with the same component over and over much faster than a direct 1D-3D coupling where a 3D transient simulation can be the major bottleneck in the overall calculation time.

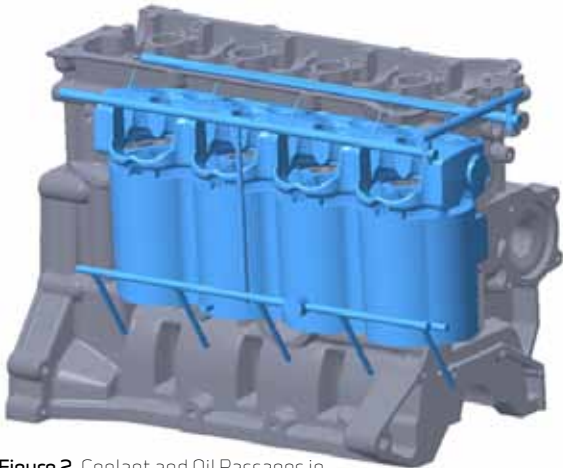


Figure 2. Coolant and Oil Passages in Detailed 3D CFD Model

Concluding Thoughts

As demonstrated here, the detailed simulation approach versus conventional engineering hand calculations can be significantly different. Use of a validated 3D CFD tool such as FloEFD, as opposed to a single empirical formula can greatly improve the accuracy of the data used in any 1D simulation like with Flowmaster. A single empirical formula can fail to capture all of the details and differences within a detailed engineering design. As can be seen in Figure 4, there are many complex details in the engine geometry and in its consequent performance results that a single formula cannot capture.

The perceived advantage of the empirical formula is that it takes less than half an hour to develop. However, in the amount of time it takes to look up the formulas, a model could be setup and a run initiated in FloEFD. From there it is only a matter of a few days of computing time to create the data

from the 3D simulation. A trade off that is well worth it for the vast improvement in accuracy. Since FloEFD is embedded within most CAD tools, any design changes to the engine and block make it easy to capture the performance changes. If there are any changes to the engine or block, the 3D simulation could be re-run with no additional setup, thereby keeping the data current. This allows the engine and block to be developed concurrently with the 1D simulation.

As we follow along this analysis method we will see a difference in the 1D modeling. A follow-on paper is expected to be delivered that highlights the differences in the 1D analysis.

Reference:

[1] SAE 2013 World Congress
"Characterizing Thermal Interactions Between Engine Coolant, Oil and Ambient for an Internal Combustion Engine"
Sudhi Uppuluri, Computational Sciences Experts Group; Joe Proulx, Mentor Graphics; Boris Marovic, Mentor Graphics (Deutschland) GmbH; Ajay Naiknaware, CSEG, LLC

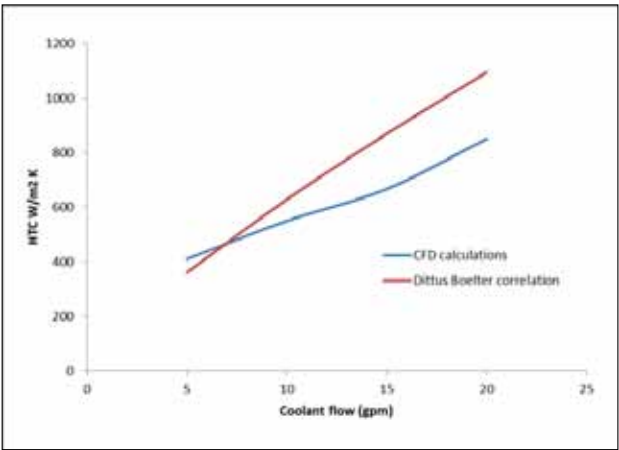


Figure 3. Comparison Chart of Empirically Derived and 3D Simulation Derived Heat Transfer Coefficient.

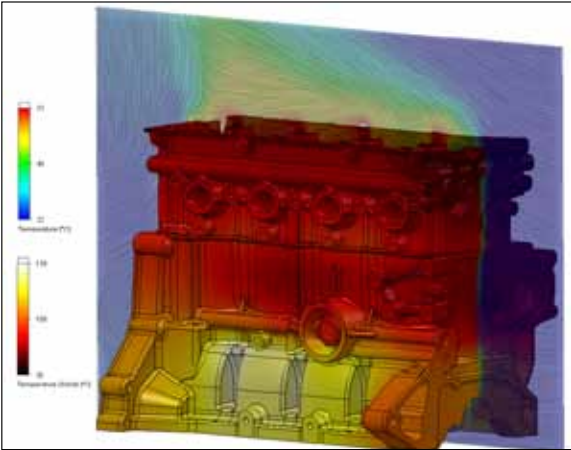


Figure 4. Surface Plot of Temperature from 3D Simulation

Megawatt Engines need Mega Cooling

By Boris Marovic, Mentor Graphics

The thought of a 20 megawatt electric engine is mind blowing; especially when you consider most road car engines are a mere 120 kW. A 90 ton, 20 meter long Eurosprinter that is capable of reaching speeds of up to 230km/h only uses 6.4 MW in its four electric motors. So when considering a 20 MW engine, in an oil or gas compressor for instance, one has to marvel at its power. An engineer however must concern himself with how to keep this monster cool.

E-Cooling GmbH in Berlin is an engineering consultancy founded by Karim Segond. Their expertise lie in providing 3D thermal and flow analysis, enhancement and development supporting electronics, electric engines, and power electronics. When E-Cooling began working on 20 MW

motors it was evident that traditional CFD was not up to the job of meshing their complex geometries. Karim undertook the task of finding an approach that could handle complex geometries, wasn't too laborious but still delivered quality results, "The pre-processing with traditional CFD tools is much too slow for the simulation of large complex machines. I decided to look for a better solution that would solve my problems faster. I was specifically looking for software that can mesh such models with a Cartesian mesh and found FloEFD™. "E-Cooling's ethos is to provide detailed, accurate data to their clients at a reasonable cost, therefore the amount of man-hours used to mesh complex geometries is a big factor to consider for Karim. "The biggest benefits I got from FloEFD was that it was embedded, I



Figure 1. Rotor of a Hydro Generator. Photo courtesy of Hydropower Consult



With thanks to Karim Segond at E-Cooling GmbH
www.e-cooling.de



"The accuracy of FloEFD was always good. It is not easy to measure electric motors that run at very high speeds but FloEFD provided good results when compared to the measurements we received from our customers. FloEFD helped me to work on contracts that involved very complex geometries, such as a stator coil end turn support system, which I wouldn't have been able to do with other CFD software."

Karim Segond, E-Cooling GmbH

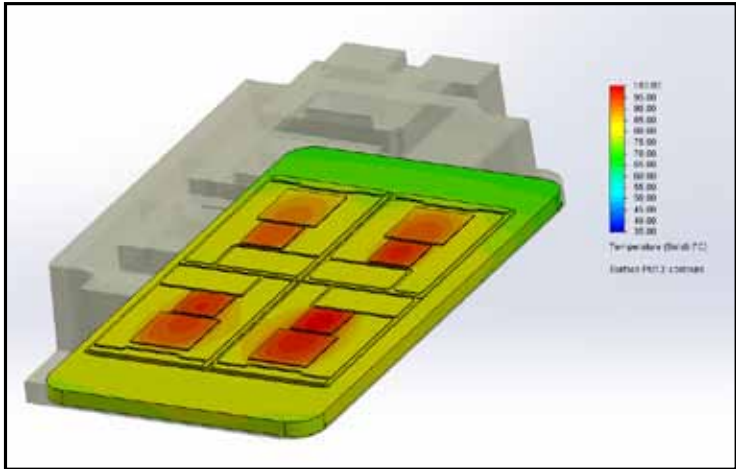


Figure 2. Surface temperatures in an IGBT casing

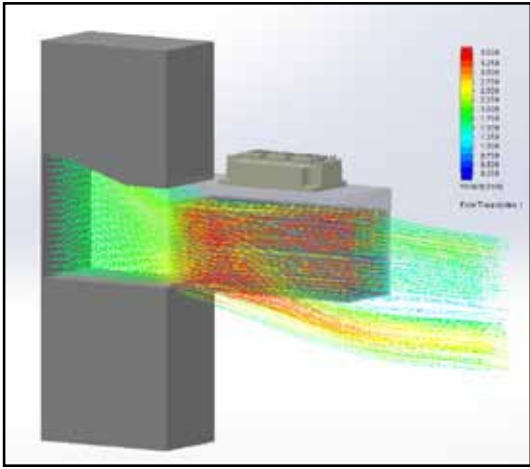


Figure 3. Streamlines through the heat sink of a power module

could work within a CAD system and use parametric CAD models. This made it easier to change any geometry and therefore run several variants very easily. Another point that lifted a heavy burden for me is the automatic meshing, so basically the meshing as I knew it became obsolete and I could spend my time with other things than manually mesh the geometry." Karim is supported by his business partner, Guenter Zwarg, for the thermal management of these mega engines; the expertise of Günter covers almost all types of large electrical motors and

hydro generators. According to Karim, his customers were always very satisfied with his work and the accuracy of the results has not suffered from the comfort of automatic meshing.

Karim is also investigating the thermal management of the power electronics components used to drive such large engines. Karim says "The cooling of power electronics is very important and should be considered as early as the concept stage of the design. Here CFD can be leveraged to optimize the design and ensure the best

possible cooling for the components."

Besides simulations of IGBTs E-Cooling has turned their attention to the overall cooling of a system. Such cooling systems are too big and too complex to simulate with 3D CFD software. Therefore it is necessary to analyze them using a 1D thermal and fluid flow circuit that is modeled in a 1D CFD tool such as Flowmaster®. This combined solution then enables Karim to provide the qualities of both tools and provide the ultimate cooling solution to his customers.

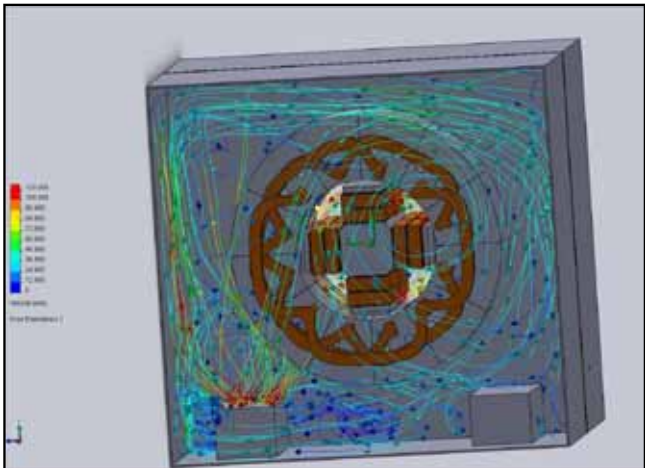


Figure 4. Streamlines of the E-Cooling tutorial electrical motor

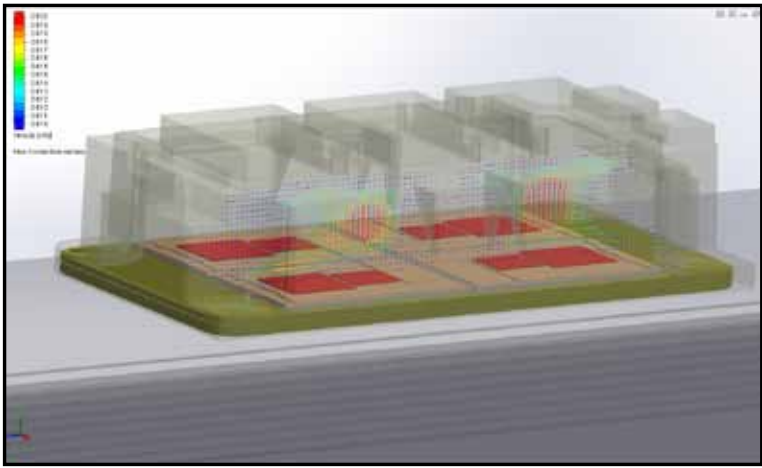


Figure 5. Flow vectors of free convection in the casing of a power module

Lights, Camera, Action!

Grass Valley Video Camera Modeling using FloEFD™

For more than 50 years Grass Valley has been the premier video technology solutions provider that broadcasters and video professionals turn to for imaging, video and media solutions. Grass Valley Netherlands BV develops and manufactures professional cameras for the broadcast market.

Their award winning cameras are a result of their commitment to innovation and performance to camera design and engineering excellence. Their range of system cameras have captured the world's highest profile, most prestigious events as well as local news and public affairs programming.

More Power means more Heat

When it comes to the design of these modular cameras, many factors must be considered as the units consist of the head, which contains sensors and video

processing, and the body that houses the electronics to transmit HD signal back to the studio. As broadcast video cameras consume a lot of power, cooling the camera's electronics is very important, making thermal design critical to any new development.

Grass Valley's latest camera was expected to consume more power, and hence produce more heat, than their existing designs. Grass Valley decided to invest in a Knowledge Transfer Project sponsored by M2i (Material Institute for Innovation), to investigate the use of virtual prototyping to optimize the thermal design. The project was supervised by B.V. Ingenieursbureau H.E.C. (HEC), who recommended using a CFD modeling tool such as FloEFD™. The 3D fluid flow and heat transfer analysis tool would be able to provide the insight necessary to ensure the best possible design.



Figure 2. Baseline model of existing camera

Analysis & Results

To gain proficiency and confidence in the simulation technology, HEC advised Ir. E. Schmit, the Mechanical Architect working on the project to first build a model of an existing camera.

With just three days of training from HEC, and under their guidance, Ir. Schmit was able to use FloEFD Embedded within their PTC Creo CAD system to build a model of Grass Valley's LDK 8000 Elite WorldCam Multi-Format HD Production Camera, for which experimental prototype test data was available.

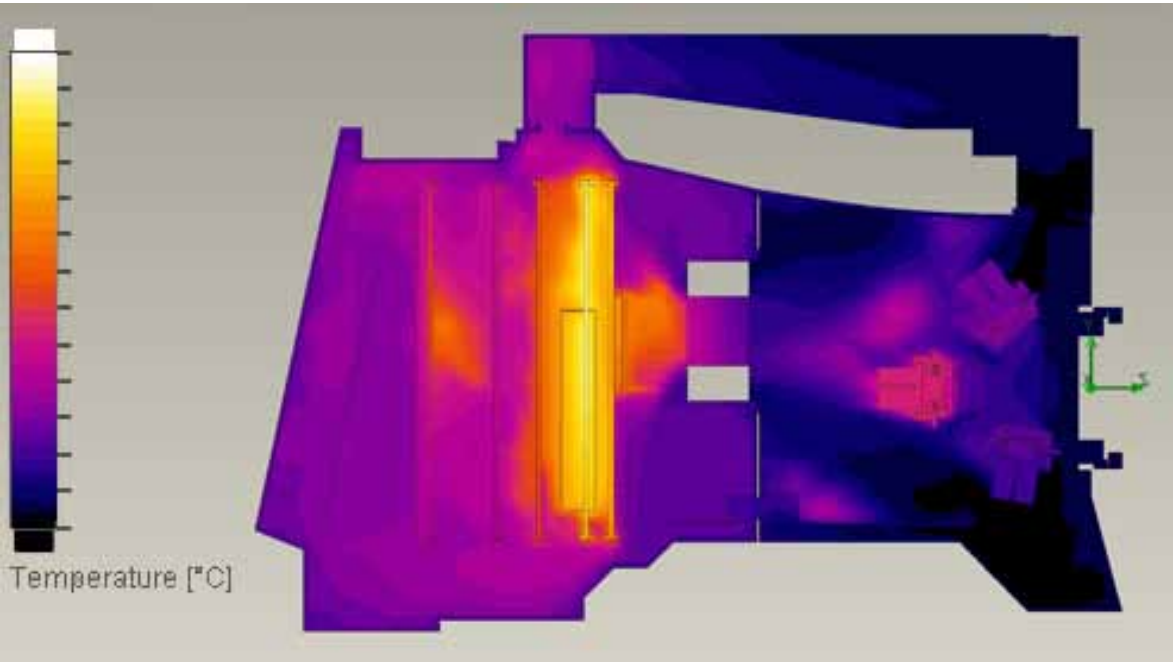


Figure 1. FloEFD results closely matching experimental data



"Working with FloEFD I had a very positive experience. It is a user-friendly package that is fully integrated into our development software - ProEngineer Creo. It has a very intuitive interface and offers many opportunities to produce insightful results. We have much more insight into the heat flow within the camera and have been able to make a number of changes to the design very early in the project that would have taken much more time to make later on. I think it's well worth the investment and we will certainly use FloEFD in future projects." - Ir. E. Schmit, Mechanical Architect at Grass Valley Netherlands BV

The temperatures observed in the simulation (Figure 1) were found to be in close agreement with the measured values for this camera, showing less than 10% variance. The total airflow through the camera was even closer to the measured value, <5%. Ir. Schmit was also able to estimate the noise level produced by the fan with a rule of thumb based on the differential pressure and flow through the fan, this also proved to be closely matched to the results created in FloEFD.

In addition, FloEFD provided numerous amounts of simulation data that would be very difficult to get from a physical prototype. Data such as the distribution of the total air flow through each vent, the pressure differential across the fan, the fan flow rate and of course the direction and temperature of the air flows within the camera. These data results were used to make predictions of how the new design would perform. Based on the simulated model, a number of five design iterations were used to improve the cooling concept, finally resulting in the optimal design.

Having successfully completed the Knowledge Transfer Project, Grass Valley Netherlands BV have now been able to make FloEFD an integral part of their product development process.

Acknowledgements:

Grass Valley www.grassvalley.com
B.V. Ingenieursbureau H.E.C.:
www.hecbv.nl
M2i (Material Institute for Innovation):
www.m2i.nl



The Family Business: How to be a World Champion

Kristan Bromley
relies heavily
on the help and
support of a
number of people
to keep him at
the sharp end of a
sport that affords
little room for error

Most sporting events can be broken down to simple phrases that belie the effort and skill and dedication required to perform them in any meaningful sense: "defend yourself at all times"; "get the ball in the back of the net"; "get to the bottom faster than everyone else". Expanding the latter even a little and the picture begins to get substantially more complicated. The ability to beat the competition is going to be a function of physical conditioning, technique (lest all your conditioning be wasted) and finally how well fitted your equipment is to you and the task at hand. When fractions of a second can cover the whole field, two out of the above three isn't going to be good enough. Now consider that any one of them is a topic that can – and does – fill volumes of research by itself.

When considered in this light, it doesn't seem accurate for any sport, let alone the Skeleton, to be considered an individual event in any meaningful sense. So it is that Kristan Bromley relies heavily on the help and support of a number of people to keep him at the sharp end of a sport that affords little room for error, somewhere he's been for an impressive 13 years.

Gym sessions are monitored closely by a dedicated conditioning coach and followed up by intense physiotherapy to help his body recover in time for the next session. Push track sessions are assisted by sports psychologists and more coaching staff all aiming to ensure that the gains made in the punishing fitness and strength sessions are converted to shedding the fragments of time that make for medals.

But Skeleton is very much a family affair for Kristan: his fiancée is current world champion and fellow Bromley development rider, Shelley Rudman, and Bromley Technologies was co-founded with brother, Richard. Making a family enterprise work is a notoriously delicate process, but get it right and the pay-off is far greater than a bit of mutual understanding over the number of evenings or weekends sacrificed, or gym bags full of laundry generated. The depth of understanding and sometimes brutal honesty that can exist between people who are close can of course lead to explosive disagreements, but when managed correctly there exists a structure that lends itself to quick decision making and the basis of a powerful and committed support network.



The Bromley Family (left to right)
daughter Ella, Kristan Bromley, fiancée
Shelley Rudman, mother Mavis, brother
Richard and father Ray.



Richard Bromley has been shouldering the burden of taking feedback from Kristan as a development rider and converting it and test and simulation data in to faster sleds for 14 years now. However, this focus is as much about a dedication to Bromley Technologies as it is about getting his brother on to the top step of the podium, and Kristan wouldn't have it any other way "Shelley and I are development riders for Bromley. It's more accurate to think of us as being sponsored by Bromley Technologies, rather than it working for us." This subtle distinction between having a brother and a shared company working for you and your medal ambitions and you being one of the test pilots for that same company is a very important one. The former set up could quickly become self-absorbed, irrelevant and ultimately insolvent, while the latter can thrive on the competitive spirit and in fact be more competitive precisely because it has broadened its outlook.

That's certainly how Kristan sees it "The success [Shelley and I have had] is down to maintaining a focus on finding a competitive edge through the innovation in our products." Thus the wheel of innovation turns for Bromley: the risk taking on the part of the development riders generates success on the track for Bromley equipped riders, which in turn generates new business



Bromley Technologies Founders: Kristan Bromley (left), & brother Richard Bromley (right)

for the company and therefore the ability to invest in further innovation. Bromley Technologies is supported by its development riders who work on behalf of their customers, a job best accomplished by trying to claim the top step of the podium themselves. Considered in these terms, it's difficult to know if it's more accurate to say that the success of Kristan and Shelley on the track is due to their relationship with Bromley Technologies, or that Bromley Technologies is a successful venture due to the ambitions of its development riders. It may even be that this blurring over who is offering the support to who is the greatest success of the Bromley brothers story.

The Road to Sochi 2014

Engineering Edge caught up with Richard Bromley to ask how the recent test session in Norway went for the team. "Norway was mainly about aerodynamic testing" explains Richard "the last 1/3 of the track is pretty fast and we know it so well that we can then separate out the aero gains from any other factors." This is ahead of St. Moritz World Championships the longest track on the circuit where aero gains are a major consideration. "We know our baseline CFD model matches well with the wind tunnel data, so we can have confidence that the trends we see in simulation as a result of any enhancements are genuine ones."

And so it proved to be in Norway, with each enhancement demonstrating an incremental improvement in performance. Such testing is about more than simply re-enforcing confidence in simulation though (although the author feels obliged to say that the CAE engineer who loses their sceptical side is on a slippery slope; no pun intended). One thing CFD can't do is predict how a given chassis modification will feel to the athlete, "the CFD will only tell us what's aerodynamically more efficient, but we also need to know how the resultant changes affect the athlete: they need to be able to hold their position or control the sled comfortably for it all to be worthwhile."

It's back to HQ now to post-process the results further, ensuring that every last bit of data is extracted from the hard weeks put in on the track, before adding the results to the already considerable library built up on their home track.



The XXII Olympic Winter Games

- 6850 Olympic and Paralympic athletes from 33 nations will compete in the 16 day event
- The Winter Olympic Games are made up of 15 sport disciplines of seven sports including Biathlon, Bobsleigh, Curling, Ice Hockey, Luge, Skating, and Skiing
- The Paralympic Games are made up of 1350 athletes competing in Alpine Skiing, Biathlon, Cross-Country Skiing, Ice Sledge Hockey, and Wheelchair Curling
- Bobsleigh is a winter sport invented by the Swiss in the late 1860s in which teams make timed runs down narrow, twisting, banked, iced tracks in a gravity-powered sled
- Skeleton racing involves plummeting head-first down a steep and treacherous ice track at 90mph on a tiny sled. It is considered the world's first sliding sport
- Curling is also known as 'The Roaring Game', it's nickname originating from the rumbling sound the 19.96kg granite stones make when they travel across the ice
- The ringing of cow bells during downhill skiing stems from the French tradition of scaring off the abominable snowman (l'homme terrible de froid) rumored to wander snow covered mountain valleys

Understanding Plume Dispersion

Predicting the External Aerodynamics of Cooling Towers using CFD

By Dr. Andrey Ivanov &
Dr. Svetlana Shtilkind



Figure 1. Natural Draft Wet Cooling Towers

Cooling towers are an integral part of power and chemical plants. Their primary function is to reject heat into the atmosphere as a relatively inexpensive and dependable means of removing low-grade heat from cooling water.

Cooling towers are characteristically tall, large, lightweight structures that are very sensitive to wind loads that can pose some problems to structural design. The design however, is not without purpose. In the case of Natural Draft Wet Cooling Towers (see Figure 1) these design features allow heated water to be evenly distributed through channels and pipes above the fill. As the water flows and drops through the fill sheets, it comes into contact with the rising cooler air. Evaporative cooling occurs and the cooled water is then collected in the water basin to be recycled into the condenser. The difference in density of the warm air inside and the colder air outside creates the natural draft in the interior. This upward flow of warm air leads to a continuous stream of fresh air through the air inlets into the tower.

Comparing Actual vs. Virtual

Following the collapse of three cooling towers at the Ferrybridge Power Station in Yorkshire, UK in 1966, these wind-sensitive structures have undergone numerous costly wind tunnel testing. These tests seek to identify those pressure distributions that lead to extreme key stress dominating the design of the tower. Wind tunnel tests and numerical investigations are generally used to obtain the wind-induced pressure coefficient distribution on outer and/or inner surfaces of cooling towers under specific surrounding or operating conditions.

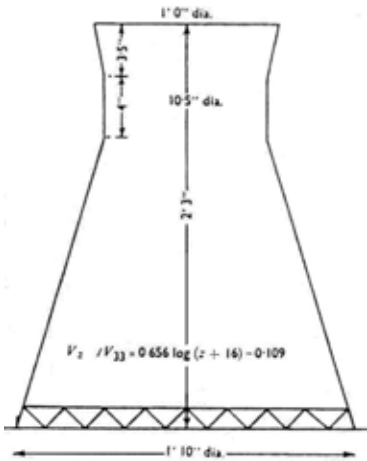


Figure 2. Cooling Tower Geometry

Geometrical Parameters	Units	Value
Overall height	in	27.0
Base diameter	in	22.0
Throat diameter	in	10.5
Top diameter	in	12.0
Cylindrical throat height	in	4.0
Upper truncated cone height	in	3.5
Air Flow Properties		
Temperature	K	293.2
Pressure	atm	1.0
Reference velocity V_{33}	m/s	103.9
Friction velocity U_*	m/s	7.86
Reynolds Number		$\approx 6.0E6$

Table 1. Cooling Tower Parameters and Flow Conditions

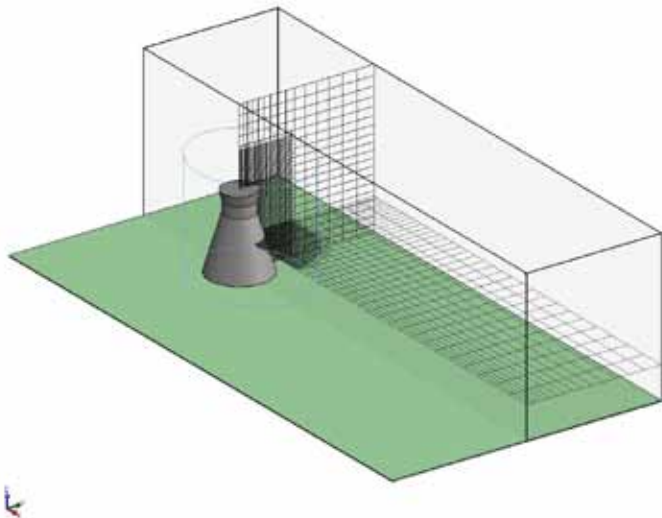


Figure 3. Computational Mesh Topology

In this given situation, the use of Computational Fluid Dynamics (CFD) can be regarded as an extremely useful tool in being able to predict cooling tower aerodynamic characteristics. Using a tool such as FloEFD™ to analyze the flow around the cooling tower could avoid costly wind tunnel tests and provide reliable data for practical structural design changes.

Setting the Parameters in CFD

To create the model in FloEFD the following parameters were set; the hyperbolic shape of a cooling tower shell is approximated by a short cylindrical throat joined onto two truncated cones, as can be seen in Figure. 2. Considering the structure is

symmetrical, boundary conditions were used to mesh half of the tower. The shell surface is relatively smooth and the cooling tower base aperture was treated as sealed. The cooling tower was defined by the geometrical parameters given in Table 1. All presented parameters as well as experimental data were taken from the wind tunnel experiments of Cowdrey and Neil; Salter and Raymer; and Zdravkovich [1-3].

The kinetic energy of turbulence and its dissipation rate profiles in the approaching flow correspond to those of the neutral atmospheric conditions. Figure 3 below shows the computational mesh topology in FloEFD.

The Results

It is worth noting that all calculations presented below were performed as stationary ones. Usually this took 500-600 iterations to get to the converged solution. Figures 4 and 5 demonstrate the comparisons of predicted and measured C_p distributions at $Z/H=0.79$ and at $Z/H=0.43$, respectively.

From almost all angles it can be concluded that the predicted results compare very well with the experimental. Predicted C_p distribution with elevation in the rear side of the structure also show excellent correlation with the experimental data (see Figure 6 overleaf).

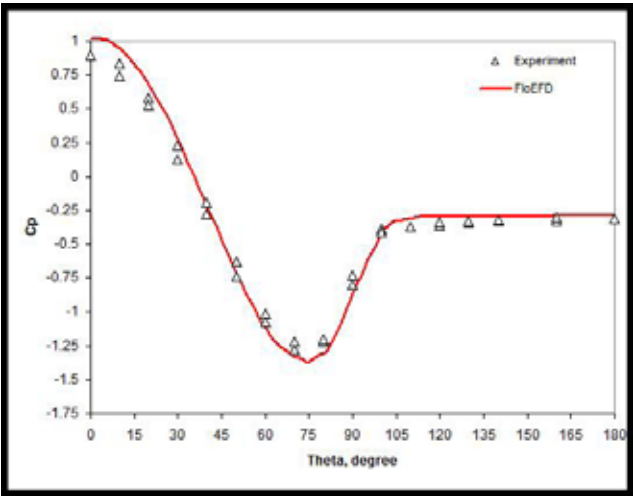


Figure 4. C_p distributions at elevation $Z/H=0.79$

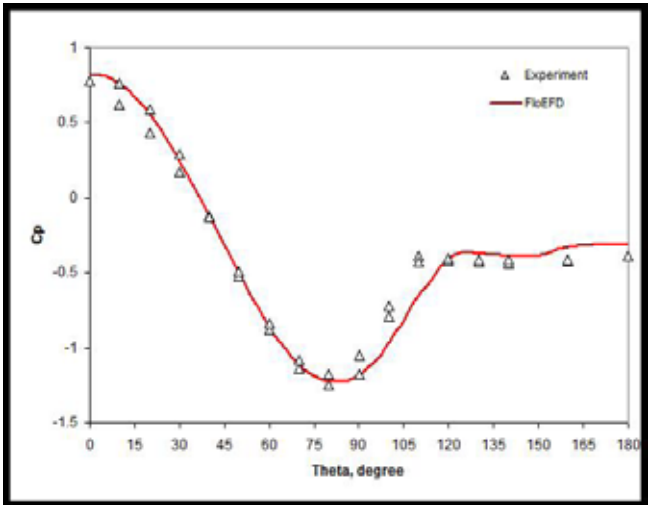


Figure 5. C_p distributions at elevation $Z/H=0.43$

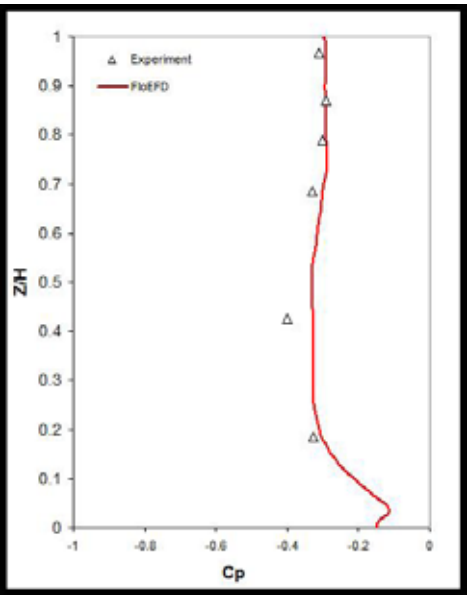


Figure 6. Cp distributions with elevation in rear side of the cooling tower (theta=180)

FloEFD can be used for complex multi-physics calculations including water vapor plume dispersion along with condensation and evaporation processes. Figures 8 – 10 demonstrate the results of the predicted visible saturated vapor plume formations complicated by a number of interesting associated physical processes.

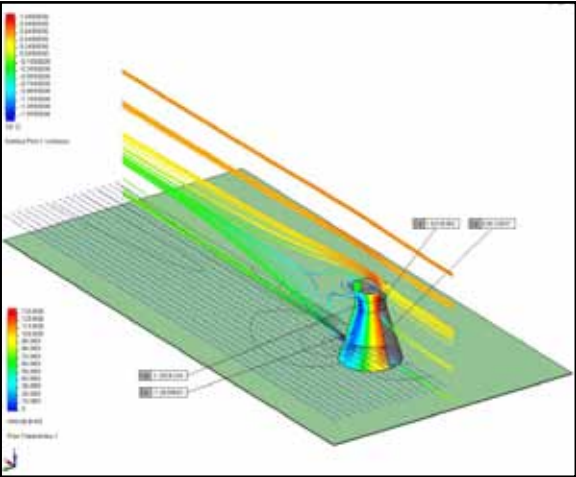


Figure 7. Cp distribution on the cooling tower shell along with flow trajectories (colored by velocity magnitude) in symmetry plane

Conclusions

Whilst it is clear that FloEFD has successfully validated the problem of predicting the external aerodynamics of cooling tower structures. This article also demonstrates its capability to accurately simulate complex multi-physics processes that occur in wet cooling tower plume. FloEFD's numerical approach can be used as a very cost effective method of evaluating cooling tower environmental impact before very costly wind tunnel or nature experiments are carried out.

References:

[1] Cowdrey, C.F. and O'Neill, P.G.G. Report of tests on a model cooling tower for CEA: pressure measurements at high Reynolds numbers. Nat. Phys. Lab., Aero. Rep. 316a, 1956.
 [2] Salter, C. and Raymer, W.G. Pressure

measurements at high Reynolds number on a model cooling tower shielded by second tower. Nat. Phys. Lab., NPL Aero. Rep. 1027, 1962.
 [3] Zdravkovich, M.M. Flow around circular cylinders. Vol. 2: Applications. Oxford University Press, 2003.

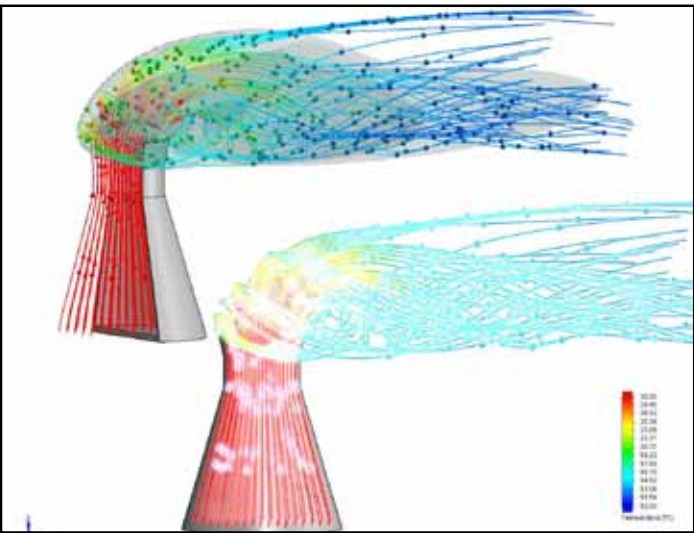


Figure 8. Condensate mass fraction isosurface with a value of 10-4 (wet plume visibility limit) with flow trajectories colored by temperature magnitude

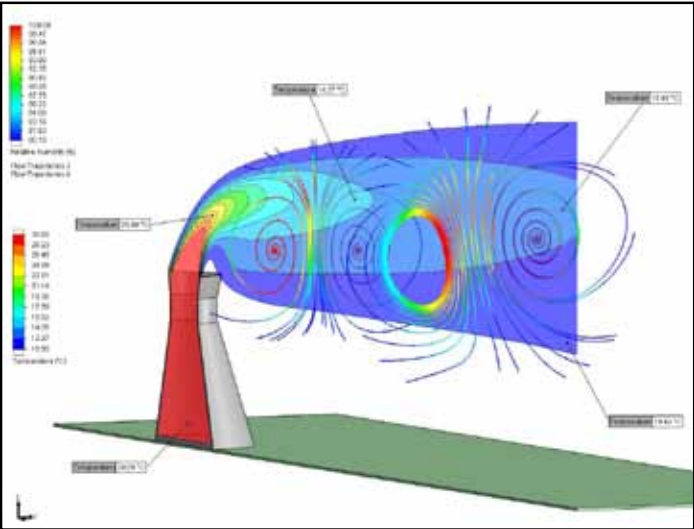


Figure 9. Temperature distribution in vertical symmetry plane with flow trajectories drawn in two lateral downstream sections and colored by relative humidity magnitude

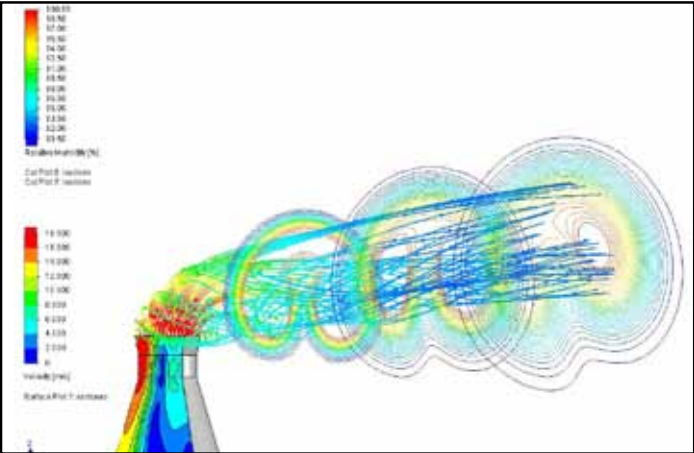


Figure 10. Velocity distribution on cooling tower shell with flow trajectories colored by temperature magnitude and relative humidity contours in three downstream cross-sections

Benchmarking takes off for NASA CRM & Tupolev Tu-214

FloEFD™ Simulation of External Aerodynamics

By Tatiana Trebunskikh & Andrey Ivanov, Mentor Graphics

External aerodynamics is a theoretical basis for aerospace technology, and aerodynamic calculations of modern aircraft and other vehicles. This branch of hydro-gas dynamics is becoming increasingly important in modern life due to the development of a new generation of commercial and military aircraft and unmanned aerial vehicles. CFD simulations in this area now play a very important role. Panel and other methods for preliminary estimates are still useful but a modern CFD approach allows for more accurate results and better information on vehicle performance, earlier in the design cycle.

FloEFD™ has been successfully used to simulate external aerodynamics in various studies, ranging from aerofoils to whole aircraft modeling, for physically feasible range of Reynolds numbers including subsonic, transonic and supersonic cases. Compared to a traditional CFD approach, FloEFD arrives at valid results with ease. There are also several additional mathematical models employed in FloEFD for detailed analysis. These are a unique model of laminar/turbulent transition, and also an innovative and effective model of boundary layer. FloEFD offers various methods for visualization of results, allowing the investigation of a complex 3D flow structure and presenting aerodynamic parameters in an understandable form.

Two models of aircraft will be discussed in this article. The first is the NASA Common Research model in the wing/body/horizontal-tail configuration and the second one is the Russian commercial aircraft Tu-214. The main purpose of this investigation was to obtain aerodynamic

characteristics of the vehicles such as lift, drag, pitching moment coefficients and pressure coefficient which were compared with experimental data.

The external flow simulation around the wing/body/horizontal-tail configuration of the NASA CRM with focus on aerodynamic coefficients is presented here. The genesis of an open geometry NASA CRM was motivated by a number of interested parties asking NASA to help develop contemporary experimental databases for the purpose of validating specific applications of CFD [1]. A transonic supercritical wing

design is developed with aerodynamic characteristics that are well behaved and of high performance for configurations with and without the nacelle/pylon group. The horizontal tail is robustly designed for dive Mach number conditions and is suitably sized for typical stability and control requirements. The fuselage is representative of a wide body commercial transport aircraft; it includes a wing-body fairing, as well as a scrubbing seal for the horizontal tail. The model of the NASA CRM is presented in Figure 1.

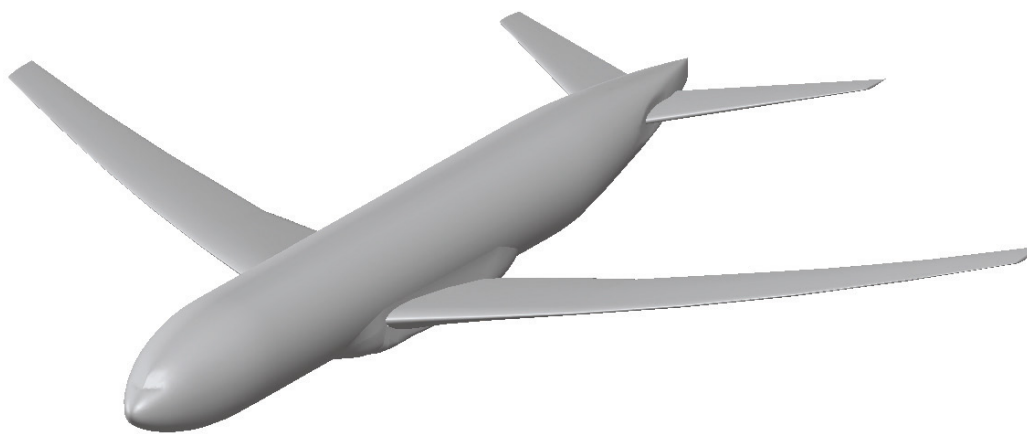


Figure 1. The model of NASA CRM

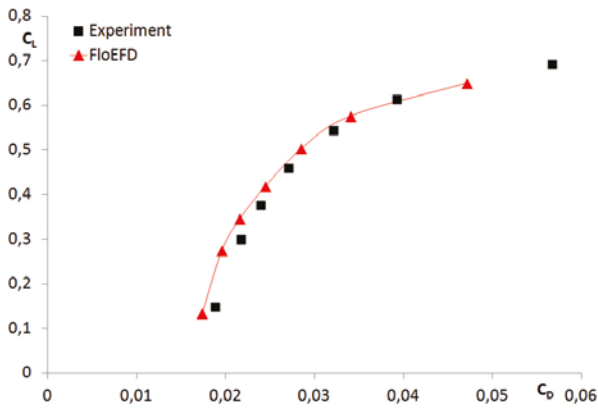
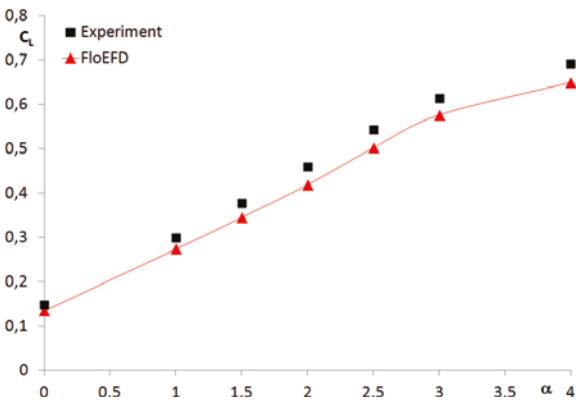


Figure 2. Lift coefficient (left) and polar (right) of NASA CRM

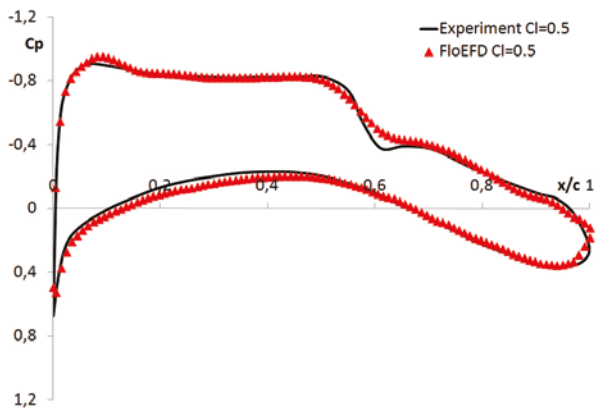
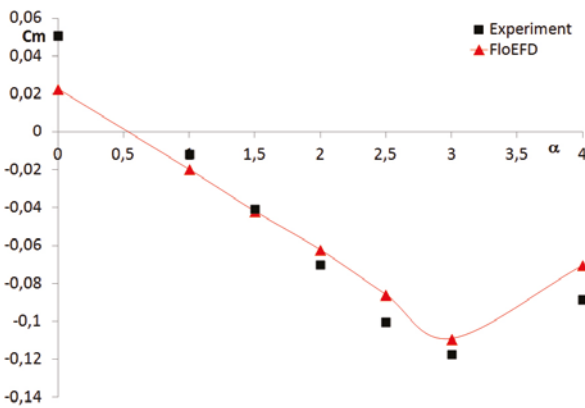


Figure 3. Pitching moment coefficient (left) and chordwise pressure coefficient distribution at 49.9% semispan (right) of NASA CRM

Calculations were provided at the following far field conditions: $M = 0.85$, $P_\infty = 201300$ Pa and $T_\infty = 210.9$ K. The angle of attack varies in range from 0° to 4° . The best results were obtained on the model with local mesh around the aircraft and several refinements during calculation by Solution Adaptive Refinement (SAR) technology in FloEFD. Attention should be paid to fine mesh resolution in the neighborhood of wing leading edge.

Lift coefficient, polar, pitching moment coefficient and chordwise pressure coefficient distribution at 49.9% semispan were obtained from calculations and experiments [2] and are presented in Figures 2 and 3. Good FloEFD prediction of the lift and drag coefficients in linear area were achieved. For pitching moment coefficient, discrepancy is bigger. Also there is some insignificant departure in C_p between calculation results and experiment. The pressure distribution with flow trajectories colored by Mach number at $M = 0.85$ and angle of attack 4° is displayed in Figure 4.

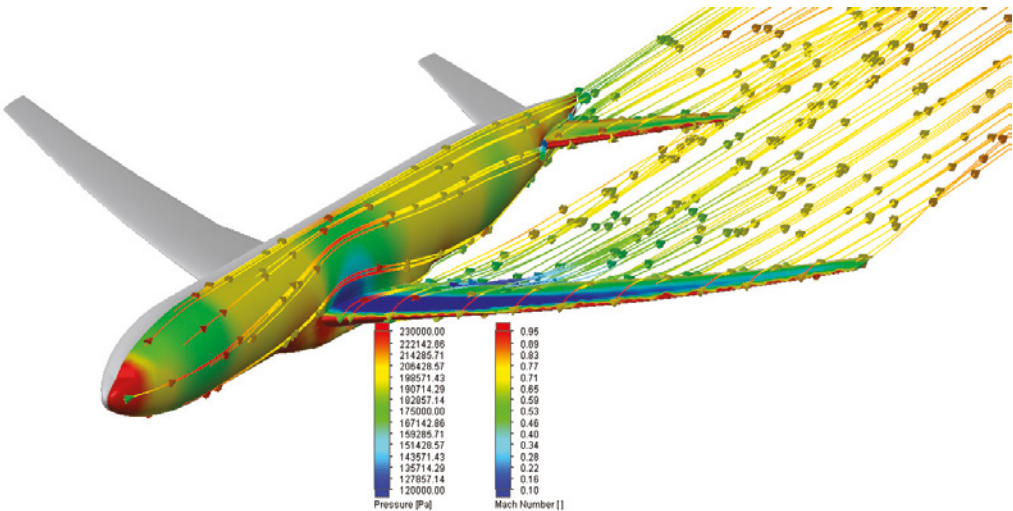


Figure 4. Pressure distribution with flow trajectories colored by Mach number at $M = 0.85$ and angle of attack 4° of NASA CRM



Figure 5. The model of Russian commercial aircraft Tu-214

The second aircraft which is considered here is the Russian commercial aircraft Tupolev-214 (Tu-214) developed by well-known Russian Aircraft Design Bureau PSC 'TUPOLEV' (Figure 5). This vehicle is a cantilever monoplane of a normal scheme with a low-set swept wing and a tail assembly placed on a fuselage with two turbojet engines mounted on pylons under the wing.

The Tu-204/214 was designed as a family of aircraft incorporating passenger, cargo,

combi and quick-change variants and relates to a fourth generation of aircraft which have a higher level of reliability and fuel efficiency [3]. For developing this family of aircraft the latest science and technological developments in aerodynamics, strength, propulsion engineering, materials, electronics and ergonomics were applied.

Calculation of this task was provided at the following far field conditions: $M = 0.6$, $P_{\infty} = 101325 \text{ Pa}$ and $T_{\infty} = 288.15 \text{ K}$. The angle of attack varies in range from -3° to 18° . Work of the propulsion system was taken into

account in these investigations. The FloEFD predictions align with the wind tunnel's tests of the Tu-214 aircraft scale model. Comparison was made with respect to integral parameters such as lift coefficient and drag coefficients, etc. All of these parameters were compared with experimental data.

Lift coefficient and polar are presented in Figure 6. It should be pointed out that good FloEFD prediction of these coefficients were achieved at Mach number

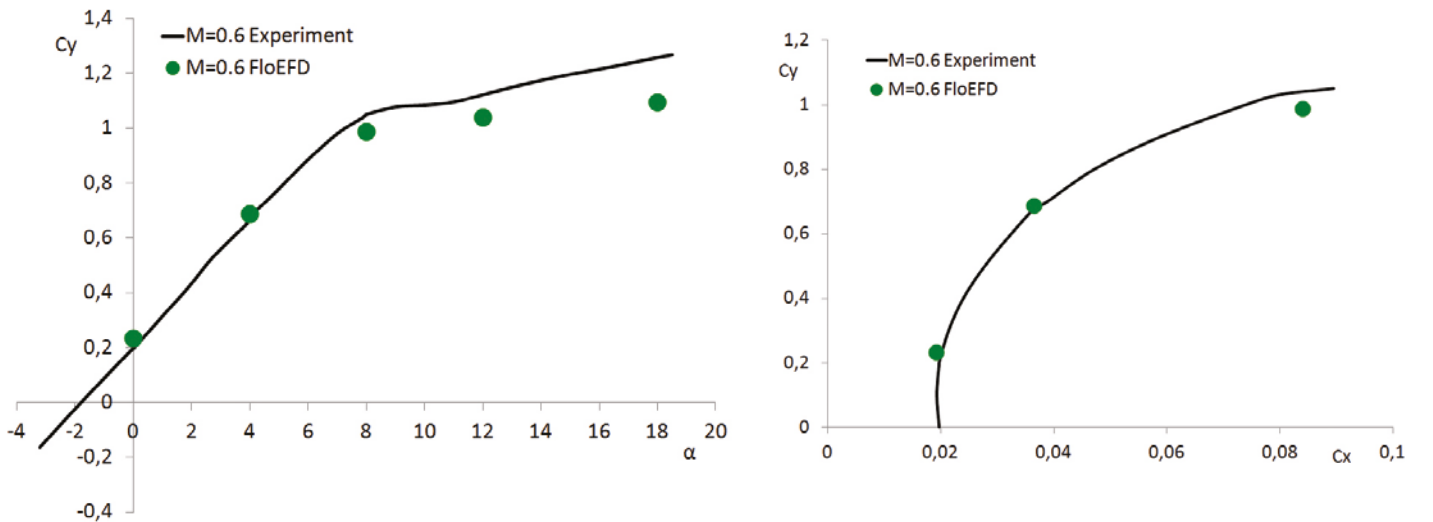


Figure 6. . Lift coefficient (left) and polar (right) of Tu-214 (results were provided by PSC TUPOLEV)

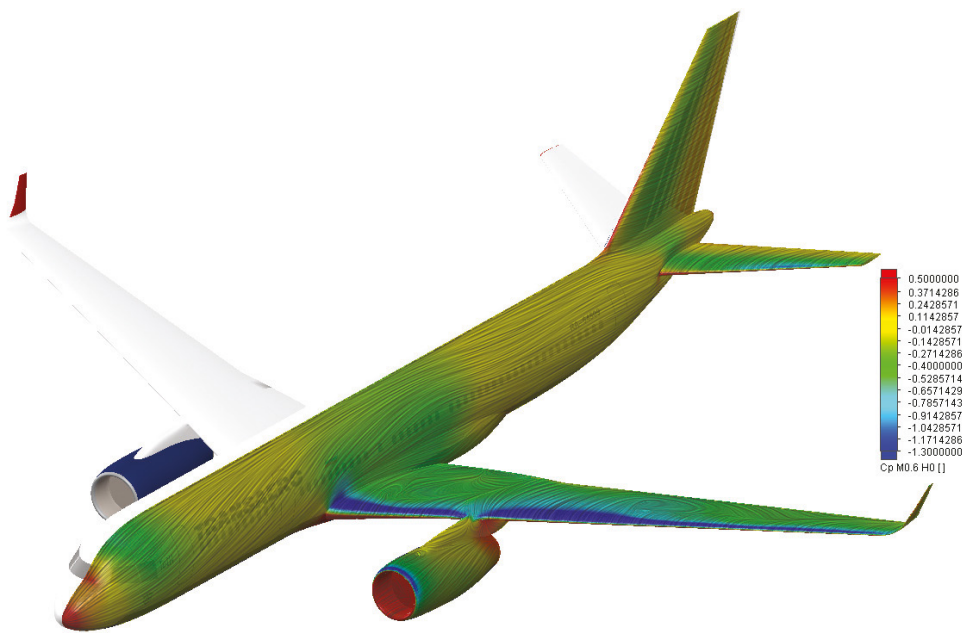


Figure 7. Pressure coefficient distribution with LIC at $M=0.6$ and angle of attack 10° of Tu-214 (results were provided by PSC TUPOLEV)

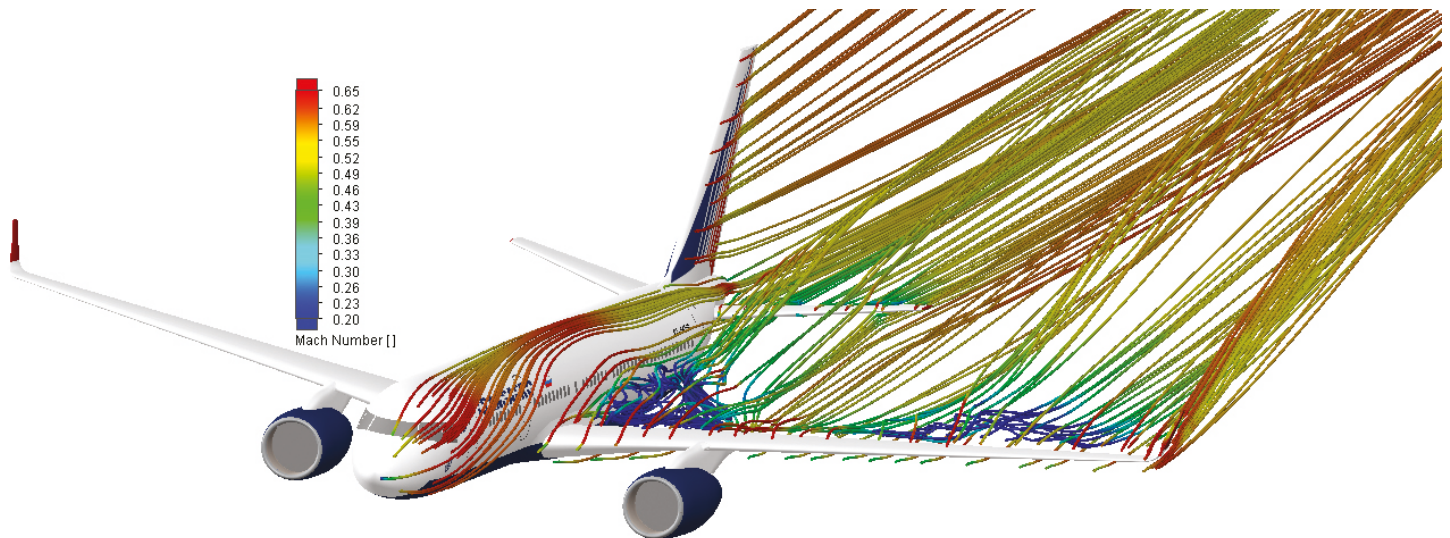


Figure 8. Flow trajectories colored by Mach number at $M=0.6$ and angle of attack 10° of Tu-214 (results were provided by PSC TUPOLEV)

under study. There is also agreement in aerodynamic derivative obtained in FloEFD and experiments with a discrepancy of approximately 1.7%. Pressure coefficient distribution with LIC in FloEFD at $M=0.6$ and angle of attack 10° is presented in Figure 7 as oil flow lines. Using LIC technology allows for good observation of clear flow structures near the aircraft's surfaces.

Comparison of measured and predicted values of the main integral parameters such as lift, drag and pitching moment coefficients show agreement for the

investigated class of tasks. Thereby FloEFD yields a series of 'what-if' aerodynamic analyses. It should be pointed out that FloEFD provides export of pressure and temperature as loads for structural analysis, on a structural mesh in NASTRAN format directly, allowing automatic parameter changes rather than a manual approach.

References

1. J.C. Vassberg, M.A. DeHaan, S.M. Rivers, and R.A. Wahls, "Development of a Common Research Model for Applied CFD Validation Studies", AIAA Paper 2008-6919, AIAA Applied Aerodynamics Conference, Honolulu, USA, August, 2008
2. 4th AIAA CFD Drag Prediction Workshop: <http://aaac.larc.nasa.gov/tsab/cfdlarc/aiaa-dpw>.
3. Koshcheev A.B., Platonov A.A., Khabrov A.V. Aircraft aerodynamics of the family Tu-204/214. Textbook. M.: Poligon-Press, 2009, 304 p. (In Russian)

The **A to Z** of Breaking a World Water **Speed Record**

It's not every day that a World Record is broken and in speed-sports it's indeed a very rare experience. To do it both safely and cost effectively requires meticulous planning, solid engineering design and quality manufacturing, plus a balance between taking calculated risks versus the accrued speed benefits to be gained.

By Koen Beyers, Voxdale BVBA





Figure 1. Voxdale F2 Speed Boat Design Process - Brainstorm & Conceptual Design (left) Architecture & SDX (center) and Engineering & Optimization (right) - Pro/E, ISDX, AAX, FloEFD

When Voxdale was approached by leading Belgian Speedboat manufacturer, Bernico International, to design an innovative Formula 2 class boat to break the then world record in 2008 and the 100 mph barrier, a new approach was needed. With a combination of PTC CAD/CAE tools, including the 3D CAD-embedded CFD tool FloEFD from Mentor Graphics, we embarked on this challenge.

The rationale behind our approach was simple — F2 Racing Boats are very expensive, and typically there is no time or budget for physical prototyping in any design process. The ideal scenario is to 'build and race' and there is not a 'classic' development path for such a process (for example, an alpha version, a beta version, an O series and a release version...) For Bernico, the success of the design of a new F2 boat would be commercially essential for subsequent sales of 'cruiser' boat sales. Bernico gave us a simple set of target specifications for the new F2 boat:

- 1) 300 HP outboard engine;
- 2) Top speed of 160km/h (~100mph) with an acceleration of 0-100 km/h in six seconds;
- 3) Cruise at 97% 'above water' for good aerodynamics, and
- 4) No rear deck and minimal turbulence in the cockpit.

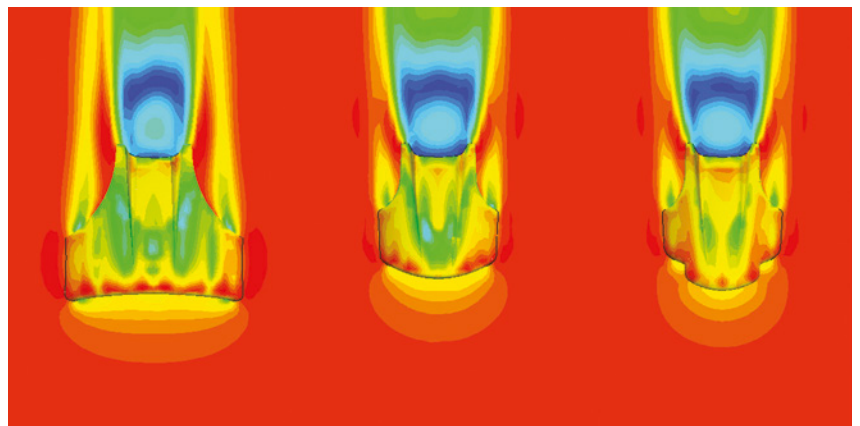
We started the project in early 2009 by taking the then Bernico F2 boat design which could reach speeds of 157.1 km/h (97.6 mph) and 3D scanning the hull and body to reverse engineer the prior design in CAD/CAE as a baseline (see Figure 1). We then did a CFD simulation on the baseline CAD geometry before we could brainstorm several parametric out-of-the-box ideas which we could virtually test in the software

and do some design optimization. With the Pro/Mechanica structural analysis tool we could also conduct concurrent structural analysis of our boat designs to yield the optimal solution which we would recommend to Bernico. Within our familiar Pro/E environment we therefore did complex surface geometry modeling of the boat, mechanical integration and engineering, structural optimization, thermal engine management, light-weight material selection, design for cost and assembly, as well as flow analysis in FloEFD to deal with aerodynamics.

CFD simulation helped us to shave off drag components throughout the new boat's shape. We looked at the boat pilot's helmet shape to produce less flow separation and therefore drag. We used a NACA shaped duct to create an overpressure in the cockpit area so there was less turbulence created, and at the rear deck Splitter and Deflector plate we evolved our aerodynamic design (Figure 2) so there was a positive lift on the rear deck and a low flow separation behind the outboard motor. In total we managed to create a drag reduction from our baseline geometry of 240 N, designed



Figure 2. Evolution of Rear Deck Deflector & Splitter Unit



the boat for a positive torque on the rear deck of 450 Nm and when it was built we managed to get to within 3 km/hr of our predicted top speed. Moreover, our design had better acceleration than we needed and crucially more stability and better 'driveability' than what we started with.

This Voxdale-designed Bernico F2 boat broke through the 100 mph barrier at Coniston Water in the UK's Lake District during the annual Power Boat Records Week on its first outing in November 2009 with a stunning World Record of 103.6 mph or 166.7 km/h (Ref 1). Its excellent naval architecture, functional design, optimized aerodynamics, low fuel consumption and lightweight materials proved to be a successful combination. Bernico quickly commercialized the boat design and a Cruiser edition was made available from early 2010 with three orders being taken on the spot during Coniston Records Week! What did we conclude from this exercise? Some boat designs are hard to test but easy to simulate, and CAD/CFD/CAE simulation certainly stimulates radical innovation and leads to workable solutions that yield performance improvement and ultimately in this case a world record breaking result.

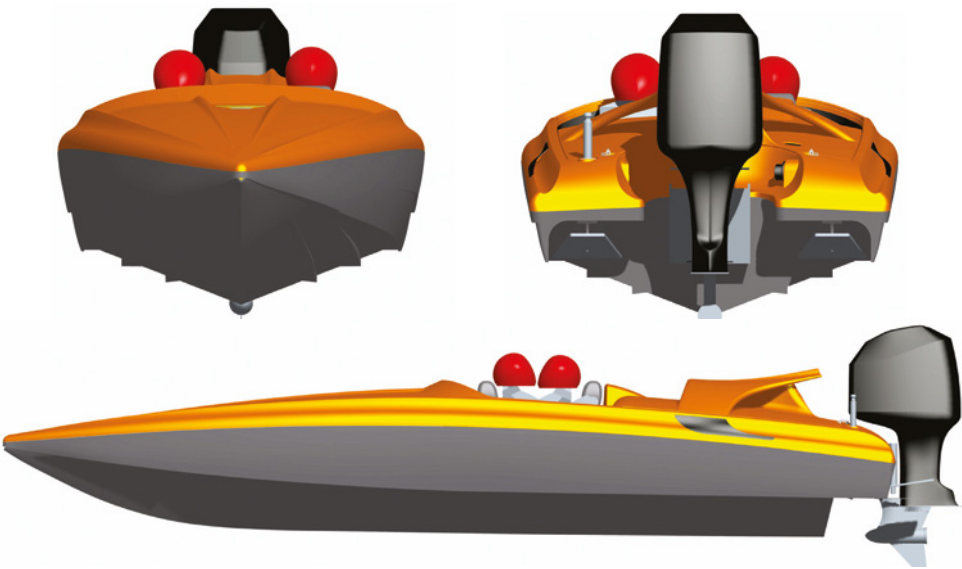


Figure 3. Final Formula 2 Race Boat Design (front, side and rear view)

References & More Information:

- 1) Coniston 2009 Powerboat Records Week Monohull Record Breaking 103mph run's video: http://www.youtube.com/watch?v=_WBggHZaWck
- 2) <http://www.voxdale.be>
- 3) <http://www.bernico.be>
- 4) <https://www.facebook.com/voxdalebelgium>

Figure 4. Record Breaking F2 Bernico Boat on Coniston Water in November 2009 with superimposed hull pressure contours from FloEFD simulation prediction





Optimizing Air-to-Air Refueling Systems

A study of a complex aero air-to-air refueling system

By John Isaac, Business Development Manager, Mentor Graphics



Photo courtesy of Wikimedia: F-15C Eagles from the 67th Fighter Squadron at Kadena Air Base, Japan, refueled by a KC-135R Stratotanker from the 909th Air Refueling Squadron during joint bilateral training with other U.S. forces and the Japan Air Self Defense Force Feb. 25, 2010

In the mil/aero industry, systems are getting more complex and the time/cost to design them getting tighter.

These systems and components may be mechanical, electrical, or a combination of both. A prime example of a complex aero system is the air-to-air refueling system. It contains not only piping for distributing the fuel, but also complex 3D components such as the fueling nozzle at the plane-to-plane connection.

Three approaches are used in the design and analysis process of these systems. One approach is to do the design, produce a physical prototype, test it, change the

design, and then repeat the process, which can be extremely expensive and time-consuming. Another option is to over-engineer, which will result in a safe solution but may be less cost-effective, add weight to an airborne system, and compromise the performance of a system intended to run in a narrow bandwidth.

The third approach, virtual prototyping with computational fluid dynamics (CFD) analysis, early and throughout the design process, can deliver an optimized system at lower cost, and get the system deployed faster.

This approach offers the opportunity for the designer to experiment with multiple design approaches and produce a more optimized design. This is not achievable if each experimental design requires a physical prototype be built and tested.

What Effects Should We Analyze in the System?

Let's assume that we work for an aerospace company that is developing a new refueling system or that we want to analyze some problems with an existing system. In the analysis and subsequent changes to the design, we want to ensure that we have a system that can deliver the following three performance criteria:

- 1) Will my system be able to deliver fuel at an acceptable rate to the receiving aircraft? Basically, will my system flow rate meet specification?
- 2) Will my system deliver fuel to the fighter tanks at an even rate? The fighter has tanks in the wings; and if the rates to the tanks are uneven, one wing will become heavier faster and the fighter will become unstable and may break off from the tanker.

3) If or when the fighter disengages from the tanker, either by plan or in an emergency breakaway, will the water hammer effect on the piping cause excessive pressure surges that may damage the system? I know the maximum pressures my system can tolerate, and the analysis can tell me if I am still well within specification.

So we need a CFD solution that will enable us to analyze these effects quickly. First, let's make changes to the design that I think will solve problems in the system. Then, we will quickly re-analyze with the trial changes that gradually focus in on an optimum design to address all of my specifications.

Choosing the Right CFD Analysis Approach

We have two types of CFD analysis tools at our disposal. One can be used to analyze the piping and could be considered a 1D analysis (i.e., the fuel only flows in the axial direction of the pipes). The other can analyze very complex components where the fuel flow is 3D, such as through the fueling nozzle. What CFD tool do I use to analyze this system, which is clearly a combination of 1D piping and 3D complex components?

The 1D CFD tool is much faster than the 3D CFD but lacks the accuracy when simulating the complex nozzle. However, if we analyze the complete system using only the 3D CFD tool, we may get the accuracy we need but the computer execution time will be excessive, defeating the goal of rapid and multiple experimenting with several design approaches. The best approach would be integrating the 1D and 3D tools and leveraging the advantages of both.

Combining 1D and 3D CFD

We will illustrate how such an integrated system works by using Mentor Graphics 1D system simulator, Flowmaster, and 3D simulator, FloEFD, in our analysis. Figure 2 illustrates how this combined 1D-3D solution works for the refueling system.

Initially, the refueling system designer defines a range of operating boundary values (such as pressure and flow rates), that may be presented to the nozzle. They determine this by understanding typical refueling scenarios, and the complete spectrum of possible conditions the system could deliver under normal and extreme conditions.

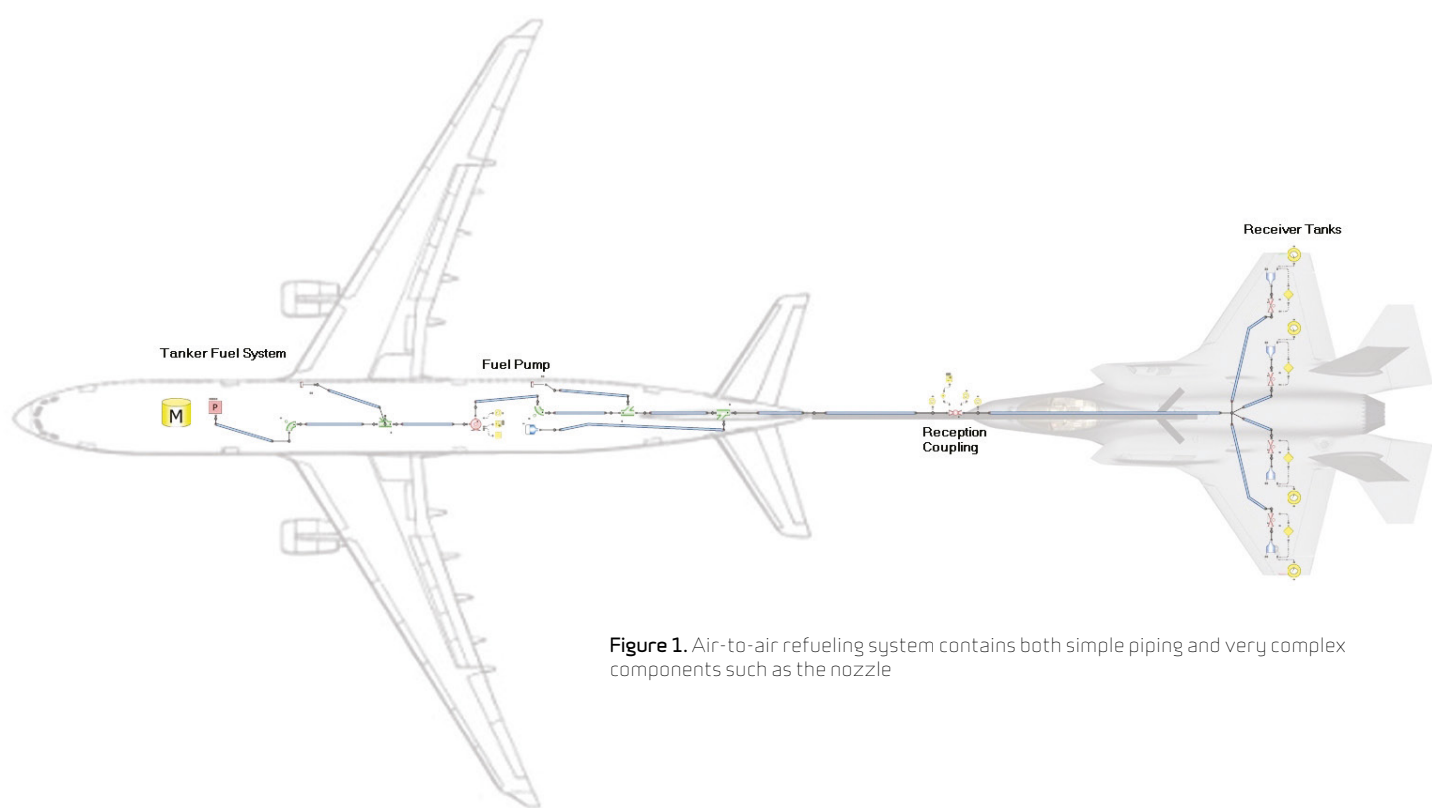


Figure 1. Air-to-air refueling system contains both simple piping and very complex components such as the nozzle

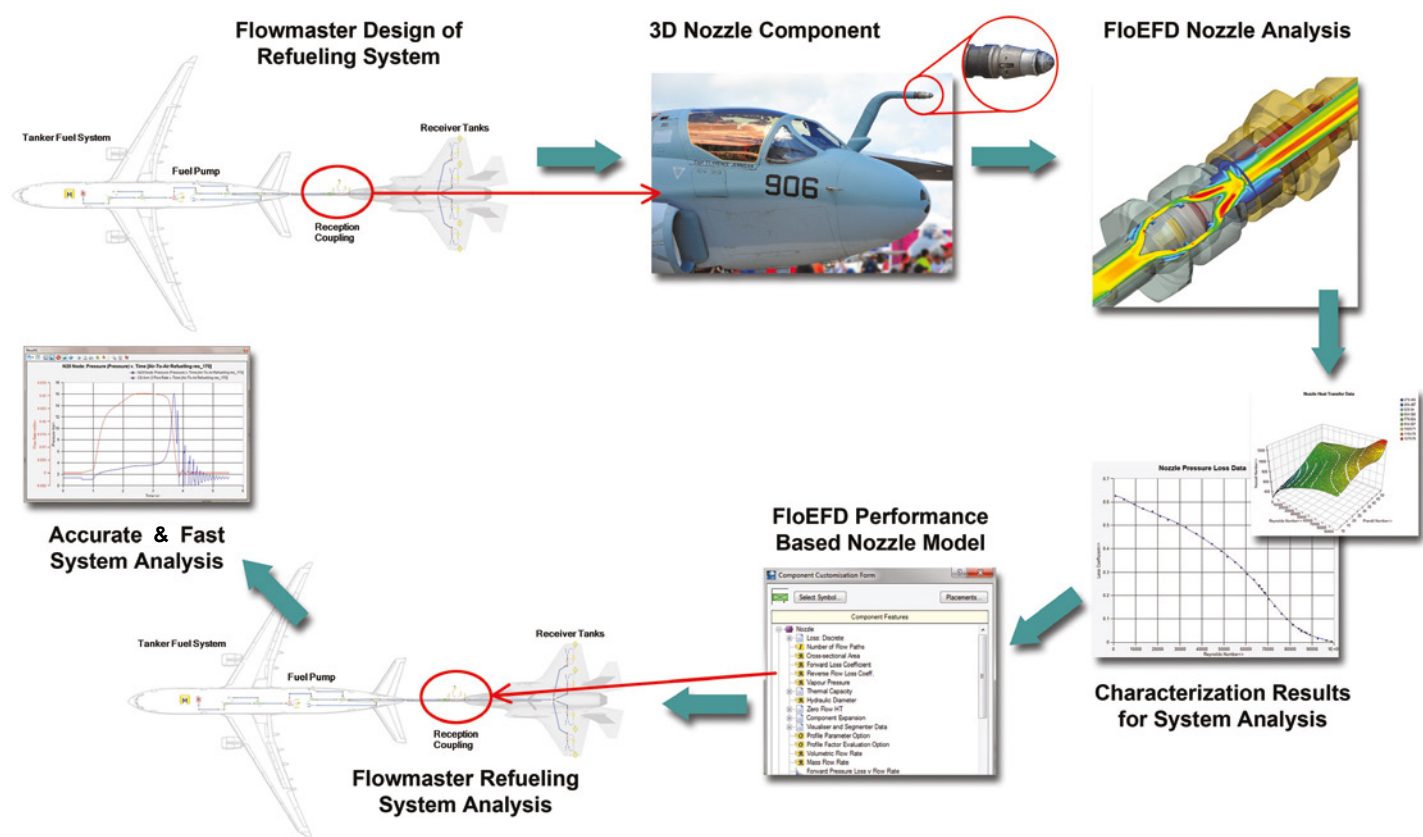


Figure 2. Combining 1D and 3D CFD leverages the advantages of both approaches and provides speed and accuracy in the analysis

The MCAD designer of the nozzle uses the 3D analysis tool embedded in the PTC Creo, CatiaV5, NX, or SolidWorks MCAD system to run detailed fluid flow analysis on the nozzle. Because the 3D analysis is embedded, the designer can perform these analyses directly within the MCAD tool using the same interfaces, an analysis model contrived directly from the MCAD model without external interfaces of data translation, and automatic meshing and convergence.

The nozzle designer sets up a set of analyses based on the nozzle boundary value spectrum presented from the system designer. The designer simply specifies the range of conditions, and the 3D analysis software automatically creates the set of conditions called Design of Experiments. This could result in 30, 40, or even more model batch executions through the 3D analysis, which, for a complex component, might have to run overnight. The resulting data of these runs is automatically condensed into detailed characterization

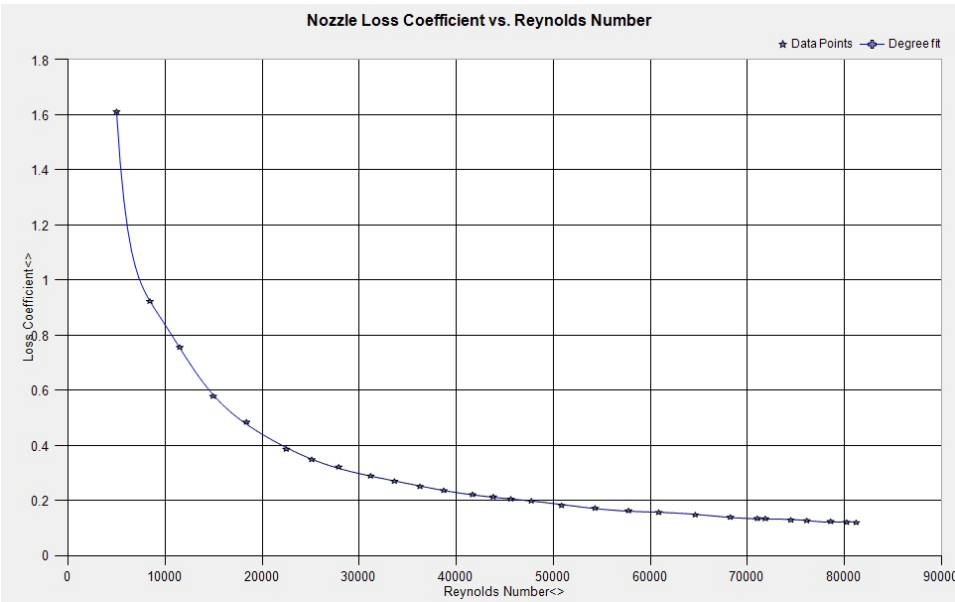


Figure 3. The results of the FloEFD nozzle characterization CFD analyses are captured in a model that spans the spectrum of possible operating conditions

graphs that now represent a complete model of the nozzle.

This model is then simply opened in Flowmaster and saved to the relational database of the 1D system analysis tool. Now, the systems designer can run the flow analysis through the series of refueling scenarios anticipated for the trial design. Design changes can be made to the system and subsequent analysis runs performed. The model of the nozzle remains valid because it covers the full spectrum of possible operating conditions.

The Results

We started out with three criteria for an optimized system: flow rate, flow distribution to the fighter tanks, and the possible water hammer effects of breakaway. The 1D analysis with the 3D-derived nozzle model quickly (in minutes) and accurately creates graphs and numerical data to represent these effects at all nodes throughout the system. The change in fuel levels of the four fighter tanks are shown in Figure 4 and the hammer effects in Figure 5.

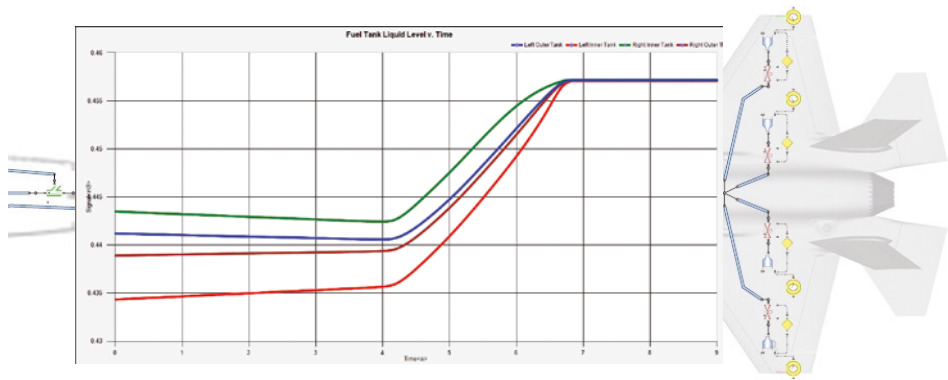


Figure 4. Flowmaster results show how the four fighter tanks will converge to full at a rate within spec that will not cause the fighter to become unstable

1D and 3D CFD Simulation

The accuracy of the 3D simulation of the complex component (nozzle) combined with the speed of the 1D piping system analysis brings the best of both worlds together. With the speed of the analysis, the systems designer is able to try several design scenarios and create a refueling system to run in the small bandwidth of optimum performance. The tanker system could

be designed to service different classes of fighter under a spectrum of operating conditions. This same combination of 1D and 3D integrated analysis methodology can be used for other aerospace systems such as onboard fuel delivery to the engines, engine cooling, interior environmental (air), etc. It also can be applied to industries such as automotive for cooling systems and exhaust, chemical processing, energy, utilities, etc.

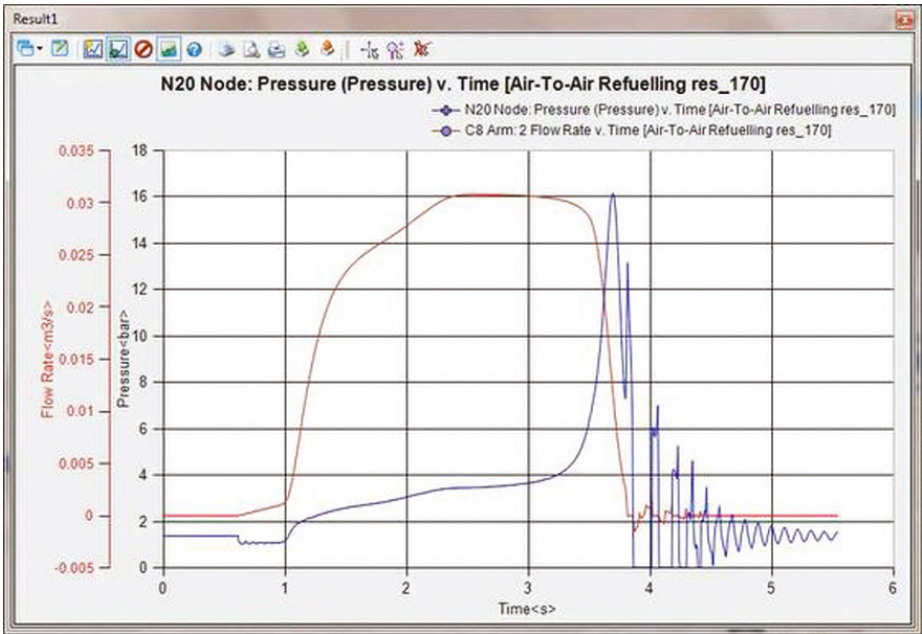


Figure 5. The system designer must analyze the 'water hammer' maximum pressure to determine if it will damage the system

Zero to 90 in 166,440 hours

It's what happens off stage that counts

By John Murray
Product Marketing Manager,
Mentor Graphics



In 1994 a young PhD candidate loaded up a transit van, pointed it east and set off for Altenberg. His intention was to meet up with the British skeleton team at one of the most notorious and demanding tracks in the world. In the back of the van was a rudimentary skeleton sled liberally covered with sensors and data acquisition equipment.

Having one of the experienced sliders from the team pilot it down the mountain at Altenberg over a series of runs would fill up the hard disk drives with information on various aspects of sled performance and handling. It was a methodical and scientific approach that would provide crucial and objective information on how a sled performs over the course of a real run. In conjunction with sector and overall times, it afforded the opportunity for real insight into performance.

The cold logic of methodical product development was about to crash headlong in to the extremely focused, tense and introverted environment of a squad of

athletes battling for a limited number of team places. "No one would ride it", remembers Professor Kristan Bromley. "At that time, the team was almost uniformly military, so the prospect of jeopardising their chance of making the team in order to help a young engineer who'd just landed up with a fairly unpromising looking sled appealed to no one." None of the athletes would ride the sled, so Kristan did.

Over the next two years, Kristan would be an intermittent and amusing distraction at practice sessions around Europe. Britain didn't make sleds and post-graduate students didn't compete on them, full stop. Except that in 1996 Kristan won the British championships on a sled he designed. The sport had just received the opening salvo from an approach that would upset the established equipment supply chain and lead to the formation of a company that, at the time of writing, supplies the skeleton teams of 23 nations.

Meeting the Bromley brothers, the co-founders of that company, supplies



individual anecdotes that taken together offer some explanation as to how it was that a Sheffield based company went on to dominate skeleton bobsled design and produce two world champions from within their stable: the Bromleys are restless. By itself, this might well have left a legacy of half-finished projects constantly superseded by the next big idea. Yet couple it with a grounding in, and respect, for the scientific method and the result is demonstrably a success.

"Our ethos is simple," says Kristan "we need to bring added value through the application of the best technologies." Actually delivering on such a mission statement in a meaningful sense requires focused and intensive effort: computationally, in the wind tunnel and on the track. Asking what was missed, what question wasn't asked, what could be done better. Being restless.

Ask the brothers who they admire from the commercial world and it's interesting that they mention Oakley, Burton, Scott: strong brands with a heritage in their respective sports, each now developed beyond those same sports. Indications of future ambitions perhaps? Kristan relays a quote that has stuck with him "The best advice anyone can get about staying ahead of the copy houses is to build a kick-ass Brand; wear the fastest running shoes in the product development arena; and always be one step ahead. By the time your competitors are copying you; you should have the next product in the market. That is why Apple comes out with so many

new models and is so successful - they run faster."

I'm initially surprised to hear the word 'brand' from that side of the table, it feels like too corporate a word from a company founded on putting itself in the full glare of the winter sports media spotlight and 'eating its own dog food' at 140kmh in front of local partisan crowds. But as Richard went on to explain, having a strong Bromley brand isn't about being able to sell their t-shirts for inflated prices; it's about defining what they do better than everyone else. As much to keep their eye on the ball as the company grows, as it is for outside consumption. The best indication of what their brand means within skeleton and what it will come to mean more broadly can be found both in their first foray outside of an elite competitive product.

This winter will see the launch of the Bromley Baseboard at a few select ski-resorts. Under development for the last four years, it's fascinating just how methodical, considered and patient the development and launch process has been. What it isn't is at all surprising. Consider the skeleton event itself; what the public sees is 90 seconds or so of action per run. What they don't see is the four years of preparation on the track, in the gym, the hours on the road, the time developing the equipment and in general the devotion to a way of life alien to most people. Teams and athletes used to living and working on those terms are more than capable of taking the

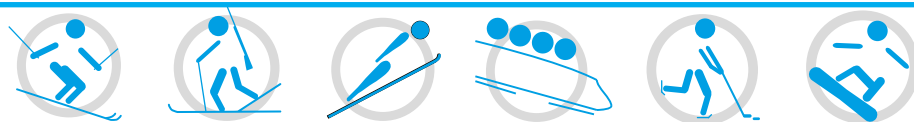


long view and ensuring that everything is engineered such that it comes together at the right time for the main event. If you're successful all you've done is make yourself a target for the competition. Complacency is as much of a foe as injury.

I would suspect that most of us have attended at least one professional training course delivered by a tutor with an armory of sporting analogies at their disposal, most, if not all, of which revolve around the event itself. Perhaps we look in the wrong place for inspiration, maybe the real lessons to be learnt are well away from the field, ring or track.

Is your business ensuring that all your customers see are the 90 seconds of the winning run?

For more information on Bromley Technologies:
www.bromleytechnologies.com



The Road to Sochi 2014

...Continues to be a demanding one. Since Lillehammer, Bromley Technologies has lost no opportunity to continue to test and develop the sled. This is an arduous undertaking which means making sacrifices in a number of areas, but not in athlete preparation. Kristan and Shelley are currently at the wrong end of a long strength and conditioning program which is, to quote Kristan, "horrible!" I'll let the reader reflect on how bad a training program has to be to get that reaction from a man who's been a competitive athlete for as long as Kristan has.

Driving Flanders to Electric Powertrain Innovation

Voxdale BVBA and Flanders' DRIVE delivering on the demand for innovation in the Automotive Industry.

By Koen Beyers, Voxdale BVBA, Belgium



Figure 1. Range Rover Evoque at Flanders' DRIVE media day with proposed driveline, April 2013

The not-for-profit organisation, Flanders' DRIVE, was set up in 1996 as an automotive industry initiative by an assortment of companies in Belgium to cope with the increasing demand for innovation in the sector. Activities started in 2001 with the support of the local Flemish Government and by 2004 the building and infrastructure of Flanders' DRIVE in Lommel, Belgium, came into operation.

At first, Flanders' DRIVE focused solely on product innovation. Since 2005 however, it expanded its focus to include process innovation for production and assembly companies as well. Over the past few

years, Flanders' DRIVE has developed into a research center for the Belgian vehicle industry, which supports the sector with a hands-on approach and a permanent and flexible focus on the actual needs of the sector. For this, Flanders' DRIVE has a team of 45 employees and state-of-the-art infrastructure available for innovation support and application-oriented research together with and for the Belgium automotive industry. It now has over 170 Partners including Volvo, Tyco, Toyota, Bombardier, Alcatel-Lucent,

Continental, DAT Trucks, Ford, IVECO, Johnson Controls, Siemens, NXP, and TI Group to name a few.

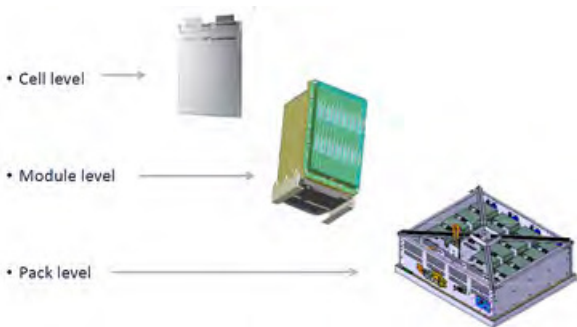


Figure 2. EV Battery Pack component levels



Flanders' DRIVE has in its aims targets for technological solutions in the fields of Advanced Manufacturing Processes, Clean & Energy Efficient Vehicles, Lightweight Solutions, Intelligent Driver and Traffic Systems and Intelligent Development Tools. In the years ahead, Flanders' DRIVE wants to play a leading part in the transformation of the vehicle industry towards a green and smart mobility industry. This will be done through focused development of strategic competences and knowledge diffusion, creation of an increase in scale through strategic and application-driven cooperation with other research centers, and further integration in European clusters and participation in international projects. Recently, Flanders' DRIVE through an "Electric Powertrain" project (with 12 partners*) wanted to prove an innovative conceptual EV drive train on a typical Range Rover Evoque car.

The project involved:

1. Developing further knowledge on state of the art battery systems (Lithium titanate oxide anode)
2. Designing, developing and integrating a full functional innovative battery pack
3. Special attention for energy management, the battery housing and thermal management so that the:
 - a) Power pack would cover regenerative braking
 - b) Development of an electrical ABS, leading to significantly shorter braking distances.

Originally the project targeted an 800V Battery Pack but eventually it opted for a 400V pack due to space reasons in the

Charge/Discharge cycle (36s) at 20 & 50 A (50% SoC)

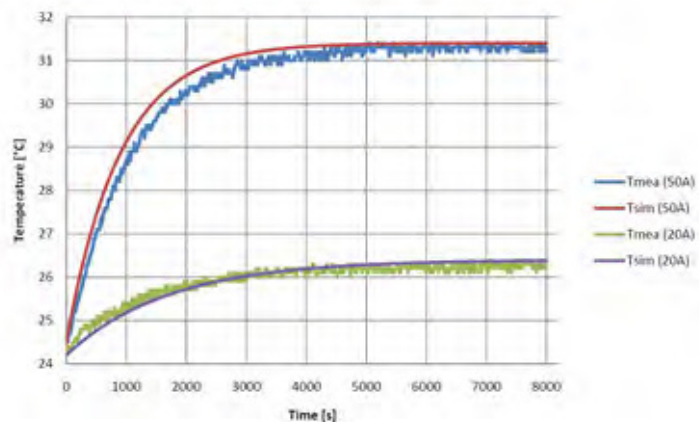


Figure 3. CFD thermal simulation versus experimental measurements.

Evoque. We were aiming for Maximum Power in = Maximum Power Out which would be good for regenerative braking. Each Pack would have 12 cells per module and 15 modules per pack and the 180 cells would take up 235 liters of space in the car with a total mass of 225 kg. Each elementary cell would be made up from six layers repeated n/6 times. Heat transfer in the battery would be predominantly by conduction. Voxdale chose the FloEFD 3D CFD package that's embedded in PTC Creo as the simulation tool for designing thermal aspects of the Battery Modules because of its ease of use and easy meshing methodology for complex repeated geometries like in this example.

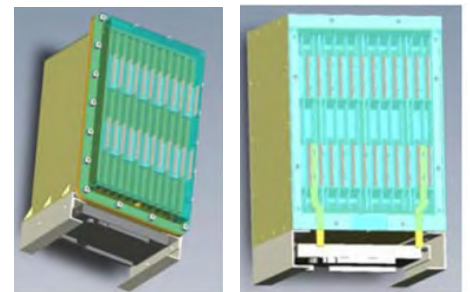


Figure 4. Battery Pack "Wet Module" (left) and "Dry Module" (right)

We initially validated our CFD thermal simulation approach versus experimental measurements in the laboratory and we got good agreement. (Figure 3).

The two Battery Pack Module concepts were investigated in the study are illustrated in Figure 4.

1. Wet Battery Module
 - a) Cells submerged in cooling liquid
 - b) Inlet and outlet for forced liquid cooling/heating
2. Dry Battery Module
 - a) Aluminium cooling ribs between cells
 - b) Cooling ribs connected to the base plate
 - c) Base plate cooled/heated by Peltier elements.

The fluid flow and heat transfer predictions revealed complex flow fields in the Wet Battery Module channels which we were able to rapidly assess with FloEFD. (Figure 5)

Parametric FloEFD predictions for the Dry Battery Module channels also showed that a set of Peltier elements were able to cool the module adequately whereas the Wet Module created considerable packaging challenges. In addition, unknown longer

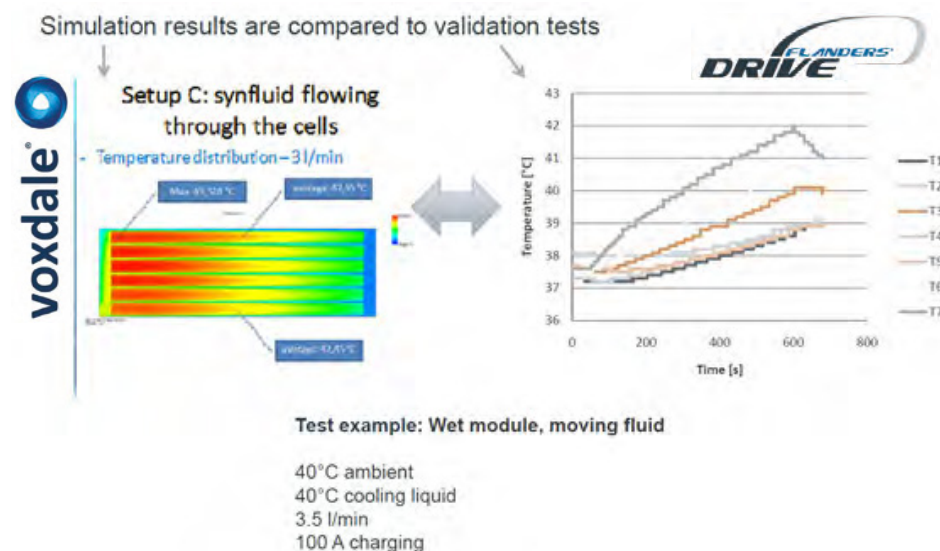


Figure 5. FloEFD simulation results versus experimental measurements for Wet Module

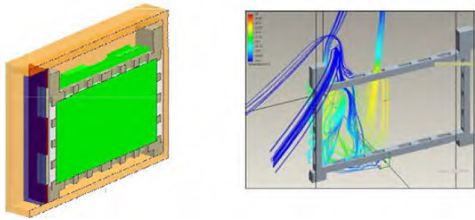


Figure 6. Geometry and detailed FloEFD thermal predictions for parts of the Dry Module

term effects on the cell packaging due to the cooling liquid meant that the Dry Module was our recommendation for the EV Battery being designed. (Figure 6)

Based on our work and that of the other consortia partners, Flanders’ DRIVE set up a press and media day in April 2013 showing the new EV Powertrain design inside a two-wheel drive Land Rover Evoque’s powertrain (Figure 1). It included four switched reluctance motors, one powering each wheel separately, thus eliminating the need for a differential between wheels. Powering each wheel with an independent motor should also lead to enhanced safety, speed and handling of the electric vehicle. Cornering would also be improved because the car’s outer wheels would spin faster than the inner wheels as the car turns. This in turn improves the car’s overall torque because the power generated by the

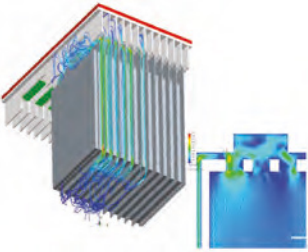


Figure 8. Aquilo concept car battery pack cooling simulation in FloEFD

batteries would be sent to where it is needed most. The Flanders’ DRIVE motors also did not use magnets – thus potentially reducing the price and helping to generate additional power for the engine through a regenerative braking system. The next step for Flanders’ DRIVE researchers will be to optimize the powertrain technology in conjunction with its European Partners which include Jaguar Land Rover and Skoda so that they can be applied to all hybrid and electric vehicle combinations.

Finally, my colleague at Voxdale, Wouter Remmerie, and I decided to see if we could think through what we had learnt from the initiative to facilitate some “blue sky” thinking related to electric vehicles with novel battery locations, a patented 3D printed chassis monocoque concept, and thermal management (via FloEFD), all inside PTC Creo. We called our Project “Aquilo” and decided to look at a fundamental new conceptual aerodynamic design process with CFD simulation prototyping related to cooling and heating of battery packs, cooling of powertrain (Figure 8), cooling of electronics, and simulation of battery



Figure 7. Voxdale concept electric vehicle chassis

cooling media, plus lightweight casings for a generic two door EV sports car chassis design (Figure 9). The battery casings were designed with FloEFD and fabricated in the laboratory to validate them.

Our final sports car design with novel monocoque, FloEFD aerodynamic styling and battery driveline was visualized in PTC Creo (Figure 9). A very interesting exercise and something that illustrates the power of tools we have available to us inside PTC Creo.

For more information visit:
<http://bit.ly/1kWdC9M>

* The Flanders’ DRIVE Electric Powertrain project was a consortium of 12 companies including Arteco, CTS, DANA, EIA Electronics, Imec, Inverto, LMS, NXP, Punch Powertrain, Triphase, Umicore and Voxdale: flandersdrive.be/en voxdale.be/en

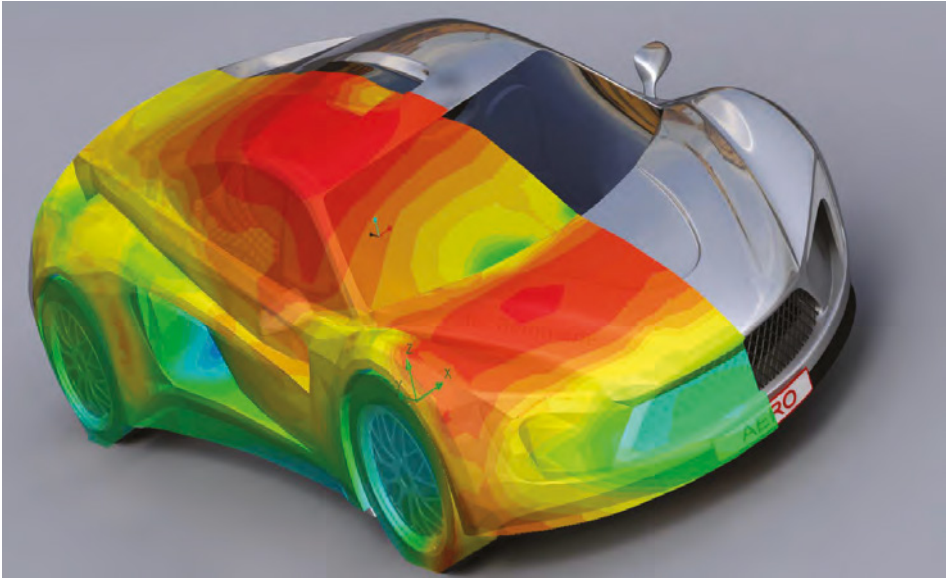
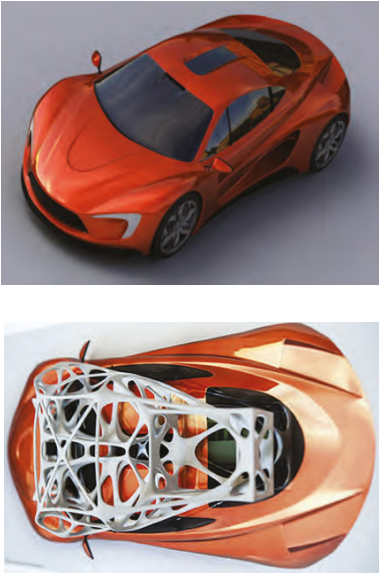


Figure 9. Aquilo concept car design in PTC Creo with external aerodynamics pressure predictions from FloEFD Simulations

Upgrading a Biomass Furnace: A Simulation Driven Approach

By D. Hasevoets, Cofely Fabricom E&E & Wouter Remmerie, Patrick Vlieger, Voxdale

Cofely Fabricom GDF SUEZ is a leading multi-disciplined engineering, project management and construction organization in the oil, gas, power and allied industries. Part of the global energy group GDF SUEZ, Cofely Fabricom employ over 5,500 people worldwide who strive for the improvement of energy efficiency, durable development and quality of life.

The Cofely Fabricom, Energy & Environment Division specializes in turnkey Engineering, Procurement, Construction and Commissioning (EPC) projects in the renewable energy sector emphasizing on balance-of-plants, flue gas treatments, and cogeneration plants. In April 2013, Cofely Fabricom E&E was awarded a turnkey revamping contract to improve the reliability and performance of the biomass furnace of the cogeneration unit in Sart-Tilman, Liège, Belgium, which is part of the central heat production and distribution across the Université de Liège (ULG) and the CHU University Hospital. The project was centered around the improvement of a number of failures experienced by the two institutions, specifically:

- Insufficient instrumentation for proper combustion control;
- Reduced performance due to a lack of recirculation of smoke gases in nominal operation;
- Incomplete coverage of grid with pellets, leading to primary air bypass non-uniform combustion; and
- Refractory damage caused by extremely high local temperatures.

In order to address these issues, a completely new combustion control philosophy was investigated.

The approach would involve:

- A mixture of 50% re-circulated smoke gases into primary and secondary air to improve performance;

- Optimizing, by means of Computational Fluid Dynamics (CFD) calculations, secondary air injections to respect legal emission limits;
- Installing new fans, frequency drives and electrical cabinets; and
- Implementing superior instrumentation, including ultrasonic flow meters and infrared cameras.

Cofely Fabricom E&E first performed the necessary process calculations for optimized combustion, accounting for flow rate, temperature, oxygen content and pressure drop, which sized the primary, secondary and recirculation fans as well as the duct diameter and valves.

The next step was to ensure the optimal configuration of the secondary air injections. Since the main objective of the project was to achieve an increase in performance, the oxygen concentration at the furnace outlet had to be reduced from its current value of 13% while respecting the legal emission limits. The secondary air injection therefore had to ensure that all produced CO was recombined to CO₂. This would be achieved by obtaining an optimal level of turbulence inside the narrowest section of the furnace, referred to as the “furnace neck”.

To gain sufficiently high velocities at the tube outlet, the secondary air injection nozzles were divided into two rows: an upper and lower ramp of 2 x 14 tubes each at the front and back end of the furnace, 112 tubes in total. At lower flow rates, the two lower rows were isolated in order to maintain a minimum velocity of 20m/s at the remaining tube outlets.

Physically building and testing different prototypes of an installation of this size would be time consuming and prohibitively expensive. In order to understand the response of the system and arrive at the optimum configuration of nozzles, Computational Fluid Dynamics (CFD) simulations were carried out using Mentor Graphics’ FloEFD by project partners Voxdale.

The first step was to create a model of the existing furnace and simulate its behaviors. This approach would allow simulation parameters and boundary conditions to be adjusted to obtain a good match between a well-known system and the simulation model. During this phase confidence in the simulation approach is established and the first insights into the system are generated.

Combustion processes weren’t directly modeled in the simulation, instead, air temperatures and flow rates were adjusted to obtain comparable behavior. This reduced the time required for each simulation without appreciably affecting accuracy, which in turn allowed for CFD to cover a large number of design iterations in a reasonable time. Figure 1 illustrates the original setup of the furnace with wood pellets that are fed into the system, forming a layer on the moving grid. Below

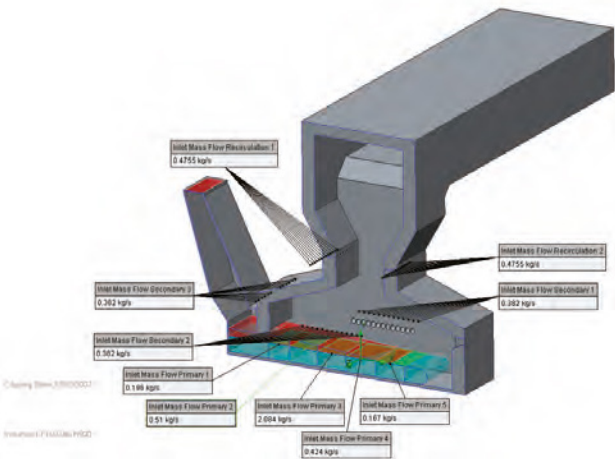


Figure 1. FloEFD simulation geometry



Figure 2. Secondary air nozzle detail results

this grid, five distinct supplies of primary air, provide the oxygen required for the combustion process. In addition, secondary air is supplied through nozzles on both the front and lateral walls. At the furnace neck, exhaust gases are injected into the furnace, providing the system with recirculation air.

In the second phase, different design proposals were set up and simulated in FloEFD. Three-dimensional turbulence plots and velocity patterns were used to assess the various configurations. One of the earlier setups is illustrated in Figure 2, in which the secondary air nozzles were moved closer to the furnace neck and the number of nozzles was greatly increased. Although this solution offered some benefits, it resulted in insufficient turbulence intensity across the furnace neck.

Based on the insight offered by such simulation and analysis, further design iterations could intelligently evolve. For example, it became apparent that offsetting the recirculation nozzles slightly with respect to each other created the desired amount of turbulence in the furnace neck. The positioning and layout of the secondary air jets were similarly optimized in order to ensure sufficient turbulence in the adiabatic chamber (Figure 3). As the simulations were performed without combustion, it could reasonably be assumed that an even higher level of turbulence, higher velocities and better mixing would occur in practice. The resulting design is shown in Figure 4.

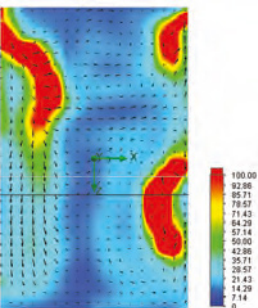


Figure 3. Turbulence intensity in the adiabatic chamber

Disassembly of the old furnace began in May 2013, with installation works running from June to September 2013. Start-up and combustion optimization took place in October - November 2013. During cold commissioning

of the new installation the simulated velocity distribution was verified inside the

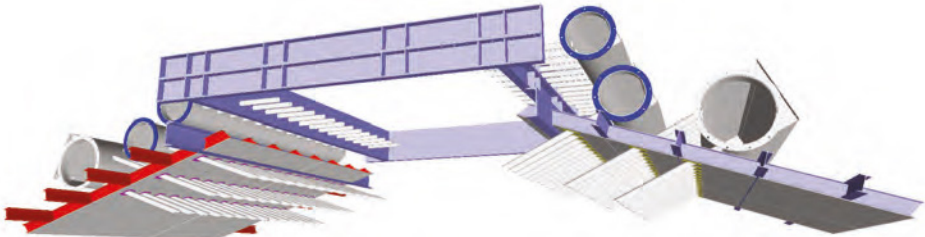


Figure 4. Furnace neck resulting design

furnace and comparable flow patterns were observed. Integrating CFD in to the design process helped Cofely Fabricom E&E deliver the project successfully and within a short time frame. Virtually prototyping various designs in FloEFD provided a reliable and inexpensive means by which different parameters could be assessed and adjusted. Ultimately, all project objectives have been fulfilled.

- Performance was increased by 8.4% (actual efficiency 89.3%);
- The furnace represents a considerable improvement over the previous design (see Table 1) and operates well below legal limits, e.g. for both carbon monoxide and nitrous oxides.

The process followed demonstrated the value of fluid simulation for such projects. It is therefore an approach which will be used for future projects, where appropriate. The installation has been in reliable operation since November 2013.

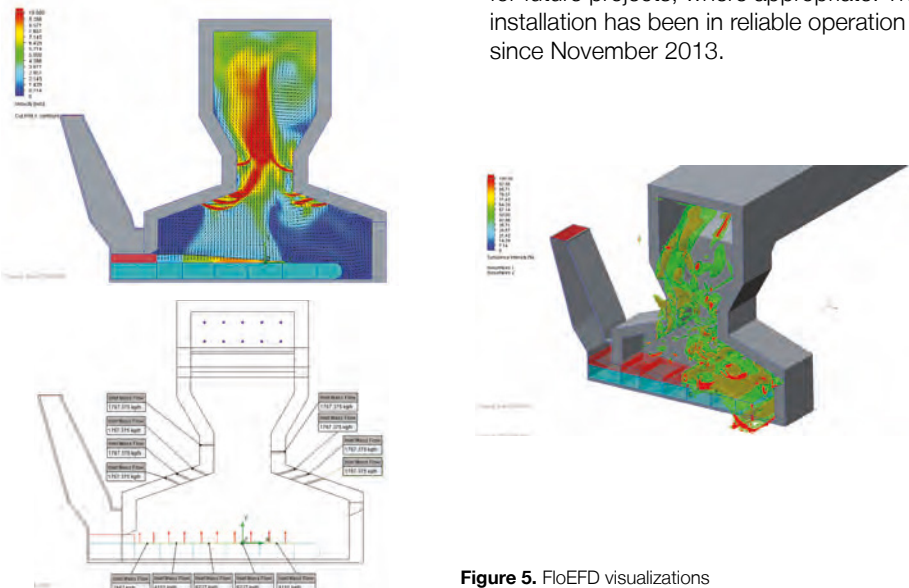


Figure 5. FloEFD visualizations

Table 1 Emission figures

Species	Old Furnace (Nm³)	New Design (Nm³)
CO	106	11
NO _x	406	203

More Power Please!

What do Tim, the Toolman, Taylor in the TV-Series “Home Improvement” and Raul Cano at Stanley Black & Decker have in common? The need for “More power!!”

By Boris Marovic, Industry Manager, Mentor Graphics



Unlike Tim, Raul Cano is a professional and is the Lead Project Engineer CAE for Stanley Black & Decker's DeWALT Professional Tools brand. He and his team are responsible for optimizing the performance of their hammer tools, namely the Rotary Hammer, Demolition Hammer, and Hammerdrills as well as concrete saws and dust extraction for large hammers.

DeWALT's reputation in the power tools and construction tools industry is unsurpassed. For almost 80 years DeWALT has earned a name for designing, engineering and building the toughest industrial machinery. The company incorporates their long standing tradition of state-of-the-art engineering into every product of their broad range of high performance portable electric power tools and accessories. Making DeWALT tools the number one selling brand of professional power tools in North America, and the fastest growing professional power tool brand in the world for the past five years.

The mission for professional tools from DeWALT is to deliver optimum performance and reliability. In order to achieve this, Raul's team investigate several numerical simulations including drop, stress and thermal simulations. One of the methods

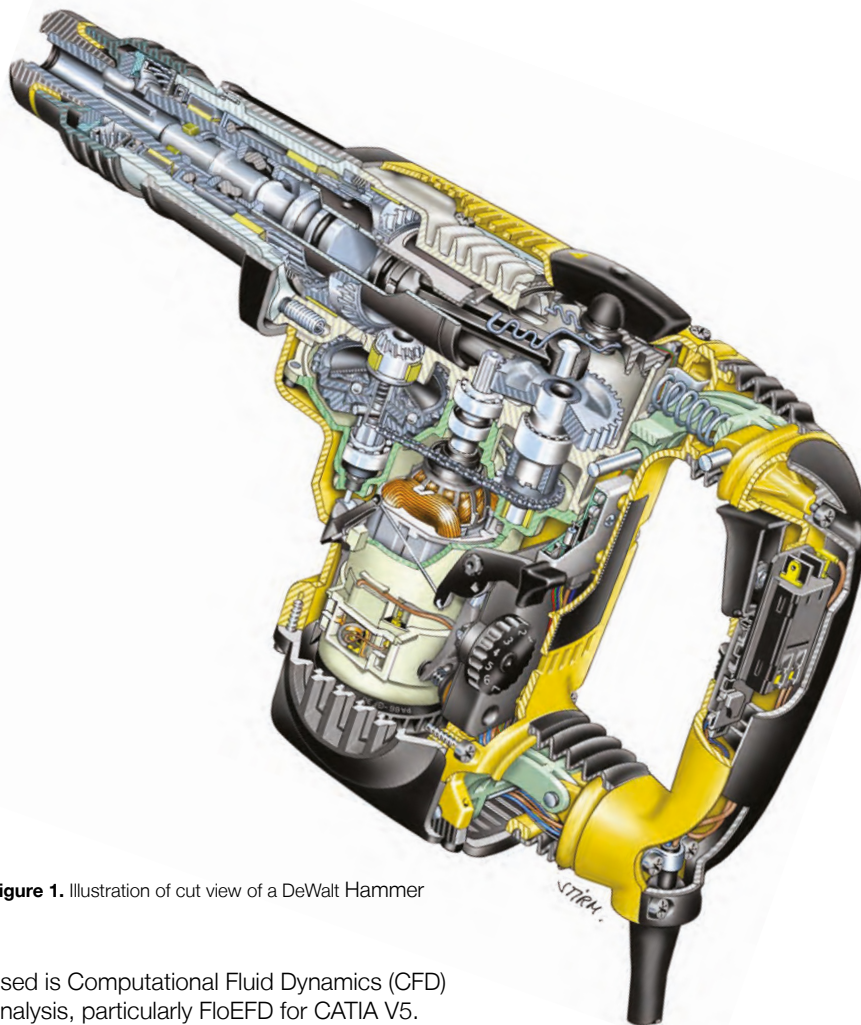


Figure 1. Illustration of cut view of a DeWALT Hammer

used is Computational Fluid Dynamics (CFD) analysis, particularly FloEFD for CATIA V5. The primary challenge for thermal simulations is the need to process complex geometries such as the narrow spaces inside a handheld power tool where the motor, gearbox, and electronics are situated. This housing is built with stiffening ribs that not only makes such a power tool so robust but also complex. As with many, if not all, tools of this nature, the challenge is thermal. The use of FloEFD in their design process helps Raul to test design variations for venting, fan position and geometries, as well as housing changes for better airflow. In the case of the metal housings of the gear box, FloEFD is used to improve the cooling performance of the gear box.

Raul comments, “The capabilities of FloEFD to handle complex geometries allows us to simply switch between different component designs such as different fans and then let the software automatically mesh and

calculate several variants over the weekend, is an enormous advantage for us.”

By having the ability to test so many variations of geometry it is possible to find the best solution for optimum airflow, both for quantitative flow rate and noise. With FloEFD, Raul is able to determine if a certain geometry change has a positive influence on the volume flow rate through the tool as well as find areas with very high velocities which can be indicative of a high noise source in the design.

The primary role of the airflow in the power tool is of course, thermal management. The better the airflow the more efficiently the motor can be cooled, thus allowing the power of the tool to be increased. One

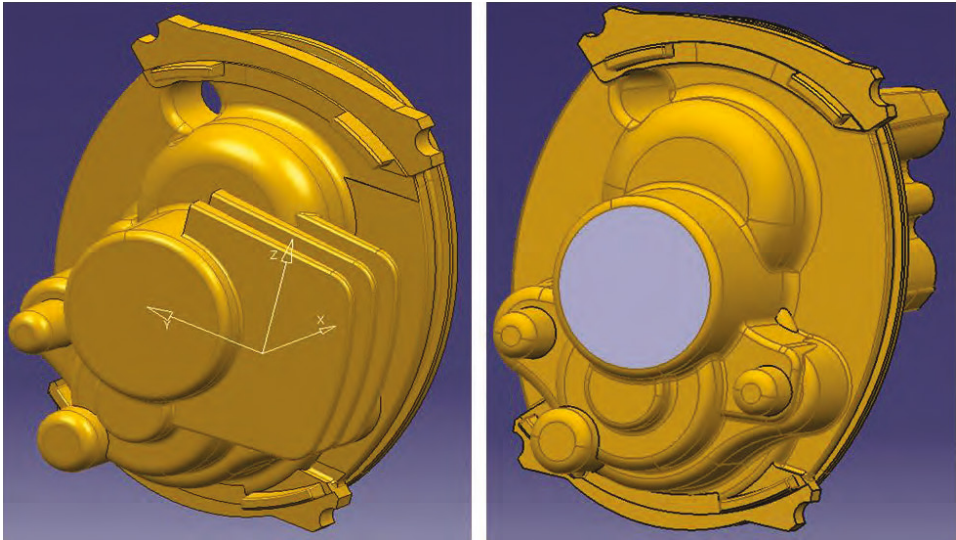


Figure 2. Bearing housing variants with (left) and without (right) cooling fins

study showed that an existing bearing housing design that contained fins for better thermal management, although it made the part more expensive and heavier, was still justified when compared to a housing version without the fins (Figure 2) as simulations have shown. In case of housing without the fins, the surface temperature of the external housing of the tool increases by 30°C in some regions (Figure 3).

In the case of the Large Hammer Dust Extraction – Hole Cleaning tool, the team at Stanley Black & Decker were able to reduce the wear of the hose attached to the unit and the vacuum cleaner. The wear at the hose was caused by the high concentration of concrete particles from the drilling of a hole that impacted the hose at a certain location causing a high abrasion rate. Just by optimizing the airflow path and its bends to reduce the impact of the particles, Raul was able to reduce the wear by around

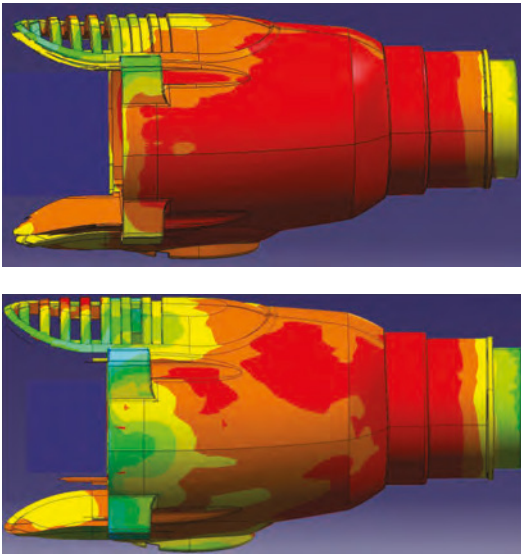


Figure 3. Temperature profile of external housing of a hammer showing the influence of the bearing housing without (top) and with (bottom) cooling fins

60%. As a result the lifetime of the hose increased by a factor of two. In another case, a range of simulation variants with different components of the Alligator Concrete Saw was conducted (Figure 4) to optimize the performance. The goal was to optimize the flow rate by making changes to the fan, fan RPM and other components. The measurements in the lab at the end showed that even the noise was reduced by 10dB. A reduction of 10dB of noise is equivalent to around an eighth of the original noise (3dB equal half the noise).

The design of the power tools at Stanley Black & Decker are influenced by several departments and requirements. “If the drop test simulations don’t go well we have to redesign the housing which might make it necessary to change locations of venting openings. On another occasion the marketing department played with the rapid prototyped sample and found it is too thick or too long at a certain area of the housing which means we need to try to change it if possible and that often influences the flow paths in the tool that might reduce the flow rate due to too high pressure losses.” explains Raul. “All the desired changes have to be evaluated by multiple factors which might increase the price, the weight or size in one way or another. At the end of the process, the design has to perform at its best and the thermal simulations with FloEFD provide us reliable results to make sound judgments on the design changes we make.”

“Stanley Black & Decker uses several FloEFD licenses in our development centers in the US, UK and Germany and I have personally used it for over five years now with great success. We have several projects over a year and in each the number of simulation runs can vary from just a few to 20-30 simulations per project.” says Raul.

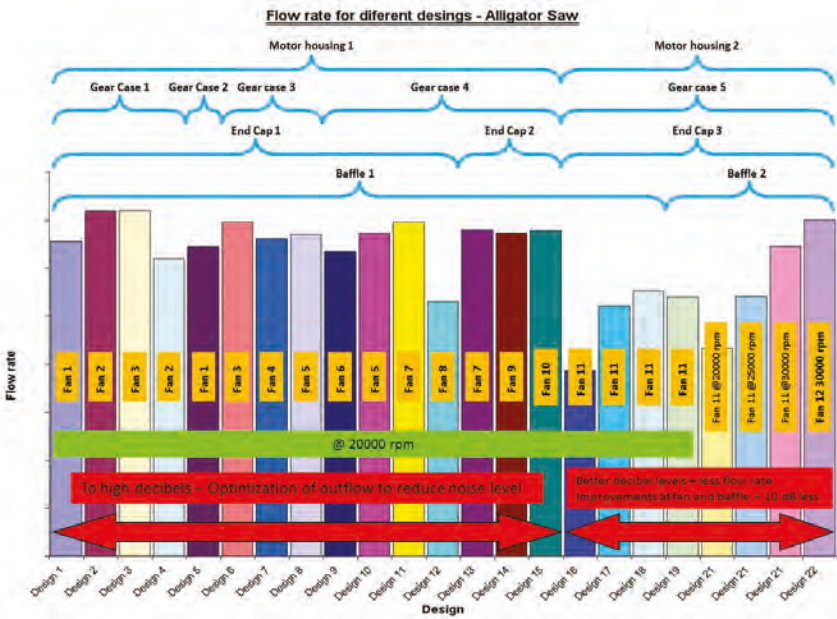


Figure 4. Flow rate variation of different component design iterations of the Alligator Concrete Saw

FloEFD™ for Cyclone Simulation

Air cyclones are a popular method for separating out particulates due to their simple design and low capital and running costs.

By John Murray, Industry Manager, Mentor Graphics

The simple operating principle belies the complexity of the air motion inside the cyclone. This is characterized by high levels of turbulence, strong anisotropy and an unsteady, swirling airflow.

The lack of a stable theory of fluid motion in an air cyclone tends to favor either incremental alteration of existing designs and/or expensive physical prototyping. However, computational fluid dynamics (CFD) can be used to have a better understanding of the intricate flow field structure of the cyclone and help designers understand important features such as hydraulic resistance, central vortex stability and cyclone efficiency, as described by the degree of air purification. Obviously, the usefulness of any such results depends upon the trust that can be placed in the CFD tool for a given application. Mentor Graphics FloEFD addresses this issue directly by continually looking for industrial benchmarks or suitable experimental data against which it can be compared.

This FloEFD CFD study is particularly interesting as the k-ε turbulence model is generally regarded as not being suitable for the swirling flow that obviously plays such a prominent role in a cyclone. It therefore provides an excellent dataset against which to judge FloEFD's enhanced k-ε turbulence model. [1]

Two separate experiments were considered: the first relates to a Stairmand High Efficiency cyclone [2], the second to a cyclone with a bin [3] (see Figure 1 & 2).

As well as the lack of a bin, the Stairmand HE cyclone differs by not having a flow straightening device at the end of the outlet pipe. Beyond geometric considerations, the two experimental datasets emphasized differing aspects and so allowed a broader range of FloEFD outputs to be assessed. Comparison with the Stairmand data will provide a good benchmark of how FloEFD handles the pressure differential between inlet and outlet. The Lorenz cyclone with bin data will allow an assessment of how accurately FloEFD is tracking the motion and settling of particles of various diameters to be simulated.

Stairmand HE Cyclone

A range of cyclone operating conditions were considered, covering inlet velocities of 5-25m/s. A comparison of the FloEFD predictions with the experimental results (Figure 4) show excellent agreement for calculated pressure drop between inlet and outlet.

Figure 1. Design of Stairmand HE cyclone: 1) cylinder part; 2) conical part; 3) outlet pipe; 4) inlet pipe; 5) expulsion; 6) dust expulsion; 7) current lines

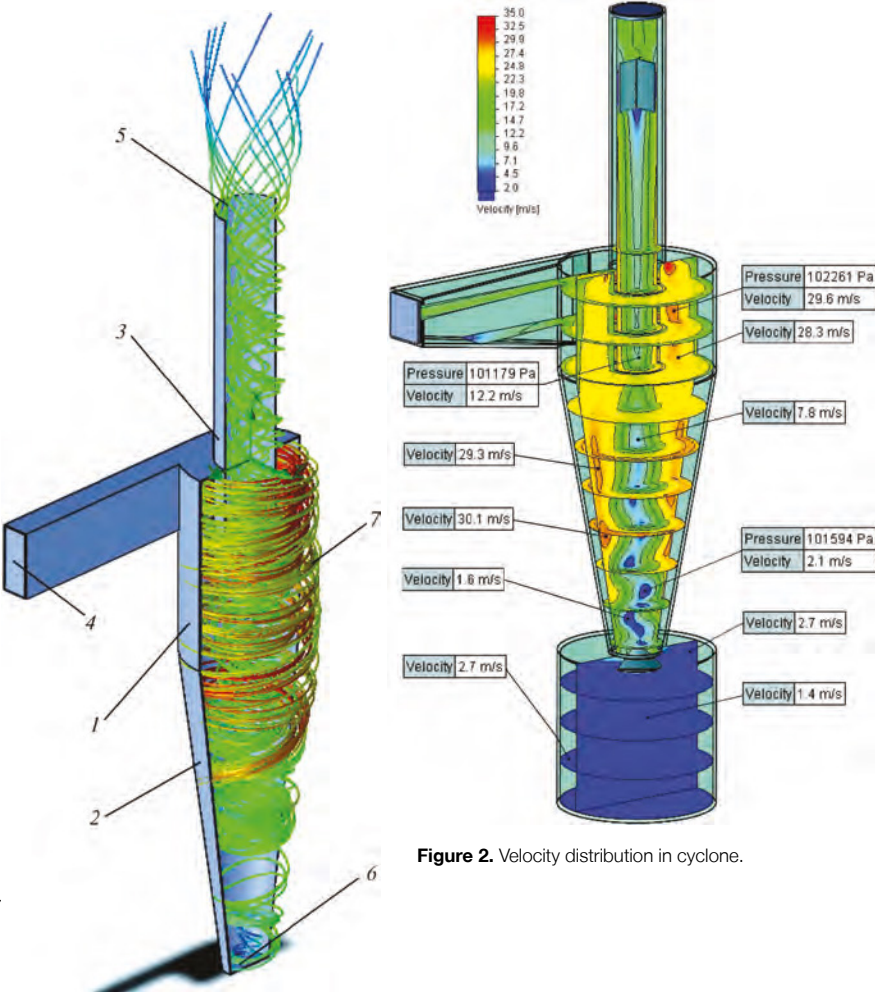


Figure 2. Velocity distribution in cyclone.

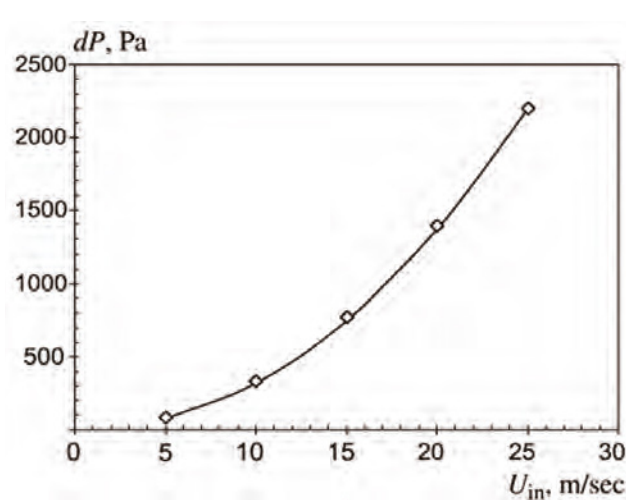


Figure 3. Dependence of hydraulic resistance of Stairmand HE cyclone on air velocity at cyclone inlet

Lorenz Cyclone with a Bin

In contrast to the above, the experimental data for a cyclone with a bin are distinguished by a wide variety of conditions and temperatures. In addition, an evaluation of the cyclone efficiency which FloEFD replicated via an assessment of the motion and settling of particles. In order to do this, the inlet surface discharged 500 particles of a given diameter, across a range of diameters, from the inlet pipe. The trajectory of each particle was then tracked and the cyclone efficiency determined as the ratio of the number of captured to the number of discharged particles of each size. In common with the Stairmand HE case, the first step was to compare predictions of the hydraulic resistance across a range of flow rates with the experimental dataset. In this case, the experimental dataset included points for a range of gas temperatures, which was in turn calculated by FloEFD, (Figure 4).

It can be seen that there is again excellent agreement between experiment and simulation for this cyclone geometry. While the error does increase at higher temperatures, even at 850°C it is little over 10%. In practice, gas flows in cyclones rarely exceed 400°C. The calculated cyclone efficiency is shown Figure 5.

Since the flow pattern in a cyclone is unsteady, the probability of particle drop-out for each diameter was calculated by averaging the results of five discharges of particles. The vertical bars at each point represent the maximum and minimum probability of drop-out of a particle with a definite diameter over five particle discharges. While the calculated cyclone curves have a slightly steeper gradient relative to the experimental data, the agreement between FloEFD and the dataset is very good, particularly below 200°C.

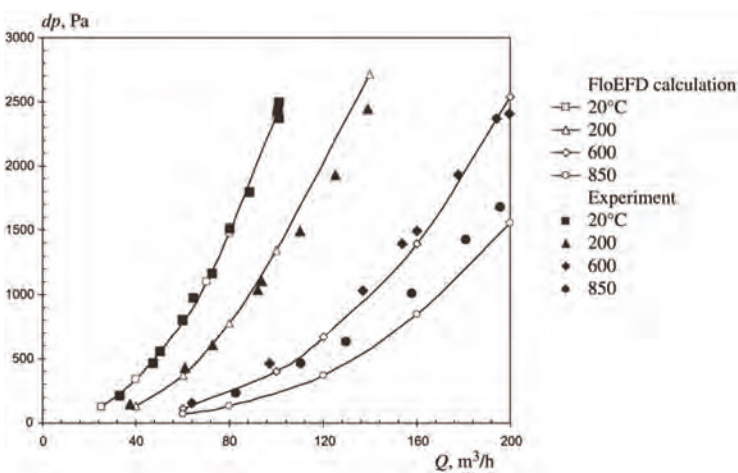


Figure 4. Dependence of hydraulic resistance dP of cyclone with bin on throughput Q at various gas temperatures

Conclusions

This work demonstrates that the modified $k-\epsilon$ turbulence model used in FloEFD is well suited to highly swirling flows. Considering the low computational overhead associated with FloEFD (the largest mesh was generated for the cyclone with a bin case, which only came to 380,000 cells) it is clearly the case that FloEFD can offer much to engineers and designers involved in the design of such systems.

References:

[1]. Enhanced Turbulence Modeling in FloEFD™, MGC 02-11, TECH9670-w, Mentor Graphics Corporation (2011).
[2]. F. Boysan, W. H. Ayer, and J. A. Swithenbank, "Fundamental mathematical modeling approach to cyclone design," Trans. Inst. Chem. Eng., 60, No. 4, 222-230 (1982).
[3]. T. Lorenz, "Heißgas Entstaubung mit Zyklonen," VDI Fortschritt Berichte, Reihe 3, Verfahrenstechnik, No. 366, VDI-Verlag, Dusseldorf (1994).

This article was adapted from an article published in Petroleum and Engineering Journal, Vol. 49, Nos. 3-4, July, 2013. Computerizing Calculations and Designing a Numerical Modeling Software Package for Computing Aerodynamic Characteristics of Air Cyclones. A. V. Ivanov, G. E. Dumnov, A. V. Muslaev, and M. V. Popov

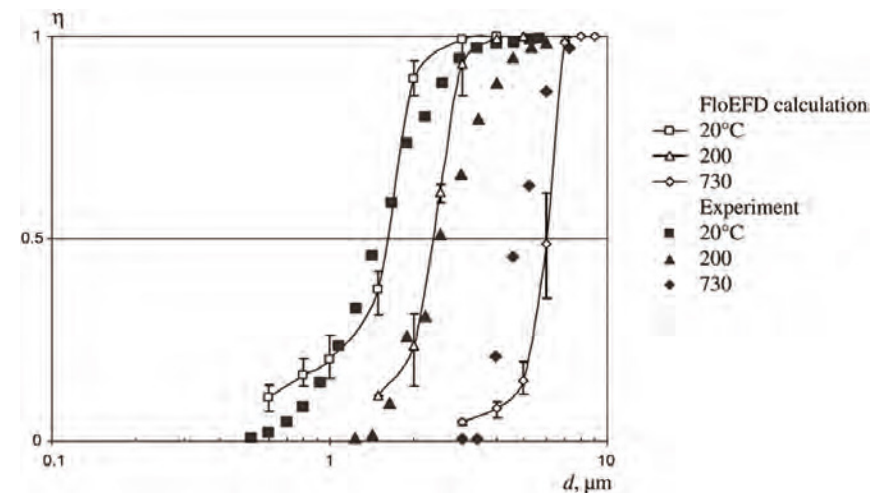


Figure 5. Dependence of gas purification degree η on particle size at various gas temperatures at 60 m^3/h cyclone throughput

Saipem S.p.A moves FloEFD Offshore

Saipem S.p.A take advantage of FloEFD
to support operations



Figure 1. The Saipem 7000: The world's second largest Semi-Submersible Crane Vessel (SSCV)

Saipem S.p.A, a subsidiary of Eni S.p.A, is a world leader in the oil and gas industry, providing engineering, construction and project management services to organizations in some of the most difficult operational environments in the world. Success in this industry requires engineers to balance experience with innovation in order that projects are delivered safely while ensuring that best practice constantly evolves with the latest tools and techniques.

The Naval Analysis Group in Saipem's London office focusses on supporting offshore heavy lift and pipeline installations for projects around the globe. As exploration has moved into increasingly challenging territory, the engineers and naval architects

have sought to continuously invest in and improve their operational practice in order to better serve the operations they support.

A practical example of this evolution is the integration of FloEFD into their suite of tools. Computational Fluid Dynamics (CFD) has been used in the offshore industry for a number of years, often focusing on specialized applications such as heat transfer or multi-phase flow. However, the wider application of CFD beyond specialist groups has been limited by the complexities involved in geometry handling, meshing, and solution procedure. Not only this, but the hardware and time frames required to deliver solutions on anything other than the most basic geometries renders it difficult to use in operational environments.

Saipem saw an opportunity to address these issues through the adoption of FloEFD and first trialled the code in 2007. Following a successful evaluation period in which FloEFD was deployed to simulate a number of geometries including a semi-submersible crane vessel (Figures 1 & 3), a J-Lay Tower, and an offshore construction vessel, the program became core to its problem solving capabilities.

FloEFD afforded users at Saipem the opportunity to consider deploying CFD on problems which would previously have been too resource or time constrained to consider it. For example, when the increase in predicted towing force required for a Mobile Offshore Unit (MOU) was raised as a concern by the local project engineer, FloEFD was used to mesh, solve, and

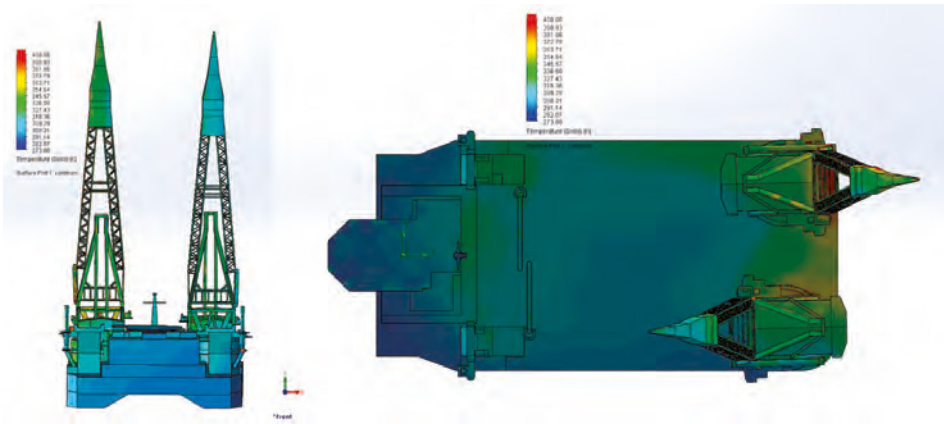


Figure 2. FloEFD Model showing Temperature Distribution during Flare Operation

provide a reliable prediction on capacity within hours of the original question being raised. In a similar fashion, FloEFD was able to provide assurances that temperature limits were not breached for crane operation in proximity to a flare stack (Figure 2). Without this reassurance, there was a real possibility that the certification of the crane would have been removed until all the cables were re-greased, resulting in considerable cost and loss of capability.

Pipeline construction is another example of where changes in operational requirements have required an innovation in the processes used at Saipem. As it becomes economic to exploit hydrocarbon reserves in deeper waters, so the traditional anchored laybarges used for pipelay and trenching increasingly give way to dynamically positioned construction vessels. Powerful

thrusters are used on such vessels in order to generate the large tow forces required to cut deep trenches.

However, these high-power devices bring with them the risk of seabed scouring when used in shallow water operations (Figure 4). This presents an environmental issue and also risks causing the soil removed during the ploughing operation to be swept away, which would affect the ability to mechanically backfill the trench.

To develop a systematic approach to this issue, Saipem employed FloEFD along with established sediment transport methods. The result was a robust and cost effective solution which allowed the team to establish

the susceptibility of the seabed to erosion by propeller wash. FloEFD could then be used to plan the operation to mitigate any potential deleterious effects.

In one notable instance of this method being deployed, FloEFD simulations were validated against a sonar survey of the seabed which was conducted following a ploughing operation. The results from the survey revealed good qualitative agreement between the simulation and the actual seabed profile.

The Naval Analysis team at Saipem have demonstrated how CFD can be deployed to aid day-to-day operations and complement existing tools. Furthermore, they've taken maximum advantage of what Saipem calls the "Engineering Orientated" nature of FloEFD on a range of projects. Being CAD embedded, providing intelligent assistance with defining the computational regime and being able to deliver results quickly without a protracted meshing process enables the users at Saipem to consider it as a genuine asset even when deadlines are pressing.

By John Murray,
Product Marketing Manager,
Mentor Graphics

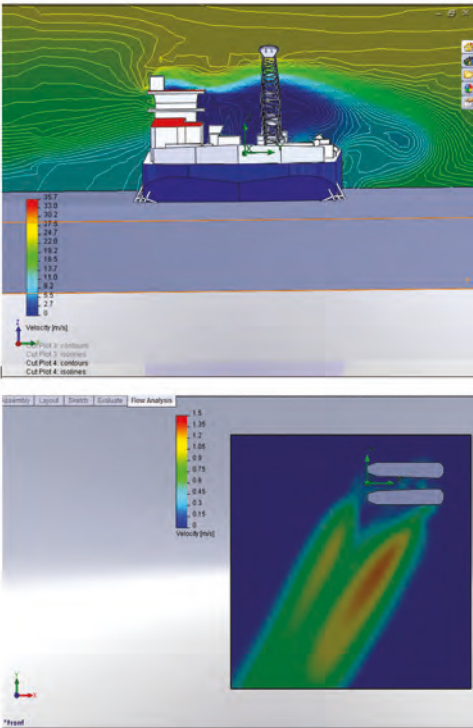


Figure 3. Velocity Contours on the Semi-Submersible Crane Vessel

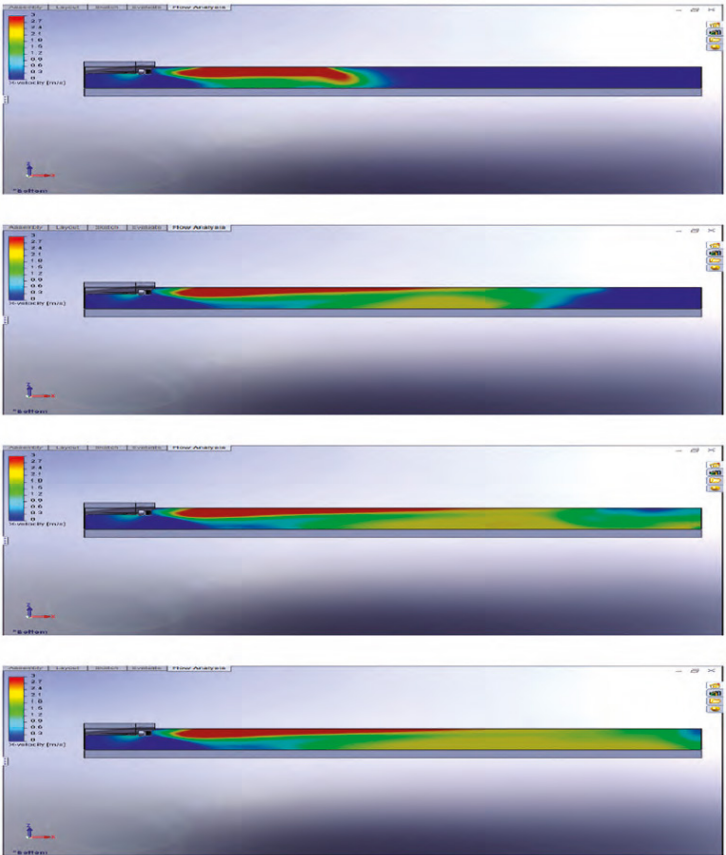


Figure 4. The Effects of Thruster Operations in Shallow Waters

Leaving on a Jet Plane

Simulation of a Jet Engine Thrust Reverser
By Boris Marovic, Industry Manager, Mentor Graphics

Some time ago we conducted simulations of a jet engine thrust reverser with FloEFD and compared them with a traditional CFD simulation tool; such measurements are often impossible to come by or extremely hard to get in order to compare with physical tests. This is what we found out about the accuracy of FloEFD simulations.

But first, what is a thrust reverser? In commercial jets every airplane is equipped with at least two powerful jet engines. These engines do not only propel the plane to its cruising speed and maintain it at that speed, but are also used to slow it down again just after touch down on the runway. Now of course that cannot be done by rotating the engines 180° or suddenly letting the engine spin the other way around. That would be like shifting your car into reverse at 180 km/h! It would wreck your gearbox.

No, this is achieved by redirecting the airflow towards the flight direction, not fully, but to a certain degree. For that there are three major types of thrust reverser (Camshell-type, Target type and Cold Stream type) and the application depends mostly on the type of engine. There are also different types of engines, but let's leave this topic aside this time.

In our simulation we considered a Cold Stream type of thrust reverser where part of the rear nacelle is moved backwards, this

reveals the cascade that contains some guide vanes directing the flow forward and at the same time closing the bypass duct of the jet engine. The bypass duct is the portion where around 90% of the actual thrusting airflow travels through the engine. Only ~10% actually goes through the combustion chamber in most modern turbo-fan jet engines.

The model is simplified to leave out any actual fan rotating or wing or the entire aircraft in order to only focus on the jet engine. Of course in reality the airflow can also be influenced by or influence the airplane geometry and the flow around it, but this is ignored in our case.

Our case considered a bypass ratio of around 8:1 as you can see from the mass flow boundary conditions in Figure 1.

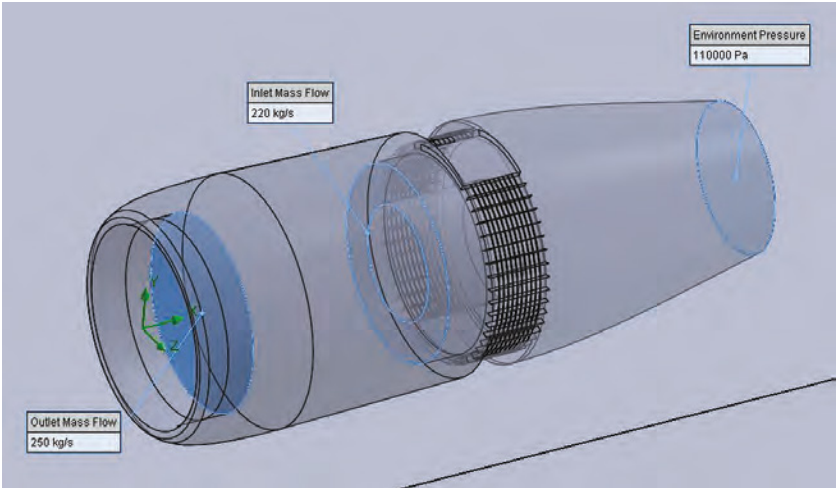


Figure 1. FloEFD Thrust Reverser Model with Boundary Condition Callouts

In the simulation we considered a groundspeed of 100 km/h during landing including the influence of the ground about 2.5m beneath the engines center line. The ambient temperature is 20°C at an atmospheric pressure of 1 atm. The bypass mass flow rate enters the cascade with 62.4°C and the core flow nozzle outflow is at 426.8°C and 1.1 bar. The whole engine was considered in half symmetry so the overall flow rate would be 500 kg/s at the intake and 220 kg/s at the bypass outlet into the cascades. That's actually a pretty small engine as the engine that drives the Boeing 787 Deamliner has 2.5-times the mass flow rate and a thrust of around 240-330 kN, depending on the engine model.

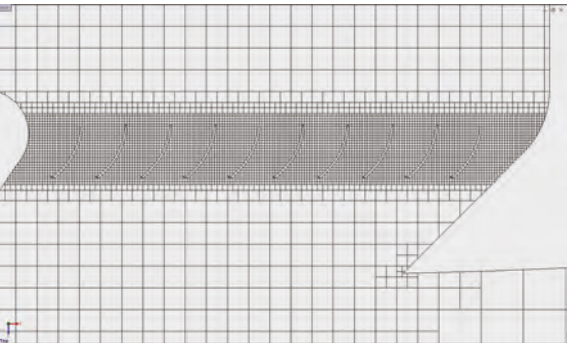


Figure 2. FloEFD Mesh with Local Refinement at the Guide Vanes

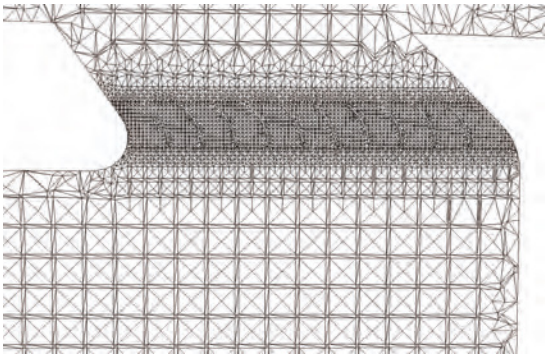


Figure 3. Traditional Tetrahedral CFD Mesh with Local Refinement at the Guide Vanes

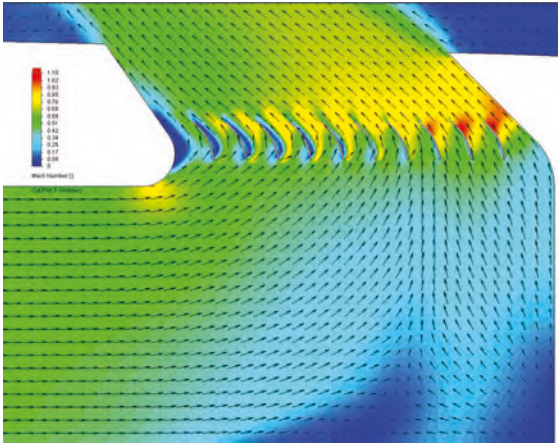


Figure 4. Velocity Contours Plot through Chamber and Vanes with FloEFD

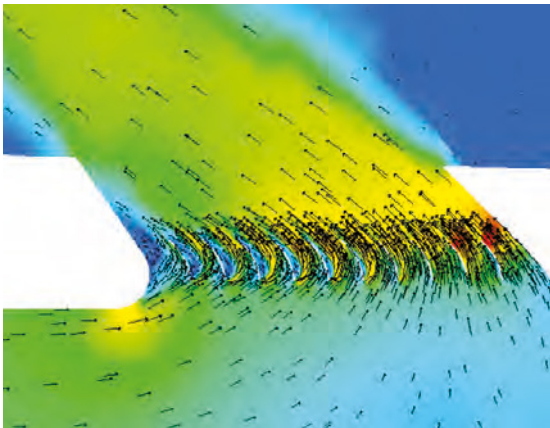


Figure 5. Velocity Contours Plot through Chamber and Vanes with Traditional CFD Tool

For the FloEFD mesh settings we applied two local meshes, one around the engine and another over the guide vanes in the cascade in order to resolve the gap between the vanes with around 10 cells. This resulted in an initial mesh of 4,995,315 cells and was meshed in ~22 minutes (Figure 2). The mesh with the traditional CFD software was made of tetrahedral cells and resulted in a mesh of 9,401,189 cells (Figure 3). The same boundary conditions were applied and also the same post processing conditions such as the reference pressure which is necessary to calculate the forces correctly.

$$R_{jet} = F_{vane} + F_{chamber} + I_{in}$$

Where F_{vane} is the force acting on the guide vanes of the cascade, $F_{chamber}$ is the force on the chamber walls before the flow exits through the vanes, and I_{in} is the inlet impulse at the inlet boundary condition of the bypass where the flow is entering for the thrust reverser cascades.

Since we want to know the reverse thrust the forces are the X-component of the forces on the model which were acquired by the use of goals on the model.

The impulse can be calculated as:

$$I_{in} = \int [(P - P_{ref}) - \rho u^2] dS$$

Where P is the static pressure at the inlet of the bypass, P_{ref} is the mentioned reference pressure of 1 atm, ρ as the air density at the bypass inlet and u is the x-component of the flow velocity at the bypass inlet. This results in an impulse of -63,700 N for FloEFD and -62,287 N for the traditional CFD.

The forces on the vanes are 54,464 N for FloEFD and 57,388 N for the traditional CFD tool and for the chamber in FloEFD the forces are 45,307 N and for the traditional CFD tool 42,654 N.

This then leads to a resulting reverse thrust of 36,071 N for FloEFD and 37,755 N for the traditional CFD tool. If we compare the calculation results to each other we can see from the resulting reverse thrust that the traditional CFD tool has a 4.5% higher thrust than FloEFD.

But remember that we compare two codes against each other. This might mean that the one result is 2.25% below the physical test and the other is 2.25% above. However, the two results are very close to each other.

When looking at the result in more detail we can see that there is flow separation at the first five vanes and the flow reaches supersonic flow at the last three vanes in both tools (Figure 4 + 5) where both color scales show the Mach number ranging from 0 to 1.1 from blue to red respectively.

All in all, there is a pretty good comparison between the two codes considering that traditional CFD tools are considered high-end CFD expert tools and FloEFD a CAD embedded CFD tool for design engineers. FloEFD was developed for the Russian Space Program, where it is still in use today, as well as a variety of aerospace applications much like this example.

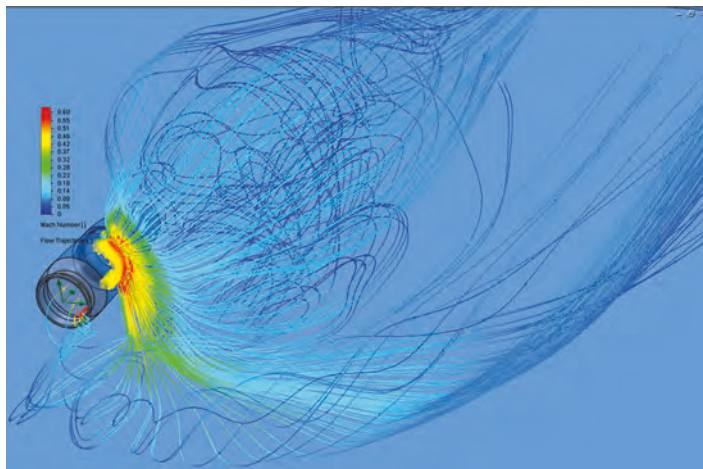


Figure 6. Flow trajectories of the thrust reverser flow in FloEFD

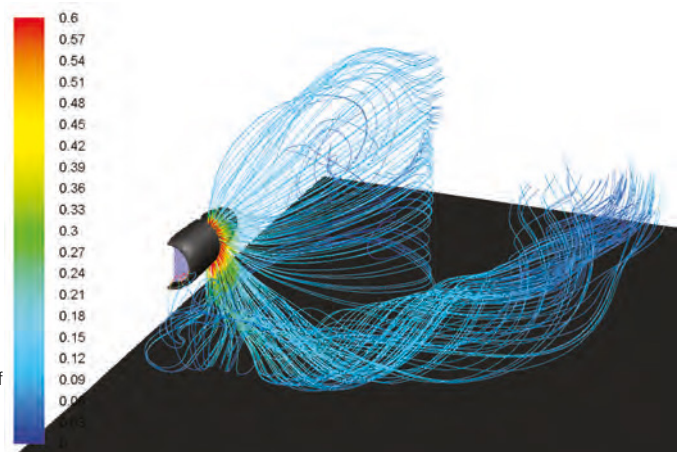


Figure 7. Flow Trajectories of the Thrust Reverser Flow in the Traditional CFD Tool

Advanced Natural Convection Cooling Designs for LED Bulb Systems

By James Petroski, Snr. Application Engineer, Mentor Graphics

The movement to LED lighting systems worldwide is accelerating as energy savings and the reduction in hazardous materials increase in importance. Government regulations and rapidly lowering prices help to further this trend. Today's strong drive is to replace light bulbs of common outputs (60W, 75W and 100W) without resorting to Compact Fluorescent (CFL) bulbs containing mercury while maintaining the standard industry bulb size and shape referred to as A19.

For many bulb designs in the USA, this A19 size and shape restriction forces a small heatsink which is barely capable of dissipating heat for 60W equivalent LED bulbs with natural convection for today's LED efficacies. 75W and 100W equivalent bulbs require larger sizes, some method of forced cooling, or some unusual liquid cooling system. Generally none of these approaches are desirable for light bulbs from a consumer point of view. Thus, there is interest in developing natural convection cooled A19 light bulb designs for LEDs that cool far more effectively than today's current designs.

Current A19 size heatsink designs typically have thermal resistances of 5-7°C/W. This article presents designs utilizing the effects of chimney cooling, well developed for other fields that reduce heatsink resistances by significant amounts while meeting all other requirements for bulb system design.

Current LED light bulb designs are essentially composed of three regions: a base at the bottom for installing into a luminaire, a central region which is a heatsink and contains space for the electrical driver (power supply), and the upper region which is the optical portion of the bulb where the LEDs reside and some type of optical beam spreading system (Figure 1).

To determine the effectiveness of a typical LED bulb, several commercially available bulbs were bought and tested to determine heatsink and system performance. There were two criteria chosen to evaluate them. First, the heatsink itself was evaluated for its convective thermal resistance. This is a straightforward calculation using the average surface temperature, power dissipated and ambient temperature.

The heatsinks showed nearly isothermal conditions under test when examined with an infrared imaging camera (a commercial FLIR SC620 was used in this investigation). Second, a modified dimensionless parameter was chosen to evaluate the bulb system level performance.

Potential Solutions for Performance Shortfall

One potential solution for this performance shortfall is to consider chimney type designs. Chimneys have existed long before the modern era and been adopted for use in electronics cooling in various applications. Perhaps the earliest example of modern research in this area is that of Ellenbaas with his work examining free convection of parallel plates and vertical tubes with parallel walls in the 1940's [2]-[3]. In subsequent decades the research has continued including up to the present time. For example, in the 1970's and 1980's much

work was conducted around shrouded heatsink concepts, though the work has continued to the present time.

However, a typical LED bulb design lacks one primary element for a chimney design - there is no central core opening. Since many chimneys are of cylindrical shape, this suggests that a design with a cylindrical light guide for the LEDs could be created and allow for a central thermal chimney.

Annular Chimney Design (V3)

One proposal for such a solution is shown in Figures 2 and 3. This bulb assembly still has the same base in the same location, but the LEDs, optical elements and the heatsink all occupy the same general region of the bulb. There is a solid central core about 26mm in diameter, then an open annular region which comprises the through chimney, and an outer area with the LEDs, light guide and

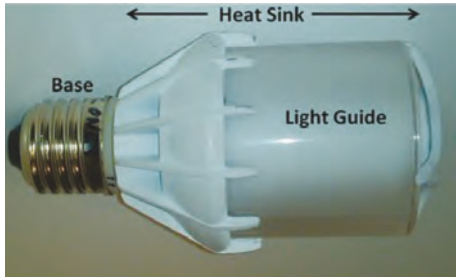


Figure 2. Prototype V3 Assembly

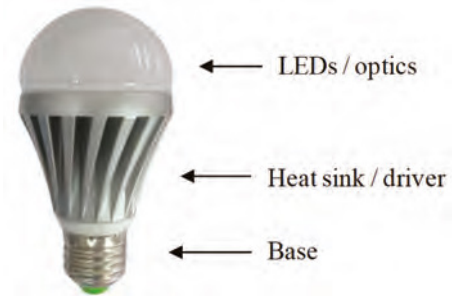


Figure 1. LED Light Bulb Construction

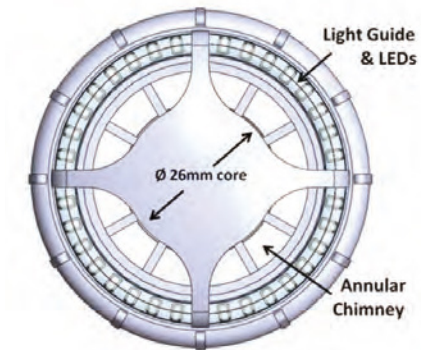


Figure 3. V3 Top View with Annular Chimney



other support structure. The entire assembly fits within the A19 envelope defined by the ANSI standard. This particular design was designated prototype V3 (version 3).

As seen in Figure 2, a prototype bulb was constructed. The main heatsink was made by the lost wax casting process with a standard aluminum casting alloy. Other parts except the base were machined, and different printed circuit boards (PCBs) were created for different testing conditions. Two types of PCBs were created: one with actual LEDs, and a second with surface mount resistors. The latter design allowed for more accurate measurement of thermal input energy. LEDs can be used but accurately knowing the thermal input energy is difficult; one must accurately measure the radiometric light output energy for an input electrical energy to measure the difference, and light energy can be reabsorbed into the system and become an input load.

The V3 design was tested to understand overall system performance and compared to computational fluid dynamics (CFD) numerical solutions using FloEFD™.

CFD simulations were conducted to correlate to the various tests. In the vertical orientations, about 150,000 cells were used and horizontally about 100,000 cells were used. Sufficient room above and below

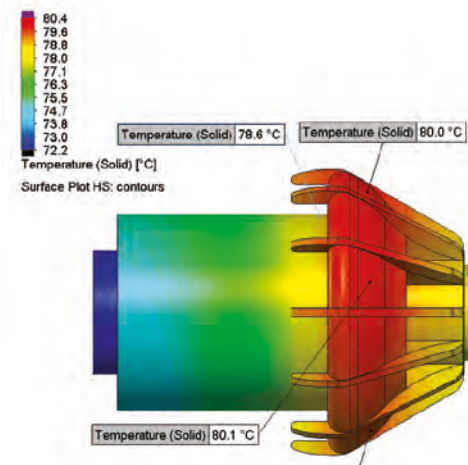


Figure 4. CFD Image of V3 Horizontal Position

Test Case	Location	T/C	IR Image	CFD
Vert Up	Outer HS Chimney	*see text	73.7	73.6
		71.6	n/a	72.5
Vert Down	Outer HS Chimney	74.4	75.2	74.4
		71.3	n/a	73.0
Horizontal	Outer HS Chimney	78.1	80.7	80.1
		75.9	n/a	78.6

Table 1. CFD Image of V3 Horizontal Position

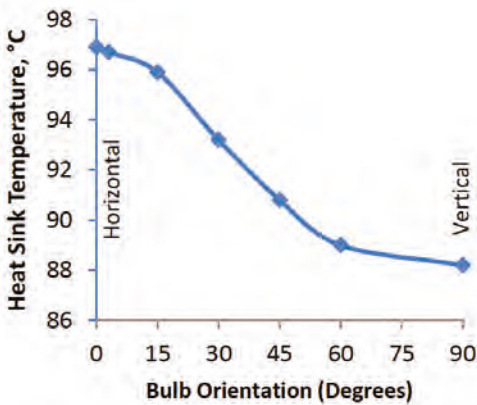


Figure 5. V3 Design Orientation Sensitivity

the lamp (as defined by the gravity vector) is used for proper flow development, and one bulb diameter around the sides was adequate for spacing around the bulb without influencing results unduly. Mesh sensitivity studies were conducted primarily by increasing the number of partial cells FloEFD uses, which refines the mesh around the fluid to solid boundaries (partial cells are part solid, part fluid and a unique cell used by FloEFD). Maximum cell counts of five to six hundred thousand cells were solved and compared to coarser meshes; results were found to be 0.1 to 0.2°C different from the coarser meshes so the coarser meshes were deemed acceptable. In all CFD simulations, radiation was selected as part of the solution routine. The heatsinks were painted with a special white paint and the emissivity was measured to be 0.975 on both the heatsinks and a special flat panel painted sample.

A few pertinent observations should be made from these results. First, the thermocouple used to measure the outside heatsink temperature in the Vertical Up orientation was not attached properly and is quite sensitive in this orientation (the “*” entry in Table 1). Although this was found later, the test was not repeated though in other orientations the thermocouples gave reliable results. Other temperature differences are within instrument errors. Second, there is a noticeable improvement in the heatsink thermal resistance (nearly 20% better than any of the commercial bulbs tested). Third, horizontal performance is worse – not surprising, since chimneys are meant for vertical operation. As seen in Figure 5, angles from 45° to 0° showed significant increases in temperature for the heatsink (0° indicates horizontal, and 90° is vertical up). This graph is based on the verified CFD model dissipating higher power levels at these angles. Variations between vertical (90°)

and tipped to 45° showed only modest increases in overall thermal resistance.

Other variations of this V3 design were modeled to see how much improvement could be made over this design. They included varying the number of internal fins in the annular chimney and varying the fin height.

Chambered Design with Annular Chimney (V6)

Given the limitations of the V3 design, another solution was sought. The vertical solutions needed to be better, and some method to improve the horizontal system performance would be needed for bulbs with higher power levels than used for tests in V3.

An advanced chimney system was devised and prototyped, still remaining within the design outline of an A19 bulb. This system involves a unique chamber internal to the chimney yet is open to the lamp bottom, sides and top. The annular chimney is thus split into separate chimneys – in this case, the “Y” shaped chamber creates the three of them – to allow the chamber access to the various sides of the bulb. This heatsink geometry is shown in Figures 6 and 7. Test results at 11.9W of thermal power showed that the V6 heatsink thermal resistance is 4.0°C/W. This is an improvement of 13% over the V3 performance at a similar power input. It is



Figure 6. Prototype V6 Assembly

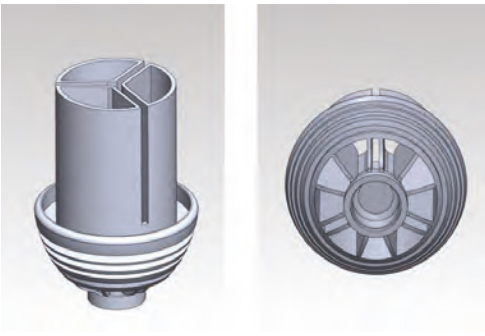


Figure 7. V6 Heatsink Detail

a fair assessment to state the efficacy of a chamber and chimney type system is a large improvement over the typical LED bulb design (a one third reduction over the typical LED lamp tested).

The significant improvement is the improvement in system thermal resistance though there is still room to improve the convective path, and the conductive path is relatively similar to before. The performance improvements were created by better airflow patterns in the design. Vertically there are strong drafts created in the chimney and chamber sections. Velocities 200mm above the bulb reached nearly 0.6 m/s in the CFD simulation, indicating a strong draft created by the bulb design, and over 10% higher than the V3 design. Reducing the LED driver core size opens the annular region in V6 to permit greater airflow, along with optimizing the flow paths.

Furthermore, the chamber design has an advantage over the pure chimney design in the horizontal orientations. As noted earlier, one drawback of a pure chimney design is poor horizontal performance. The V3 design horizontal R_{θ} gains 0.74°C/W to 5.34°C/W. In the V6 design, there is a slightly larger difference but the overall system performance is significantly better than V3. The V6 temperature gain is 10.2°C and the thermal resistance gain is 0.86°C/W. Table 2 shows a summary of the performance differences in the orientations. For horizontal use, the chamber construction is designed for external air to

Parameter	Vert Up R θ , °C/W	Horiz R θ , °C/W
V3 Chimney	4.6	5.34
V6 Chamber	4.0	4.86

Table 2. V3 and V6 Heatsink Differences by Orientation

pass through the “Y” shape. From a CFD analysis in one horizontal orientation, one can see the airflow through the chamber as shown in Figure 8. As expected, the chamber provides cooling in horizontal orientations that standard chimney designs such as V3 cannot.

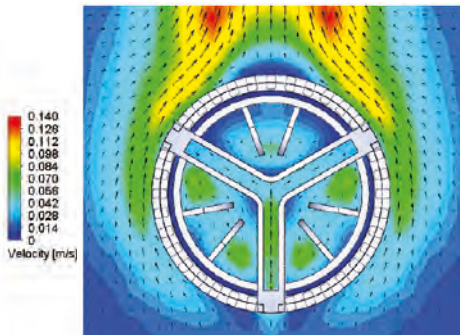


Figure 8. Airflow in Chamber, Horizontal Orientation

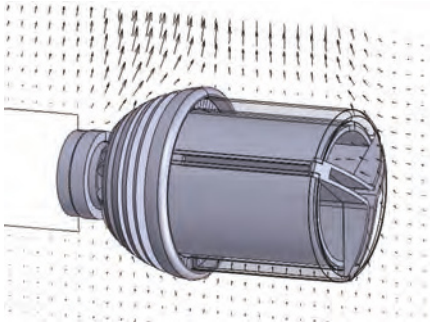


Figure 9. Air Flow into Chimney Core

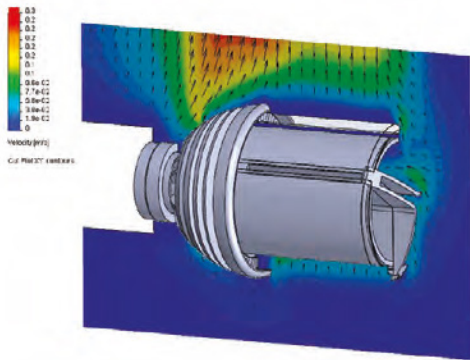


Figure 10. Velocity Vector & Contour Plot

However, one surprising finding from simulation was that the chamber created the movement of air into the chimney regions when horizontal which provided more cooling. The velocity vector plot of Figure 9 shows this air flow (seen near the top cap in the right of the figure). Figure 10 shows a similar view with color contours.

This airflow inducing effect of the chamber will be studied in a later paper. It is primarily due to the chamber creating a particular draft that imparts momentum to surrounding air and pushes this external air into the surrounding chimneys.

Chambered Design with External Fins (V8)

While V6 is better than V3, it was clear the thermal performance is not enough for a 100W equivalent bulb dissipating 18W. At 4°C/W and a 55°C ambient, the boundary condition temperature for the LED printed circuit board (PCB) would be 127°C, and the resulting junction temperature would likely be 135°C or higher (exact temperature would depend on the LED model and drive current applied). To keep the junction temperature below 120°C (a common maximum), the heatsink should not exceed 110°C. This 55°C rise over ambient for 18W applied means the heatsink resistance should not exceed 3°C/W as a design goal. To achieve this, a similar heatsink to V6 was created with a 2mm larger outer diameter for the annulus outer core, and external fins

added outside the light guide section. The lower heat sink section was redesigned for better inlets. Other dimensions were kept the same as V6 and the overall outline was kept within the A19 envelope. Even with the addition of the fins and larger chimney annulus, the heatsink areas are nearly identical between V6 and V8 (39,035 vs 38,705 mm²). Figures 9 to 11 show the V8 bulb and heatsink. The V8 prototype was tested and simulated at a number of power levels and orientations. A resistor PCB was used with input powers of approximately 6, 9, 13, 17 and 21W, and simulations were conducted

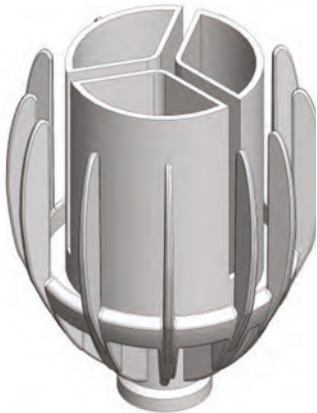


Figure 11. V8 Heatsink detail



Figure 12. Prototype V8 Assembly

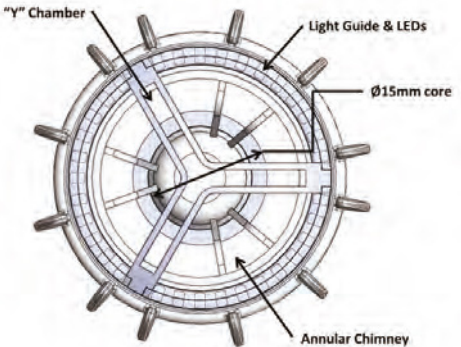


Figure 13. V8 Assembly Top View

with 9, 13 and 21W of input power. IR and thermocouple data were within 1.5°C for all tests. Simulation mesh dependency studies were conducted similar to the process described for V3 to ensure adequate mesh density for the simulations. Figures 14 and 15 show some of the test and simulation results.

The V8 prototype performed significantly

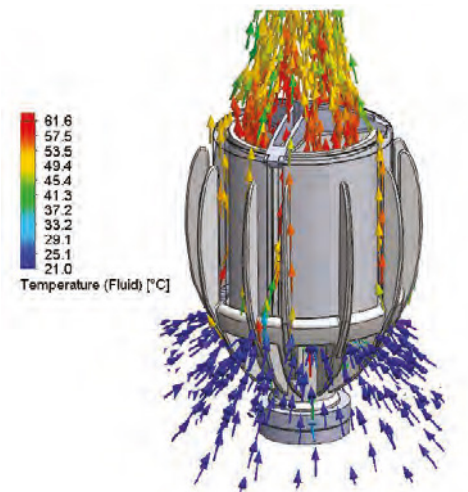


Figure 14. CFD Simulation of V8 Vertical Up Test

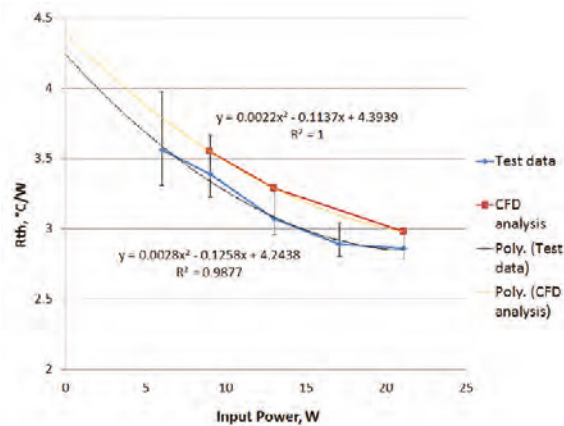


Figure 15. Performance of V8 in Vertical Up Orientation

better than the V6 design. As seen in Figure 15, the results show reasonable agreement for the tests and the simulations. By performing an examination across a wider range of thermal input powers, a general performance diagram of the heatsink can be generated. Table 3 shows results for the vertical up orientation. The test data is the average of the thermocouple and the IR image data, and the error estimates based on the possible worst errors for the type of measurement. For each data set, a second order polynomial curve fit was applied and the equations shown.

A few important observations are found

from this performance chart. The simulation solutions are conservative compared to the actual tests though close to the upper end of the experimental error band. Small air currents in the lab may account for this as the simulation assumes perfectly still air. The outer fins are very effective at removing heat in the presence of low air currents. Second, the V8 design performance is a large improvement over the V6 design. At 11.9W of input power, the heatsink resistance is about 3.1°C/W, almost a 25% improvement in the vertical orientation. At the higher power levels for 100W equivalent bulbs (18W input), the heatsink tests just below 3°C/W, meeting the design target. Third, the two key changes in the V8 design account for the improved performance – the larger annular region (2mm larger outer diameter) and the fins. Simulations show the outer fins account for about 2/3 of the improvements, and the larger annular region the other 1/3.

The values for Table 3 use approximately 12W of input power for V3, V6 and V8 designs. The commercial LED lamps ranged from approximately 7W (40W equivalent bulb) to 13W (60W equivalent). Even as the convective resistances of the new designs are an improvement over the commercial units tested, it is still a significantly higher resistance than the conductive resistance in the system. Finally, the horizontal performance of the V8 prototype is also significantly improved over the V6 design. The external fins provide significant new cooling paths in the horizontal orientation.

Conclusions

Several interesting results have been found during this study. First, the current design of LED bulbs performs adequately for the current power dissipations but will not be enough for future 75 and 100W equivalent bulbs. Second, rather than a standard central LED engine design, a cylindrical LED layout and light guide with a chimney enhances thermal performance and can still fit within the desired A19 design envelope. Last, a novel chimney and chamber design was developed for enhanced performance. Unusual air flows were noted as well in horizontal positions and will be evaluated in future work.

Though the V8 prototype design is far better than current designs, it is a bit marginal of a system that will adequately cool the 100W equivalent light bulb at 2.9°C/W. Future work will look at designs beyond the types shown in this paper (and beyond this paper’s scope) that again reduce the overall system thermal resistance – allowing a 100W natural convection cooled LED bulb to fit within the A19 envelope.

References:

[1] Proceedings of the ASME 2013 International Technical Conference and Exhibition on Packaging and Integration of Electronic and Photonic Microsystems InterPACK2013 July 16-18, 2013, Burlingame, CA, USA

[2] W. Ellenbaas, “The Dissipation of Heat by Free Convection from the Inner Surface of Vertical Tubes of Different Shapes of Cross Section,” Physica, 9, pp 865-874, Sept 1942.

[3] W. Ellenbaas, “Heat Dissipation of Parallel Plates by Free Convection,” Physica, IX, No. 1, Jan 1942

Parameter	Vert Up Rθ, °C/W	Horiz Rθ, °C/W
V3 Chimney	4.6	5.34
V6 Chamber	4.0	4.86
V8 Chamber	3.1	3.83

Table 3. Heatsink Differences by Orientation (12W power)



Avoiding Hot Spots

Discom B.V. use FloEFD™ to ensure Temperatures are kept within Bounds



In their 30 years as designers and suppliers of exhaust gas systems, Discom B.V. have seen the requirements regarding noise and emissions change and tighten considerably. Investment in research and development is therefore critical to creating new designs and ensuring the continued success of the company.

The challenges they face come not just from meeting or exceeding regulatory requirements, but also to ensure that the systems offer high reliability over their design lifetime. These requirements are made more complex due to the need to ensure that the final design can be practically installed and maintained within the often tight spaces set aside for them.

Given these requirements, it's essential that the tools that support the design process are integrated within the overall suite used, and can provide clear and reliable results with the minimum of user intervention. It's for these reasons that FloEFD, operated by HEC on behalf of Discom, can prove so valuable. For instance, when considering the lifetime estimation of thermal loading on an exhaust silencer for a train, the CAD embedded nature of FloEFD allowed for even this complicated geometry to be prepared and discretized with minimum effort. The results from the simulation can then be fed in to the structural finite element package to define the boundary conditions for the resulting simulations.

Underpinning all such work are two key aspects of the FloEFD package: a comprehensive materials library, which allows for the thermal properties of both metals and insulation materials to be accounted for. In addition, an advanced

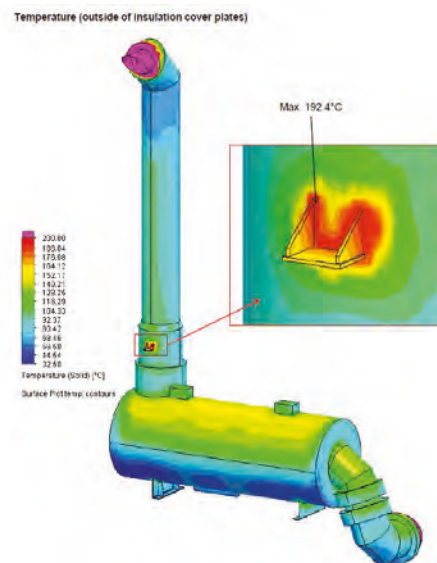


Figure 1. Identification of Local 'Hot Spot' in Train Exhaust Systems

radiation model allows for the effects of these materials, their surface finish and even solar radiation to be accounted for. When such detail is applied alongside a detailed CAD model, it is easy to identify and predict individual hot-spots should they occur. Being able to do all this 'upfront' in a virtual environment ensures that the optimum configuration can be derived before any metal has been cut.

For more information:
www.discom.eu



Figure 2. Discom B.V. headquarters in The Netherlands

ShowerPower®

Turbulator keeps

IGBTs Cool

FloEFD™ Efficiently Cools IGBT Power Modules

By Klaus Olesen, Thermal Design Specialist,
Danfoss Drives, Germany



The ShowerPower® liquid cooling heat exchange turbulator (Figure 1) was designed in 2005 by Danfoss GmbH engineers to efficiently cool IGBT power modules. The driver at the time was the fact that every electronic circuit generates heat during normal operation (except perhaps for superconductivity scenarios which are rare in industrial situations).

availability of liquids in certain applications. Liquid cooling outperforms air cooling by producing heat transfer coefficients several orders of magnitude higher, thus enabling much higher power densities and more compact module and inverter solutions. The acceptance of liquid cooling varies from business segment to business segment. The automotive industry for example has been using liquid cooling

for internal combustion engines for more than a century, so the idea of liquid cooling of power electronics in an automotive application is considered a non-issue. In other industries the idea of having fluids flowing through power electronic assemblies often finds resistance and concerns. The term “turbulator” for the ShowerPower is a little misleading: under normal flow conditions, liquid flow in the flow channels

This heat generation is due to conductive and switching losses in active devices as well as ohmic losses in conductor tracks. And since every new generation of power semiconductors becomes smaller than the preceding one, and the market expects smaller and more compact solutions, the demands to be met by the thermal design engineer kept growing. Sufficient cooling of power electronics is therefore crucial for good operational performance. The dominant failure mechanisms in power semiconductor components are related not only to high absolute temperatures but to changes in temperature during cycling; temperature swings produce thermo-mechanically induced stresses and strains in the material interfaces of the components (that have mismatches in coefficients of thermal expansion) which in turn lead to fatigue failures.

Liquid cooling of power electronics has been around for many years, primarily because of the ever-increasing power densities demanded, and due to the

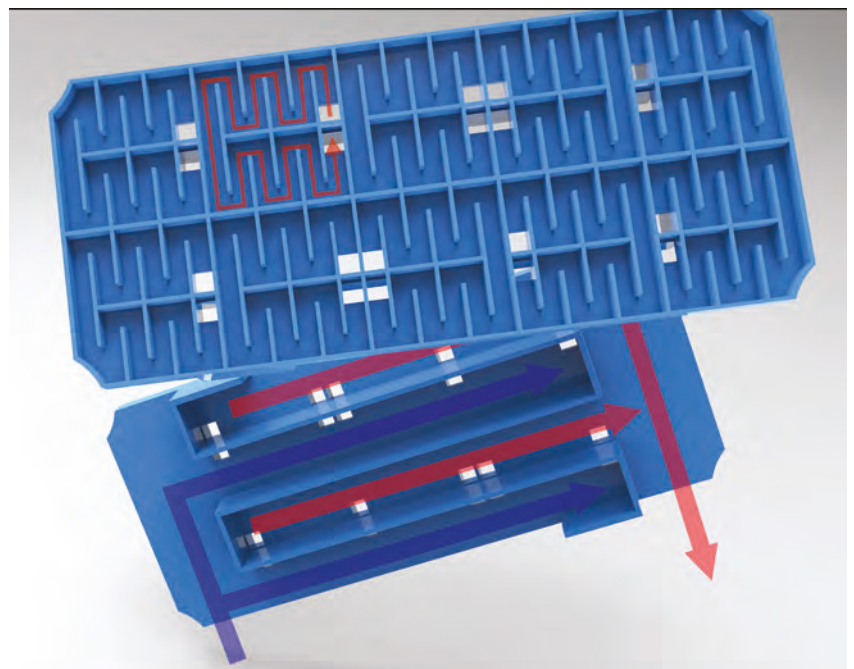


Figure 1. The general Danfoss ShowerPower® turbulator concept (cooling liquid in blue; warmed up liquid in red)

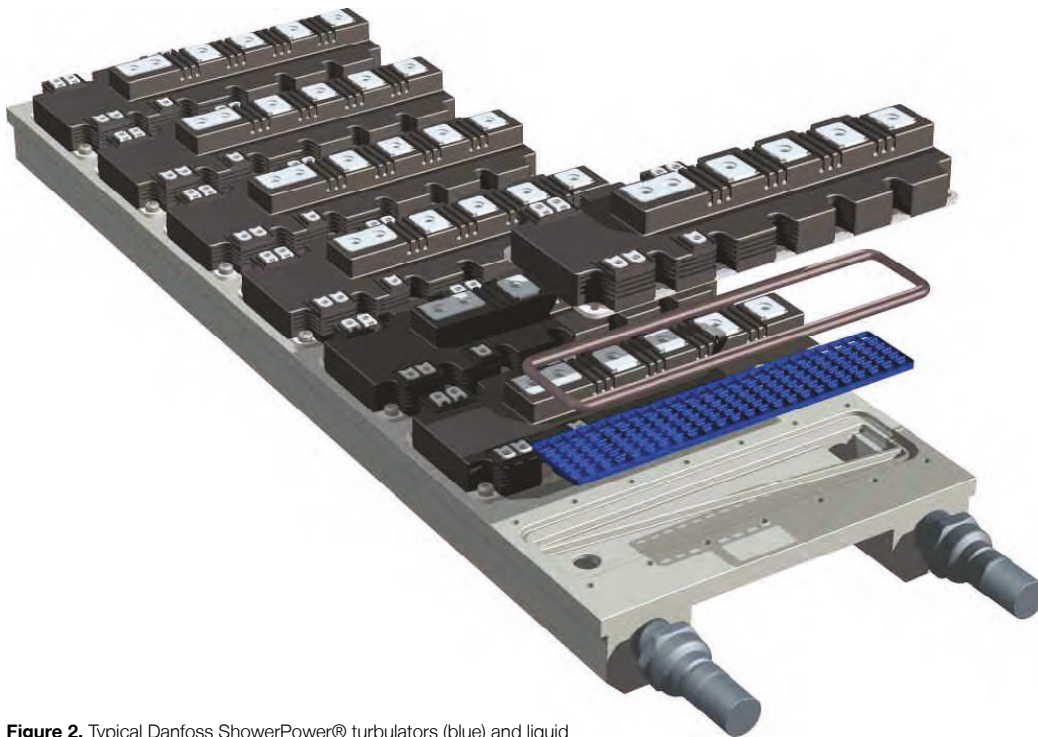


Figure 2. Typical Danfoss ShowerPower® turbulators (blue) and liquid cooling base plate for seven P3 power electronics modules in parallel

is laminar; typical Reynolds numbers range around 500 and the transition into the turbulence regime occurs at a Reynolds number around 2,400.

Liquid cooling solutions may be divided into two groups - indirect and direct liquid cooling. Indirect cooling means that the power module is assembled on a closed cooler, e.g. a cold plate. Cold plates may be manufactured by for example gun drilling holes in aluminum plates or by pressed-in copper tubes in aluminum extrusions. When dealing with cold plates it is necessary to apply a layer of TIM (Thermal Interface Material) between the power module and the cold plate. Direct liquid cooling on the other hand means that the coolant is in direct contact with the surface to be cooled. Here the cooling efficiency is improved by increasing the surface area and this is commonly done by various pin fin designs. Direct liquid cooling (Figure 2) eliminates the otherwise required layer of TIM. Because the TIM layer accounts for 30%-50% of the R_{th} , junction-coolant, this TIM-elimination results in an improved thermal environment for the power module. Since dominant failure mechanisms are temperature-driven, this will lead to higher reliability of the power module.

The ShowerPower cooler assembly in Figure 2 is for a wind turbine application featuring seven P3 IGBT modules, turbulators, sealings and a manifold. The design ensures that all chips in all modules are cooled

equally efficiently. The concept enables tailored cooling if hot spots need extra attention; this is simply done by designing the cooling channels individually. For further information on the principles of ShowerPower please refer to References 1 and 2. The general ShowerPower plastic part (in blue) has several cooling cells in the X and Y directions and needs a manifold structure on the backside of the plastic part; this ensures that each cooling cell receives water at the same temperature. Since the P3 module is relatively long and narrow only one cell is necessary across the module; this makes the plastic part much simpler since the manifold structure on the backside becomes obsolete.

Overall, the ShowerPower concept has several inherent benefits:

1. The ability to homogeneously cool large flat baseplate power modules, and systems of modules, thereby eliminating temperature gradients thus improving life and facilitating paralleling of many power chips;
2. Eliminating the need for TIM - No TIM-related pump-out and dry-out effects;
3. A very low differential pressure drop,
4. Compact, low weight, high degree of design freedom enabling 3D designs; and
5. Low manufacturing costs: metal-to-plastic conversion into simple plastic

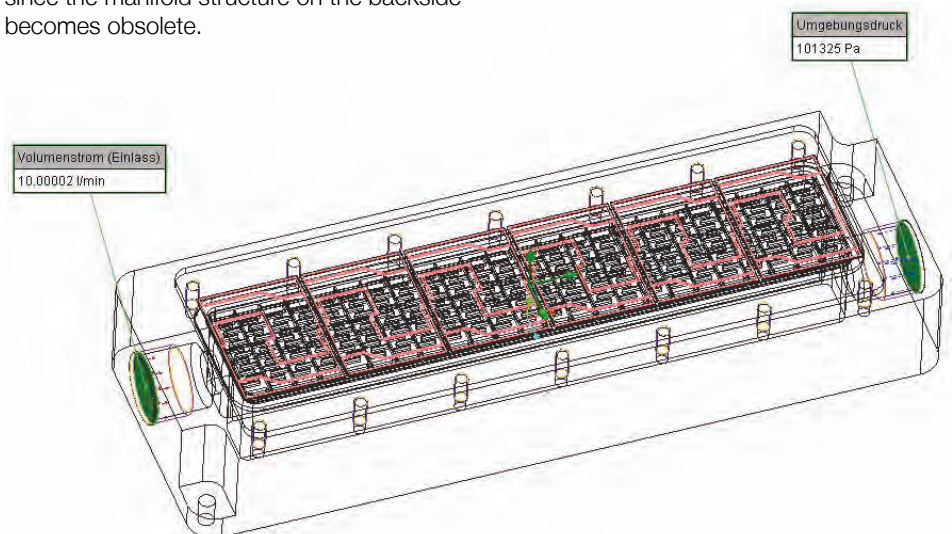


Figure 3. Typical Danfoss ShowerPower® liquid cooling CFD simulation of a Power Module geometry inside FloEFD for Creo

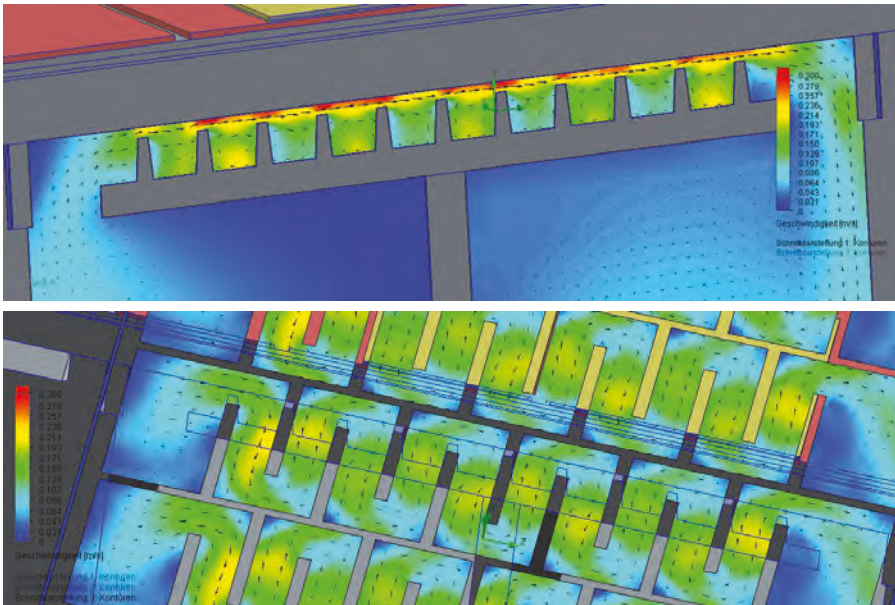


Figure 4. Typical Danfoss ShowerPower® liquid cooling CFD simulation of a Power Module geometry showing sectional views of flow vectors and velocity magnitude contours.

parts.

Numerous CFD simulations and test measurements have been done over the years on various Danfoss ShowerPower designs to validate the concept and to extend it to niche and custom applications. Engineering simulations, (thermal, fluid, mechanical, stress, vibrational etc.) are a crucial part in any Power Module product development project, the obvious reason being, to reduce the number of time-consuming and costly experimental tests necessary. Computational Fluid Dynamics, CFD, is the best way to simulate a ShowerPower liquid cooling system. CFD will predict fluid flow so that the correct heat transfer rates and pressure drop conditions are found and thus the relevant temperatures, e.g. semiconductor junction temperatures are calculated and maintained.

When designing a liquid cooled system in the FloEFD for Creo CFD package (Figure 3) we consider several issues in order to ensure a reliable solution that is capable of delivering the performance needed over the required lifetime of the system. We also consider other factors such as corrosion, “tightness”, sedimentation (including bio growth) and anti-freezing issues for instance. The permutations in the turbulator geometry are quite large:

- Width of channel;
- Depth of channel;
- Height of bypass;
- Amount of channels per meander; and
- Channel cross section area to avoid the risk of blockage.

Figure 4 illustrates such a CFD prediction for a typical ShowerPower application. With FloEFD we can easily create several

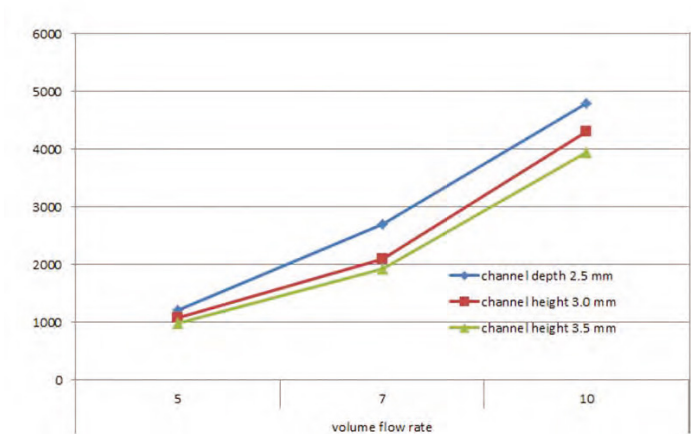


Figure 5. FloEFD Pressure drop curves for different volume flow rates in the ShowerPower®

different simulation cases to allow the design engineer to make optimization judgements. Finding the best design out of many CFD cases is supported by effective parametric results comparison in the software. We are able to look at many different channel dimensions for a range of flowrates (Figure 5). FloEFD ultimately gives us predictions of the surface temperatures on the IGBT/ShowerPower system before we iterate to a final prototype and build and

test it (Figure 6).

References:

1. K. Olesen et al., “ShowerPower® New Cooling Concept”, PCIM Conference Proceedings 2004, Nuremberg.
2. K. Olesen et al., “Designing for reliability, liquid cooled power stack for the wind industry”, EWEA Conference Proceedings, Copenhagen, Denmark, 2012.

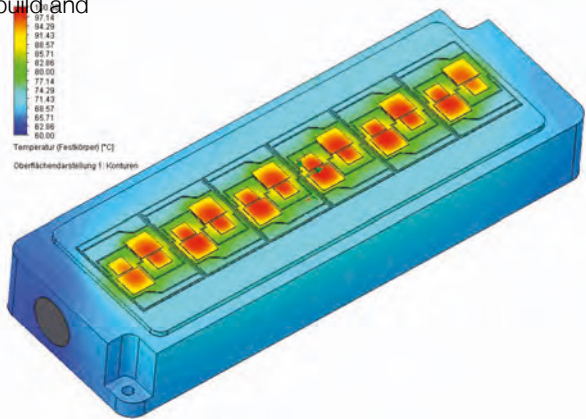


Figure 6. CFD temperature surface plot on a Danfoss Power module with an operating ShowerPower®



The Three Waves of Commercial CFD

By Ivo Weinhold, User Experience Manager
and John Parry, Mentor Graphics

In recent years, many papers have been published on the history of flow simulation. Many early CFD pioneers like Brian Spalding, David Tatchell, Ferit Boysan and Michael Engelman have talked or written about their memories. This pool of historical facts, technical information and personal impressions give a remarkably consistent description of the way engineering simulation software evolved from academic research codes towards the modern CFD products we know today. Developed and supported on an industrial scale by multinational software companies.

Closely linked to the performance of available computing hardware, this development was, particularly in the early stages, driven primarily by research and development projects for aerospace and defense, but latterly also increasingly by interest from civilian industry. Looking back, three major phases of the development of CFD software for industrial applications can now be recognized:

- The First Wave: The beginnings of commercial CFD software in the 70s and 80s.
- The Second Wave: In the 90s, CFD enters the research and development departments of large industrial enterprises.
- The Third Wave: After the millennium, CFD becomes an indispensable part of the product development process.

The First Wave: The beginnings of commercial CFD software

Since 1958 the codes of the CFD software engineers in the first phase had its roots in the work of the Fluid Dynamics Group T-3 at the Los Alamos National Laboratory (USA), and the research activities under Prof. D. B. Spalding at Imperial College London in the 1960s and 1970s.

In the late 1960s, Concentration, Heat and Momentum (CHAM) Ltd., founded by Spalding, and initially located at Imperial College London, dealt with consulting work. The era of commercial CFD software began in 1974, when CHAM Ltd moved to its own offices in New Malden near London. Initially, the development of customized CFD codes was central to the business activities of CHAM. That became too time-consuming and inefficient, so CHAM decided to develop a general-purpose CFD package for in-house consultancy work, and released this as a commercial product, PHOENICS, in 1981. This may well be regarded as the birth of the CFD software industry (see CHAM Ltd, 2008). Others quickly followed suit. For instance, Fluid Dynamics International (USA) followed in 1982 with FIDAP, a FEM-based CFD package, and in 1983 Creare Inc (USA) released the finite-volume CFD code, Fluent. Computational Dynamics/ADAPCO (UK/USA), co-founded by Prof. David Gosman, another professor at Imperial College London, released StarCD in 1989.

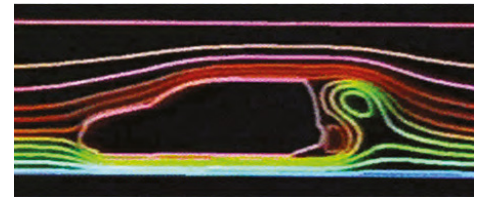


Figure 1. Fluid flow simulation in the 1980s, taken from Hanna & Parry (2011)

The basic technologies behind most of the CFD packages of this era had been created by former employees or guest scientists of the two aforementioned research institutions in London and Los Alamos, or were based on their scientific publications. But there were also other developments of CFD technology: in the 1980s alternative approaches for CFD simulation emerged as part of the military and civilian aviation and space program of the former Soviet Union, largely unnoticed by the Western scientific community due to the political situation. Their technical tasks for CFD simulations were similar to those in the West, but the available computing resource for their solution was much more limited. Conversely, because of the high political priority of these research programs, very extensive experimental data for numerous fluid flow and heat transfer phenomena, especially in the near-wall area, were generated. This situation led to the development of alternative CFD methods, which, building on known methods for

The Second Wave: CFD enters the Research and Development Departments of the Industry

Using technology typical of the first phase, Flomerics Ltd., founded in 1988 by David Tatchell and Harvey Rosten in Kingston-upon-Thames (UK), played a pioneering role in marketing CFD software developed exclusively for industrial applications with its software package FloTHERM, first released in 1989. Both founders worked for CHAM Ltd in senior positions before leaving to found Flomerics, with the aim of “providing good science to industry” (Tatchell, 2009). FloTHERM was a first paradigm shift in the CFD industry, away from the focus on complex CFD technology, towards the solution of engineering tasks in industry as the central goal. This also meant that from then on engineers working in product development, and not scientists, were the main target users of this type of CFD software. The available CFD technology, computer hardware and operating systems imposed certain limits on such an innovative approach. Therefore Flomerics concentrated initially on only two application areas: electronics cooling (with FloTHERM) and built environment HVAC (with FloVENT). The requirements of engineering-oriented CFD software for these application areas were relatively clearly defined and, more important, also just feasible.

This concept opened up completely new market opportunities, because for the first time engineers in product development without special knowledge of numerical methods and without extensive CFD

experience were empowered to employ CFD simulations as a development tool. The solution of a technical engineering task became the center of attention, while the underlying CFD technology was more or less just a means to an end.

Obviously, other CFD providers also recognized the beginning of this paradigm shift and especially the new business opportunities associated with it, responding to this trend with their own product offerings. Overall, huge investments from all CFD software vendors in better user interfaces, robust solvers and reliable physical models could be observed, with the clear objective of entrenching CFD into the research and development departments of large industrial enterprises and thereby attracting a new generation of CFD users.

After establishing CFD as a successful tool for the functional design, verification and optimization of product designs, features, processes and physical effects in large industrial companies in the early 2000s, the reputation of this technology amongst engineers improved significantly. As a result, the demand for CFD simulations showed strong growth, especially in medium-sized and small companies keen to reduce the costs associated with physical prototypes. Another important aspect was the need to integrate CFD simulation into the regular product development process, as these companies usually had as yet no

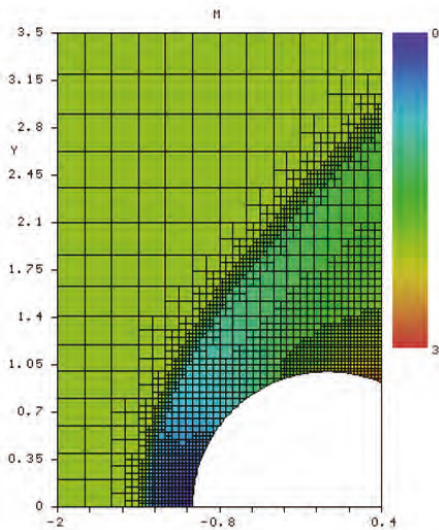


Figure 2. Result plot of Aeroshape-3D (Parry et al., 2012)

Cartesian grids as published in the scientific publications in the West, were based on a combination of numerical, analytical, and empirical data. This innovative approach yielded high-quality simulation results in virtually, arbitrarily complex computational domains while maintaining the low resource requirements and the effectiveness of methods using Cartesian grids. With the gradual economic liberalization in the Soviet Union in the late 1980s, several teams of scientists have commercialized this CFD technology and, since the early 1990s, sold their products and services in Europe and Asia. The best known products of this kind were Aeroshape-3D by Prof. V. N. Gavrilouk and team (Petrowa, 1998 & Alyamovskiy, 2008) and FlowVision by Dr. A. A. Aksenov and team (Aksenov et al., 2003).

From the beginning of the 1990s, the conditions for CFD software and simulations changed quite rapidly. Computer hardware, mathematical methods and physical models all experienced huge performance gains. Numerical methods such as unstructured Finite Volume methods, multi-grid methods, sliding mesh, etc., suitable for complex geometry and optimized for HPC, became commercially available as well as more reliable, more flexible and more broadly applicable physical models. CFD technology became much more feasible, and for the first time, quite realistic model sizes, for real industrial applications were possible. These new capabilities heralded a new phase in the usage of commercial CFD software - entry into the research and development departments of industry across the board.

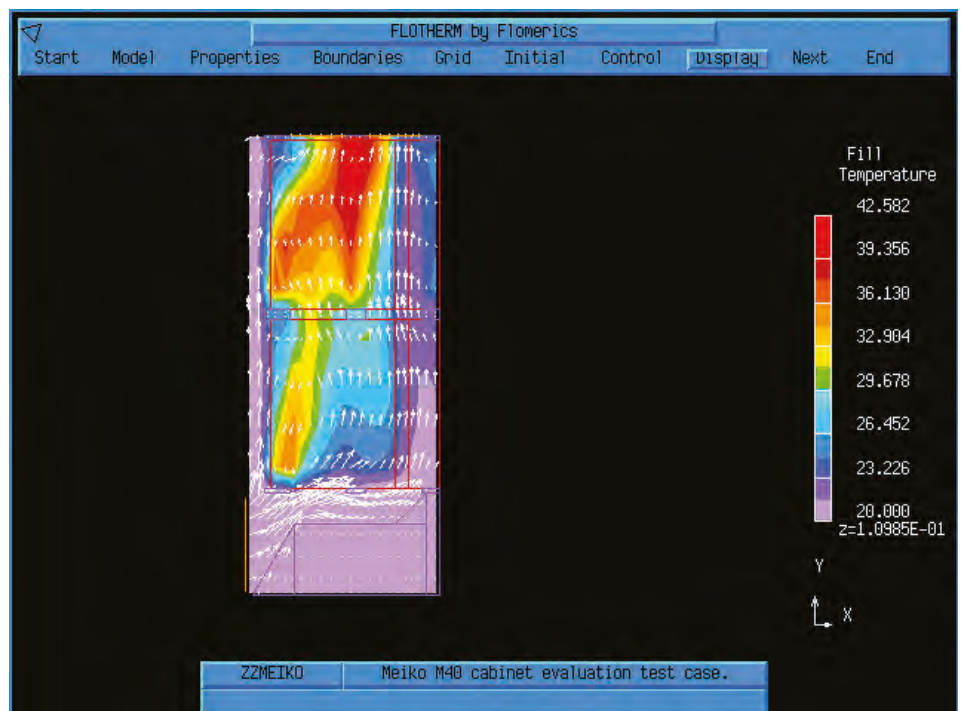


Figure 3. Early version of FloTHERM (Hanna & Parry, 2011)

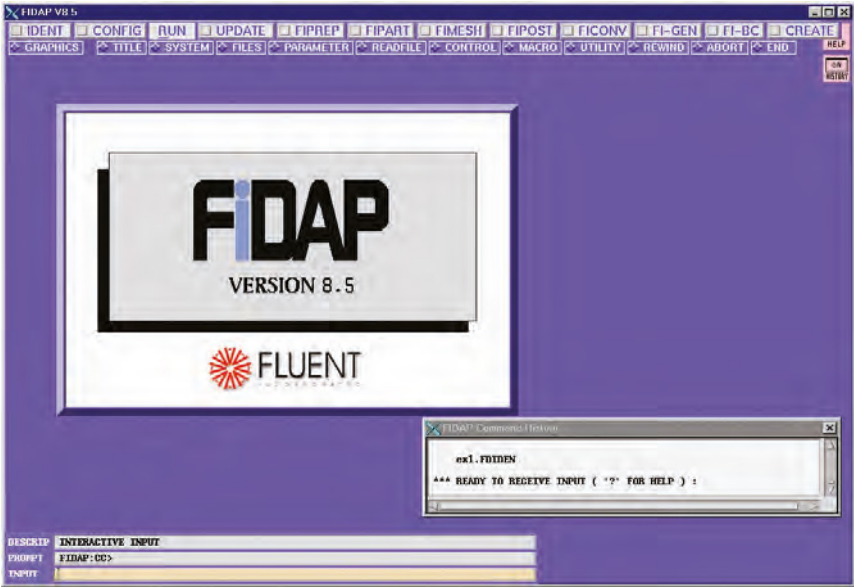


Figure 4. FIDAP User Interface in the late 1990s (University of Delaware, 2007) URL

dedicated simulation departments. This meant that qualified engineers from product development or design groups would perform the simulation themselves. The efficiency with which simulation projects were conducted had to be increased, so CFD results would be available sufficiently in sync with the product design cycles, for the results to help guide proposals for design improvements. In this context the handling of industry-level geometry played a key role. At that time this was already being provided as 3D CAD data which should, of course, be used with as little simplification and modification effort as possible to be useable by the subsequent and preferably fully-automated mesh generation step. The CFD software market responded to these demands with new and improved products – and a third wave of CFD software for industrial product design began and continues to this day.

The Third Wave – CFD Becomes an Essential Element of the Product Design Process

The major CAD and Product Lifecycle Management (PLM) vendors play a key role in this third phase. Since the 1990s, they have been successfully introducing the concept of PLM, which encompasses CAE. As a result, customers have put pressure on commercial CFD software vendors to conform to this concept and to take steps to integrate their products into the major PLM systems. In the 2000s, virtually all CFD software providers upgraded their systems with, at the least, CAD import interfaces. Some have developed bi-directional links with major CAD/PLM systems, and a few have even embedded their CFD technology directly into the 3D CAD systems themselves. New CFD techniques to support these requirements were also developed, partly from scratch, and partly as enhancements of existing technology.

The company NIKA GmbH, founded in 1999 as a German-Russian joint venture, was a typical example of a new commercial CFD software vendor emerging at the start of this third wave. NIKA exclusively developed, based on the above mentioned Aeroshape-3D technology, CAD embedded CFD software, which is now offered as FloEFD for several major 3D CAD systems.

The current third wave has allowed newcomers from other areas the opportunity to enter the CFD market, refreshing it with new technologies. But all have one thing in common: The industrial user, with his or her need for easy-to-use, task-oriented, automated, reliable, efficient and readily-available CFD software as an indispensable tool for digital prototyping is the focus. The result of changing development processes and, as a consequence, the changing role of the simulation engineer. Aspects like process integration, reliability, modeling safety, and reproducibility are becoming the center of attention, and influence purchasing decisions for CFD software. The further development of CFD software based around

these requirements will bring exciting new technologies and products to market. A new fourth wave may be expected to follow soon...watch this space.

References:

Aksenov, A. A., Kharchenko, S. A., Konshin, V. N., Pokhilko, V. I. (2003), FlowVision software: numerical simulation of industrial CFD applications on parallel computer systems. In Parallel Computational Fluid Dynamics 2003: Advanced Numerical Methods, Software and Applications, Elsevier, 2004, pp. 401-408

Alyamovskiy, A. A. (2008), SolidWorks 2007/2008. Компьютерное моделирование в инженерной практике, bhv-St. Petersburg, 2008, pp. 467-468

CHAM Ltd (2008), Earlier versions of PHOENICS: -81 to -1.6 A brief history. Available: http://www.cham.co.uk/phoenics/d_polis/d_chron/earlyver.htm

Hanna, K., Parry, J. (2011), Back to the Future: Trends in Commercial CFD, NAFEMS World Congress, Boston (Paper and Presentation Slides)

Parry, J., Kharitonovich, A., Weinhold, I. (2012), FloEFD – History, Technology & Latest Developments, Mentor Graphics, 2012

Petrowa, J. (1998), GUS - Informationstechnologien im CeBIT-Spiegel: Partner gesucht. ComputerWeekly, Volume 8, 1998. http://scripts.online.ru/it/press/cwm/08_98/gus.htm

Tatchell, David (2009), David Tatchell's Blog, Mentor Graphics, 2009. Available: <http://blogs.mentor.com/daviddtatchell/>

University of Delaware (2007), FIDAP/ GAMBIT. www.udel.edu/topics/software/special/statmath/fidap/

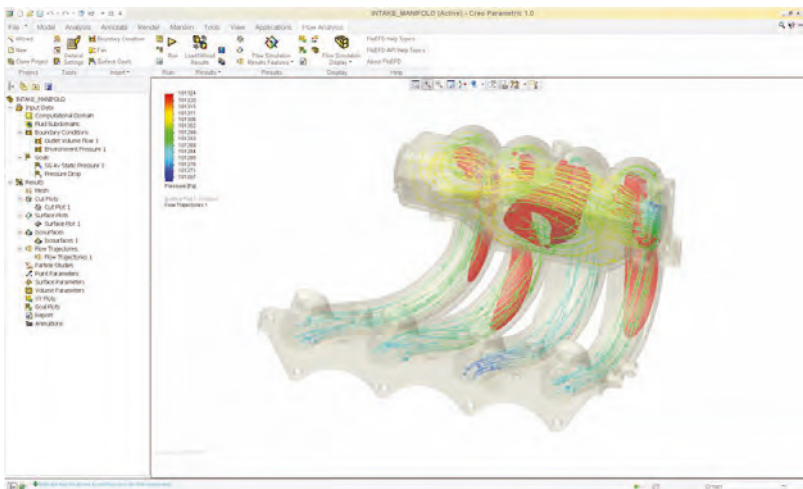


Figure 5. FloEFD for Creo by Mentor Graphics

Engineering Techniques for a Helicopter Rotor Simulation

By P.N. Subbotina, T.V. Trebunskikh, Mentor Graphics;
B.S. Kritsky, Sc.D., M.S. Makhnev, R.M. Mirgazov, Ph.D.,
TsAGI, Zhukovsky

The Central Aerohydrodynamic Institute named after N.E. Zhukovsky (TsAGI) was founded on December 1st, 1918 under the initiative and leadership of N.E. Zhukovsky, the father of Russian Aviation. It was the first scientific institution to combine basic studies, applied research, structural design, pilot production and testing.

During its distinguished history TsAGI has developed new aerodynamic configurations, aircraft stability/controllability criteria and strength requirements. It was a pioneer in the theory of flutter, along with many other theories, applications and experimental studies [1].

Today TsAGI is one of the largest scientific research centers in the world. Over the last few years, it has established contacts with a majority of research and development centers and aircraft manufacturers in Europe, the United States and Asia and has participated in a large number of joint research programs including the development of next-generation aircraft.

One of the main areas of TsAGI activity is investigating new configurations of helicopters in general, and helicopter rotors in particular. The new sliding technology of rotation brings FloEFD™ into the world of challenging problems in aerodynamics such

as the modeling of a helicopter rotor. This has allowed the validation of the single blade rotor model in cooperation with TsAGI. This technology became available in the latest release of FloEFD V14.0 which provides extended capabilities for simulations of rotating equipment such as pumps, fans, and blowers. With its new sliding technology the software extends the boundaries of simulating turbo-machinery equipment to the cases where fluid quantity is highly non-uniform around a rotating part.

The FloEFD code validation is performed against the experimental data obtained by L.S. Pavlov in 1979 [2] and the numerical data obtained by a traditional CFD code and by the TsAGI specialized software product [3,4].

The model rotor consists of one rectangular, untwisted NACA0012 rigid blade mounted on a hub containing a drive shaft with a balance weight (Figure 3). The model rotor is defined by the geometrical parameters given in Table 1.

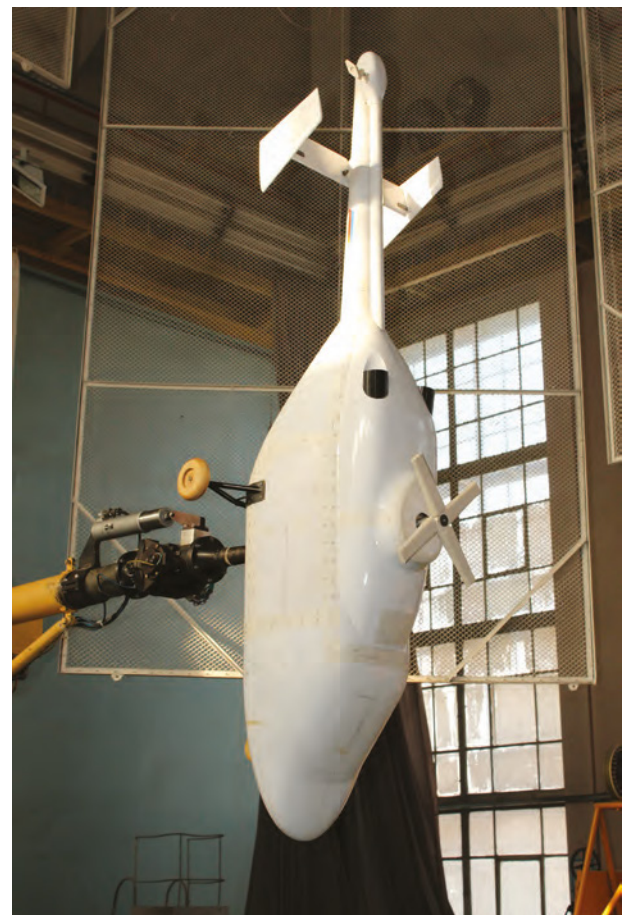


Figure 1. Light Helicopter model tests in wind tunnel T-105.

Pressure distributions have been measured at 10 cross-sections of the blade

$$\bar{r} = \frac{r}{R} = 0.2; 0.3; 0.4; 0.5; 0.6; 0.7; 0.8; 0.9; 0.95; 0.99$$

In the simulation the following forward velocities were considered: hover mode ($V_{\infty} = 0$) and horizontal flight ($V_{\infty} = 11.5$ m/s).

The ambient temperature is 15°C at an atmospheric pressure of 101325 Pa. The blade rotates with an angular velocity of 36.5 rad/s. All presented parameters as well as experimental data were taken from the T-105 wind tunnel experiments of L.S. Pavlov [2].

The mesh settings within FloEFD were set to a uniform mesh with a high mesh density in the vicinity of the rotor and extended to the boundaries of the Computational Domain. Two local meshes, one around the rotor and one on the blade surface, were applied to resolve the tip of the leading edge of the blade. This resulted in an initial mesh of about 2,700,000 cells (Figure 4) and was meshed in about five minutes. The mesh with the traditional CFD (ANSYS Fluent) was made of tetrahedral cells and resulted in a mesh of about 8,500,000 cells.

The FloEFD calculations were performed as transient (unsteady) analysis in three stages with different time steps decreasing from

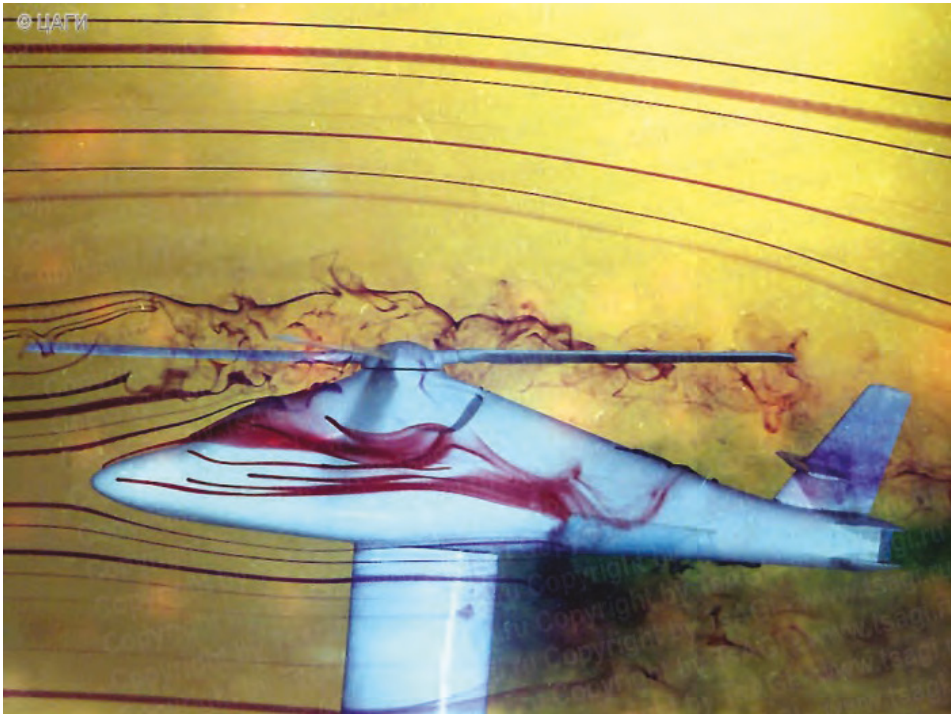


Figure 2. Helicopter model flow tests in the hydro tunnel

Table 1.

Geometrical and Air Flow Parameters:	
Rotor radius	$R = 1.2$ m
Chord length	$c = 0.15$ m
Rotor collective pitch angle	$\varphi = 8^\circ$
Angular velocity of rotation	$\omega = 36.5$ rad/s

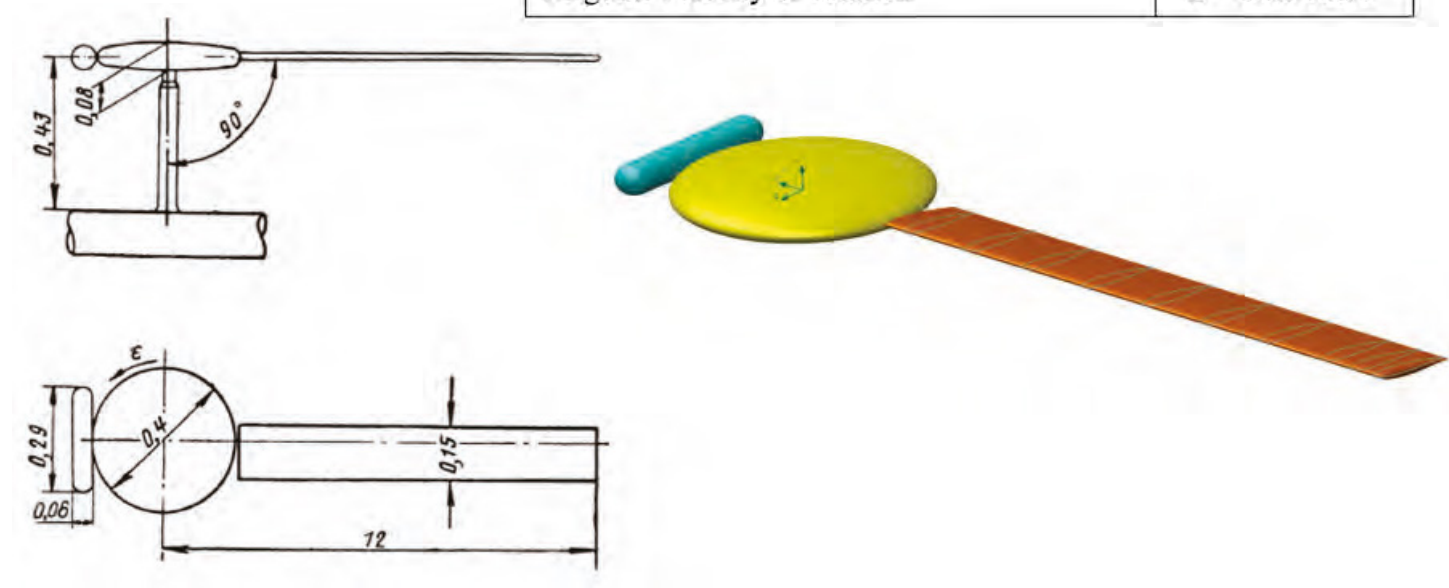


Figure 3. Rotor Blade Model

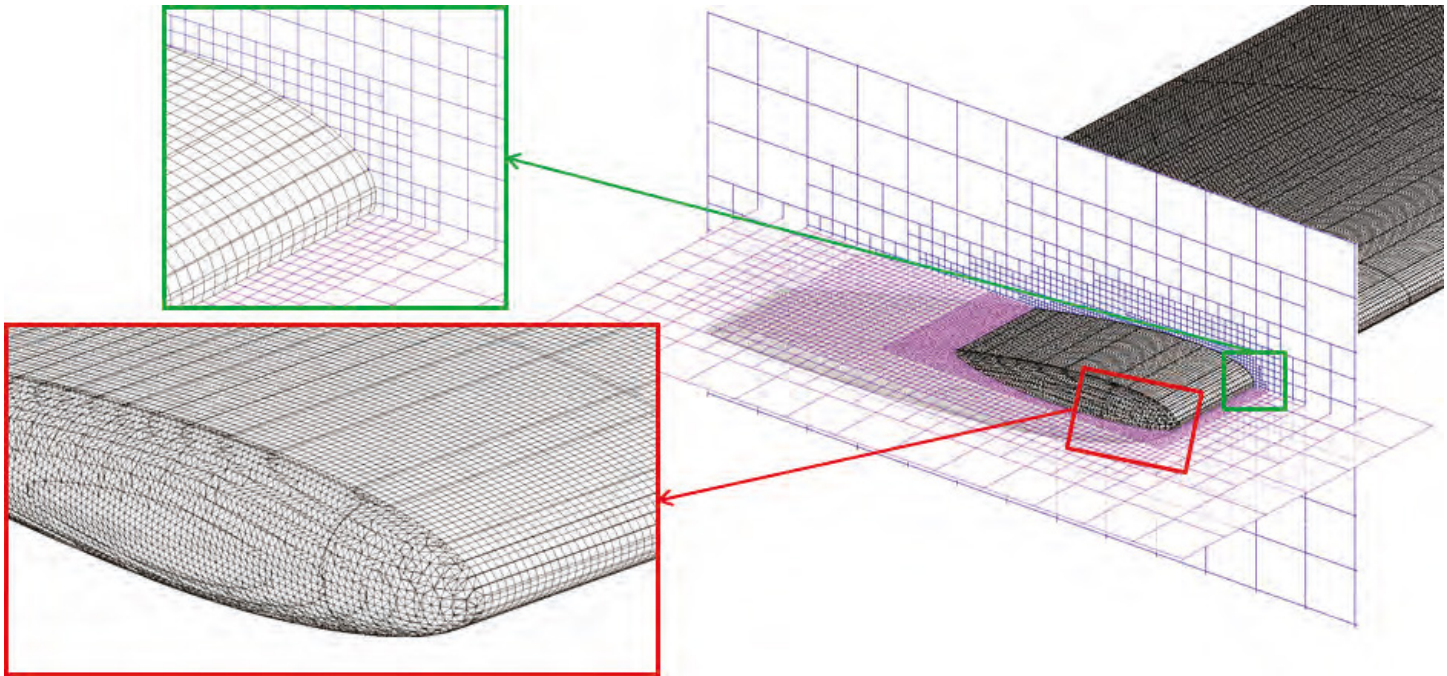


Figure 4. FloEFD mesh with local refinement on the rotor blade surface

the azimuth angle of 9° per one iteration to the azimuth angle of 1° per one iteration for the last revolution on which the presented results were obtained. It has taken about 36 hours to simulate each case on Intel Xeon 2.7 GHz, 8 CPU, 32 Gb RAM and about 30 minutes to specify the project.

The calculations by using ANSYS Fluent were performed on the cluster of 24 computers with Intel Xeon 2.8 GHz, 12 CPU, 100 Gb RAM (the total number of CPU was 288). It has taken about 48 hours to simulate each case and about seven days to specify the project and the calculation mesh.

Also the simulation was performed by using the TsAGI specialized software RC-VTOL based on a nonlinear vortex theory (S.M. Belotserkovsky's school) [3,4]. The calculations were performed on Intel 3 GHz, 4 CPU, 8 Gb RAM and took about 20 minutes per each case.

The wake vortex structures calculated by FloEFD (left) and RC-VTOL (right) are demonstrated in Figure 6. Predicted pressure coefficient (C_p) distributions at the cross-section $r = R$ also show good correlation with ones predicted by the traditional CFD tool and the experimental data (Figure 7).

Figure 8 shows the blade section normal force coefficient along the blade radius predicted by FloEFD and RC-VTOL and

the experimental data. It can be seen that there is again good agreement between experiment and simulations.

This study demonstrates that all software tools have successfully validated the problem of predicting the helicopter rotor blade characteristics. RC-VTOL is the least resource-demanding software, but it cannot provide the pressure distributions on the

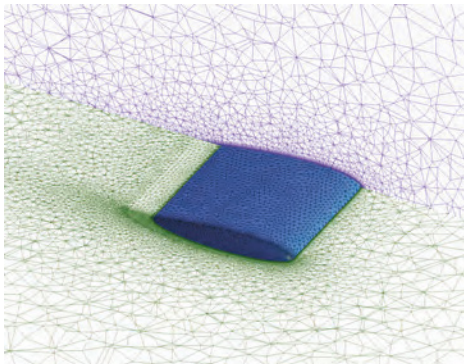


Figure 5. Traditional tetrahedral CFD mesh with local refinement on the rotor blade surface (ANSYS Fluent mesh topology)

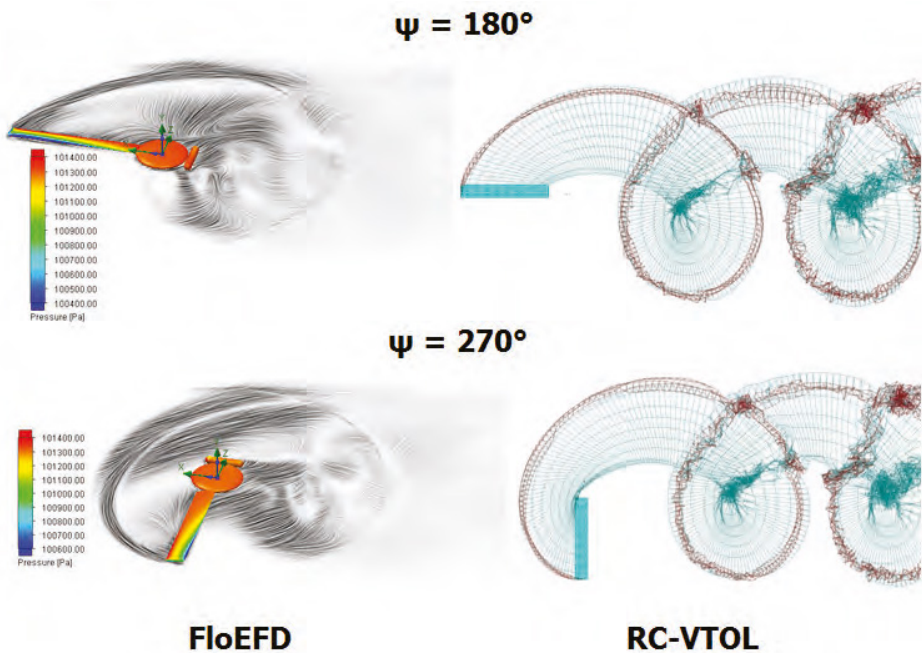


Figure 6. The wake vortex structure and the pressure distribution on the blade at the forward velocity of 11.5 m/s and the azimuth angles of 180° and 270°



surfaces. It is worth noting that FloEFD is less demanding of computer resources than the traditional CFD approach: it takes about 30 minutes to prepare a project for calculation including the mesh creation; the calculation mesh required to obtain the acceptable results was three times less than one for the traditional CFD tool.

References:

- [1] www.tsagi.ru
- [2] Pavlov, L.S. Pressure distribution in rectangular wing (blade) sections during curvilinear motion in an incompressible medium. Uchenie Zapiski TsAGI (Scientific Notes of TsAGI), vol. 10, no. 2, 1979, pp. 104-108 (in Russian).
- [3] Belotserkovsky, S.M., Loktev, B.E., Nisht M.I. Computed-aided investigation of aerodynamic and aeroelastic characteristics of helicopter rotor. Mashinostroenie, Moscow, 1992 (in Russian).
- [4] Kritsky, B.S. Mathematical model of rotorcraft aerodynamics. Trudy TsAGI (Works of TsAGI), no.2655, 2002, pp. 50-56 (in Russian).

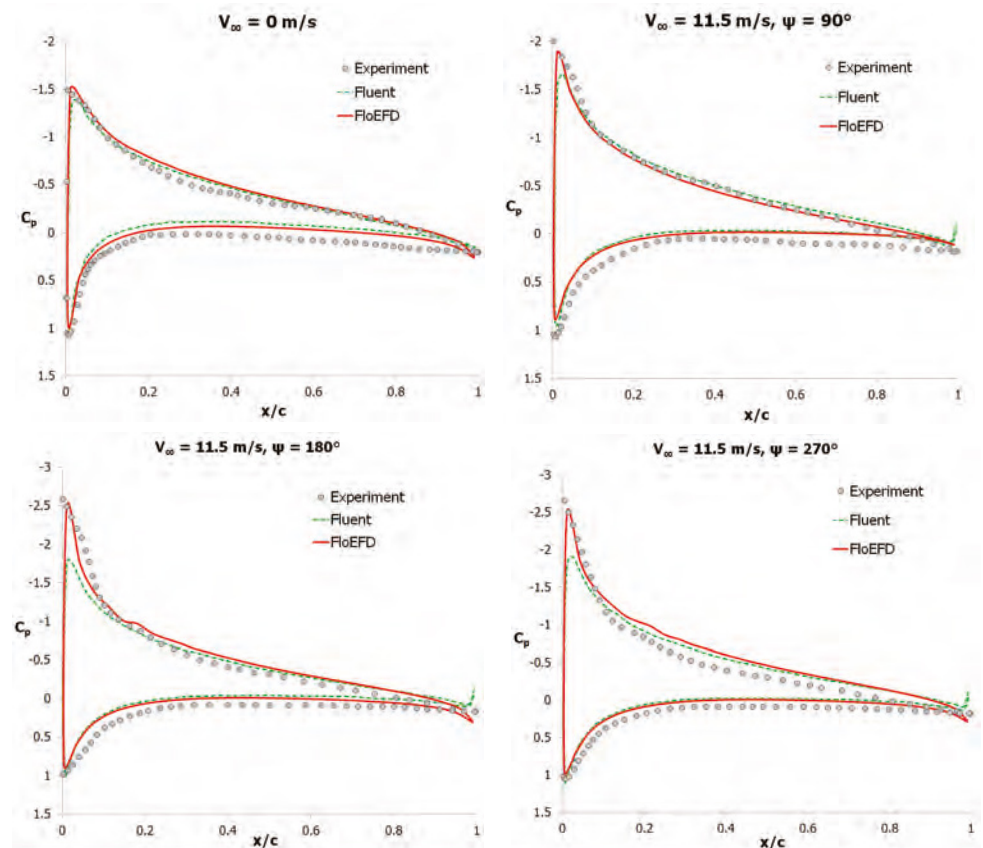


Figure 7. Pressure coefficient C_p distributions at cross-section $\bar{r} = 0.8$

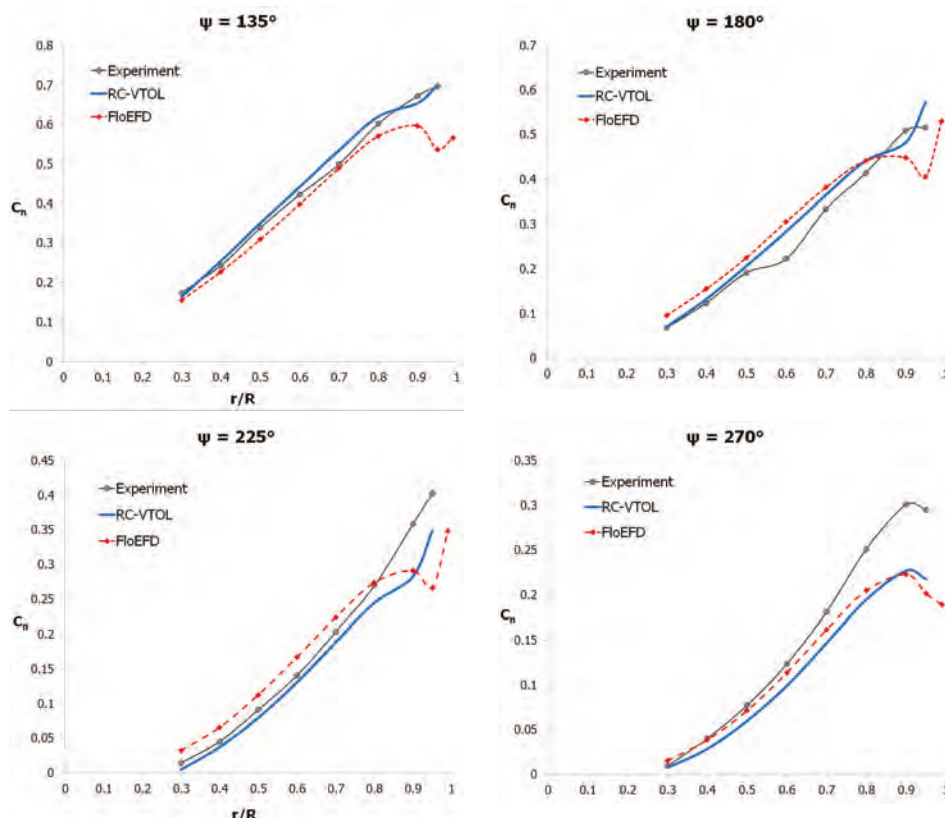


Figure 8. The blade section normal force coefficient distributions at the forward velocity of 11.5 m/s





Lighting the Way

Development of the Bertrandt Full-LED Headlight Thermal Simulation and Design

By Kibriye Sercan, Michael Hage, Mario Dotzek and Eugen Tatartschuk, Bertrandt Group, Cologne, Germany

The style of a car is very much characterized by its lighting system. The final product is created by the collaboration between three areas of competence: Design, Thermal Management and Photometry in the pre-development phase. To show their expertise, Bertrandt engineers developed their own full-LED headlamp and exhibited it at the IAA 2013 in Frankfurt, Germany. The thermal analysis of the IAA exhibit was carried out using the thermal simulation software FloEFD™ from Mentor Graphics.

General Considerations

The creation of light inherently generates heat [1] [2]. The most common light sources nowadays are incandescent lamps and LEDs. Incandescent lamps are thermal radiators (black bodies) which emit a tiny fraction of energy in the visible spectrum. LEDs are semiconductors which release photons through the recombination process. Just as there are differences in the light creation processes, there are also different demands regarding the thermal management of the light sources. Incandescent bulbs need a minimum temperature for the filament to produce light. LEDs are "cold" emitters and require efficient cooling of the optically active junction layer to meet the requirements of service life and the emission spectrum. Compared to halogen bulbs, light-emitting diodes have a higher optical efficiency, lower heat generation and a longer service life. In addition, they provide designers with more creative freedom due to their smaller dimensions, directed light emission and greater freedom within the constraints of lighting legislation [3]. Given these advantages, the tendency towards using LEDs in the automotive industry is steadily growing. As a consequence, the demands on the LED lights are also higher. They are expected to offer higher performance

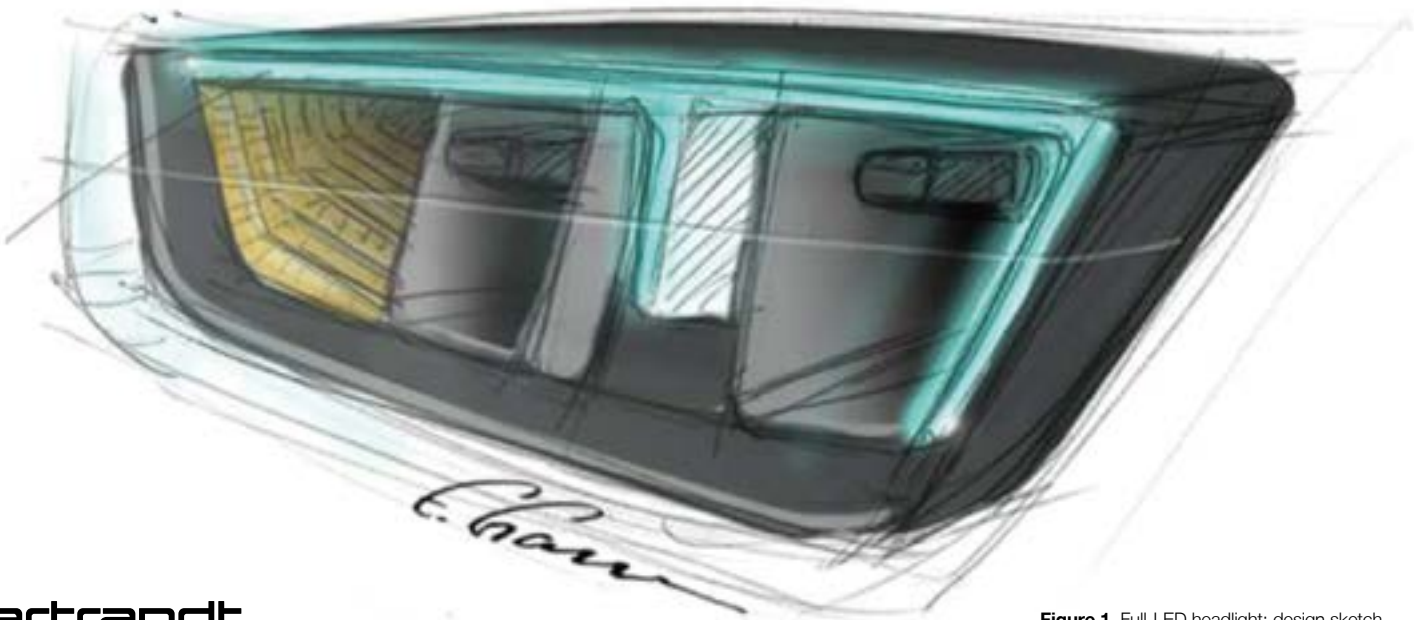


Figure 1. Full-LED headlight: design sketch

while still providing a higher quality of light and be aesthetically more appealing than their halogen lamp counterparts. Additional degrees of freedom in the development of LEDs are created by the variety of types and their ability to operate over a wide range of currents, thus varying the light output, the service life and the power dissipated. The introduction of fans and heatsinks in headlight systems also presents developers with new challenges, as the luminous flux, which is very important for the lighting design, is highly dependent on optimum thermal conditions.

Requirements and Development Process

Bertrandt engineers wanted to develop a headlight for a lower mid-size vehicle without a standard-equipment AFS function in which the static cornering lights could be implemented at low cost by using fog lights. This meant that the photometric requirements for the low beams were higher. The static low beam was to illuminate the road as well as possible in every given situation. The luminous flux should be in the region of 600 lm, therefore the low-beam LED was to emit at least 1,000 "hot" lumen. In addition, the high-beam and daytime running light functions were to be a special design element (dimmed as a position light), and indicator lights were to be accommodated in the headlamp itself (see Figure 1). High and low beam were each to be achieved with a shovel reflector (the low beam mounted on the vehicle facing outwards to allow conversion for the North American market [4]). To increase the number

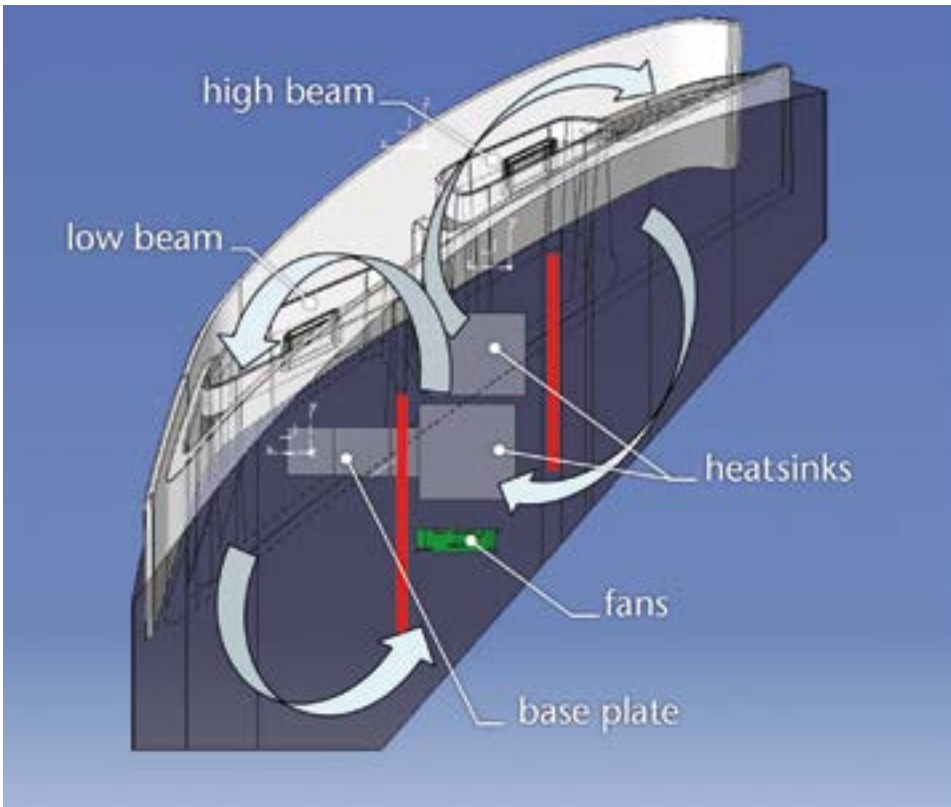


Figure 2. Concept representation of the intended airflow and simulated flow distribution in the headlight

of common parts, the same LED, an OSRAM OSTAR Headlamp Pro, was used for the high and low beam. For daytime running and turn indicator lights, several Advanced Power TOPLEDs were used. In addition to the photometric considerations, a thermal system analysis was carried out. Two key scenarios were identified:

- 1. Low beam, high beam, turn indicator and position lights were activated for the most critical night time scenario, which was consequently also the scenario with the maximum power consumption.
- 2. Daytime running lights and turn indicator lights were activated simultaneously as the most critical day time scenario.

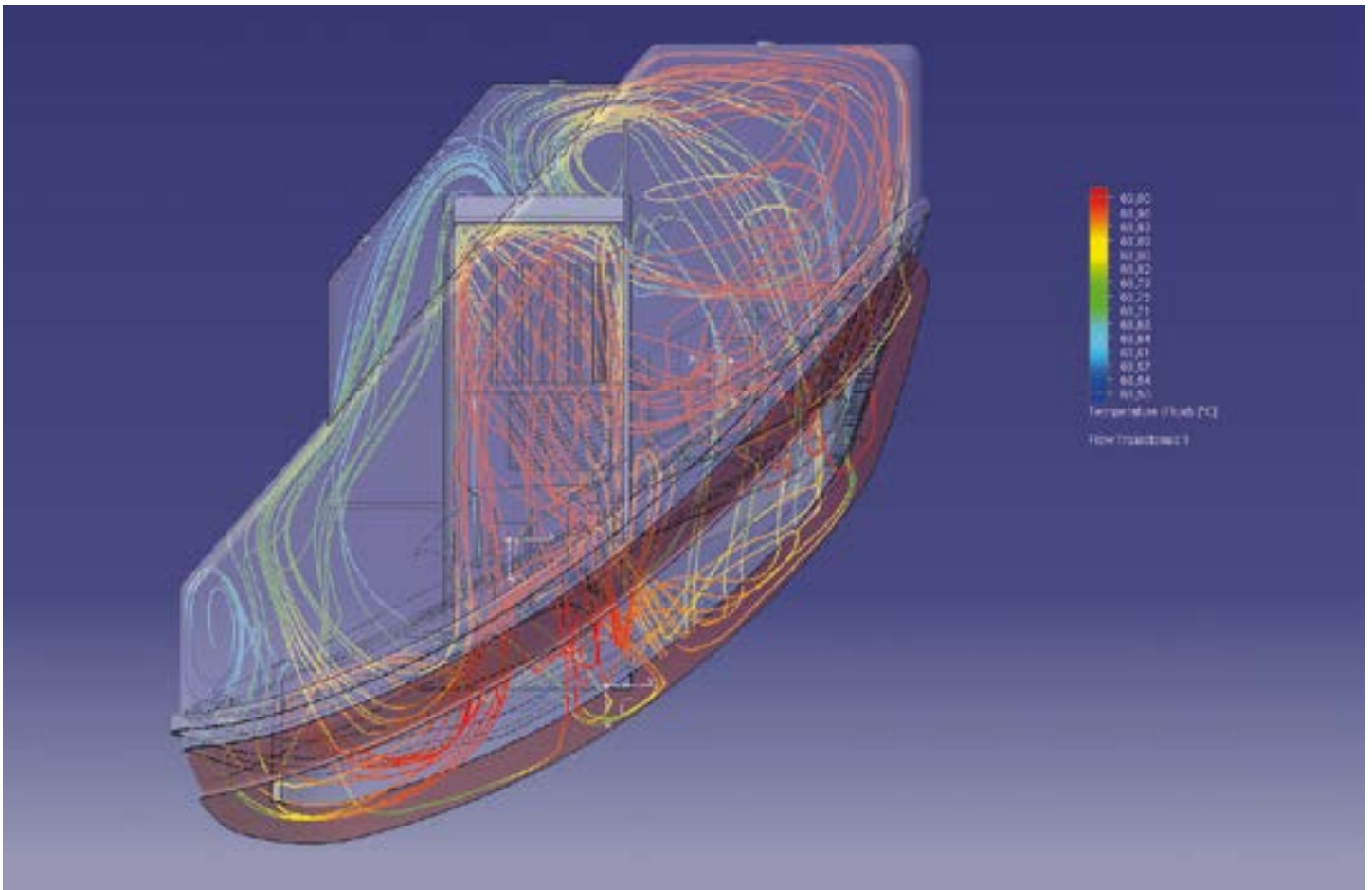


Figure 3. First airflow simulation without a cover frame. The circulations develop as planned. Part of the warm air slips through the cooling channel at the position where the base plate of the LED leaves a gap

In these two scenarios as a continuous condition, the junction temperatures of the LEDs should not exceed the maximum permissible values. A further aim was to direct the warm air from the main lighting functions (low and high beam) to the front of the cover frame, both to defog the lens and to cool the air in the lamp.

The development was carried out in the following steps:

3. Concept phase:
 - LED pre-selection
 - Heatsink positioning
 - Number of fans and possible positions
4. Dimensioning/layout:
 - Heatsink size and shape
 - Size of base plates
5. Adaptation of LED type
6. Design of the heatsink ribs and adaptation:
 - Size
 - Shape
 - Airflow direction

7. Air routing and cover frame
8. Fan selection

Through this process, which was partly iterative and partly connected with other disciplines such as lighting design, the developers succeeded in achieving the photometric objectives and the design of an efficient cooling system to attain the desired LED lifetime.

Cooling Concept

To meet the photometric requirements of the low beam, a powerful four-chip LED was chosen during the design phase. Based on the thermal resistance of the LED and estimates for the heatsinks, checks were run on whether the required luminous flux under the junction temperature of $T = 150^{\circ}\text{C}$ could be achieved. A particular challenge for cooling the low-beam LED is its position at the top of the headlight. With these design specifications, the low beam is deemed thermally more critical than the other functions. As a result of limited space in the upper housing portion, the LED was not placed directly on the heatsink, but had to be connected to the heatsink via a base

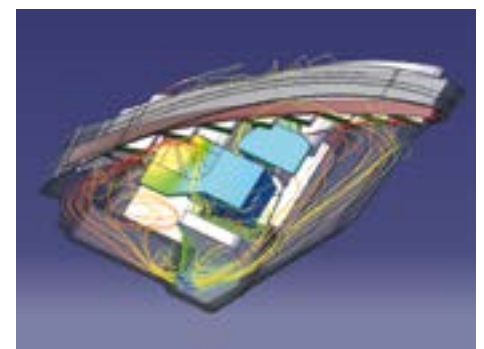


Figure 4. Thermal simulation with fully designed heatsinks and cover frame. Through several iterations and changes of the airflow guide, it was possible to design the airflow to be similar to the original plan. The base plates of the LEDs are wide enough to conduct the necessary amount of heat.

plate. This resulted in additional thermal resistance, which was confirmed both by simulations and by analytical assessments. The decision was then made to move to the five-chip LED LE UW U1A5 01, which has a thermal resistance of 1.5K/W [5], because it could be operated with a lower current and achieve the same luminous flux. Since the natural convection was hampered by the heatsink shape and position, a fan was



Figure 5. Photo of the final prototype.

utilized. This allowed good circulation of the air in the headlight, and a reduction in the size of the heatsinks (Figure 2).

The heatsink of the high beam was placed in front of the low beam heatsink, between the reflectors for the main lighting functions. Directly behind it, there is a fan that blows air through the two heatsinks in the vehicle's direction of travel. As a result, an air channel is created between the reflectors (Figure 3) which contributes to efficient cooling and air circulation. With the aid of Mentor Graphics' FloEFD™ 3D simulation software, the flow distribution was determined and the bezel geometry defined accordingly. The warm air was blown out of the heatsinks through an opening in the bezel below the centre section of the daytime running lights and against the cold lens, where the air cools down and simultaneously defogs the front lens. In two cycles, the cold air flows back behind the bezel and into the fan. The resulting cooling circuits are shown in Figure 2 (red lines indicate the air guide). It should be noted that two circuits are easier to control than one circulating around the entire headlight.

Using a parametric model of the heatsink and the FloEFD parametric study feature with post-processing [6], the heatsink fins were designed for the main lighting functions in order to ensure the most efficient cooling for a given airflow. The model was then completed for the signal light LED functions as well as

their heatsinks. Based on the aerodynamic resistance of the system, an axial fan was chosen to work in conjunction with this system at its optimum operating point.

Results

Once the system was fully represented as a CAD model with the housing, lens, cover, air duct, fan, and heatsink, it was possible to run a simulation with precise LED parameters, a characteristic fan curve and boundary conditions in the two aforementioned scenarios. From these simulations, the operating current was calculated, which allowed an LED to operate below the critical temperature in typical conditions. All lighting functions were achieved at an ambient temperature of around 50°C at the lens and at 90°C on the housing in accordance with ECE regulations and performance requirements. This was also demonstrated with in-house measurements in continuous operation of the headlight [7].

Summary

Through regular consultation with the design department, production-ready road illumination was achieved with an almost unchanged aesthetic design of the headlight from the initial sketches to the finished prototype (Figure 5). With the direct integration of the simulation software into the CAD system CATIA V5, this process was significantly simplified and accelerated.

References

- [1]: Electrical Properties of Materials von Laszlo Solymar, Donald Walsh, Richard R. A. Syms. Oxford University Press, May 2014
- [2]: Chinese Physics B Volume 20 Number 1 Internal quantum efficiency drop induced by the heat generation inside of light emitting diodes (LEDs) Chen Yi-Xin, Shen Guang-Di, Guo Wei-Ling, Xu Chen and Li Jian-Jun. 2011 Chinese Physical Society and IOP Publishing Ltd.
- [3]: <http://www.unece.org/trans/main/wp29/wp29wgs/wp29gen/wp29docstts.html>
- [4]: FMVSS [Federal Motor Vehicle Safety Standards] (2006). Standard No. 108: Lamps, reflective devices, and associated equipment. In, Code of Federal Regulations, Title 49. Washington, D.C.: Office of the Federal Register. <http://www.nhtsa.gov/cars/rules/import/FMVSS/>
- [5]: OSRAM OSTAR Headlamp Pro Datasheet Version 2.1 LE UW U1A5 01
- [6]: Parametric Study of an IGBT Cold Plate Geometry in Thermal Simulation. <http://go.mentor.com/4cpdt>
- [7]: Stz 11/2013, produktentstehungsprozess für scheinwerfer und heckleuchten, decker, hage, jerg, tatartschuk



Cost Optimization of LED Street Lighting

LED Lighting Technologies from Vestel Engineering

By Emre Serdar & İsmail Güngör, Sr. Mechanical Design Engineers, Vestel Electronic – LED Lighting

With LED lighting technologies, the mechanical design of the luminaire is the most important aspect in meeting industry demands for cost and performance.

The shape of the body, type, and number of the fins on the external casing, and the selection of the casing and other materials are the main mechanical parameters affecting the cooling of the luminaire. All these parameters also affect the weight and cost of the luminaire, so mechanical optimization is critical to optimizing the product cost.

All LED manufacturers try to design smaller and more thermally effective luminaires through the use of CFD. For Vestel's Ephesus street light luminaire, FloEFD™ was used to optimize both the thermal design and to check the drag force on the luminaire when pole mounted, to ensure compliance with national standards for wind loading.

LEDs are unique amongst light sources in that they are designed to operate at low temperatures through the efficient conduction of heat away from the LED. LEDs generate little or no IR or UV, but convert only 15%-25% of the power into visible light; the remainder is converted to heat that must be conducted from the LED die to the underlying circuit board and heatsinks, housings, or luminaire frame elements in order to limit the junction temperature during operation, otherwise the light output falls [1]. In addition to reduced lumen output, excess heat directly shortens LED lifetime, and the lifetime of any control circuitry within the luminaire.

The challenge facing lighting companies is to design a luminaire that has the maximum thermal performance while minimizing the costs related to the materials used and

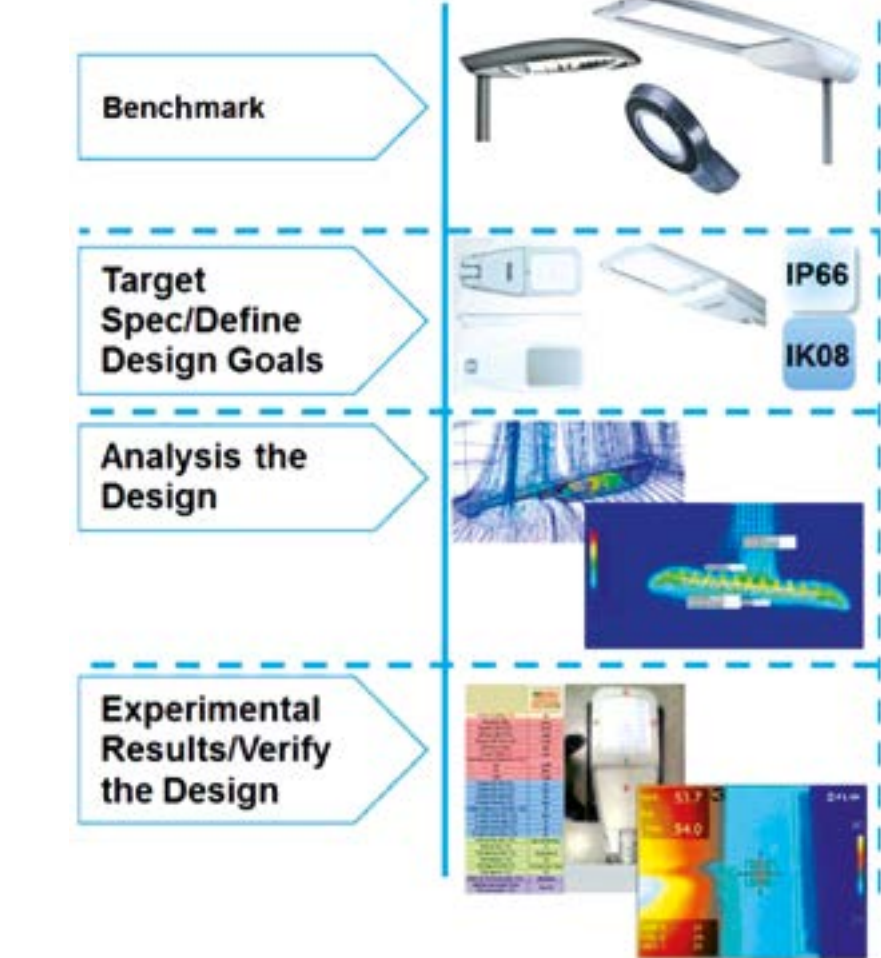


Figure 2. Design Steps

the mechanical design. As these are the largest overall contribution to the cost of the luminaire, there is a strong drive to minimize the mechanical cost through optimization of the thermal design.

The design goals for a luminaire should be based either on an existing fixture's performance or on the application's lighting requirements. So, the design steps start with researching existing product designs as benchmarks, used to develop a target

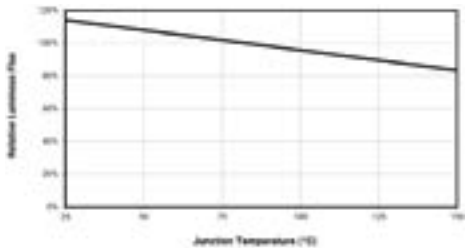


Figure 1. Relative Luminous Flux vs. Junction Temperature of White Cree XT-E (350 mA forward current)

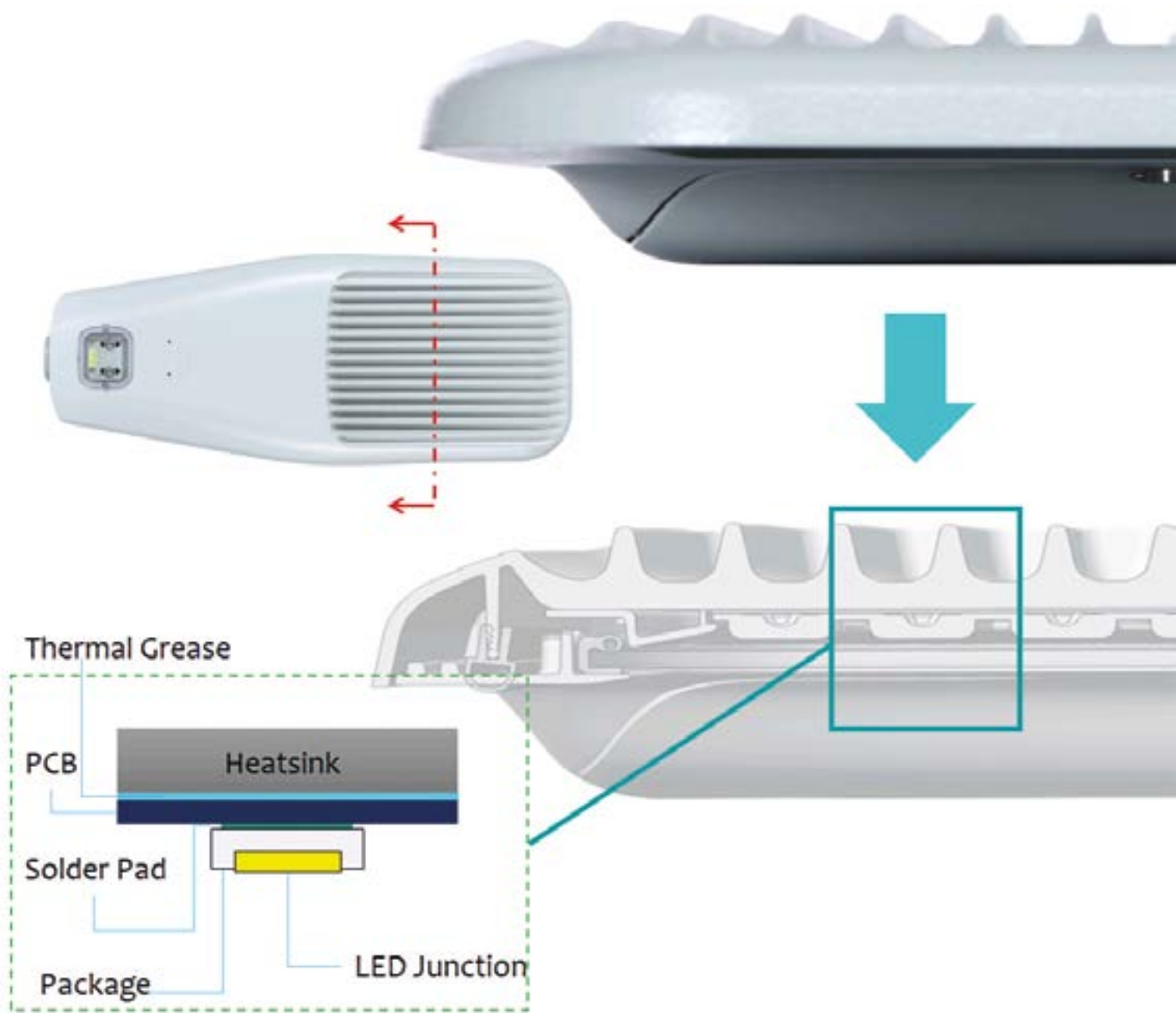


Figure 3. Cross Section of VESTEL Ephesus- Fundamental of System Configuration

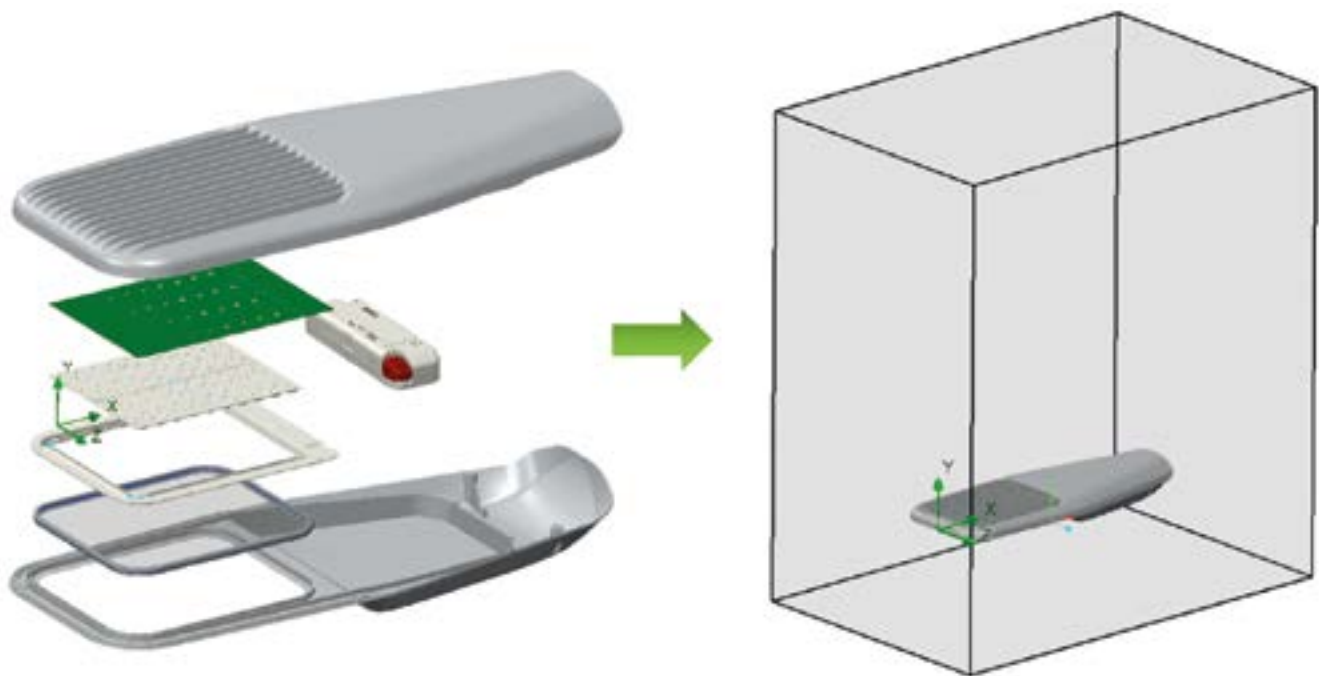


Figure 4. Thermal Analysis - Junction Temperature



specification for the product. The designer should specify any other goals that will influence the design, such as special optical and hardware requirements, like the selection of LED chips, drive current, etc. directly impacts thermal performance, and hence the mechanical design.

After the defining goals, in accordance with the optical and hardware requirements, choosing the type and number of LEDs and the drive current for the LED chips, the designer should start the mechanical design. Once an acceptable mechanical design is achieved this can be used for a first thermal analysis, and subsequent optimization study.

System Configuration

To design an effective cooling solution as part of the luminaire design, designers and analysts need to fully understand those aspects of the design that affect thermal performance, and the principle of thermal resistance. Three things affect the junction temperature of an LED chip: drive current, thermal path, and ambient temperature. In general, the higher the drive current, the greater the heat generated at the die. Heat must be moved away from the die in order to maintain expected light output, color, and lifetime

The inset in Figure 3 shows a 1D heat flow path from the LED junction down to the heatsink. The thermal resistance of the thermal grease or pad is one of the important parameters affecting the junction temperature. The designer can use the better thermal grease/pad that has a lower thermal resistance to help reduce the junction temperature. However, it should not be forgotten that a higher performance thermal grease/pad can increase the cost of your product, and so forms part of the cost optimization challenge when designing a luminaire.

To optimize the thermal design, the influence of the number of fins on the outer casing was investigated as a parametric study with 10, 15, 20, and 25 fins. The design with 15 fins was found to offer the best thermal performance.

A prototype was built, and FloEFD was found to have predicted temperatures on the casing to within a degree, and the junction temperature of the LEDs to within 2.8°C of experimental values.

Having successfully optimized the thermal design, it was necessary to complete an

aerodynamic analysis on the luminaire as it is mounted on a 15m high pole. The specification for the test comes from TEDAS, the Turkish Electricity Distribution Company. At a wind speed of 57 m/s side on to the luminaire, the drag coefficient is 0.46, resulting in a drag force of 47.2N giving a bending moment based on the height of the pole as 0.71kNm. This is substantially less than the maximum 19.8kNm set in the specification. Front on to the flow, the drag coefficient is only 0.1, so the bending moment is correspondingly less.

In conclusion, Vestel's Ephesus street light design was analyzed and thermally optimized with FloEFD, fully meeting the thermal design criteria for the product. Wind forces on the pole-mounted luminaire were also simulated and the Vestel Ephesus M3 design was confirmed not to pose any safety risk due to aerodynamic loading.

References:

[1] "Thermal Management of White LEDs" Building Technologies Programme PNNL-SA-51901, February 2007.

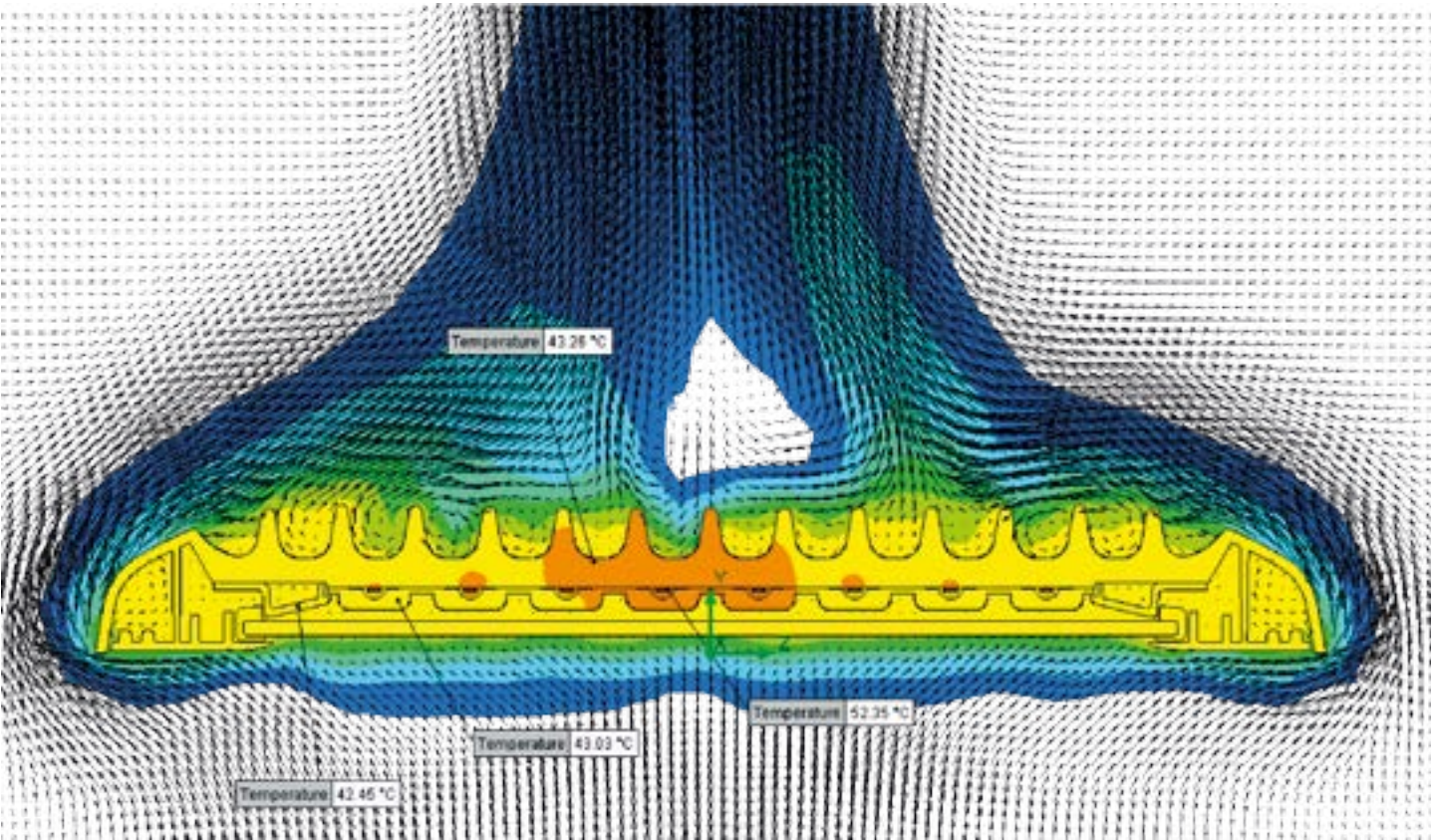


Figure 5. Top Surface Junction Temperature





Up, Up and Away!

Using CFD tools to develop a Real-Time Flight Model

By Gerardo Olivares Ph.D.; A. Barragan; J. M. Gomez; and
H. Solano, National Institute for Aviation Research



The traditional development of aircraft of any type usually goes through a long design process until the first full-scale prototype is built to test flight behavior. Such an approach is extremely costly considering the capital investment required for large passenger liners. Considering the challenges faced by the recent development of the Airbus A380 and Boeing 787 Dreamliner, manufacturers and component suppliers are understandably under increased pressure to deliver right, on time, every time.

There is therefore a need to streamline the development process and improve the prediction accuracy in flight behaviors in real-time flight simulators. Dr. Olivares and his team at the National Institute for Aviation Research (NIAR) of the Wichita State University set out to develop a method to increase the prediction accuracy of flight behaviors with the real-time flight simulator, MIURA. Conventional aerodynamic calculations used by the simulator were not accurate enough, especially predicting stall and other effects such as propeller performance or the wing-fuselage interference. The NIAR team conducted several simulations with Mentor Graphics' FloEFD™ Simulation Software on their test model, a push propeller UAV (Figure 1), in order to get more accurate data to feed into the simulator for a better prediction of flight characteristics as well as to validate the FloEFD results with wind tunnel measurements.

The goal of the NIAR research team is to better predict, not only the aerodynamics, but also take into account more models, (such as the controls and electrical systems), in the virtual engineering environment while also collecting data throughout the flight envelope and feed that back into stress simulations of the aircrafts structure. This article is based on the presentation given by Dr Olivares at the COE 2015 Annual PLM Conference & TechniFair in April 2015.

Aerodynamic Surface Stall Prediction

Stall prediction is a critical point in the aerodynamics of an aircraft because beyond the point of stall the aircraft loses its lift and maneuverability and will fall out of the sky since no lift is generated to keep it aloft. A trained pilot is able to recover the aircraft after stalling but not without a large loss in elevation. Stalling maneuvers such as those seen at airshows with fighter jets or acrobatic aircrafts, are tested by test pilots in new aircraft prototypes. The standard development process of an aircraft includes initial aerodynamic calculations starting with the selection of an airfoil. The aerodynamic parameters of airfoils however are based on a 2D profile which behaves differently to a 3D wing. There are analytical methods to predict the 3D behavior based on the 2D profile data, but this method often lacks accuracy compared to wind tunnel measurements or 3D CFD calculations. The MIURA prediction of the 3D wing and the comparison of the 2D and 3D experimental data are shown in Figure 2. It can clearly be seen that the default prediction of the stall behavior of MIURA is at a much lower lift coefficient (CL) and lower angle of attack. In a simulation the aircraft would stall at a

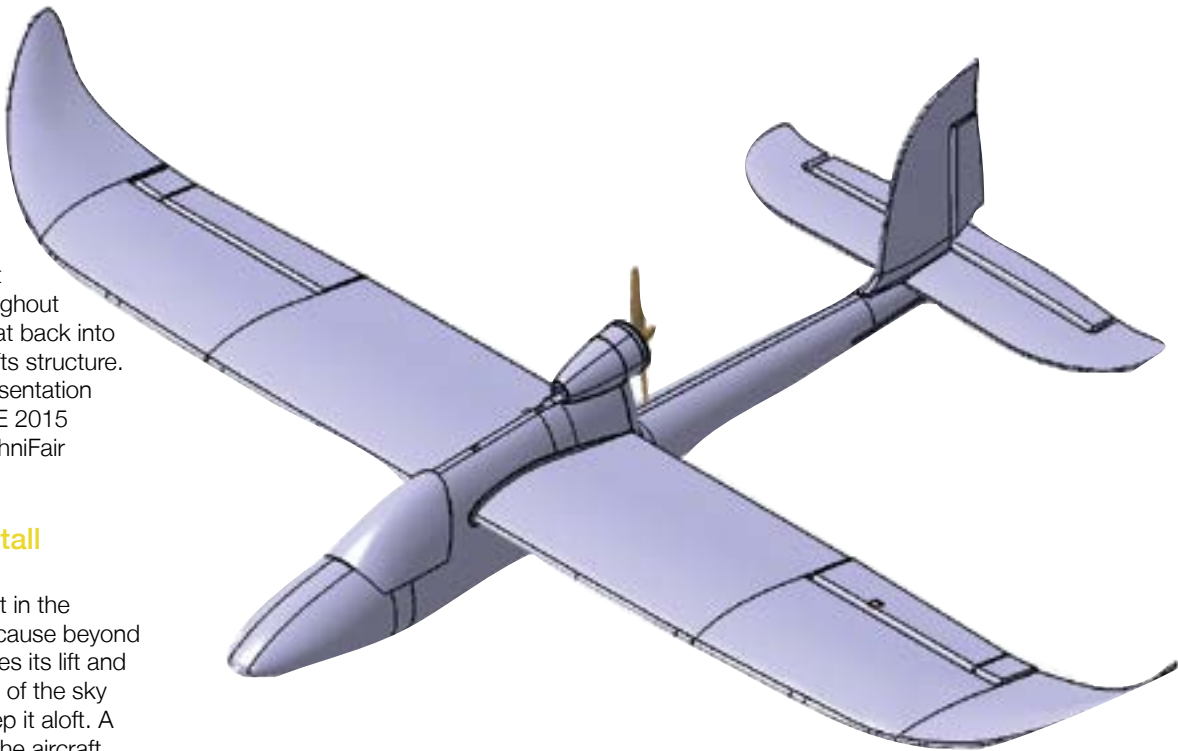


Figure 1. The NIAR push propeller UAV CATIA V5 model..

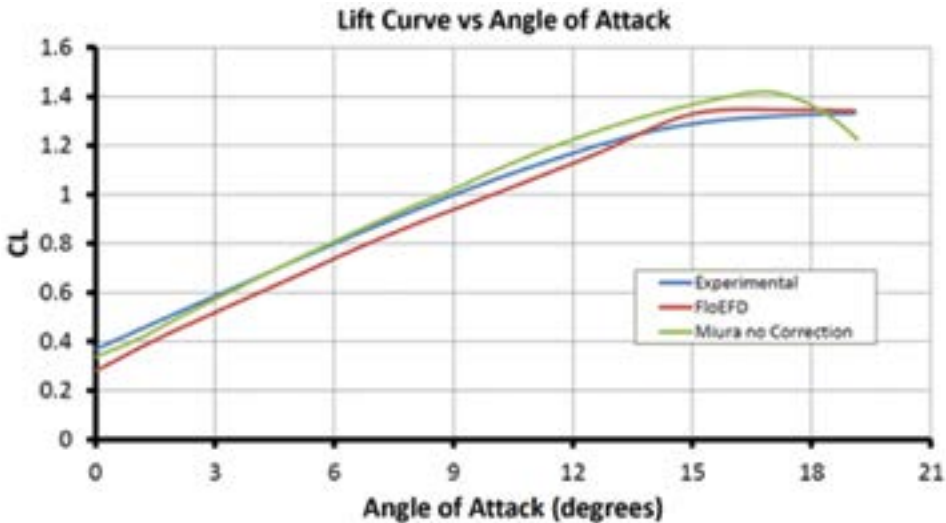


Figure 3. Comparison of lift coefficient vs AOA between wind tunnel, FloEFD and MIURA (without correction)

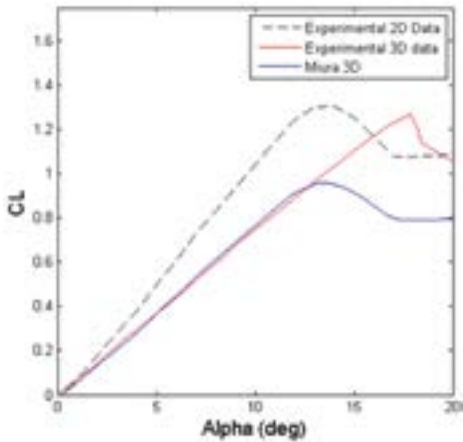


Figure 2. MIURA results without correction for stall prediction.

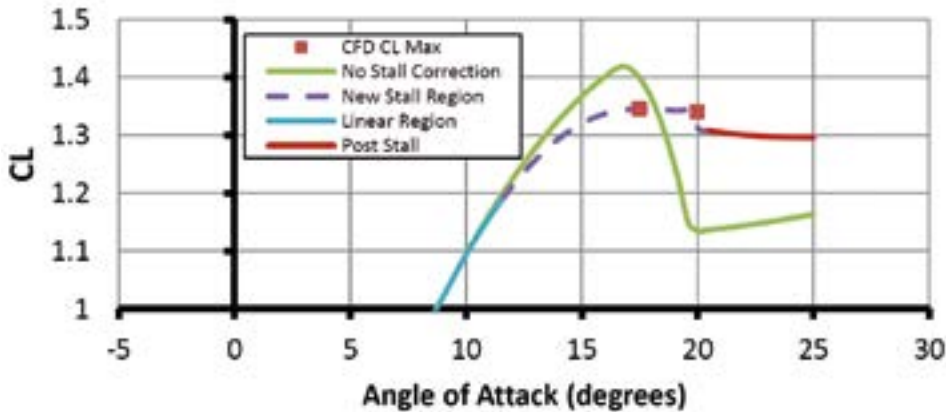


Figure 4. Lift coefficient vs. AOA showing effect of stall correction for MIURA



much smaller angle and lower lift compared to the reality. The NIAR team built a 3D wing as an extrusion of the 2D airfoil SD7062 and measured its aerodynamic performance in the closed loop Beech Wind Tunnel at the Wichita State University (WSU). They then conducted a FloEFD simulation at a range of angles of attack (AOA).

The results from the experiment, FloEFD and MIURA (without correction) are shown in Figure 3 and shows that FloEFD has the same lift curve slope and stall pattern as the wind tunnel data. MIURA on the other hand captures the initial slope but over - predicts the stall at 17° AOA.

The vital parts of the lift curve that MIURA must correct are after the linear section so as not to over-predict the lift and drop too strongly after the maximum lift. In order to do that, MIURA enables the user to input the CLmax and an additional point after that, and consequently calculates the post-stall again on its own (Figure 4).

This method leads to a drastically improved stall behavior (Figure 5). The corrected MIURA calculation fits the stall behavior of the experimental data much better than the uncorrected calculation.

Propeller Performance

Since the polars used in airfoils also apply for the propeller blades, the same problem affects the propeller performance and can be seen in the thrust and power coefficient vs. advance ratio of the propeller diagrams shown in Figure 6.

This is especially true in the crucial take-off and climb phase where the curves differ drastically and would result in extremely different flight behavior by the simulator.

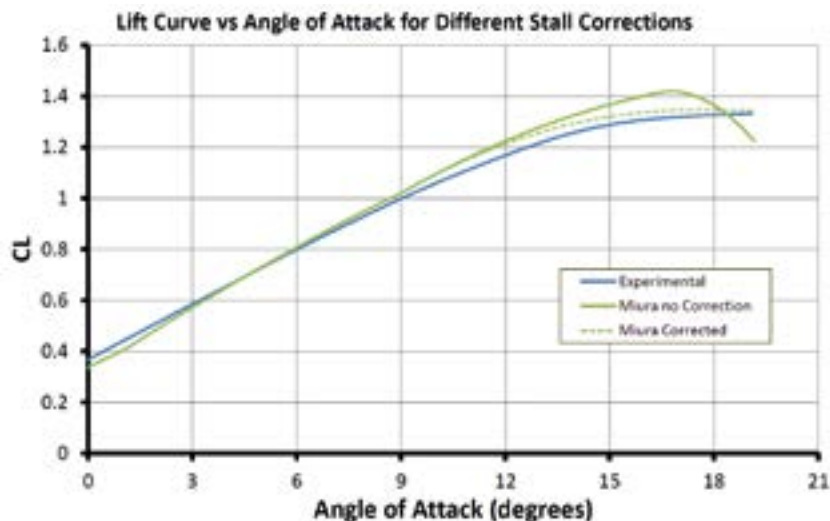


Figure 5. Lift coefficient vs. AOA showing the corrected MIURA results compared to the experiments

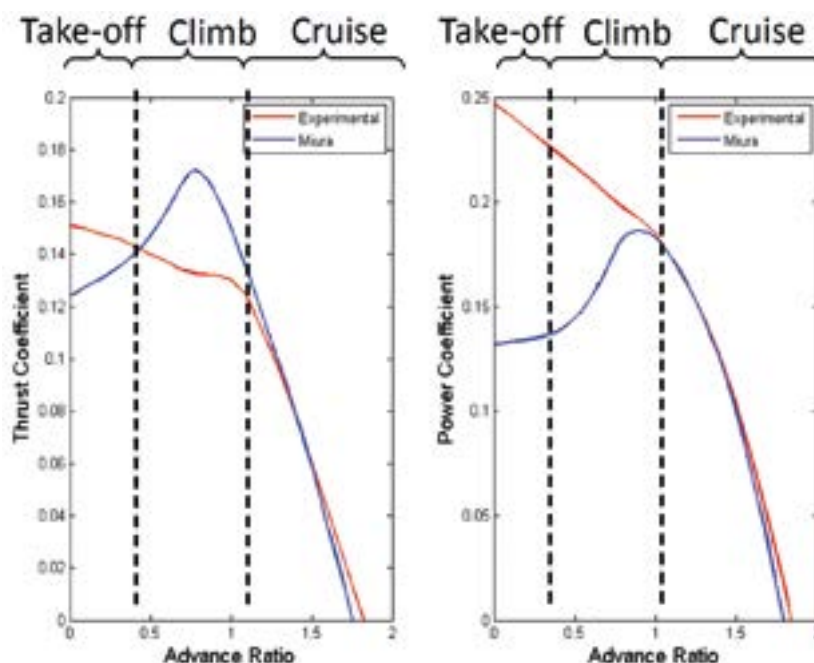


Figure 6. Thrust and power coefficient prediction of MIURA compared to experimental data

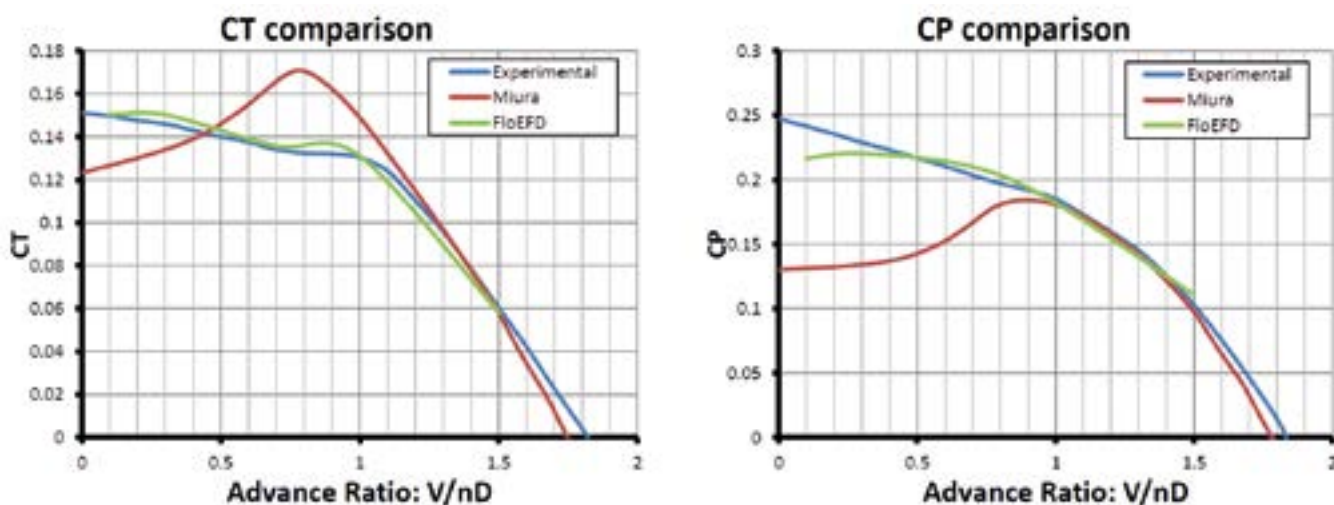


Figure 7. Thrust and power coefficient (CT and CP respectively) comparison between wind tunnel, FloEFD and MIURA (not corrected)

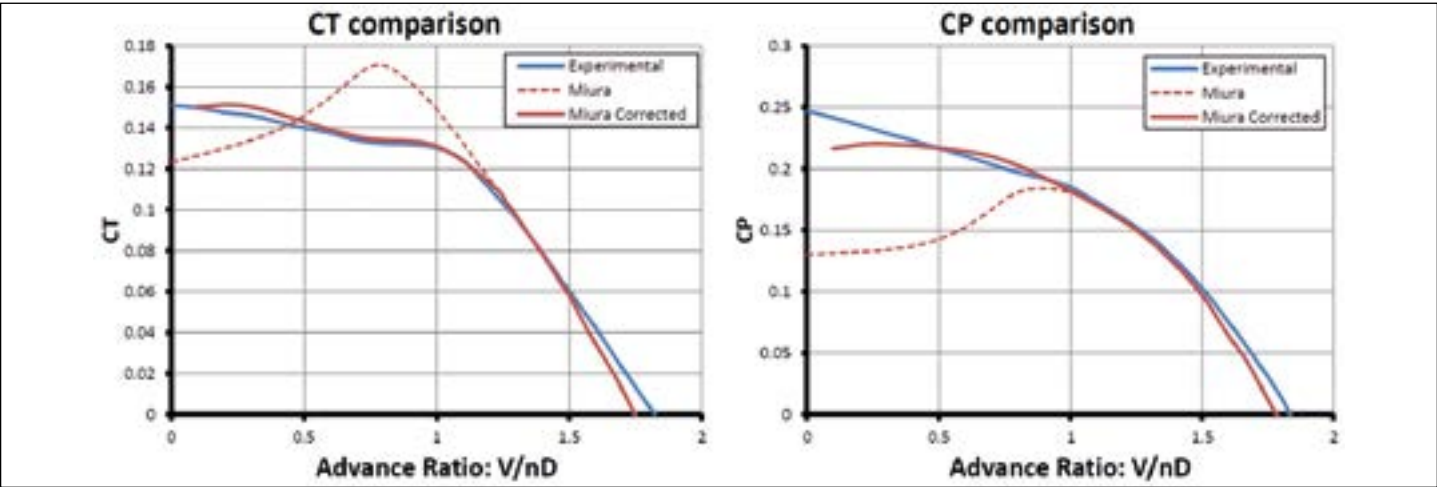


Figure 8. Corrected MIURA results for thrust and power coefficient compared to not corrected results and experimental data

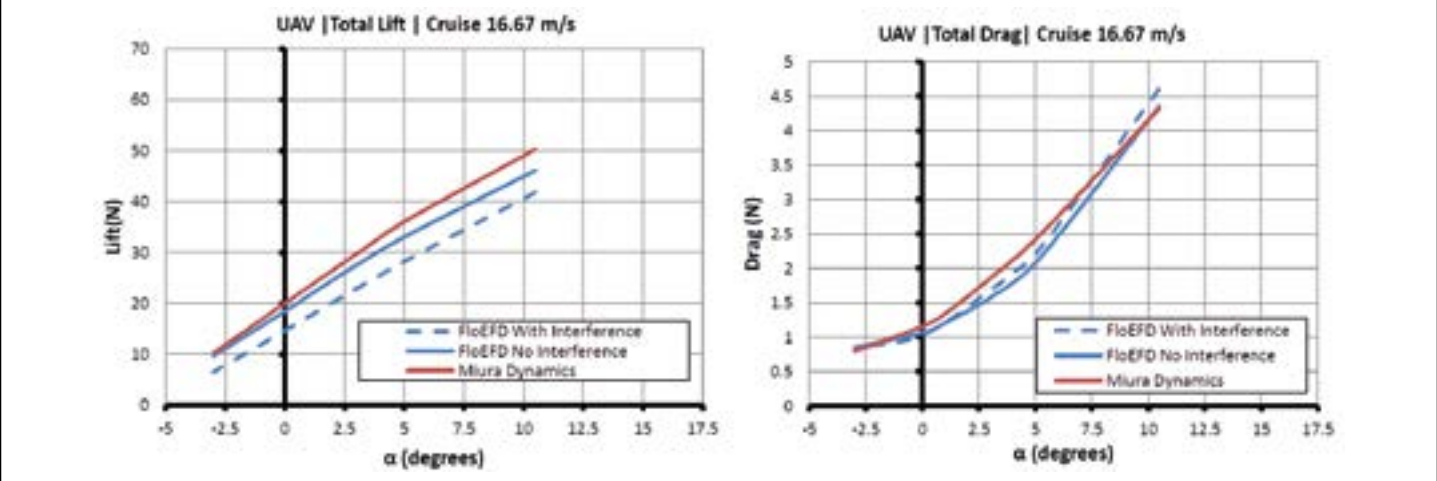


Figure 9. Lift and drag vs. AOA for not corrected MIURA results compared to FloEFD results with and without interference

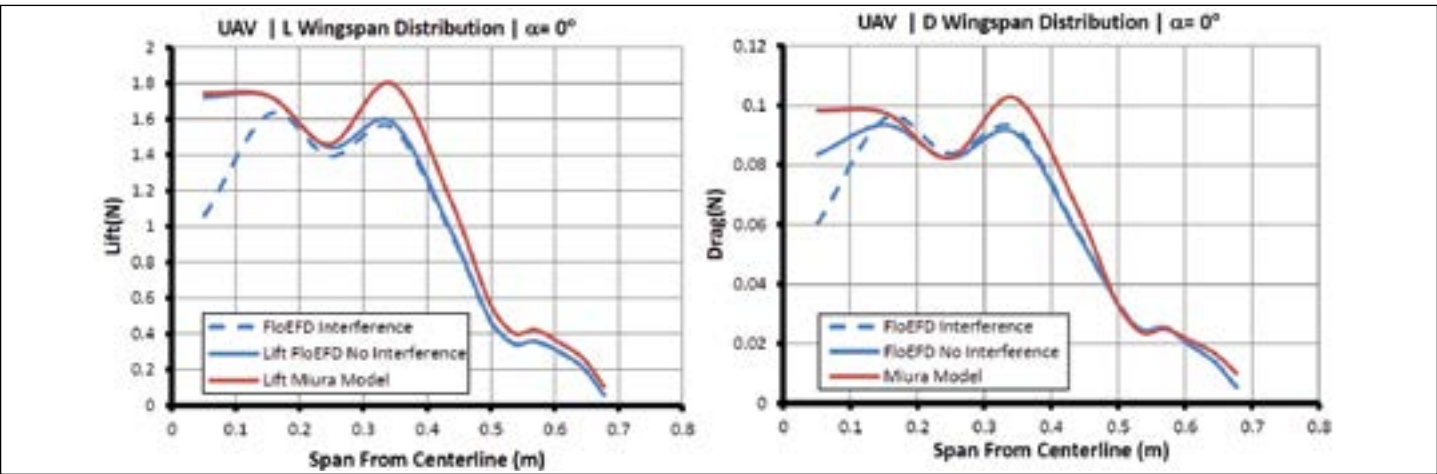


Figure 10. Spanwise lift and drag for not corrected MIURA results compared to FloEFD results with and without interference

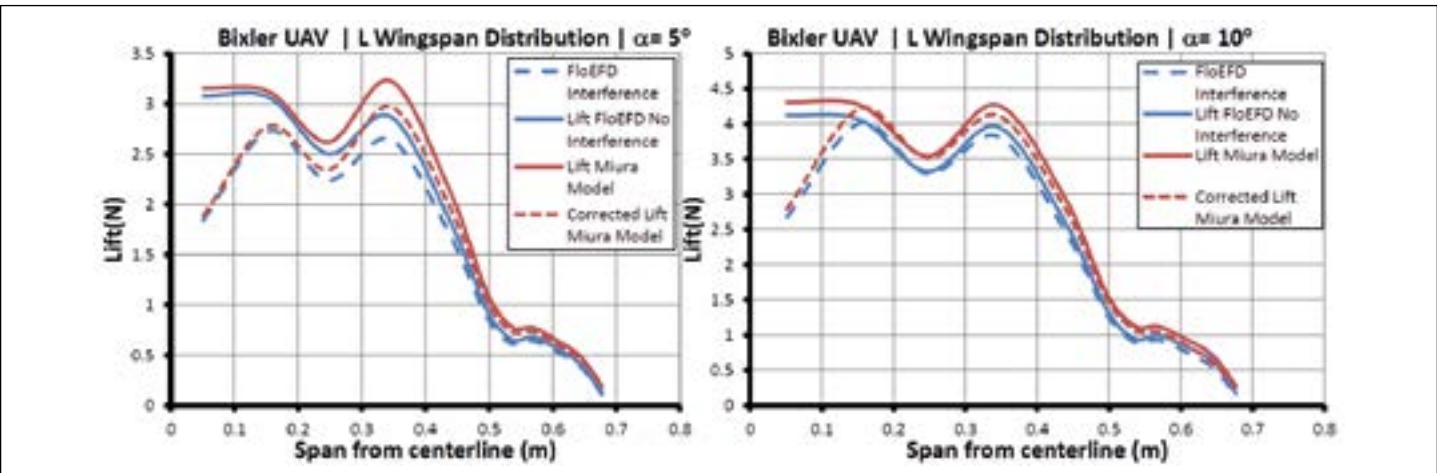


Figure 11. Spanwise lift and drag distribution with corrected and not corrected MIURA results compared to FloEFD results with and without interference

“The four distinctive features that make FloEFD the best candidate for this kind of application are its CAD embedded approach, the Immersed Body Meshing technology, the parametric study, and the solver accuracy”

Gerardo Olivares Ph.D, National Institute for Aviation Research

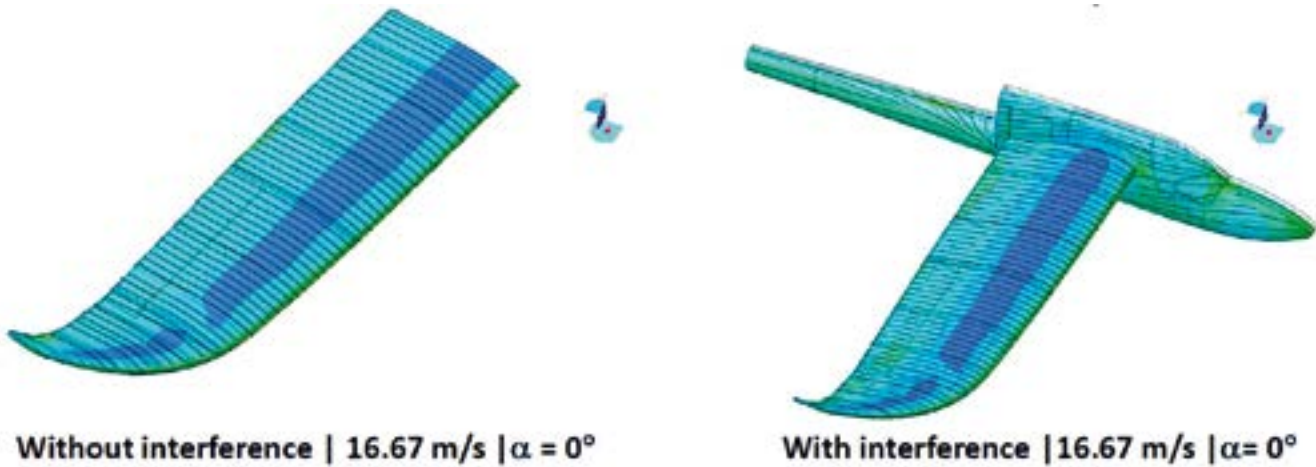


Figure 12. Pressure surface plot showing the influence with and without wing-fuselage interference

The NIAR team used one propeller from the NACA Report No. 594, “Characteristics of six propeller including the high speed range” and again measured in the wind tunnel and simulated with FloEFD then compared with the prediction of the uncorrected MIURA calculations (Figure 7).

It can be seen that the Blade Element Theory approach of MIURA works well for the power coefficient prediction above an advance ratio of 1, and for the thrust coefficient above an advance ratio of around 1.2. The NIAR team introduced correction points for the advance ratio smaller than 1, with a “Joint Point” at 1 so the interpolation of the corrected curve would utilize the results of the FloEFD simulation to achieve a higher accuracy (Figure 8).

Interference Effects

In order to analyze the interference effects of a 3D wing intersection with the fuselage of

the UAV, the aircraft was 3D scanned and a CAD model generated. The CATIA model was again simulated in FloEFD, once with only the wing and once with wing and fuselage joined together. The two different scenarios were analyzed and compared with the MIURA calculations. The lift and drag vs. AOA curves shows little deviation between MIURA and FloEFD with no interference (only the wing) but larger deviation if the interference is taken into account (Figure 9).

By taking a closer look at the spanwise distribution of lift and drag, a strong difference can be detected between wing only (no interference) and wing and fuselage (with interference) (Figure 10). FloEFD was able to predict the difference between both cases and therefore the correction of the MIURA model will improve the accuracy (Figure 11). The interference is clearly visible and in an aircraft surface plot of the pressure, the

change in the distribution can be seen close to the wing-fuselage intersection (Figure 12).

Conclusion

Dr. Olivares and his team were able to improve the simulator flight characteristic drastically with the help of the CATIA V5 embedded FloEFD simulations. The improved accuracy of stall prediction, propeller performance and interference effects enabled his team to conduct the first steps to develop a Virtual Engineering Method that is superior to the Traditional Engineering Method with regards to product development time (Figure 13) and costs.

References

[1] A. Barragan, J. M. Gomez, H. Solano, G. Olivares, “Comparison of a Simplified Real Time Aerodynamic Model with a 3D CFD Model of a UAV”, COE 2015, North Charleston (SC, USA), 28th April 2015

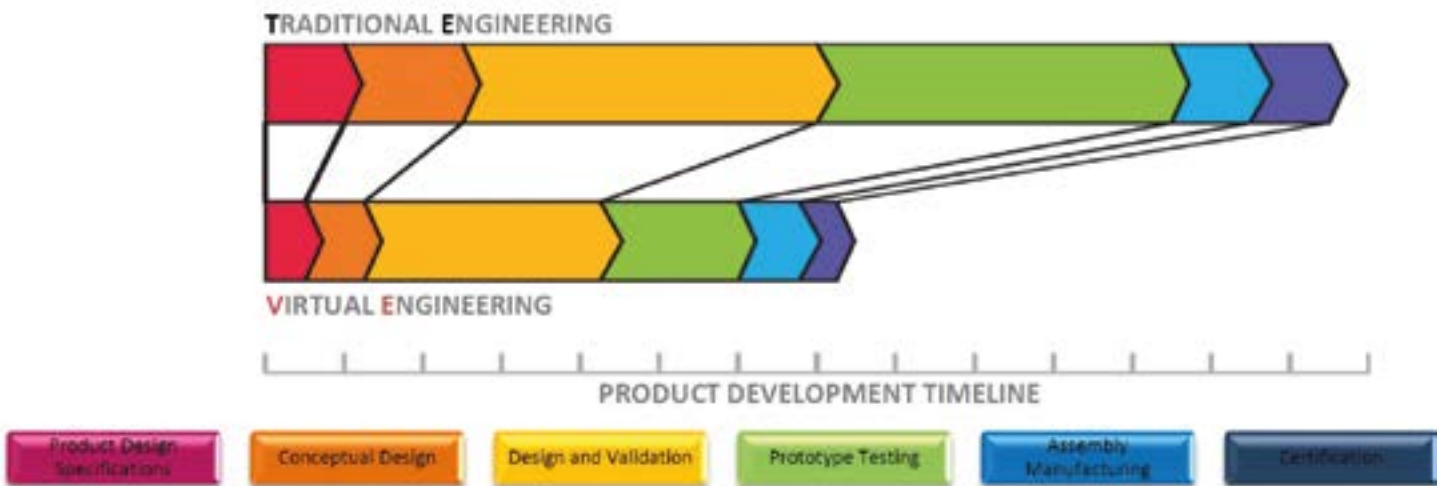


Figure 13. Advantages of the Virtual Engineering Method for the product development timeline



How to Gain 3 Seconds Per Lap

By Patrick Vlieger, Koen Beyers, Voxdale; Joren Bastiaens & Bram Dockx, Formula Electric Belgium

voxdale 

Formula Student is the biggest engineering competition in the world, with over 500 universities competing worldwide. The goal for each team is to design and build an open-wheel race car. During the summer these cars are put through a series of static and dynamic events at different

competitions. With the merging of Thomas More Innovation and Formula Group T, two teams joined forces as one larger team: Formula Electric Belgium (FEB). FEB became the only Belgian Formula Student (FS) team, consisting of more than 30 engineering students of KU Leuven University.

Compared to the 2013-2014 cars, the focus for the new FEB car was on a 20% overall weight reduction, improved reliability and an aerodynamic package. Major improvements, like the two self-developed permanent magnet motors, were made, to achieve the set goals. Over the past race year, the Umicore Luna saw the light: an





	Thomas More Innovation	Formula Group T	Formula Electric Belgium
Car Name	UTM-2	June	Umicore Luna
Year	2014	2014	2015
Weight [kg]	290	240	208
Acceleration 0-100 km/h [sec]	< 4	3.0	2.7
Lift coefficient	\	0.098	-1.200
Drag coefficient	\	0.456	0.545
Body	Steel tubular spaceframe with flax fiber body	Carbon-fiber-reinforced polymer (CFRP) monocoque	Carbon-fiber-reinforced polymer (CFRP) monocoque



Figure 1. Model history of Formula Student cars

electric FS race car, with a weight of 208 kg and an acceleration to 100 km/h in just 2.7 seconds!

The Umicore Luna was also set out to be the first Belgian FS car to feature a fully developed aerodynamic package, consisting of a front wing, diffuser, and rear wing. The package was to be added to the Umicore Luna to generate a higher amount of downforce with the aim of achieving higher cornering speeds on the track. The research on this topic was completed in the context of a Master's Thesis to obtain a degree in Industrial Engineering in Electromechanics. During the design of this aero package, the students were supported by Belgian design, engineering and research company, Voxdale bvba.

Voxdale specialize in automotive, medical and industrial sectors, as well as space

and aerospace industries. In its design and engineering process, Voxdale uses FloEFD™ for the optimization of designs. Most recently it has been used in drag reduction of trucks and Indycar race cars, as well as for structural analyses and thermal management projects.

Together with Voxdale the students came up with a plan of action, with weekly progress meetings.

The design of the aero package for the race car started out with the search for an airfoil for the front and rear wing, suitable for the needs of the Formula Student competition. Since the average speed of a Formula Student car is relatively low, an ideal high lift and low Reynolds airfoil was chosen. As a result of the gain in downforce and overall efficiency of the wing, a two-stage wing was chosen.

The angle of attack, gap and overhang of both wing stages were simulated in 2D. A manual mesh dependency test was performed successfully for the 2D wing and showed a steady result around 1.25 million cells. Using the Automatic Refinement option in FloEFD, the number of cells dropped to 250,000, resulting in an enormous reduction of calculation time, while still obtaining correct results.

The parameter for this optimization was to obtain the highest possible square lift coefficient, while minimizing the drag coefficient (max CL^2/CD). Over 100 simulations were performed to obtain the best value.

The angle of the diffuser was simulated in the same way: different angles were simulated in 2D, while numerous diffuser lengths were observed in 3D. The pitch of

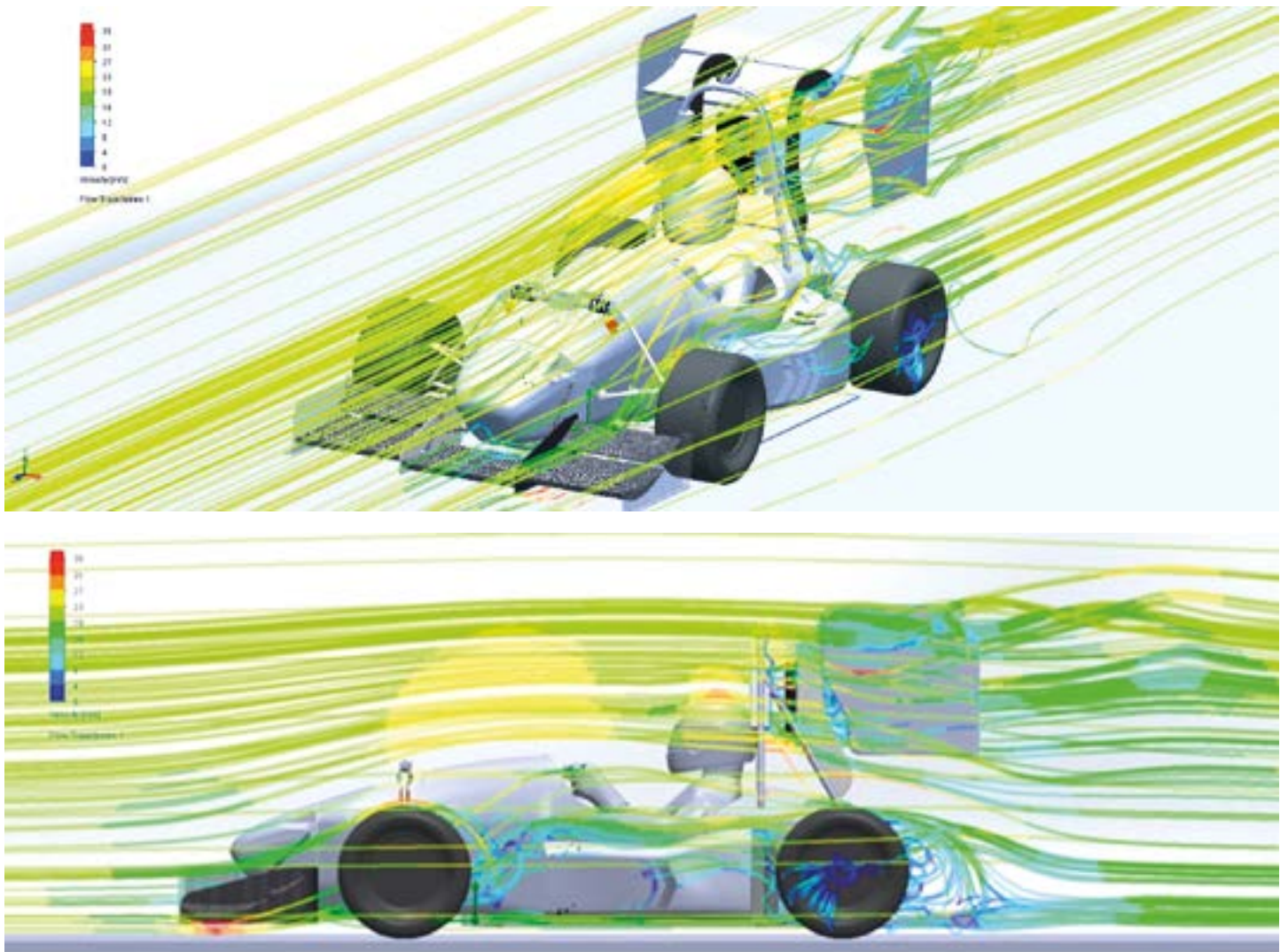


Figure 2. Flow Trajectories showing velocity over the new Umicore Luna model

the full car was also taken into account for this optimization.

After the optimization of both the diffuser and wings, a full 3D car model with aero package was simulated in CFD. The angle of attack of the rear wing was chosen to be adjustable in order to have an ideal setting for the different events at a Formula Student competition. In doing so, different settings of drag and downforce were possible and available for further validation, both on the track and in wind tunnel tests.

For the 3D simulations, a symmetry condition was used, splitting the car down the middle. This proved very useful in reducing overall calculation time. To simulate the different angles of attack of the rear wing, at first half of the car was simulated for one situation. As only the rear wing can change, EFD Zooming was performed at the rear part of the car. This again helped to reduce calculation time,

which was critical to meet the deadlines of the Formula Student project.

The results of the full 3D simulations were validated in a wind tunnel using a 3D printed $\frac{1}{8}$ scale model. Here, the same overall pattern as obtained using the flow simulation software was determined.

By adding the aero package, the positive lift the car originally generated, was converted into downforce. At 80 km/h this corresponded with an amount of 400N of downforce.

With the use of a simulation program that includes, among others, available power, rolling resistance and aerodynamic values, a lap time is determined. In previous years the new car, without aerodynamics, achieved a simulated lap time of 87.23 seconds. The new car with aerodynamics achieved a lap time of 84.32 seconds, a gain of almost 3 seconds.

When all simulations were completed and conclusion drawn, the aero package was built to be used during the Formula Student events, where results of the simulations could be validated further.

After a successful start at the FSUK event in Silverstone, United Kingdom, the FSG event in Hockenheim, Germany delivered a promising 16th place out of 97 competitors. Now the Formula Electric Belgium team is preparing the Umicore Luna for the last event at the end of this summer, at the Autodrom Most circuit in the Czech Republic.

Although the 2014-15 season hasn't finished, next year's team is already preparing the design of the new car, hoping for new racing success together with Voxdale and FloEFD. The first test of the season will be a full scale wind tunnel test in the newly built Flanders' Bike Valley wind tunnel, co-founded by Voxdale.

FloEFD™ Shines a Light on Automotive Lighting

Condensation and Radiation Modeling Technologies in Automotive CFD Simulation

By Chris Watson, Andrey Ivanov, and Svetlana Shtilkind, Mentor Graphics

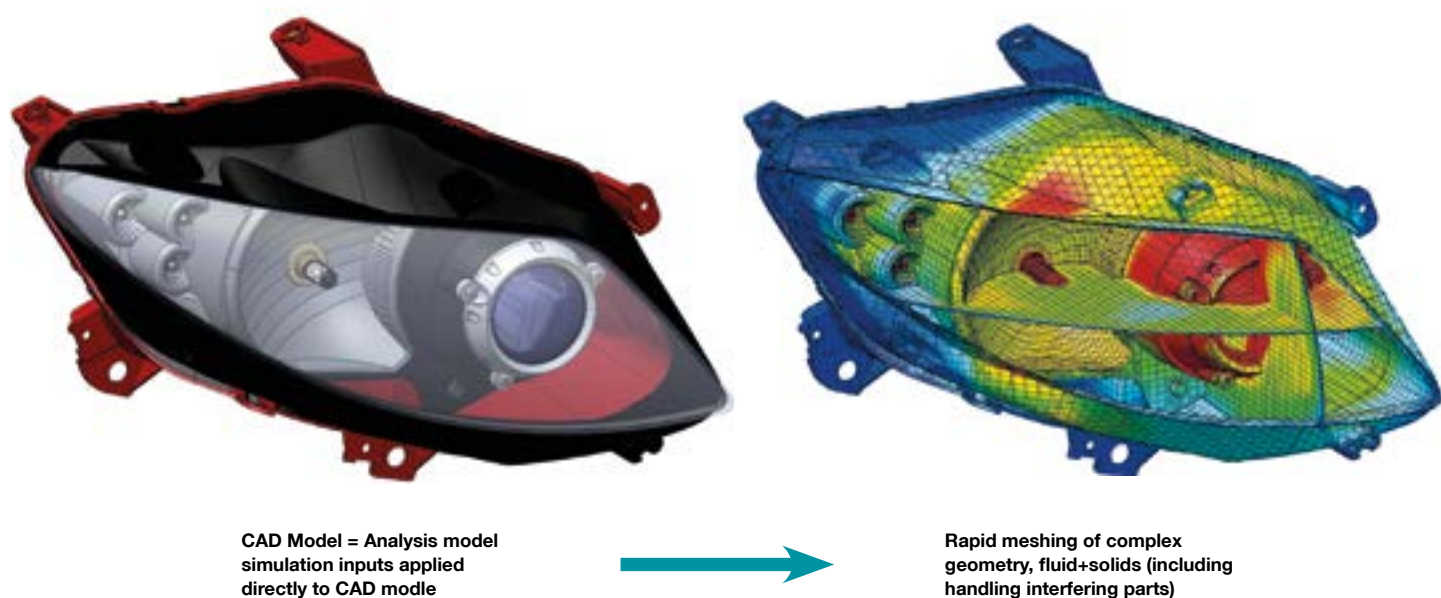


Figure 1. CAD model to final mesh

Mentor Graphics was approached several years ago by a leading automotive lighting supplier to help them find a better way of numerically simulating their headlights. Like most automotive suppliers and OEMs they already had existing commercial CFD tools which they had been attempting to use in their engineering process. However, the time and effort involved in conducting these analyses needed to be reduced. The biggest bottlenecks in the process were related to handling the complex geometries inherent in headlights and in turn creating a computational

mesh of those geometries that could be effectively analyzed. Of course the source of the geometry for one of these headlights is a CAD model, and an assembly defining one of these models can be comprised of scores of parts, including many sweeping, stylized components that are used in modern lights. The intersections of all of these parts can create complex geometrical conditions that are often quite challenging to mesh with traditional approaches.

FloEFD, Mentor Graphics' general purpose CFD software, has several key strengths that aggressively address the difficult, time

consuming aspects of preparing a headlight model for analysis that make it attractive. The first benefit is that the users can work directly on the native CAD model in their CAD tool. This eliminates the step of transferring a neutral file format model to the analysis tool, followed by the typical need to clean up any translation errors due to this process. Next, the benefit of the immersed boundary style of meshing used by FloEFD also impacts the geometry preparation. Because of this meshing the laborious step of simplifying and de-featuring the model can be greatly reduced. Geometric conditions that give other meshers difficulties, like interfering parts, small gaps and sharply pointed objects are handled by the FloEFD mesher

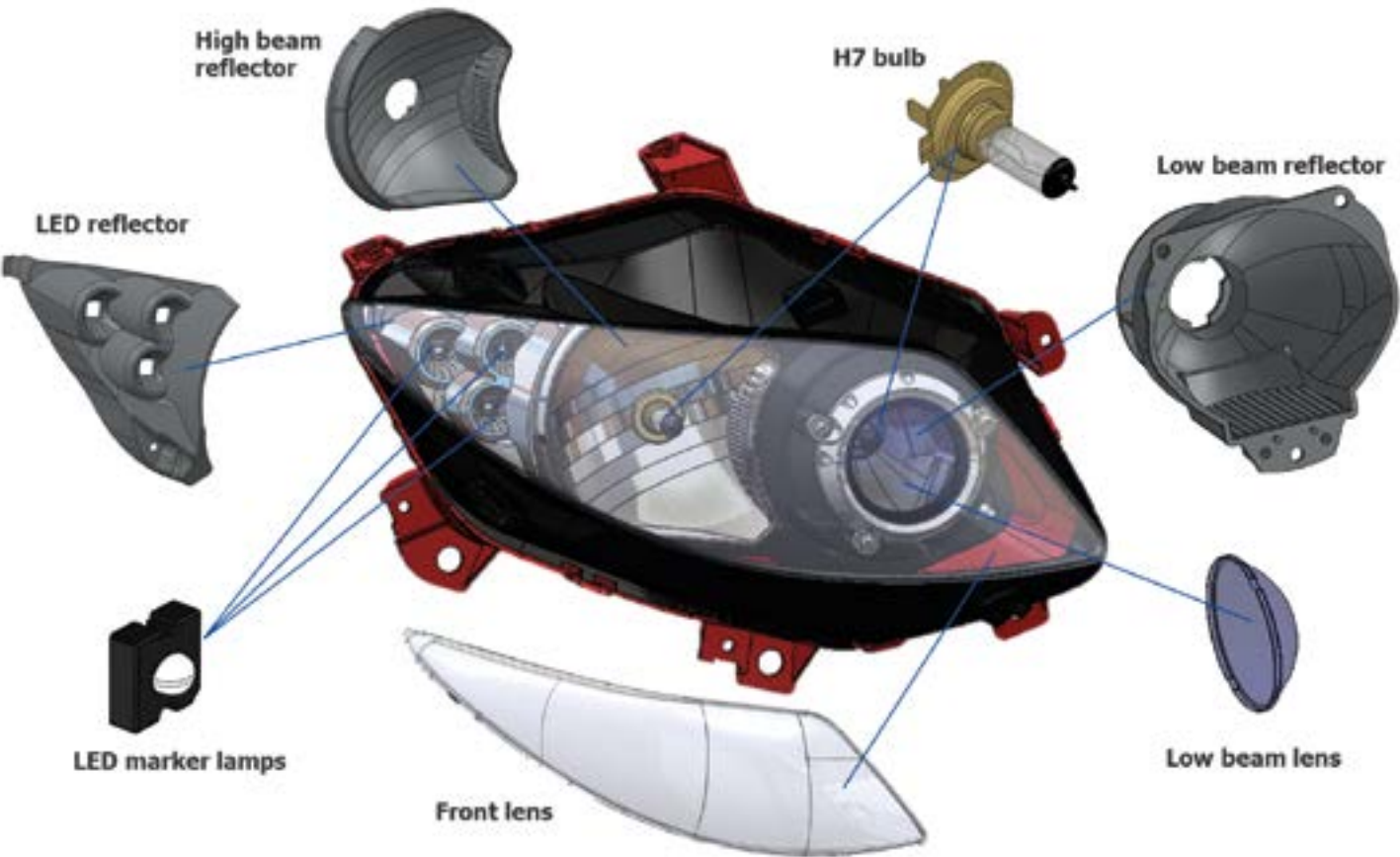


Figure 2. Assembly and relevant parts

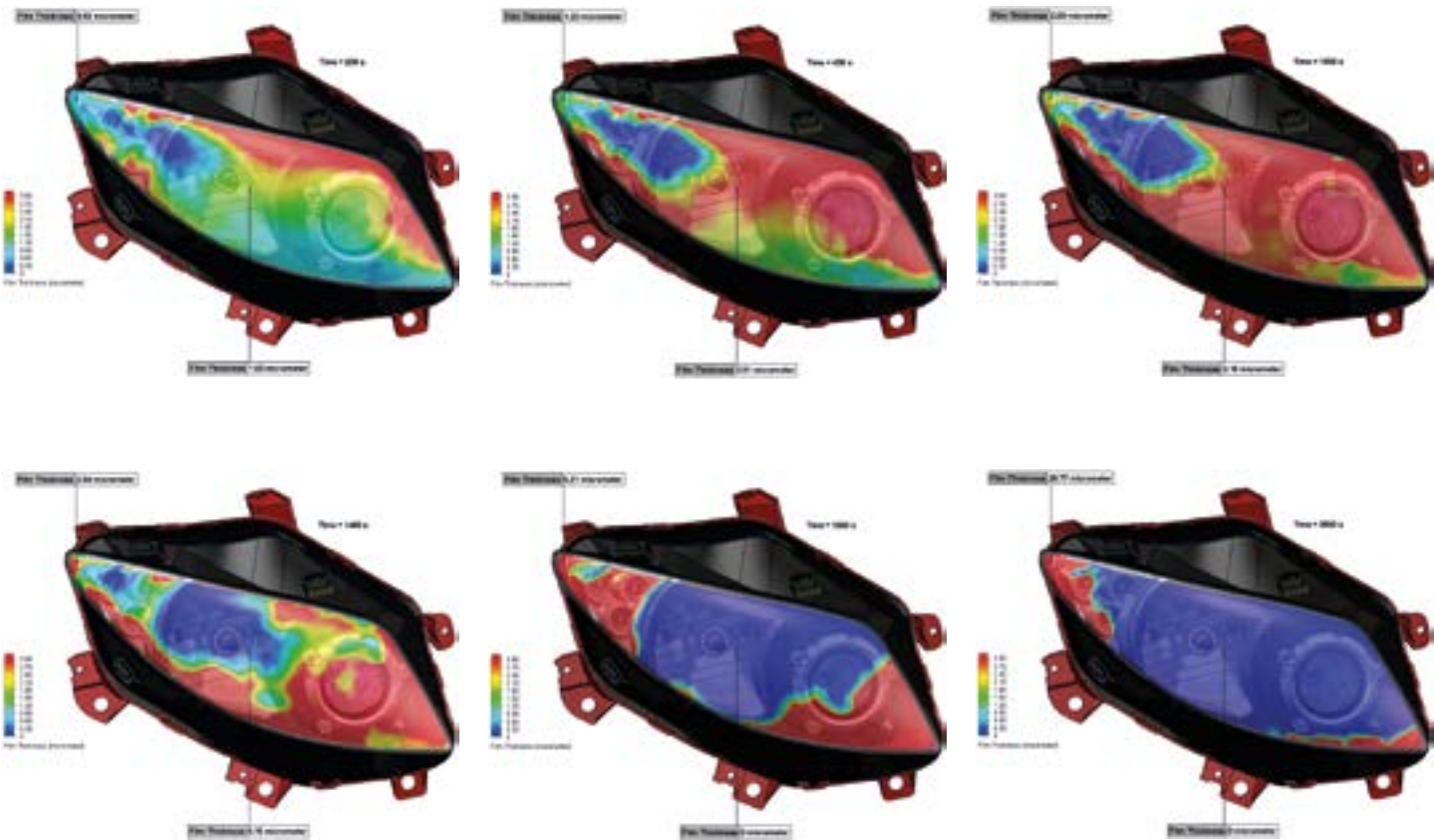


Figure 3. Film thickness development at different points in time

and solver. The net effect is a tool that can efficiently and quickly overcome the most user-intensive, time consuming hurdle of conducting these types of analyses.

So the automotive lighting supplier began adopting FloEFD to tackle these problems. Since the main bottleneck in their process had been addressed by FloEFD, as can be human nature after a relatively brief “honeymoon” period, these strengths became accepted as the “new norm” and the attention shifted to adding advanced functionality to address the demands of a complete headlight analysis. The Mentor Graphics FloEFD development team worked closely with the customer to understand their requirements, and in each of the successive releases of FloEFD enhancements were added to help make it a complete, expert tool to tackle automotive lighting applications. Many of these enhancements focused on advanced radiation capabilities, like spectral dependencies for radiative properties, like absorptivity and emissivity (implemented in a sophisticated ray-based approach), reflectivity options like diffuse, spectral, and Gaussian reflection, and improved handling of focusing and refraction for cases in which optical effects are important as well as thermal effects in semi-transparent solids. A module to FloEFD was introduced that included these enhancements as well providing the ability to create LED compact models, in which thermal and optical data from Mentor Graphics’ T3ster® and TeraLED® devices could be used to create a more accurate representation of an LED in a CFD model. The LED compact model is unique in that the user simply assigns the forward current to the device (rather than the typical input of heat generation rate, which may not be clearly defined) and the output from the analysis will include the junction temperature of the LED, its resulting heat power, and the luminous flux.

Another capability added to FloEFD to address an area of concern for headlight designers is the ability to simulate condensation. As newer headlight designs have incorporated lighting sources that generate less heat (in particular LEDs), condensation on the lenses of headlights can become a bigger issue. FloEFD’s water film evolution capability is able to model condensation, evaporation, and phase change (allowing for icing predictions), and display this information in a variety of quantitative and qualitative means.

Headlight Example

The following example highlights FloEFD’s capabilities in simulating headlights, with a particular focus on surface condensation modeling. Figure 2 displays the model and the relevant parts that were included in the simulation.

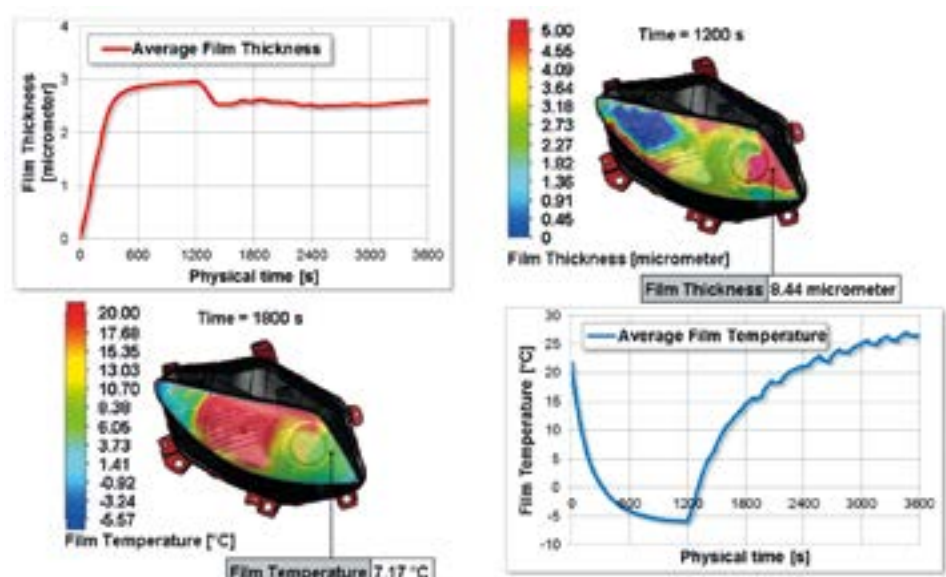


Figure 4. Development of film mass and temperature over time

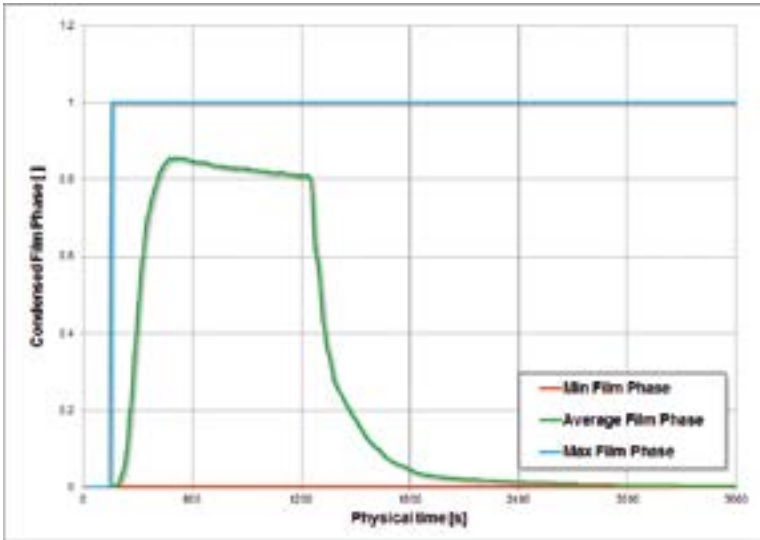


Figure 5. Transient history of film phase

The full conjugate heat transfer problem is modeled, including convection, conduction, and radiation. Appropriate material and radiative properties are assigned to each of the parts, including the lenses being modeled as semi-transparent to radiation with a specular dependency. The air space within the headlamp assembly is modeled. Transient heat transfer boundary conditions on the external faces of the assembly are used in this example, although the external air domain could have been included as part of the analysis as well. The pressure and temperature of the air within the assembly are initialized to 101325 Pa and 25°C respectively, the initial external temperature is set to -10°C, and the relative humidity is set to 95%. The inside surface of the front lens is set as “wettable” and is the region of interest to determine whether condensation occurs. The simulation scenario being modeled is:

- 1. A vehicle stopped in a cold humid environment: condensation starts;
- 2. After 750 seconds the LEDs are switched on; and
- 3. After 20 minutes (1200 seconds) the engine and lights are switched on: melting starts.

As the simulation begins the solid components start to cool due to the cold external temperature. Since the air within the headlamp is initialized with a high relative humidity, condensation begins to form on the inside surface of the front lens. Figure 3 shows the progression of the film thickness of the condensation at different points in time. At 1200 seconds the halogen bulbs, as well as the engine, are turned on. This starts to add heat to the system, and it is seen from these images that the film begins to be cleared, especially in the region in front of the high beam reflector.

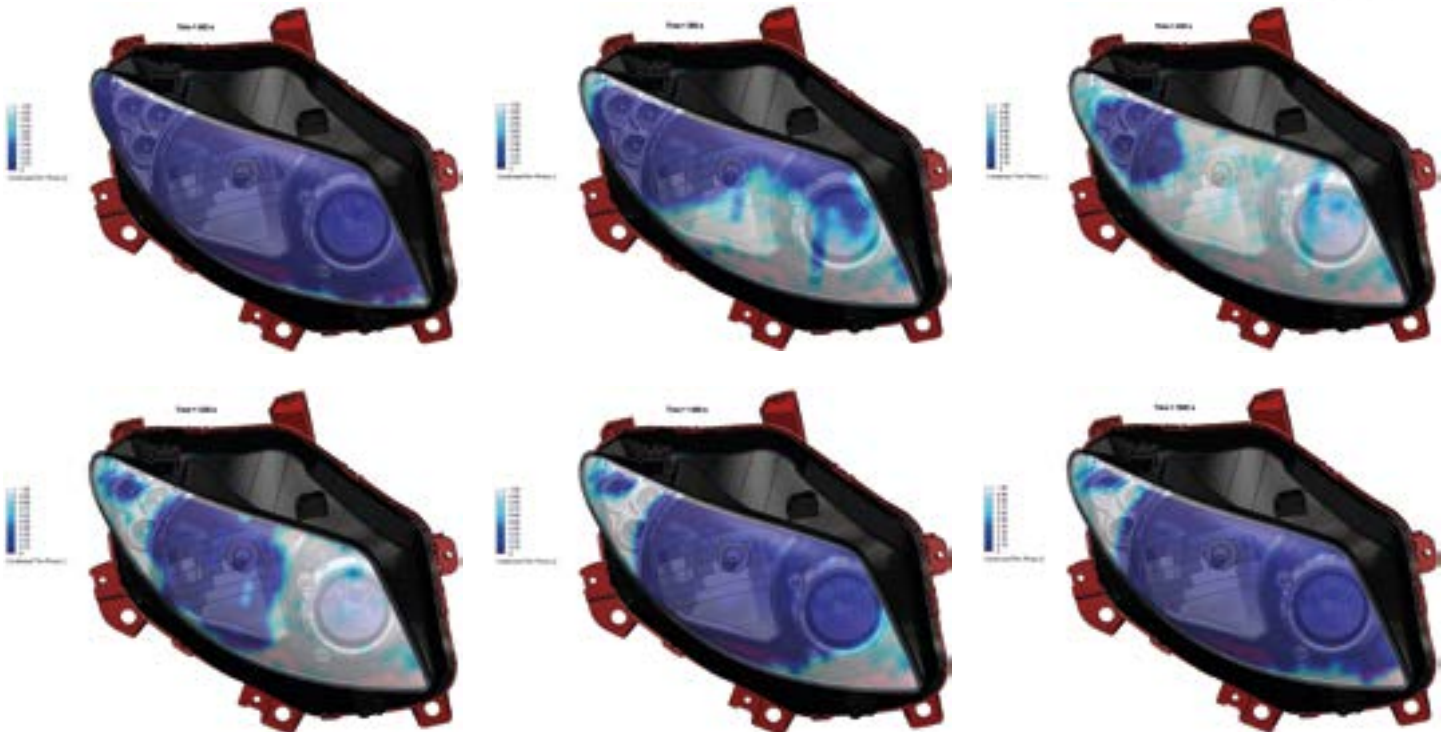


Figure 6. Development of condensed film phase on inner surface of outer lens over time

Besides the contour plots that show the distribution of condensation, FloEFD can output integrated information about the film history as well. Figure 4 shows the progression of the film thickness over time. As expected the average film thickness grows initially, ultimately flattens, and at 1200 seconds (when the lights and engine turn on) begins to decrease. However, after an initial decrease the film thickness flattens again. If one examines the contour plots of film thickness it appears that most of the lens is cleared. So why does the film thickness graph seem to not reflect this? As the heat from the bulb immediately clears the condensation from the lens in front of the bulb, this moisture is re-introduced into the airspace with the headlamp and increases its humidity. This humidity in the air is able to re-condense on colder surfaces in the corners of the headlamp. So although the overall area that contained condensation was substantially reduced once the engine/lights were started, there were some smaller colder regions in the corners that allowed a thicker film of condensation to re-form.

Another interesting phenomenon being shown in this simulation is that not only does condensation form on the inside of the outer lens, but this condensation freezes. The graph shown in Figure 5 tracks the phase of the film over time, and clearly by around 500 seconds most of the film has frozen. This continues to 1200 seconds when the lights/engine turn on and are able to melt the frost from the lens.

The images in Figure 6 show contour plots of the condensed film phase (with 0 being

LED (Input)	
Type	Osram Golden Dragon QA
Current	Dependency
LED (Output)	
T junction	102.0 °C
LED Heat Generation Rate	0.915 W
Luminous Flux	95.92 lm

LED (Input)	
Type	Osram Golden Dragon QA
Current	Dependency
LED (Output)	
T junction	100.2 °C
LED Heat Generation Rate	0.914 W
Luminous Flux	97.41 lm

LED (Input)	
Type	Osram Golden Dragon QA
Current	Dependency
LED (Output)	
T junction	101.5 °C
LED Heat Generation Rate	0.915 W
Luminous Flux	97.07 lm

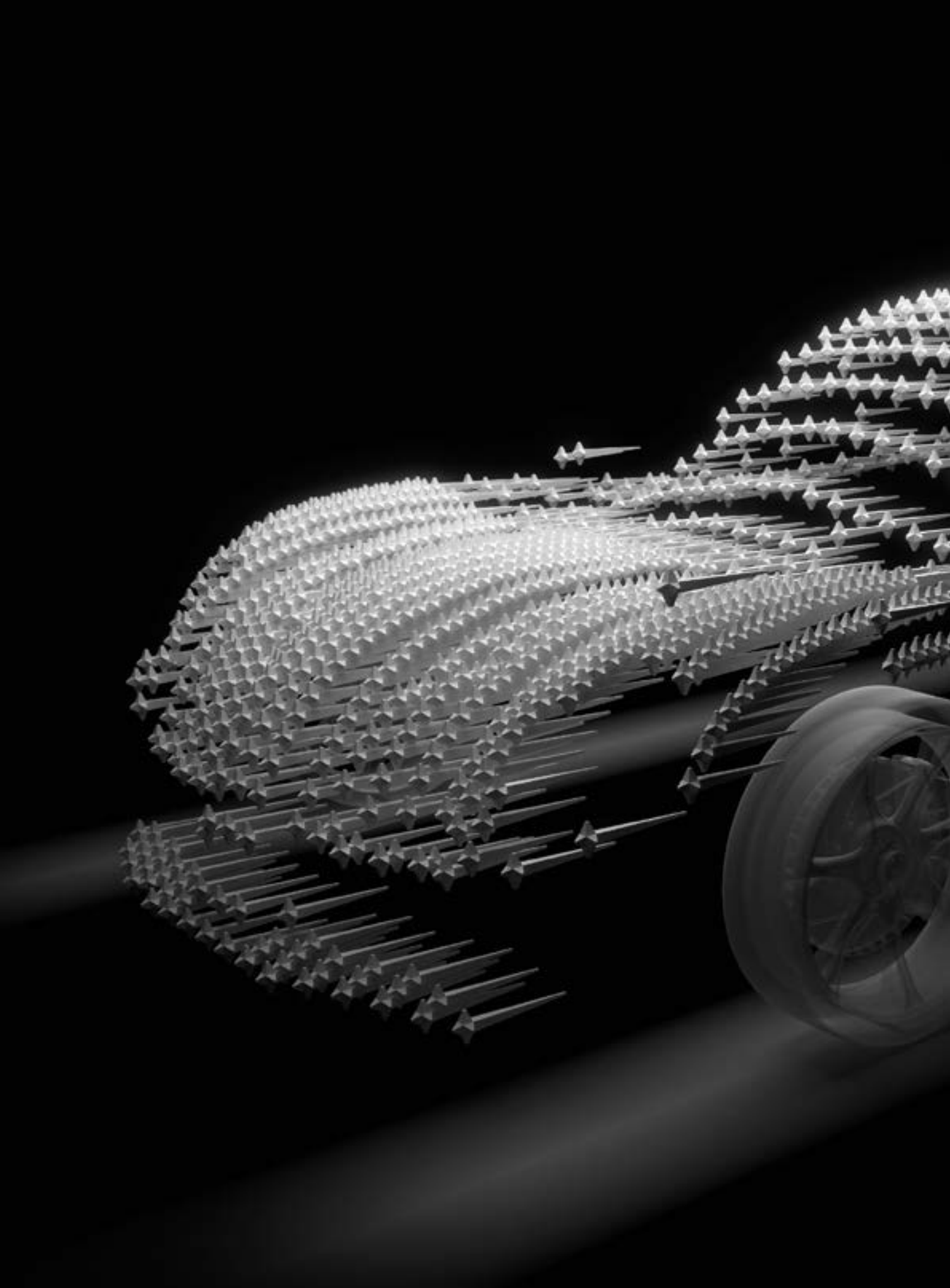
Figure 7. LEDs performance

liquid and 1 being solid). They show the development and distribution of the ice forming on the lens and ultimately melting.

Additionally, the LEDs were modeled using FloEFD's LED compact model (based on T3ster and TeraLED data). So the simulation is able to quantify various parameters of



interest as seen in the image in Figure 7. FloEFD's fundamental strength of easily meshing complex native CAD models coupled with functionality introduced to meet the requirements of lighting applications make it the ideal tool for automotive lighting simulation.





JSAE Benchmark of Automotive Aerodynamic Test Measurements

Ahmed-Type Car Body Versus CFD
Software Predictions

By Boris Marovic, Automotive Industry Manager, Mentor Graphics



The Society of Automotive Engineers of Japan (JSAE) recently conducted a blind benchmark for commercial Computational Fluid Dynamics (CFD) software to demonstrate their accuracy against test validation data on a new car shape [1]. Participants simulated a 1/4-scale wind tunnel car model. The aerodynamic test model consisted of the “Ahmed” vehicle body (see Figure 1) with a full vehicle length of 1,100mm without the “additional part” at the end of the vehicle (Case 1) and at a length of 1,250mm with the additional part attached (Case 2). The height of the vehicle was 355 mm, the width 320mm, and the underfloor vertical gap was 15mm.

Each CFD software package had to analyze the airflow around the model and compare their prediction accuracies to experimental data without knowing the data beforehand. In particular, JSAE wanted to verify how accurate each CFD tool was at predicting boundary-layer separation, pressure distribution, and body forces on the model. It was up to the participants in the benchmark to choose the best meshes and turbulence models in their CFD codes to offer their best prediction.

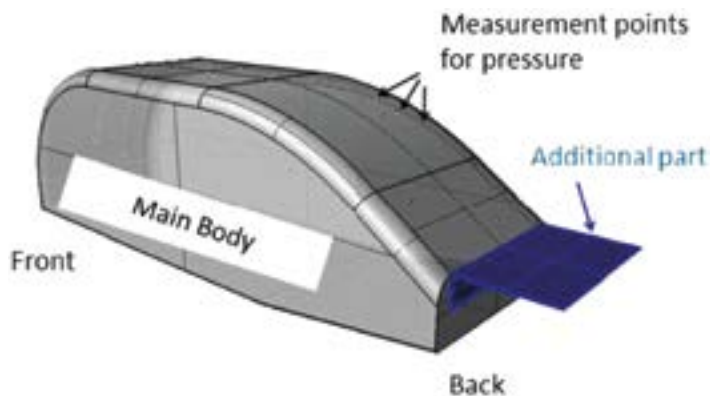


Figure 1. The JSAE Aerodynamic Test Ahmed Vehicle Body with and without the additional part at the end of the vehicle

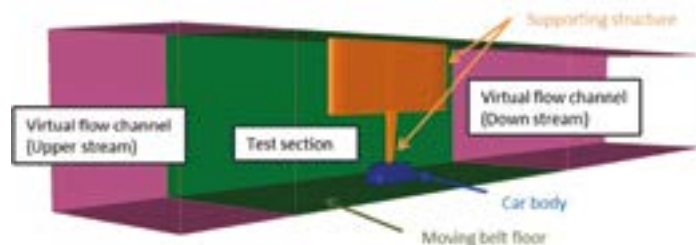


Figure 2. The model of the test chamber for the wind-tunnel experiment

The commercial CFD participants were provided with data that included support pole shape, test section shape, and vehicle model shape plus the specification of the wind tunnel test section (Figure 2). The participants were provided with reference tunnel data as well as the specified conditions for the test. Simulations were all to be at a velocity of 25.0 m/s; the fluid properties were given as a density of 1.17 kg/m³ and a kinematic viscosity of 1.56 x 10⁻⁵ m²/s, which resulted in a Reynolds number for the test of 1.76 x 10⁶.

All CFD simulation software had to provide results for drag, lift, and pitching-moment coefficients as well as pressure coefficient at various sections of the vehicle body. Sections vertically to the car were compared to measurements at the center plane ($y/W = 0.0$), 12.5% off center ($y/W = 0.125$), and 25% off center ($y/W = 0.25$), where W is the width of the body. The underfloor section was only analyzed at the vertical center plane as it was not disturbed by the wind-tunnel fixture as the top side was. The section horizontal to the car was compared at 25% ($z/H = 0.25$) of the car height as shown in Figure 3 where 'H' is the height of the body.

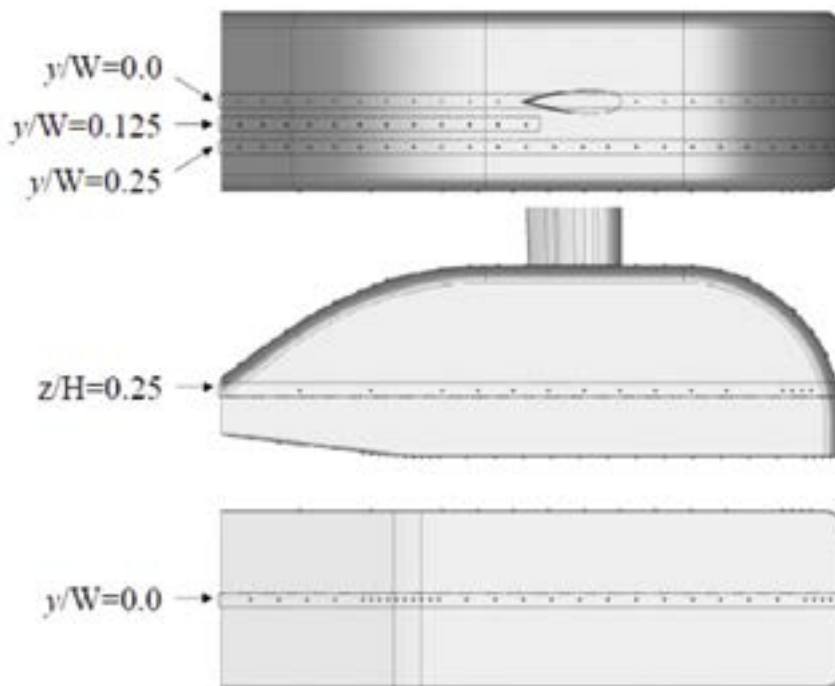


Figure 3. Pressure coefficient measurement point distribution on the JSAE car body

The airflow wake predictions behind the car model were analyzed at the vertical lines of $x = 1,000\text{mm}$ (line 1), $x = 1,050\text{mm}$ (line 2), $x = 1,100\text{mm}$ (line 3) and $x = 1,200\text{mm}$ (line 4) – see Figure 4 - and compared to experimental measurements in the Blind Benchmark.

Seven organizations (Table 1) provided submissions to the JSAE blind benchmark (encompassing most of the main commercial CFD codes available in the market today) and they all had three months to submit their simulation results and technical information on their CFD computation approaches, physical models, and resolution scales. KKE Inc., a Mentor

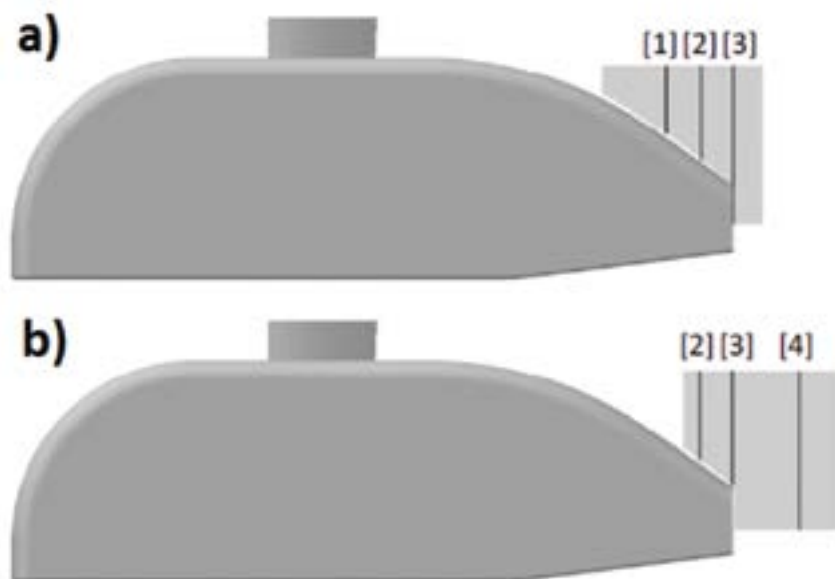


Figure 4. Wake measurements at $y/W = 0.0$ for the JSAE car body: a) the case without the additional part and b) the case with the additional part

Graphics reseller in Japan, submitted simulation results using the CAD-embedded CFD software, FloEFD™.

Table 1 shows that the cell count was 4 to 11 times lower for FloEFD than the other CFD tools for the cases considered, it uses partial cells that can contain several sub-control volumes and a special boundary layer treatment that does not need a fine cell resolution of the boundary layer as other tools do. Also, it is worth noting that a large number of CFD calculations shown in Table 1 were conducted in transient mode, which usually results in very high CPU time for the calculation even with a high number of cores due to the large number of cells employed. More information on each code's CFD simulation set-up can be found in the original JSAE benchmark paper [1].

Results

For the FloEFD simulations, KKE Inc. used the Cartesian mesh approach with solution adaptive refinement (Figure 5) on an octree basis and local meshes around the body [2-3]. Each cell level refinement was easily set-up in FloEFD and the rest of the mesh generation adaptation process was automated. The adaptive refinement can also be limited to a certain region of the domain by a maximum level being applied to the cell count so that the code does not explode the mesh size and thus helping to prevent very high CPU times. Table 2 shows the computational effort used by the seven software tools used in the blind benchmark.

Compared to the other tools, FloEFD required less resources and less calculation time to come up with good overall results, and it shows quite good agreement with the wind-tunnel experimental measurements too (Figures 6-8).

Figures 6 - 8 show the simulation prediction results for all of the CFD codes employed in the benchmark plus the error margin of the test experiment data for drag, lift, and pitching moments. The blue dashed lines show the upper and lower error margin for Case 1, without the additional part, and the red dashed lines show the margin for Case 2, with the additional part. In Figure 6, the drag coefficient (CD) of AcuSolve (Inflow 2), FloEFD, and STAR-CCM+ (IDDES) were all within the margin of error for Case 1 followed by SCRYU/Tetra (DES) with a lower value and then iconCFD again with a little lower CD. For Case 2, none of

Participants	Software	Compressible/Incompressible	Steady State/Transient	Turbulence Model
JSOL Corporation	AcuSolve Incompressible	Incompressible	Steady state	Spalart Allmaras
ANSYS Japan K.K.	ANSYSFluent R14.5	Incompressible	Transient	Scale Adaptive Simulation (SAS)
Kozo Keikaku Engineering Inc.	FloEFD	Compressible	Steady state	Modified k-Σ
Icon Technology & Process Consulting Ltd.	iconCFD	Incompressible	Transient	Spalart Allmaras
ESI Group	PAM-FLOW	Incompressible	Transient	SGS
Software Cradle	SCRYU/Tetra	Incompressible	Transient	SST-DES, SST-SAS
CD-adapco	STAR-CCM+ v7.06	Compressible, Incompressible	Transient, Steady state	IDDES (SST), SST k-ω

Software	Mesh Type	Number of Cell Layers in the Boundary Layer	Number of Cells Without Rear Flat Panel (Case 1)	Number of Cells With Rear Flat Panel (Case 2)	Mesher Used
AcuSolve	Tetrahedral mesh	7	24,755,000	25,795,000	AcuConsole1.8b
ANSYSFluent R14.5	Unstructured grid	17	16,000,000	16,700,000	ANSYSMeshing R14, TGridR14
FloEFD	Cartesian mesh based on octree technology	-	3,520,000		FloEFD
iconCFD	Hexahedral dominant mesh	7	37,640,000	38,300,000	foamProMesh
PAM-FLOW	Tetrahedral mesh	6	38,260,000		PAMGEN3D
SCRYU/Tetra (DES, SAS)	Tetrahedral mesh with prisms	10	27,000,000		SCRYU/Tetra
STAR-CCM+ v7.06 (IDDES, SST k-ω)	Hexahedral dominant mesh	20	16,690,000	16,835,000	STAR-CCM+ v7.06

Table 1. Participant Companies and CFD Codes in the JSAE blind automotive aerodynamic benchmark

			Calculation Time (h)		
Software	Computer Characteristics	Cores	Steady State	Transient	Time Step (s)
AcuSolve	HP ProliantDL360p Gen8, Xeon E5-2660 (2.2 GHz)	16	No Flat Panel: 4.2 With Flat Panel: 5.9	-	-
ANSYSFluent R14.5	Dell PowerEdge R720 (2.9 GHz)	32	4	60	2.0 x 10-4
FloEFD	HP Z600, Intel Xeon X5670 (2.93 GHz)	6	17	-	-
iconCFD	Intel® Xeon® Processor E5645 (2.4 GHz)	72	-	No Flat Panel: 254 With Flat Panel: 267	5.0 x 10-5
PAM-FLOW	HP BL460c, Intel Xeon E5-2680 (2.7 GHz)	16	40	155	5.352 x 10-5
SCRYU/Tetra (DES)	Intel Xeon E5-2690 (2.9 GHz)	48	-	33	1.0 x 10-4
SCRYU/Tetra (SAS)			-	34	1.0 x 10-4
STAR-CCM+ v7.06 (IDDES)	Dell Power Edge, Intel® Xeon® CPU X5675 (3.07 GHz)	120	-	~200	1.0 x 10-4
STAR-CCM+ v7.06v (SST k-ω)		12	17.5	-	-

Table 2. For the participating CFD Codes in the JSAE blind automotive aerodynamic benchmark, computational resource and time required for the calculations

the codes were exactly within the error margin but iconCFD made it the closest, followed by STAR-CCM+ (IDDES) and then AcuSolve (Inflow 2).

In Figure 7, the same dashed lines show the error margins also for Case 1 and 2 but here the graph shows the lift coefficient (CL). For Case 1 only, FloEFD was exactly within the margin. Slightly out of margin were STAR-CCM+ (SST k- ω), SCRYU/Tetra (SAS), and AcuSolve (Inflow 1) all at the same level, followed by AcuSolve (Inflow 2) with a larger CL. For Case 2, the test margin was very narrow and none of the codes were exactly within it. STAR-CCM+ (SST k- ω) was the closest, followed by ANSYS Fluent and then AcuSolve (Inflow 1), but with larger discrepancies.

The pitching moment coefficient predictions are shown in Figure 8 where they have the same margin color notation as before. In this graph, the error margin for Case 1 is very narrow and none of the CFD codes made it exactly within the margin. The closest were STAR-CCM+ (IDDES), followed by PAM-FLOW, and then SCRYU/Tetra (SAS) and STAR-CCM+ (SST k- ω) who were equally distant but on the lower margin compared to PAM-FLOW. Case 2 has a larger margin, and only FloEFD made it inside the margin, followed by ANSYS Fluent slightly outside the lower margin line and then with a slightly lower value SCRYU/Tetra (SAS) and AcuSolve (Inflow 2), with the same distance but on opposite sides of the margin.

It can therefore be concluded from the results of the JSAE benchmark that FloEFD was very accurate for both drag and lift in Case 1 and had the best pitching moment prediction in Case 2. STAR-CCM+ also comes out very well from the exercise if an expert user chooses the right turbulence model for the particular case

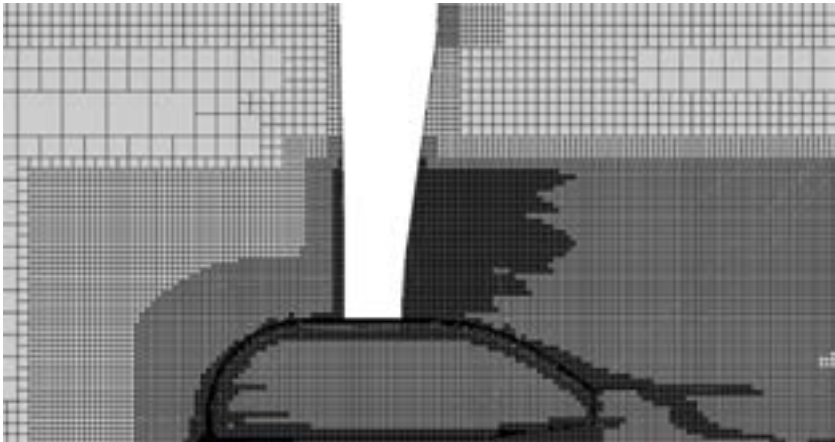


Figure 5. Computational mesh used by FloEFD for the JSAE benchmark model

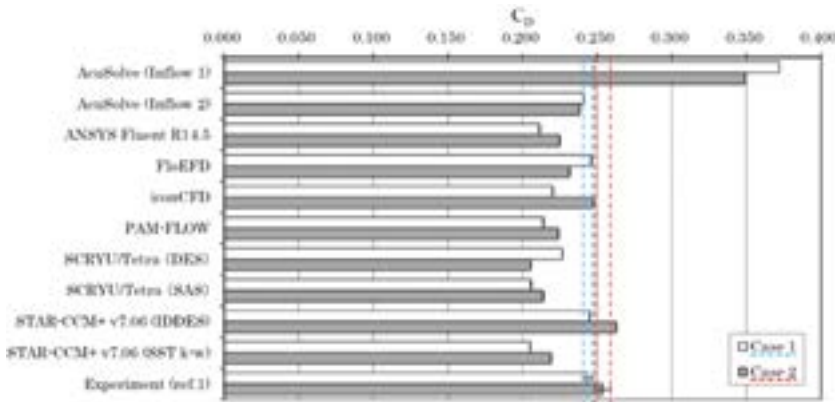


Figure 6. Drag coefficients for all CFD codes for Cases 1 and 2 with the experimental Test Data error margins in blue dashed lines (Case 1) and red dashed lines (Case 2)

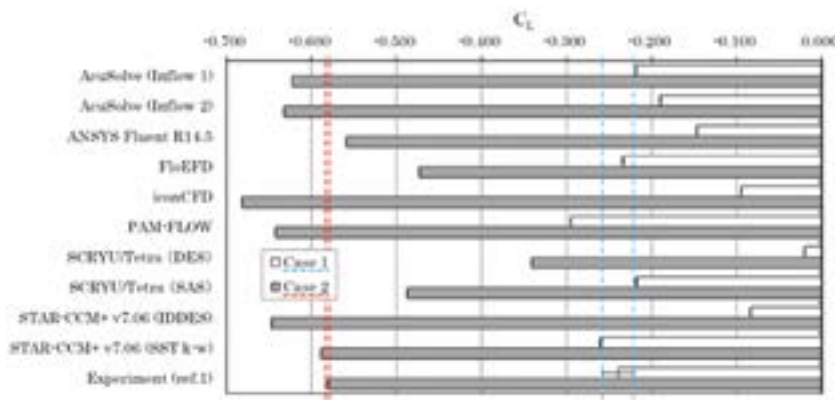


Figure 7. Lift coefficients for all CFD codes for Cases 1 and 2 with the experimental Test Data error margins.

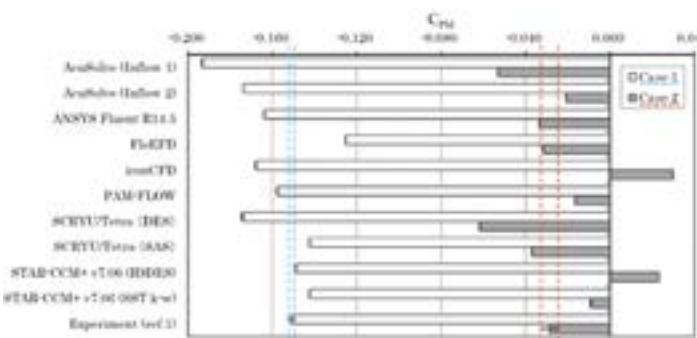


Figure 8. Pitching-moment coefficients for all CFD codes for Cases 1 and 2 with the experimental Test Data error margins.

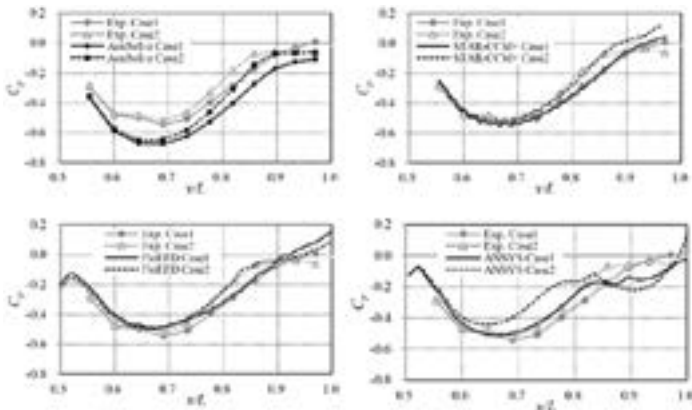


Figure 9. Comparative CFD results versus experimental measurements for the pressure coefficient at the top surface of the JSAE model at $y/W = 0.125$ for $x/L > 0.5$



being simulated. When looking at pressure coefficients measured on the car body surface (see Figure 3 for locations), Figures 9 through 12 show comparatively how well AcuSolve (Inflow 2), STAR-CCM+ v7.06 (SST k- ω), FloEFD, and ANSYS Fluent R14.5 matched the experimental data for the two cases being considered.

Finally, Figure 13 illustrates the experimental test results from particle imaging velocimetry (PIV) measurements as a contour plot post-processed to compare with most of the CFD simulation software predictions. FloEFD and STAR-CCM+ (SST k- ω) can be seen to most closely match the wind-tunnel experimental results the best.

Conclusions

Although the meshing and solver technology of FloEFD is a non-traditional CFD approach, this JSAE blind benchmark has proven that FloEFD is as accurate as, or better than, other traditional commercial CFD software in a difficult automotive external aerodynamic study. FloEFD ranks well alongside STAR-CCM+, whilst using fewer cells, a single sophisticated turbulence model, and lower CPU times to achieve the same level of results. In addition, it was worth pointing out that with FloEFD's out-of-the-box software, it also takes less time to set-up and optimally mesh the automotive body model, in addition to activating the single transitional k- Σ turbulence model compared to the many turbulence models some of the other codes employed, that required expert interventions.

References

- [1] Nakashima, Takuji; Sasuga, Nobuhiro; Ito, Yuichi; Ikeda, Masami; Ueda, Ichihiro; Kato, Yoshihiro; Kitayama, Masashi; Kito, Kozo; Koori, Itsuhei; Koyama, Ryutaro; Shimada, Yoshihiro; Hanaoka, Yuji; Higaki, Tatsuhiko; Fukuda, Kota; Yamamura, Jun; Li, Ye (2013). Benchmark of Aerodynamics CFD of Simplified Road Vehicle Model: JSAE. Paper Number: 20134343. Pages 8 – 28, http://bookpark.ne.jp/jsae/pdf_e.asp
- [2] Advanced Immersed Boundary Cartesian Meshing Technology in FloEFD: Mentor Graphics, <http://go.mentor.com/2gogl>
- [3] Enhanced Turbulence Modelling in FloEFD™: Mentor Graphics, <http://go.mentor.com/2glzd>

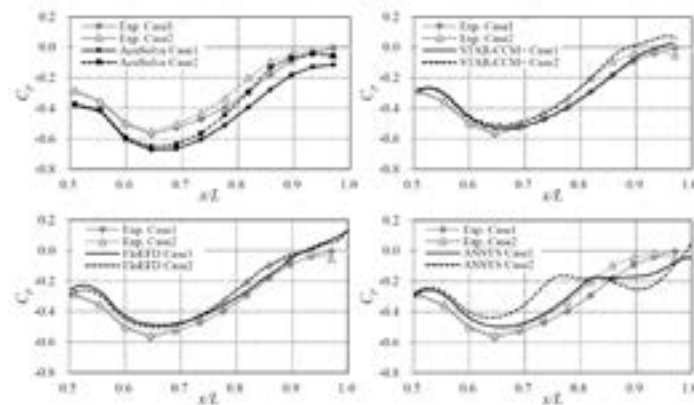


Figure 10. Comparative CFD results versus experimental measurements for the pressure coefficient at the top surface of the JSAE model at $y/W = 0.125$

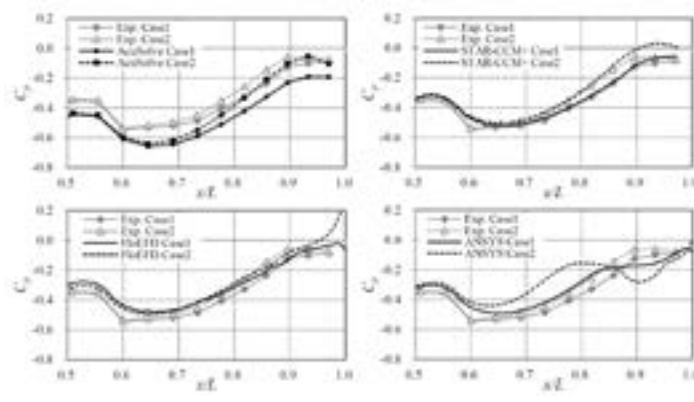


Figure 11. Comparative CFD results versus experimental measurements for the pressure coefficient at the top surface of the JSAE model at $y/W = 0.25$ for $x/L > 0.5$

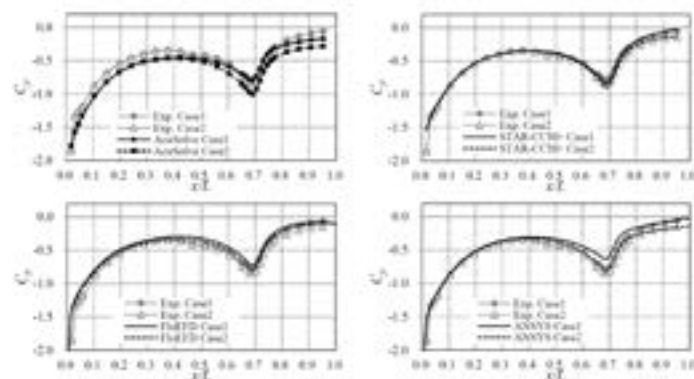


Figure 12. Comparative CFD results versus experimental measurements for the pressure coefficient at the top surface of the JSAE model at $y/W = 0.0$

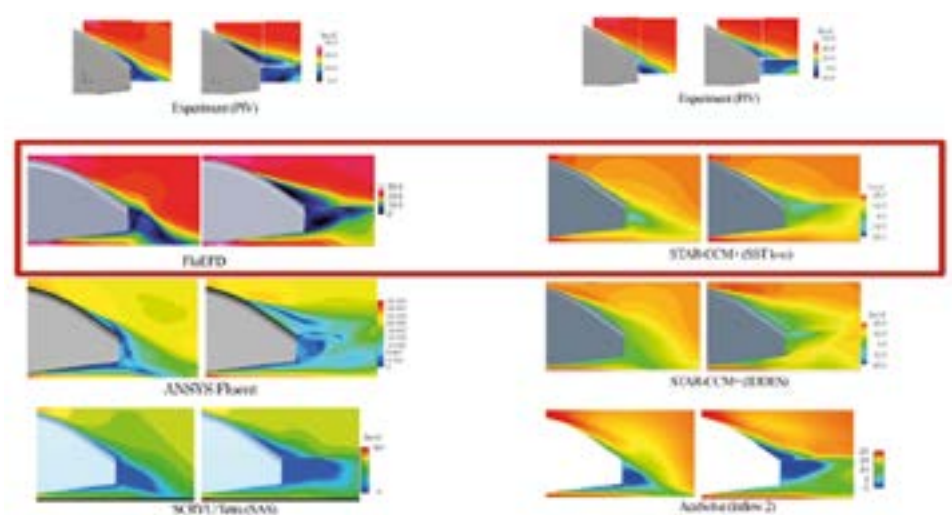


Figure 13. Centerline velocity distribution test results versus CFD code predictions for JSAE Cases 1 and 2



Making Light Work of Lifting

Liebherr-Werk Nenzing GmbH use FloEFD™ for Creo™ in their Mobile Harbor Crane Designs

Interview Kolio Kojouharov, CFD Expert, Liebherr-Werk Nenzing GmbH,
by Thomas Schultz, Application Engineering Manager, Mentor Graphics

Liebherr Werk-Nenzing GmbH, manufacturer of maritime cranes, crawler cranes and foundation equipment, demonstrates the importance of modern “Frontloading” simulation tools which go far beyond classic FEA-Analysis within the heavy duty industry.

From your experience how is the heavy duty simulation world doing at present?

The simulation world is more than ever dominated by strict regulation due to emissions, performance and comfort. It has become more and more important over the years to think beyond the classic FEA-Analysis, which most people immediately associate with our industry and applications.

Recognizing the potential for FEA-Analysis, how does CFD fit?

From a simple hydraulic block to a full power pack there is an almost infinite number of tasks waiting to be analyzed. The large number of potential cases which might consume needless power has been realised over the past years. However, external simulation services to solve this soon turned out to not be efficient enough and too expensive. At Liebherr we have high standards, so finding the tools to meet them was not an easy process and took a long time.

Why was FloEFD chosen?

As a company we were aware of FloEFD™ and indeed the concurrent approach of the technology. The over-riding reason was the strong pre-&post processor in combination with the efficient meshing. Alongside the advantage of full CAD-integration into our CREO environment, allowing quick analysis of full power packs in our own CAD system. This gives me the ability to analyze more projects at the same time, something competitors are not able to achieve.

How does FloEFD help with the complex structure of power packs?

Power packs basically contain everything below

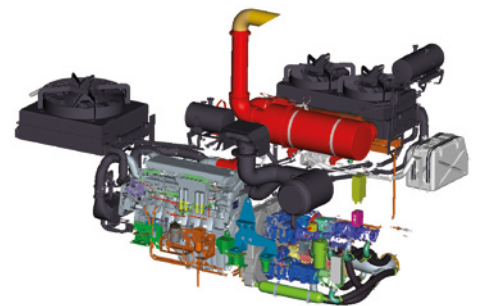
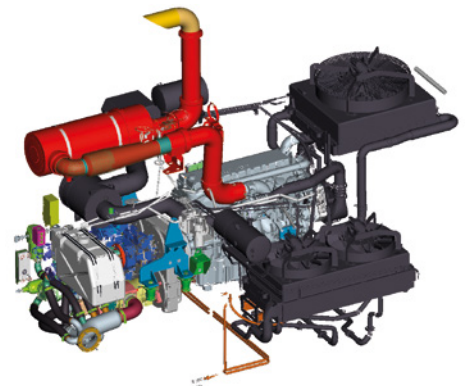


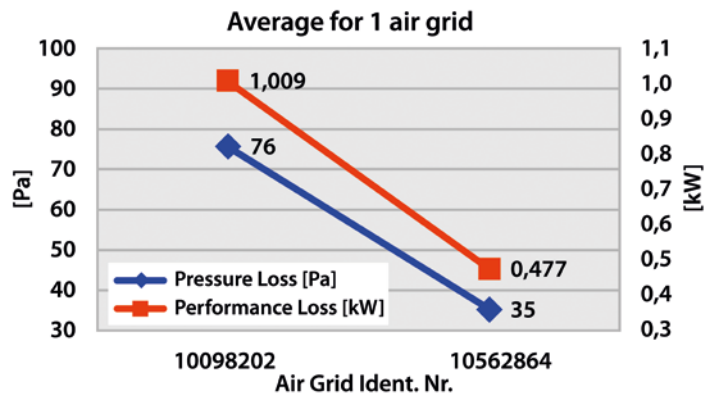
the engine hood, and typically include many devices such as cooler (diesel, water, air and oil), fans, exhausts, and hydraulics. This means that our CAD models can be rather large, with up to tens of thousands of components including all screws.

The requirements on the CFD software are therefore tough and it became apparent that most commercially available codes were not able to handle this kind of complexity, hence our need to turn to FloEFD.

The whole development cycle is influenced by this and the flexibility FloEFD allows, means that I can make decisions before, and not after, when it is too late.

There are many examples, a practical example of how FloEFD has helped with our mobile harbor crane, the LHM 550 and the inlet section of the power pack. I wanted to look at the efficiency and optimization of the protective grids. The basic inlet hood contains two rows of baffles to avoid unwanted particles such as dust or rain being inhaled by the engine. On the other hand, a set of baffles means that we have a potential performance loss between the environment and the engine. The idea is that we can save energy when we reduce the resistance.





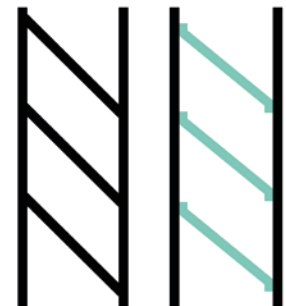
Did you use the full CAD-crane model to set up the FloEFD project?

Theoretically with FloEFD we could, but in this context it was not required. For the first step it was sufficient to have the coolers with two fans and the grids. The exhaust system was also integrated to see thermal effects near the sheet metal walls. We soon realized that the angular position of the baffles was not optimal, so we needed to locate the optimum. We used FloEFD's parametric study feature to let the software find the best angle position with the lowest pressure loss. However, always with respect to an acceptable protection against particles.

We also removed the middle beam which obviously represents a barrier for the airflow. The whole process including meetings, documentation, and decision-making, took two working days.

Are you experienced in transferring such geometry and generating the mesh?

No, not really. However, unlike the other CFD tools I experienced, FloEFD follows a completely different approach by being CAD embedded which allows me to fully skip the transferring geometry step. With regard to the mesh, people typically struggle with body fitted meshes and its manual creation of boundary layers etc. Indeed it takes much less time for the mesh generation compared to classic

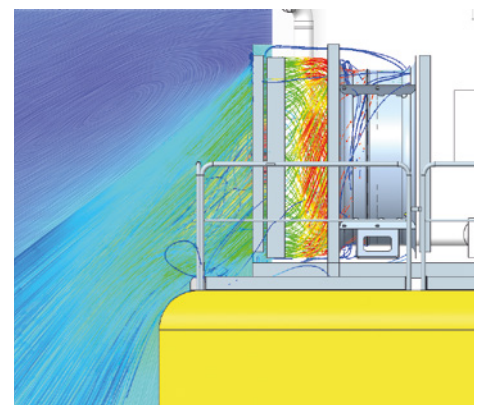
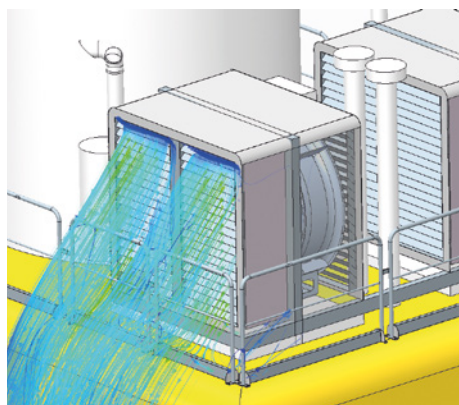


CFD-approaches. It saves us not just hours or days but weeks, this in turns gives us the benefit of not only saving time but money too. The amount we save with the reduction of man-hours spent on the project can be easily put into numbers. Not to mention the manufacturing cost savings per unit and year.

The target of increasing the performance and reducing emissions was achieved. A very welcome side-effect was that we automatically improved and simplified our manufacturing process which saves further costs. We now glue the baffles onto the frame instead of welding them.

Did you face any problems following this change in design?

We didn't face any real problems, other than the assembly team told us that removing the beam from the middle results in one single baffle for each row, instead of the initial two, so now the team has to carry double the weight while mounting.





Layer by Layer

battenfeld-cincinnati use FloEFD™ to Model High-spec Extrusion Pipes

By Heinrich Dohmann and Carsten Bulmahn,
battenfeld-cincinnati Germany GmbH

battenfeld-cincinnati is a global extrusion systems manufacturer with production facilities in Bad Oeynhausen and Kempen (Germany), Vienna (Austria), Shunde (China) and McPherson, KS (USA).

Energy efficiency, conservation of resources and reduction of material consumption are topics that battenfeld-cincinnati has long been focusing on. As a member of the VDMA's Blue Competence Initiative [2] they play a part in promoting sustainable economic development. Their aim is to provide "leading solutions" to their customers, both in terms of performance and energy efficiency.

battenfeld-cincinnati manufactures energy-efficient, high-performance extruders and complete extrusion lines according to customers' specifications and has found practical, innovative solutions for developing components and tooling. battenfeld-cincinnati is the market and technology leader in Polyolefin (PO) pipe extrusion, particularly for large diameter pipes. Numerous projects for lines with diameters of up to 2.6 meters at a wall thickness of 100 mm have already been realized and successfully placed in the field. Other products include extrusion lines for smaller pipes which are used in telecommunications, where the smallest dimensions can be up to a diameter of 4mm at a wall thickness of 0.5 mm with an extrusion speed of up to 200 meters per minute, building services (such as underfloor heating), and automotive applications, among others. These can have several different layers and various color stripes.

For over a decade FloEFD 3D Simulation Software has supported battenfeld-cincinnati engineers in their product development. We met with Heinrich Dohmann (Head of R&D Pipe Heads and Mechanical Engineering Downstream) and Carsten Bulmahn (Mechanical Engineering Pipe Heads) from battenfeld-cincinnati. "The current short project lead times between ordering and hot-commissioning require the use of advanced simulation tools like FloEFD," explains Heinrich Dohmann.



Figure 1a. battenfeld-cincinnati supplies large diameter pipe lines with diameters up to 2.6 m (photo © battenfeld-cincinnati)

Designing and building large diameter pipe heads is a huge challenge. battenfeld-cincinnati is driven by a customer-centric approach to design solutions, whereby customers can select the most suitable pipe head for their specific application from a wide range of tooling options. In the early days, battenfeld-cincinnati used FloEFD for melt distribution optimization. The increasingly complex geometries could not be calculated with the available, reliable tools anymore. Hence, the implementation of a 3D simulation tool became necessary. In addition, a confidential development project in co-operation with an established pipe manufacturer was successfully developed with the usage of FloEFD. Since then, battenfeld-cincinnati has applied FloEFD to a wide range of applications to achieve a uniform velocity distribution in the annular gap at the melt die outlet. The challenge here is to optimize the pressure drop simultaneously. This can amount to up to 400 bar for the entire line and thus has a significant impact on the overall efficiency and the installation space required. The shear flow and the material dwell times have to be considered accurately at the same time.

One of battenfeld-cincinnati's innovative products is the high performance "helix VSI-T+" pipe die. With its two-step distribution concept, it is a highly efficient solution that has proven itself in more than 600 dies worldwide. It consists of a spiral mandrel and a lattice basket distributor element,

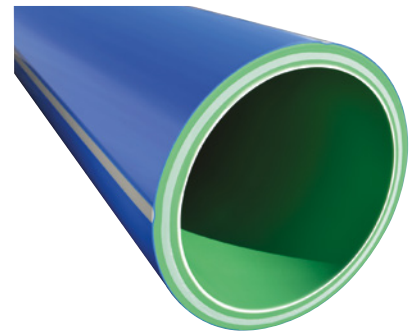


Figure 1b. battenfeld-cincinnati offers a variety of co-extrusion solutions and multi-layer pipe heads for special applications. Pictured: 4-layer PP-RCT-Pipe with glassfibre reinforced centre layer (photo © battenfeld-cincinnati)



Figure 1c. 5-layer PE-RT pipe with EVOH oxygen barrier layer (photo © battenfeld-cincinnati)

for which battenfeld-cincinnati holds the patent. Thanks to the two-step concept the melt is ideally distributed and optimally homogenized. This allows a smaller design for the distribution component, while at the same time ensures excellent pipe quality

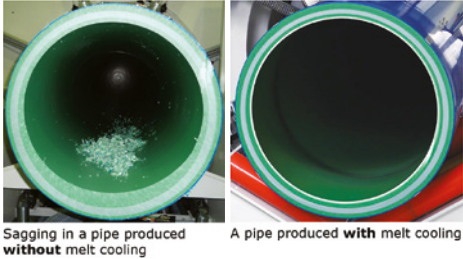


Figure 2. (© battenfeld-cincinnati)

and high outputs. With the help of PTC Creo embedded FloEFD, the battenfeld-cincinnati engineers give the pipe heads their ideal dimensions. Material flow channel and steel parts are designed compactly and efficiently. battenfeld-cincinnati's helix VSI-T+ die features active internal melt cooling to reduce melt temperatures already in the die and a reduced sagging effect, which is a big advantage in producing pipes with large wall thicknesses and a high line output.

The pipe head is one of the key factors for the customers. Its design and features ensures the production of large pipes with even wall thickness distributions and reduced pipe ovality. It also reduces sagging significantly (see figure 2). The efficient cooling concept allows for shorter cooling lengths in the line and thus enables space savings. The complete line components are custom-made and produced at battenfeld-cincinnati's manufacturing facilities.

Another application for the FloEFD flow simulations is in the development of multi-layer (co-extrusion) tools. In this process, several different layers are produced. In direct extrusion up to seven layers and in coating up to five layers can be produced. Various color stripes can be introduced into the pipe. The quality requirements are also very high in this case. Even the slightest deviations of the tone and thickness of the color stripes are not accepted. "In addition to the time optimization the simulation supports us in terms of product quality and reliability, such as at the color stripes. The detailed engineering is carried out within our development processes in the same team," says Carsten Bulmahn.

With CAD embedded FloEFD the battenfeld-cincinnati engineers can directly use the native 3D CAD data. The fluid space is automatically captured and the mesh is generated automatically from just a few settings within the software. Special calculation models for non-Newtonian fluids are applied for the simulation of the used materials. In this specific case the Carreau model is applied. The parameters for the non-Newtonian fluid model are determined on the basis of customer supplied material samples.

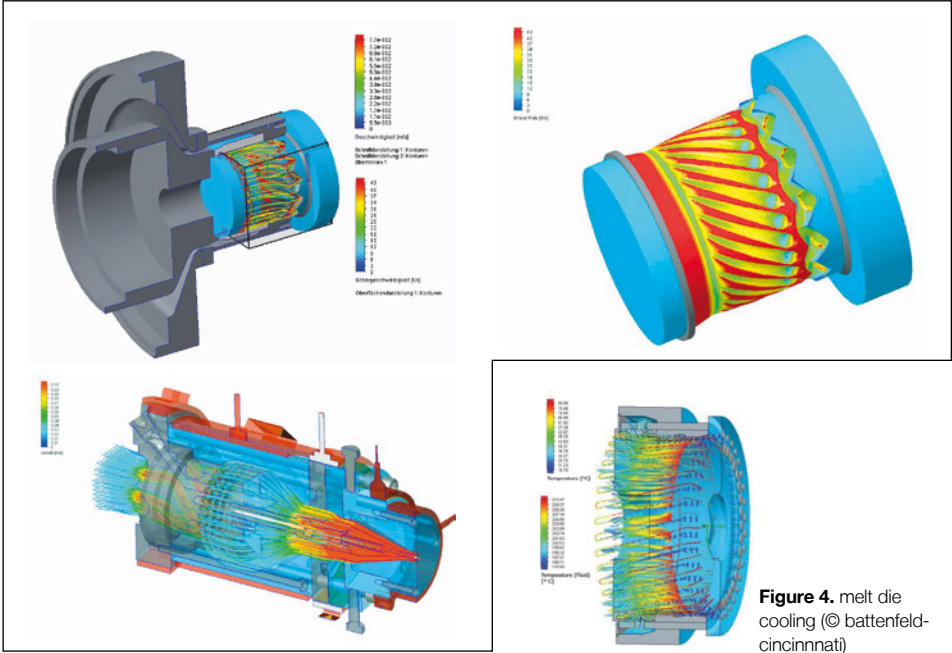


Figure 3a, b, c. melt flow through the melt die (© battenfeld-cincinnati)

Figure 4. melt die cooling (© battenfeld-cincinnati)

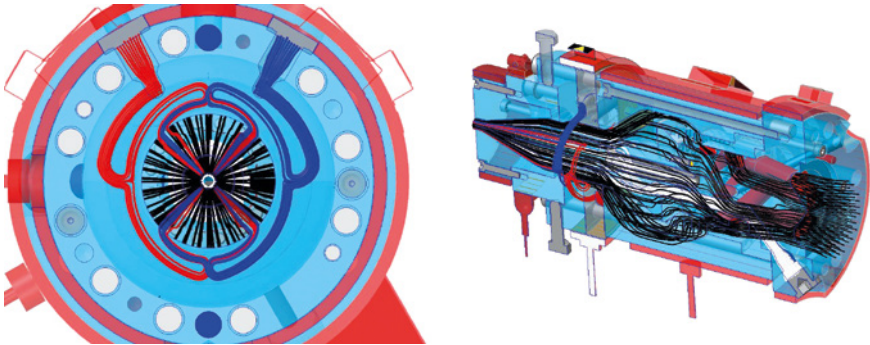


Figure 5a, b. Inner layer, middle layer (grey and black) and two color stripes (blue and red, depending on operating status) (© battenfeld-cincinnati)

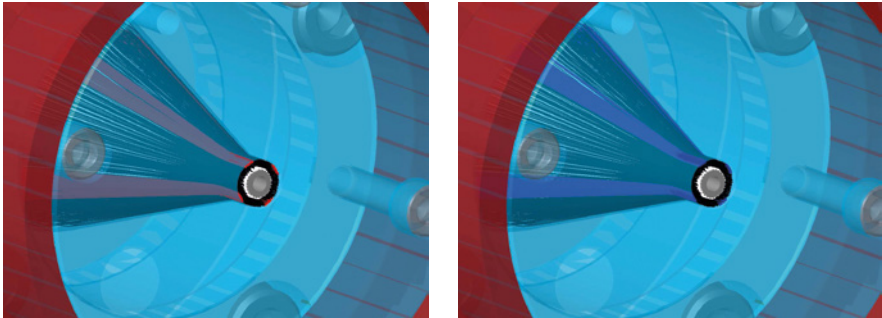


Figure 5c, d. melt distribution at the die outlet

Future conceivable applications where FloEFD might be used, are granulate preheating and pipe cooling. Both are examples of the energy optimization of the overall process. For granulate preheating the waste heat can be re-used in the process. The pipe cooling can already be ensured, but there may be potential for a further reduction of energy consumption and thus increasing overall efficiency in future.

In all of these challenges, FloEFD supports battenfeld-cincinnati's development engineers

early in the development process. Efficiency means savings of electricity and raw materials simultaneously.

References:

- [1] www.battenfeld-cincinnati.com
- [2] www.bluecompetence.net
- [3] <https://www.youtube.com/watch?v=vef7MvrOvt4>

Optimizing an Automotive Air Handling Unit for Uniform Temperatures using FloEFD™

By Lu Ping, Pan Asia Technical Automotive Center, Shanghai, China

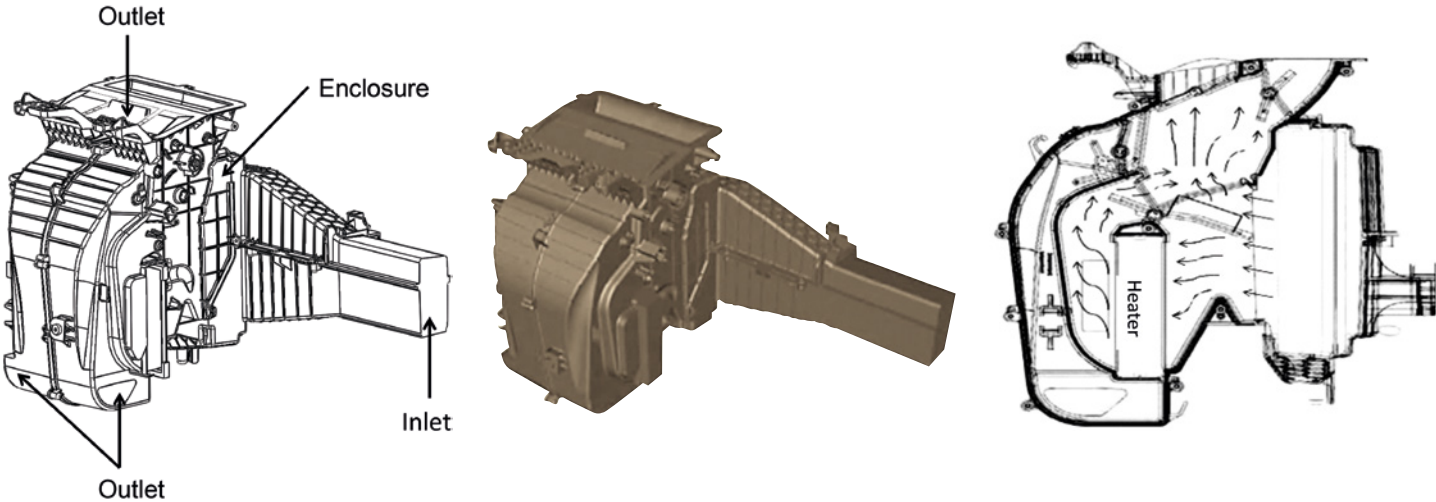


Figure 1. AHU geometry, its CAD Model, and a Sectional Schematic of Airflow Paths through it

The number of car owners in China is increasing exponentially. China will soon have nearly as many drivers as the U.S. With this band of newly qualified drivers, a demand for higher standards in vehicle ride “comfort” is developing. One such area is the standard of cabin comfort. This is directly related to a car’s air-conditioning unit with discharge temperature uniformity which is one of the key factors impacting perceived comfort levels.

On the one hand, discharge air temperature from the HVAC air box has to be uniform for passenger comfort, but on the other, uniformity can reduce the extent of the automatic air-conditioning calibration workload. However, due to packaging limitations in typical vehicle development, its air conditioning unit has to be as compact as possible, which usually make it a poor or inadequate mixture of cold and hot airflow inside the air conditioning unit and finally leads to an non-uniform discharge temperature. In the development of automotive HVAC air handling units (AHU), to control the discharge air temperature uniformity, performance is

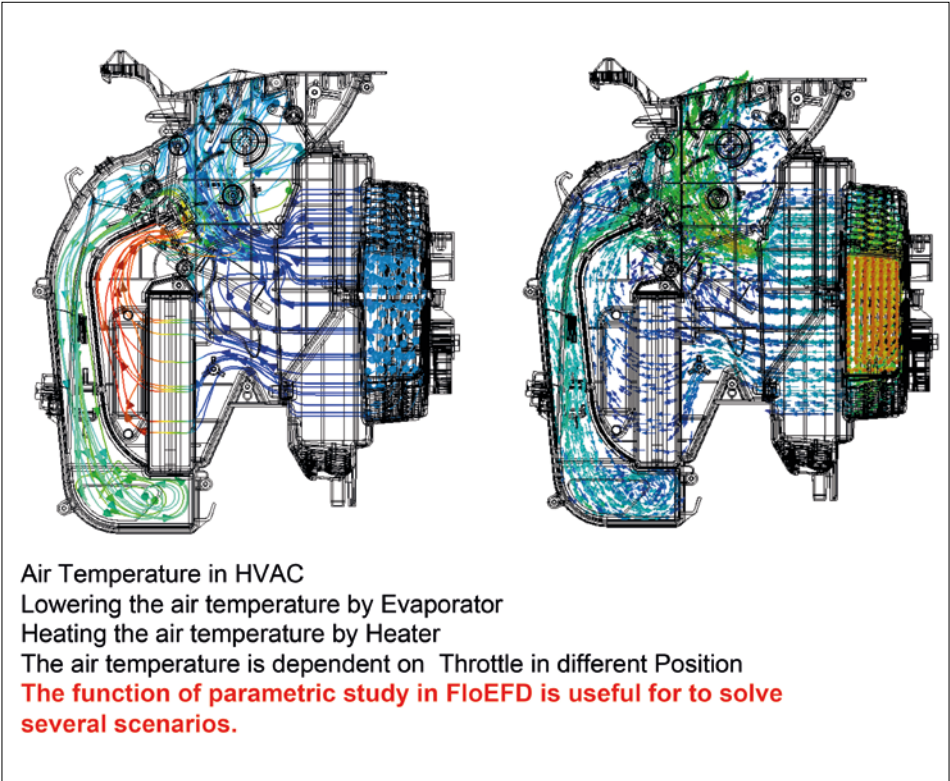


Figure 2. FloEFD predictions of airflow Vectors (right) and Temperature Distribution (left) inside the AHU

Temperature flap door in different position

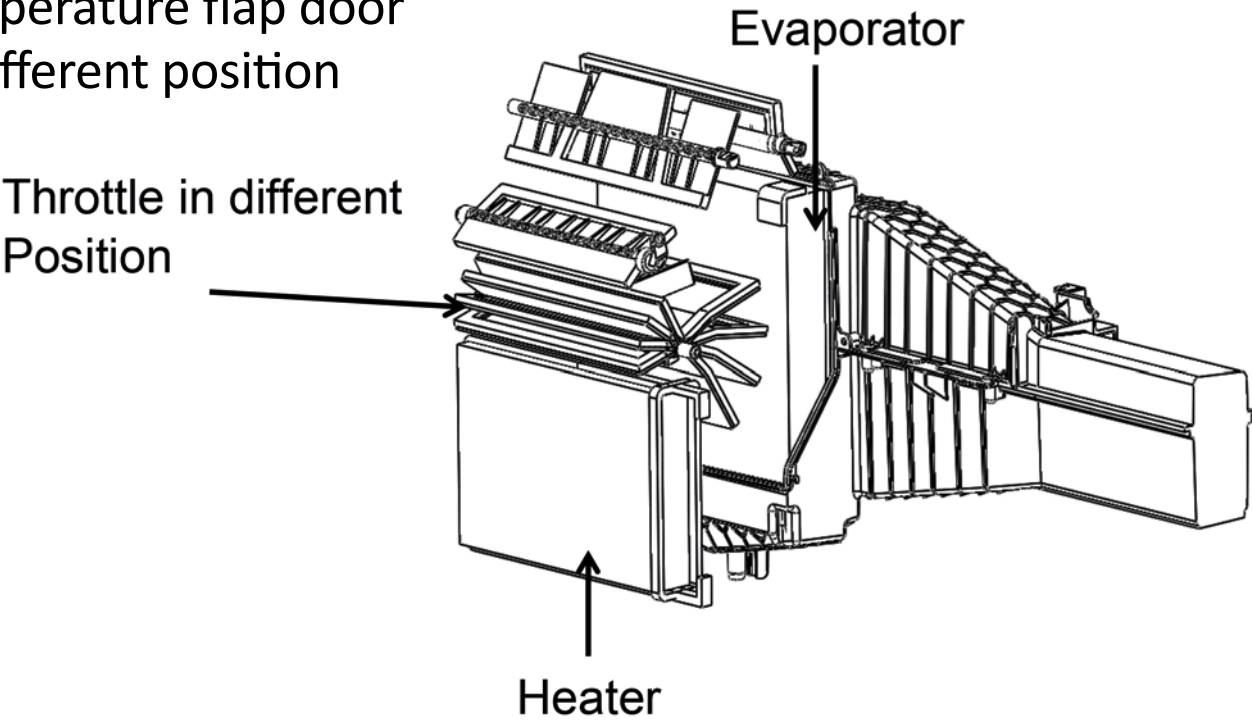


Figure 3. Air Handling Unit geometry showing details of the Evaporator, Heater and Temperature flap door under different positions

key, and it is important to consider the factors mentioned above for the development of a car’s HVAC air handling unit (AHU).

Figure 1 shows the specific AHU being evaluated in this study. Flow through it involves complex tortuous passageways and the mixing of both cold and hot airflows. The unit has one inlet and two outlet zones, and its complex geometrical nature means that it is most realistic to simulate fluid flow and heat transfer inside a CAD package using a CFD tool such as FloEFD. The AHU itself consists of air box housing, an evaporator, a heater, and flap door components. During normal operation, airflow enters the air conditioning unit through the intake housing, and then flows through the evaporator to be cooled down. After cooling, the airflow partially goes through the heater core to be warmed up while part goes towards the outlet area with the flow guiding of a temperature flap door. These two hot and cold air streams then re-converge and mix to achieve a proper and comfortable temperature. Conditioned airflow is finally delivered to passengers through the air box outlet. A typical FloEFD simulation prediction for airflow vectors and temperature effects inside the AHU is shown in Figure 2.

The position of the temperature flap door effectively acts as a control valve inside the unit and ultimately determines the hot and cold airflow “mixing ratio”. It can be altered

	Runner Hedge Angle (°)	Runner Area Ratio (%)
Case 1	120	44
Case 2	120	49
Case 3	120	39
Case 4	116	44
Case 5	116	49
Case 6	116	39
Case 7	124	44
Case 8	124	49
Case 9	124	39

Table 1. The nine AHU CFD Simulation Scenarios examined in this study

to different positions (Figure 3). The “hedge angle” and “area ratio” of the cold and hot airflow channel have an important influence on the final mixed airflow temperature distribution.

The CFD boundary conditions simulated in this AHU study extended from airflow rates of 15l/s to 60l/s at an air inlet temperature of 20°C with 875W heat transfer rate from the heater component. Nine parametric

CFD simulations inside FloEFD were used to determine an optimized cold and hot flow channel “hedge angle” together with runner “area ratios” as shown in Table 1.

This parametric study focused on the AHU outlet airflow temperature distribution under different temperature flap door setting. More focus is around the middle position, that is, for angle degree of outlet damper door

from 25° to 50°, considering the middle position is relative to a customer's actual high frequency usage scenario (see Figure 4). The temperature difference is seen to be optimal for Case 3 for the two temperature flap door conditions. Hence, the cold and hot airflow channel hedge angle and runner ratio area under this case is the most ideal which was verified visually (Figure 5) by outlet CFD temperature contours under these two temperature flap door positions.

Finally, we validated the CFD simulation Case 3 prediction against an experimental test of the actual car AHU. We chose an air conditioning box inlet temperature of 0°C, and the heater inside operating with a 90°C fluid so as to replicate a real vehicle use of air conditioning over cold and hot atmospheric conditions. By adjusting the temperature flap door in the AHU to control air-conditioning of cold and hot air mixing, we were able to verify the box's linear temperature uniformity performance target. We positioned 4 thermocouples on each outlet and measured the average exit air temperature. Figure 6 shows the actual measured performance data of the AHU. Aligned with the CFD simulation results, we achieved the maximum temperature difference within 4°C among four vent outlets when the temperature flap valve is adjusted between 35% and 65%. We reached the requirement of a linear thermal design, while at the same time it was basically consistent with the virtual design CFD results.

In conclusion, we adopted the commercial CFD software, FloEFD, for this study because of its ease of use in meshing when compared to the tetrahedral or prismatic meshing approaches in traditional CFD codes. We found that FloEFD gives more accurate and more efficient CFD simulation results. Since it works within the mechanical CAD environment, it is a highly engineered universal fluid flow and heat transfer analysis software. FloEFD was able to examine a range of AHU hedge angles for hot and cold airflow channels. The hedge angle and area ratios of 120° and 39% respectively were found to be the most optimal. FloEFD with its parameterized calculation function was highly efficient in varying a range of AHU parameters that we studied. It showed great design performance improvements in terms of achieving an optimized design while at the same time reducing our overall cost of development.

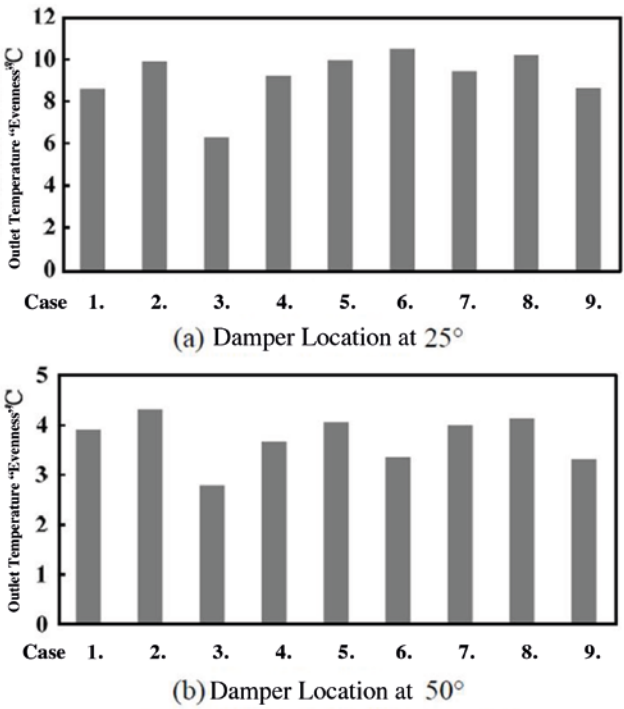


Figure 4. CFD predictions of Outlet Air Temperature "Evenness" for the nine different hedge ratio Cases at two Temperature Flap Door Angles

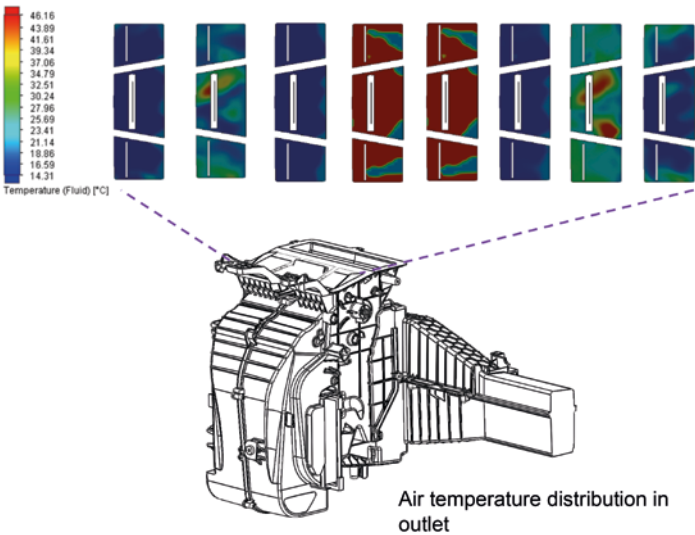


Figure 5. Air Handling Unit predicted Air Temperature Contours in the outlet face for the different hedge ratios

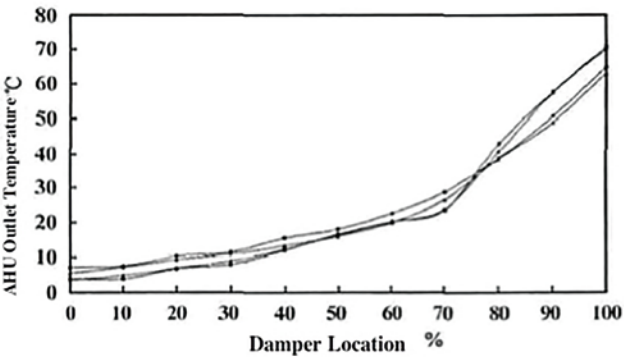


Figure 6. Data from four experimental Thermocouples of Outlet Air Temperature versus Temperature Flap valve Location for Case 3

Steering Towards Flow Optimization

FloEFD™ is an established part of the development process at Robert Bosch Automotive Steering GmbH

By Rolf Haegele, development engineer acoustics / simulation, Robert Bosch Automotive Steering GmbH.

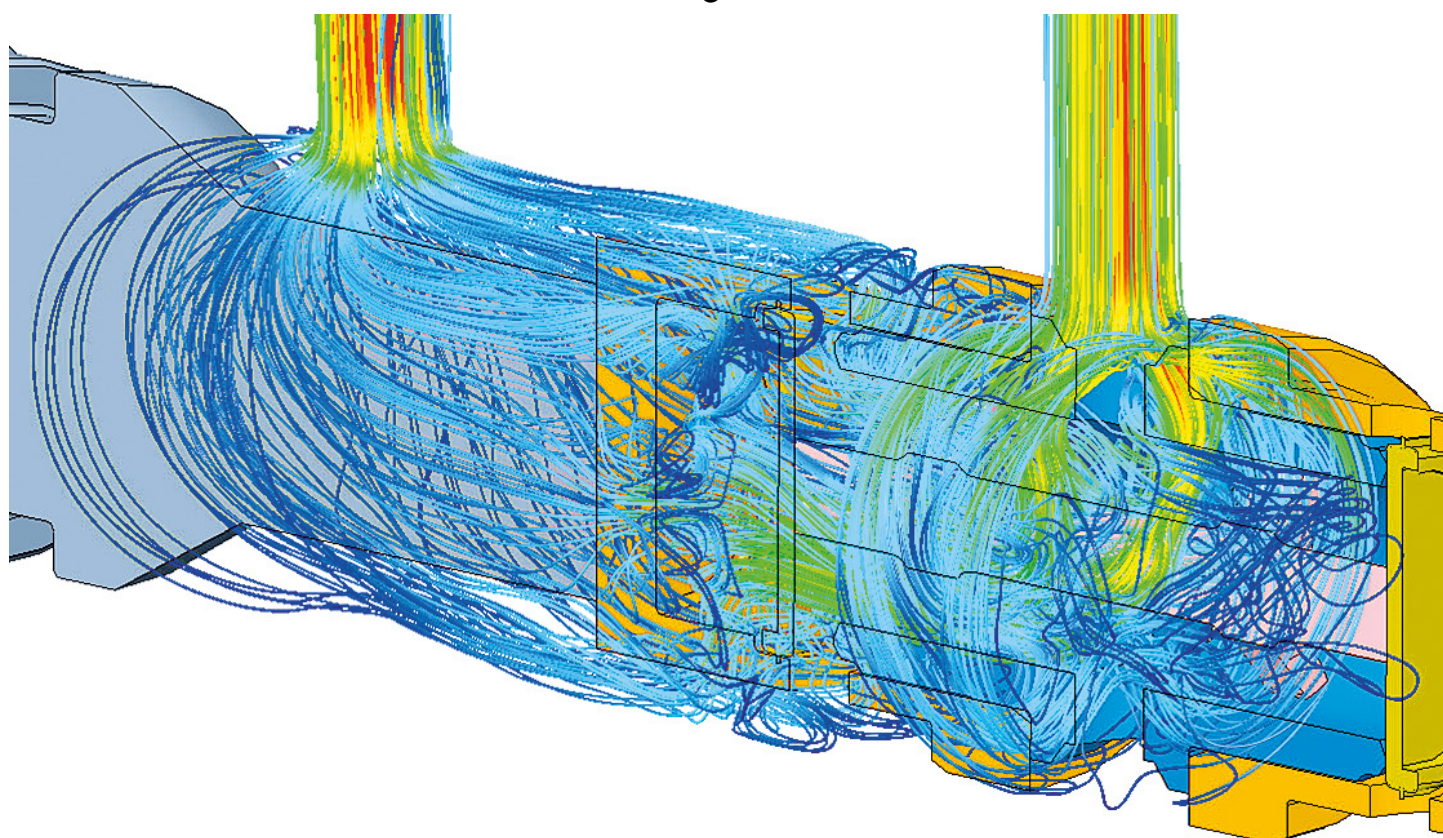


Figure 1. Flow Trajectories Inside the Valve.

The ever-shortening product cycles and decreasing development times in the automotive industry raise the need for up-to-date simulation tools equipped with reliable physical calculation methods. The use of Mentor Graphics' FloEFD Concurrent CFD software enables an evaluation of future automotive components at the earliest possible stage during the development cycle. This allows problem identification and correction when the concept is first evaluated at the feasibility stage of the project.

Steering assistance in commercial vehicles is performed by means of a hydraulic system

circuit. The double valve (Figures 1 and 2) is used to supply the feed pump as a control valve. The double valve consists of one inlet and two outlets. The two outlets are opened by pressing against the corresponding spring force depending on the operating condition. Each outlet is opened by undershooting the environment pressure in the requesting partial circuit. A pin controls the distance and the partial circuit is supplied with hydraulic oil after that. To supply the drive with the required flow rate capacity, the pressure drop arising within the valve must be overcome. If the pressure drop is too high, there will be insufficient flow to the drive, and the system will not function correctly. In addition,

a lower pressure drop reduces the power consumption of the hydraulic system, and thus the amount of energy required to steer the vehicle, contributing to the overall fuel savings and energy efficiency.

Hence the objective is to supply the required volume flow for each operating case, taking into account the given pressure conditions and keeping the pressure drop at required volume flow rates to a minimum. Simultaneously, cavitation effects have to be avoided. This is a critical consideration because the valve is opening by undercutting 0.95 bar below ambient (initial design shown in Figure 2). This pressure should be prevented from dropping

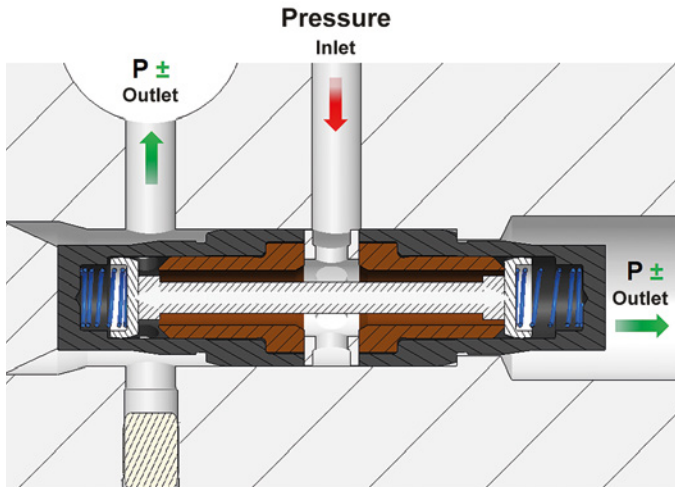


Figure 2. The initial design opens on the left by undershooting the environment pressure.

too low while being sufficiently negative to open the valve. At the same time, external factors constraining the design, such as available installation space and manufacturing capabilities have to be considered.

Several design variations for the double valve were investigated in FloEFD. Aside from the main geometry modifications, detailed changes to individual components and their effects were analyzed. For example, the pin designs shown in figures 3 and 4. The insights gained were incorporated at an early stage in the development of the product concept. The most efficient overall design based on the simulation results (Figures 5 and 6) was manufactured as a prototype and measured in a test setup. The measurements confirmed that the simulation results were accurate, reducing the number of physical prototypes to just one.

Using FloEFD for this application, the available flow rate was increased by approximately 300%, while the pressure drop was reduced by approximately 20% to approximately 0.8 bar below environment pressure. The time saving achieved compared to the conventional prototype-based development process was around five

weeks for the application described above. By “frontloading” simulation – simulating each design iteration at the beginning of the development process – the development process is streamlined, and optimized to ensure that each design iteration leads to an improvement in performance.

For FloEFD simulation Bosch Automotive Steering uses native 3D CAD data directly within the PTC Creo Parametric environment. During the modeling process, the fluid space is automatically captured and the mesh is generated from just a few settings within the software. Today Bosch development engineers use the parametric study capability within the PTC Creo environment to quickly prepare FloEFD simulations that are both fast and reliable to run, eliminating the need and cost of integrating with other software, or face the problems associated with using CAD neutral files including loss of parametric information and feature history.

In this case, by frontloading the CFD simulations Bosch Automotive was able to optimize the design of the pin in detail, allowing it to be designed for use across a series of such valves in the future. In

addition, with the simulation models being available for future analysis where the impact on the resulting weight and the quantity of material can be evaluated. Therefore cost optimizations have already been achieved at the product concept phase for the series.

“Using FloEFD within our PTC Creo environment has allowed us to front-load full CFD simulation into our design processes, cutting design times and making optimization possible from the very start of the development process. FloEFD has helped us meet today’s requirement for short development cycles.”

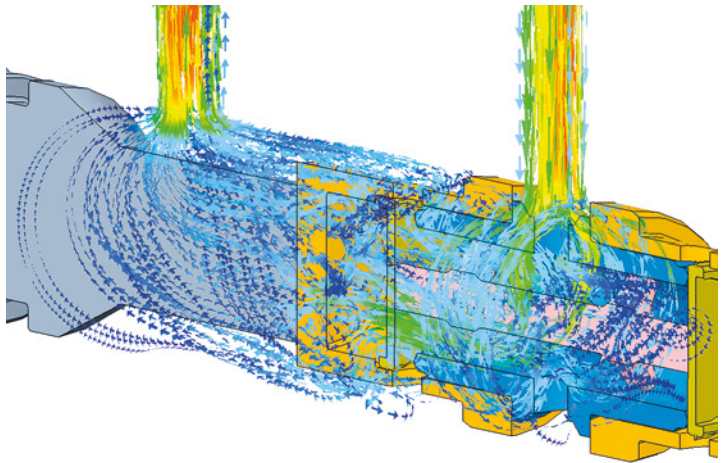


Figure 6. Flow Vectors Inside the Valve.

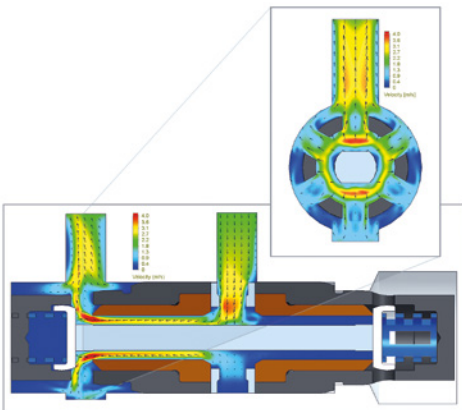


Figure 3. Design variation

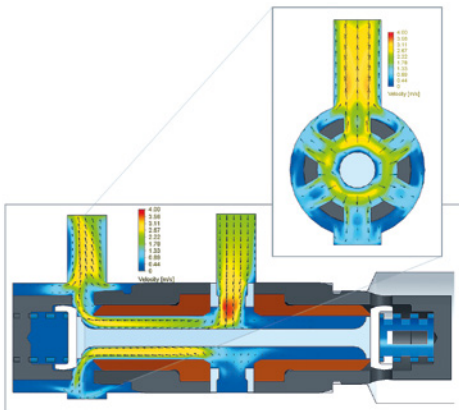


Figure 4. Design variation

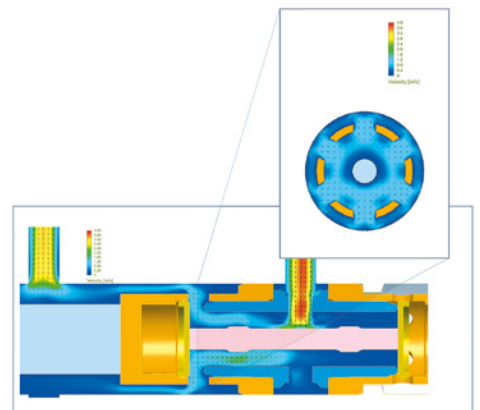


Figure 5. Design variation

Innovation isn't Optional

Mercury Racing® use FloEFD™ in the design of their latest intercooler filter

By Prasad Tota, Application Engineer, Mentor Graphics

Mercury Racing® is known worldwide for its leadership in powerboat racing and production of high performance consumer and race marine products. Founded in the 1970's as a division of Mercury Marine®, Mercury Racing's philosophy of "innovation isn't optional" has served them well and led their customers to winning multiple championships including the Unlimited Offshore World Championship and Abu Dhabi Grand Prix Class 1 World Championship.

Their product line includes sterndrive and outboard engines, drive and propellers. We met up with Hiro Yukioka, Technical Specialist, at Mercury Racing and their latest project, a design study of an intercooler filter on a sterndrive engine- QC4V (figure 1) using FloEFD™ 3D CFD simulation software from Mentor Graphics.

The 9L V8 engine with an output of up to 1650hp, has two turbochargers. The engine uses a charge air cooler (CAC) to cool the compressed air from the turbo charger. The CAC uses seawater as a coolant and comes with some challenges owing to the debris it picks up, such as sand, sea shell etc. Mercury Marine has found from field experience that not all seawater boat filtration systems are capable of preventing this debris from accumulating in the CAC.

In the existing design, the size of the passage where seawater enters into the CAC is less than 0.033" (0.84 mm), figure 2. However, it would be a mistake to assume that all the debris that enters the CAC will exit the CAC with the heated water leaving the unit. Depending on the flow velocity, some of the debris entering the CAC can settle or accumulate in the unit. If the water speed inside CAC is too low then debris could settle inside it. At such low velocities the debris accumulation is also influenced by gravity i.e. weight of the particles. FloEFD simulation software was used to study the performance of the existing filtration system and to come up with an improved design.

FloEFD for Creo is a CAD-embedded general purpose CFD software designed for engineers,



Figure 1. QC4V engine with compressed air cooler (CAC)

this focus makes the software easy to use by designers and engineers in an environment that they are already familiar with. The virtual test setup involves a CAD model with a flow inlet where the debris enters with the seawater, travels through a rubber tube into the CAC where some debris gets filtered and finally leaves from the flow outlet. It is important to note that the flow outlet is at a higher elevation than the inlet and hence the pump needs to deliver enough pressure for it to work against the adverse hydrostatic pressure.

At a flowrate of 60 litres/min the velocity inside the tube is about 3 m/s, but the velocity inside the CAC is less than 0.5 m/s. At such low velocities debris would settle inside the CAC. Hiro Yukioka had an idea to use the particle studies feature in FloEFD to virtually visualize if debris particles of a certain size would be carried by the seawater all the way to the outlet or remain in the unit. The particle study was conducted for debris size of 0.2 to 0. 5mm in diameter in increments of 0.1 mm. The particles were fed in at a mass flow rate of 0.01 kg/s which is less than 1% of the fluid mass flow rate. Activating the gravity field in the model accounted for particles settling under their own

weight. The images in figure 3 show the particle trajectory colored by velocity magnitude.

Based on the findings, a sea strainer was created with wire mesh positioned around the inside of a cylindrical perforated part (Figure 4). The mesh element should have openings smaller than 0.3 mm and an off the shelf (OTS) wire cloth was chosen that met the criterion.

"If we wish to run a CFD simulation incorporating this new design the number of computational grid cells needed to refine the fine geometry of wire mesh is extremely high and impractical on a typical designer

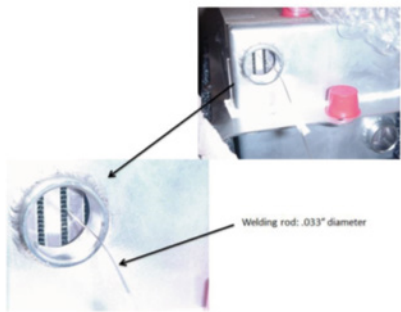


Figure 2. Fluid passage size at CAC entry



Figure 3. Virtual Debris test, Debris size from left to right (a) 0.2 mm (b) 0.3 mm (c) 0.5 mm

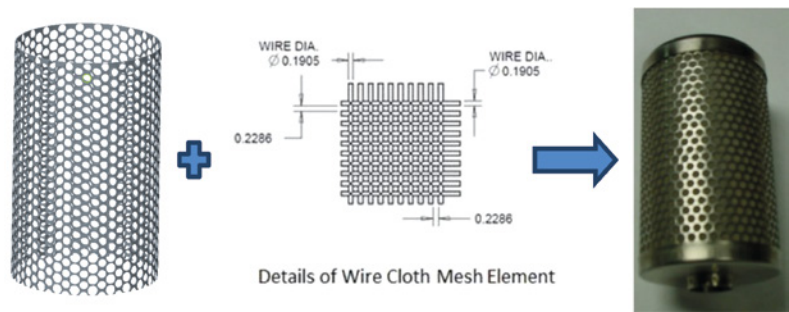


Figure 4. Sea strainer formed with a perforated part and wire mesh rolled on it

workstation. Fortunately FloEFD has a modeling technique where an object can be defined as a porous media which allows flow to go through the media with a pressure loss,” said Hiro. A resistance curve was attached to the porous object to emulate the flow vs pressure drop characteristics of the actual device. For this particular geometry an axisymmetric porous media is ideal where the flow loss coefficient (K) can be defined normal to flow direction (r, radial) and along the axis (L, length) of cylinder (Fig.5).

The resistance characteristics of the wire mesh can be either obtained in physical testing or virtual tests set up in FloEFD. In this case a section of wire mesh was tested in a virtual wind tunnel set up within FloEFD to come up with a flow vs. resistance curve that was then attached to the cylindrical part in the overall model for CAC.

The final FloEFD model with the wire mesh incorporated is shown in Figure. 7. The fluid flow simulations showed that the sea strainer results in a pressure drop of 20 kPa at a flowrate of 80 l/min.

The next step was to analyze the effect of debris accumulation on the pressure drop when a part of the overall height in cylindrical volume is completely covered with debris. This was easily tested with small modifications to the FloEFD model where a shell was added, blocking 50% of overall volume and using the parametric study feature in FloEFD this height was varied to 75% and 85%. The results show that there is minimal increase in pressure drop with debris accumulation. (Figure 8)

A prototype was built to validate the CFD results using thorough hardware testing. Physical tests showed a pressure drop of 25-30 kPa for the sea strainer that is new (no blockage) to 90% blockage to mimic the effects of debris accumulation. These findings are in good agreement with FloEFD predictions of 25-26 kPa for a flowrate of 80 l/min where blockage was varied from 0% to 85%.

Conclusion

After testing the prototype on a test rig for

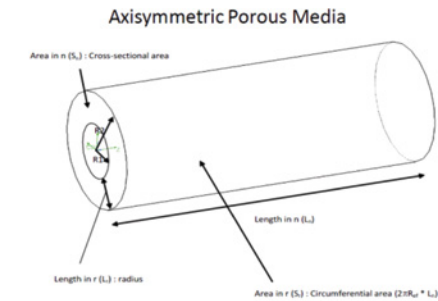


Figure 5. Axisymmetric Porous Media in FloEFD software

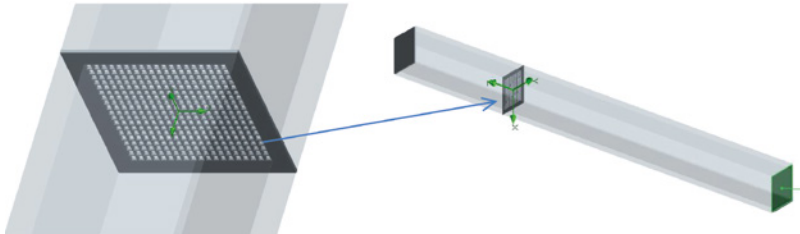


Figure 6. Virtual wind tunnel set up to characterize the wire mesh

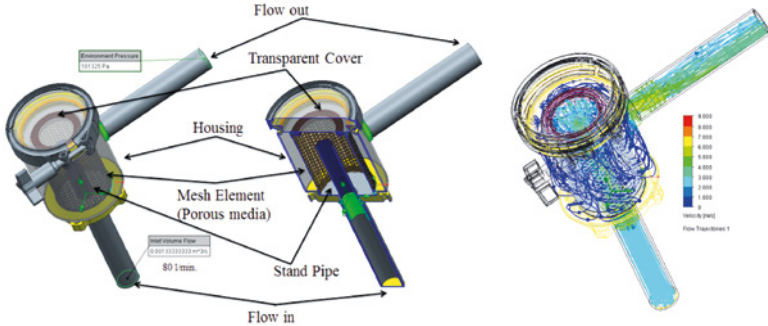


Figure 7. Cross section view of sea strainer and flow trajectories colored by speed (left to right).

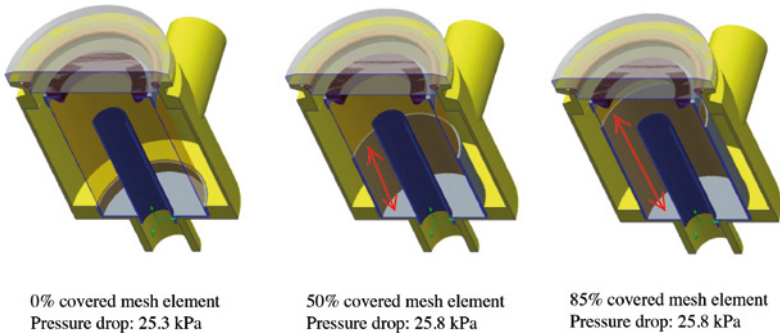


Figure 8. Debris accumulation effects on total pressure drop

several of Mercury Racing’s customers, the redesigned CAC on the field in various conditions, the customer feedback was overwhelmingly positive. Performance was not compromised and the CAC filter was presented at the Miami Boat show in February 2015 and was very well received.

“Without the FloEFD software it would have been very difficult to develop this CAC filter in such a short time. The software is embedded within CAD environment and easy to use, which allowed us to test various ideas and design virtually without the need to create multiple prototypes and several days of physical test.” said Hiro Yukioka.

Lastly I would like to express my gratitude to excellent customer support from Mentor Graphics. During this design activity I contacted them several times and every time I was impressed by their professionalism and great technical advice. FloEFD itself is an excellent product and, in my opinion, their support group adds significant value on this product.” Hiro Yukioka

Reference

[1] <http://www.mercuryracing.com/sterndrives/engines/1550-2/>



Fluid Dynamics Simulation Of Aqueous Humor In A Hole Implantable Collamer Lens Ks-Aquaport™

Concept and development history of the Hole Implantable Collamer Lens

By Takushi Kawamorita, CO, PhD, Department of Orthoptics and Visual Science, Kitasato University School of Allied Health Sciences, Sagamihara, Japan.

Implantable collamer lenses (ICL) have many advantages in the treatment of refractive errors, especially for cases involving high and moderate ametropia. In addition, the ICL has been known to be effective for the correction of refractive errors when compared to the LASIK procedure. However, cataract development has been a concern after ICL implantation (Figure 1).

It has reported that the incidence of cataract formation was approximately 10 % after the implantation. One of the causes of the cataract was thought to be a change in the circulation of the aqueous humor to the anterior surface of the crystalline lens. Therefore, Prof. Kimiya Shimizu created a centrally perforated ICL in 2006 (i.e., the Hole-ICL KS-AquaPORT™) to improve aqueous humor circulation in addition to work performed on the development of the Hole-ICL (Figure 2).

Basis examination in Hole ICL Aqueous humor circulation
After observing improved aqueous humor circulation with the use of the Hole-ICL, Fujisawa [1] reported that no cataracts were formed when Hole-ICLs were implanted into

porcine eyes. The study concluded that the Hole-ICL allowed sufficient flow of aqueous humor and distribution over the anterior surface of the crystalline lens through its central hole. In addition, Shiratani et al. [2] showed the possibility of preventing cataracts with the Hole-ICL by using minipigs.

We investigated the fluid dynamics of the aqueous humor in a Hole-ICL using the thermal-hydraulic analysis software program FloEFD V5 (Mentor Graphics Corp.) (Figure 3).

The analysis confirmed an improvement in the aqueous humor circulation when using a Hole-ICL [3]. The total flow velocity between the anterior surface of the crystalline lens and the posterior surface of the Hole-ICL was higher than that between the crystalline lens and the conventional ICL (Figure 4).

The difference was of particular note in the center of the lens, as shown in the figure. An outward flow from the hole in the Hole-ICL by trajectory analysis was noted (Figure 5). The validity of the FloEFD software utilizing computational fluid dynamics was confirmed through the agreement between the theoretical and experimental data.

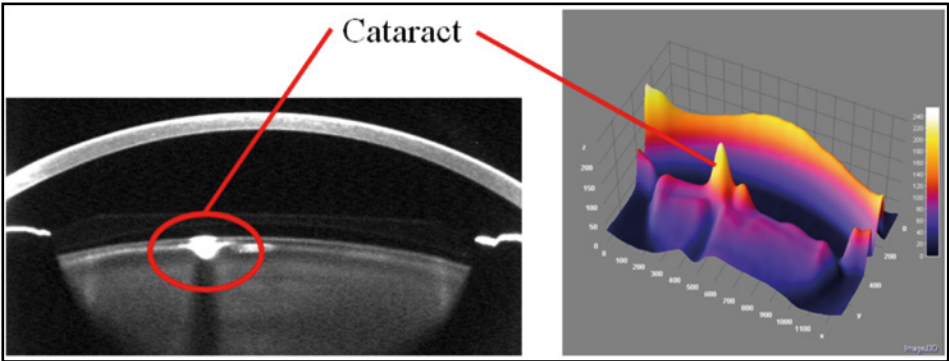


Figure 1. Cataract development of an eye with an ICL taken by Scheimpflug photography (left) and 3D densitometry by Image J 1.47v (NIH, USA) and the plug-in “Interactive 3D Surface Plot v2.33 by Dr. Barthel” (right)

In addition, many surgeons also perform peripheral laser iridotomy (LI) prior to ICL implantation to prevent the failure of aqueous humor circulation (Figure 6). The advantages of the Hole-ICL include improvements in aqueous humor circulation; hence, there is no need for the LI procedure as it may cause complications including the elevation of intraocular pressure.

There are several examples of optical systems with a centrally perforated lens, such as astronomical telescopes or special contact lens. Shiratani et al. [2] showed that the modulation transfer function of an ICL with a central hole of diameter 1.0 mm obtained using optical simulation software was similar to a conventional ICL. Uozato et al. [4] investigated the optical performance of the Hole-ICL with a diameter of 0.36 mm in an optical bench test as well as optical simulations. The authors concluded that a minimal central hole in an ICL may not have a significant impact on the optical performance for various ICL powers and pupil sizes. If the central hole size of the Hole-ICL were to increase, the circulation of aqueous humour in the surrounding crystalline lens would improve. However, the retinal image quality decreases. This indicates the existence of a trade-off between fluid dynamics and optical characteristics. Therefore, we investigated the ideal hole size in a Hole-ICL from the standpoint of the fluid dynamic characteristics of the aqueous humor using the FloEFD software (Figure 7).

The results of the computer simulation determined the desirable central hole size as 0.2 mm or larger based on fluid dynamics. The current model, based on a central hole size of 0.36 mm, was close to the ideal size. The optimization of the hole size should be performed based on results from a long-term clinical study to allow for analysis of the optical performance and incidence rate of secondary cataracts. A slight decrease in optical properties is considered an effective measure of risk mitigation when compared to low retinal image quality that can occur because of the potential for secondary cataracts to develop. In the future, the optimum hole size should be determined based on these simulation results, the results of optical analysis containing illumination optics, and long-term clinical results regarding visual performance, optical performance and complications.

Clinical results of the Hole ICL

Our results suggest that Hole-ICLs improve the circulation of the aqueous humor to the anterior surface of the crystalline lens. The Hole-ICL is expected to continue to lower the risk of cataracts. Currently, the Hole-ICL

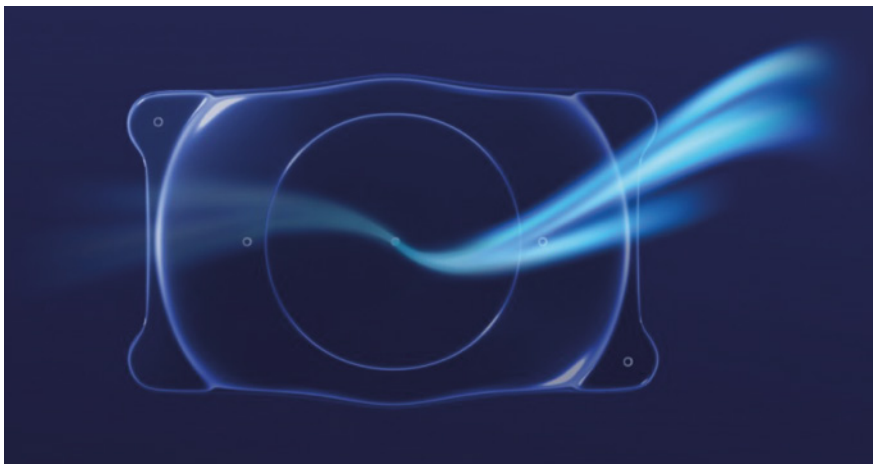


Figure 2. Illustration of the Hole-ICL KS-AquaPORTTM (STARR Surgical CO Ltd.)

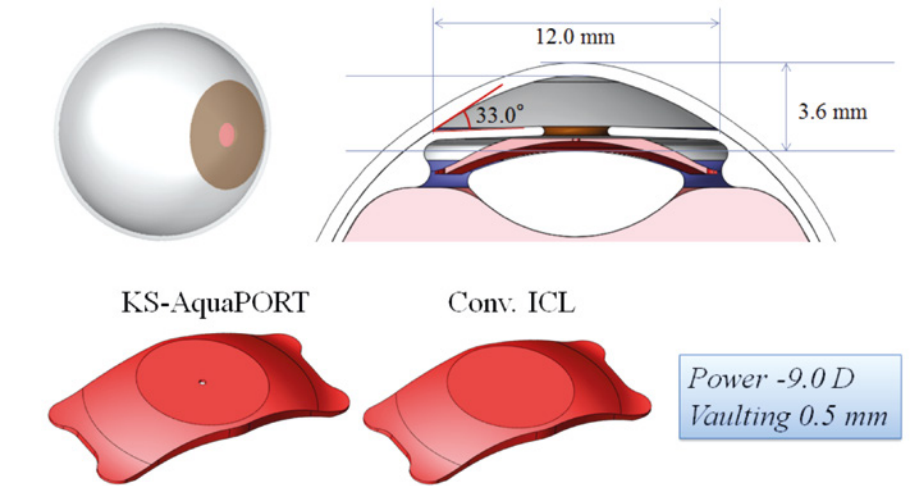


Figure 3. 3D models of eyes with ICLs created with FloEFD software. Appearance of the eye model (top left), Anterior ocular segment (top right), Conventional ICL (bottom left), Hole-ICL (bottom right)

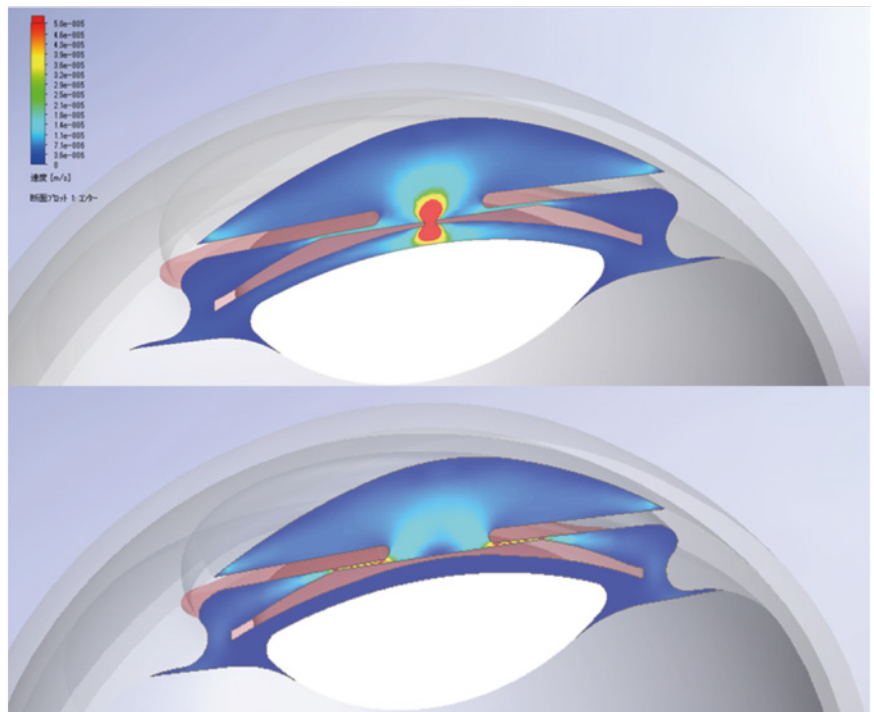


Figure 4. Flow distribution along the long axis of the cross-sectional surface of the Hole-ICL (upper) and the conventional ICL (lower)

has been used approximately 200,000 times with lenses from approximately 70 countries. There are useful clinical reports with similar visual functions as the conventional ICL (Figure 8) [5, 6]. In conclusion, the thermal-hydraulic analysis software program FloEFD contributed to the optimization of the lens design.

Acknowledgment

The authors thank Prof. Kimiya Shimizu, Prof. Hiroshi Uozato, Prof Nobuyuki Shoji, Kozo Keikaku Engineering Inc. (Mr. Osamu Kuwahara, Mr. Soichi Masuda, and Dr. Tsuyoshi Yamada), Cybernet Systems Co., Ltd. (Mr. Takayuki Sakaguchi) for technical support, and Editage for critical reading of the manuscript. This study was supported by a grant from the Kitasato University School of Allied Health Sciences (Grant-in-Aid for Research Project) (T.K.), a Kitasato University Research Grant for Young Researchers 2010-2016) (T.K.), and a Grant-in-Aid for Young Scientists (B) (T.K.).

References

[1] Fujisawa K, Shimizu K, Uga S, et al. Changes in the crystalline lens resulting from insertion of a phakic IOL (ICL) into the porcine eye. *Graefes Arch Clin Exp Ophthalmol*. Jan 2007;245(1):114-122.

[2] Shiratani T, Shimizu K, Fujisawa K, Uga S, Nagano K, Murakami Y. Crystalline lens changes in porcine eyes with implanted phakic IOL (ICL) with a central hole. *Graefes Arch Clin Exp Ophthalmol*. May 2008;246(5):719-728.

[3] Kawamorita T, Uozato H, Shimizu K. Fluid dynamics simulation of aqueous humour in a posterior-chamber phakic intraocular lens with a central perforation. *Graefes Arch Clin Exp Ophthalmol*. Jun 2012;250(6):935-939.

[4] Uozato H, Shimizu K, Kawamorita T, Ohmoto F. Modulation transfer function of intraocular collamer lens with a central artificial hole. *Graefes Arch Clin Exp Ophthalmol*. Jul 2011;249(7):1081-1085.

[5] Kamiya K, Shimizu K, Saito A, Igarashi A, Kobashi H. Comparison of optical quality and intraocular scattering after posterior chamber phakic intraocular lens with and without a central hole (Hole ICL and Conventional ICL) implantation using the double-pass instrument. *PLoS One*. 2013;8(6):e66846.

[6] Shimizu K, Kamiya K, Igarashi A, Shiratani T. Intraindividual comparison of visual performance after posterior chamber phakic intraocular lens with and without a central hole implantation for moderate to high myopia. *Am J Ophthalmol*. Sep 2012;154(3):486-494 e481.1

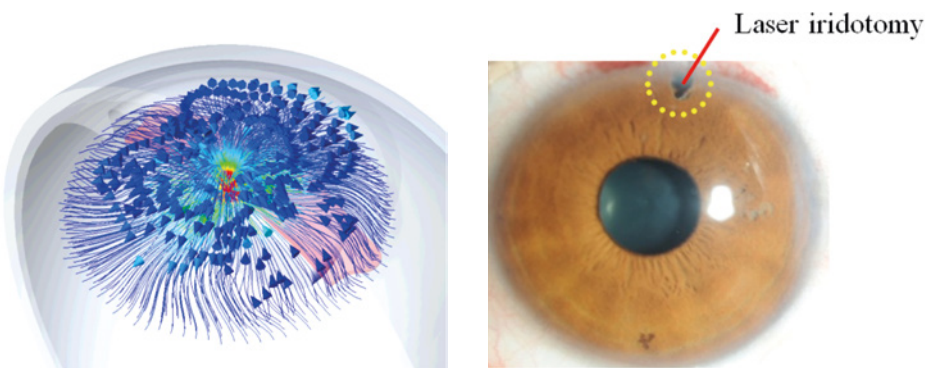


Figure 5. Trajectory analysis within the Hole-ICL

Figure 6. Photograph of laser iridotomy

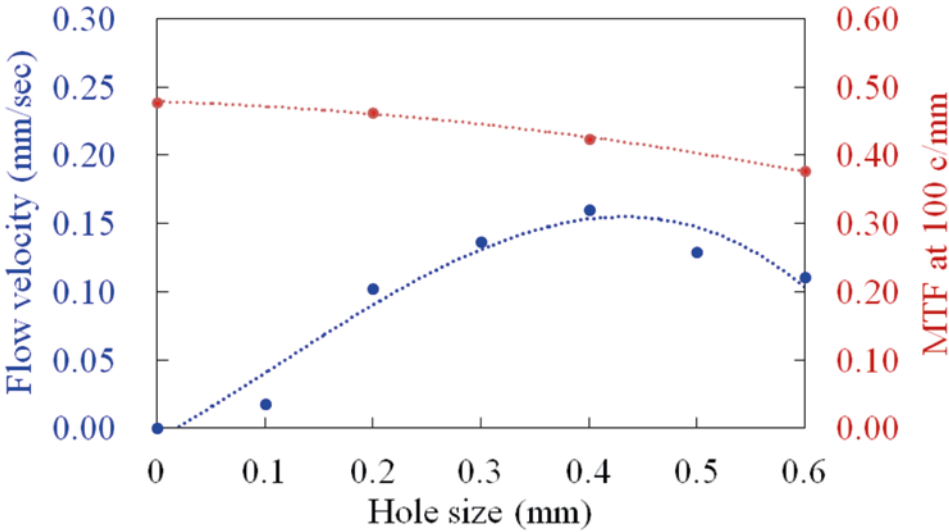


Figure 5. The relation between hole sizes and velocity of the aqueous humor fluid, including the modulation transfer function at a spatial frequency of 100 c/mm



Figure 8. Photograph of an eye implanted with the Hole ICL KS-AquaPORTTM (STARR Surgical CO Ltd.)

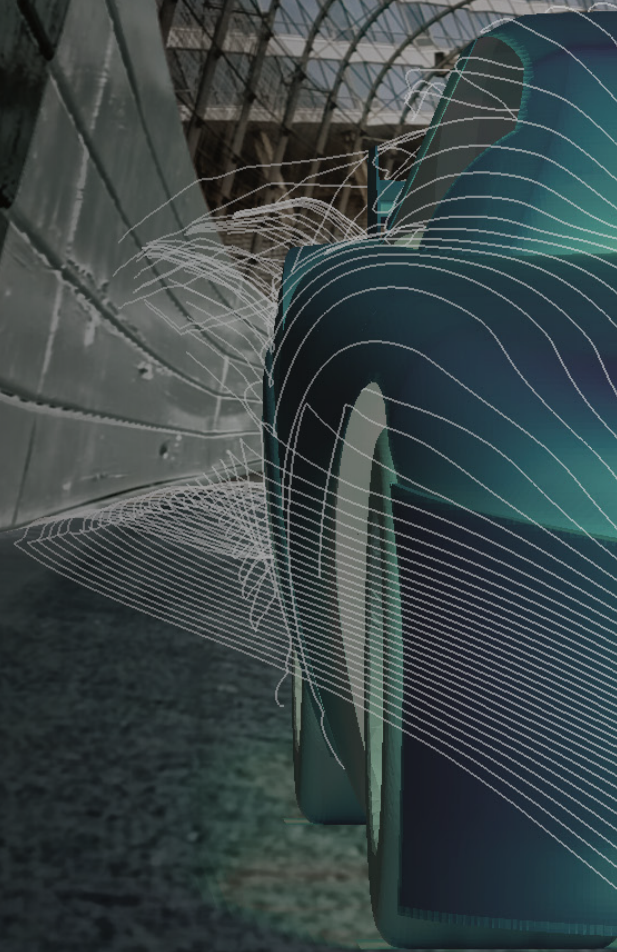
Optimizing a NASCAR Racing Machine

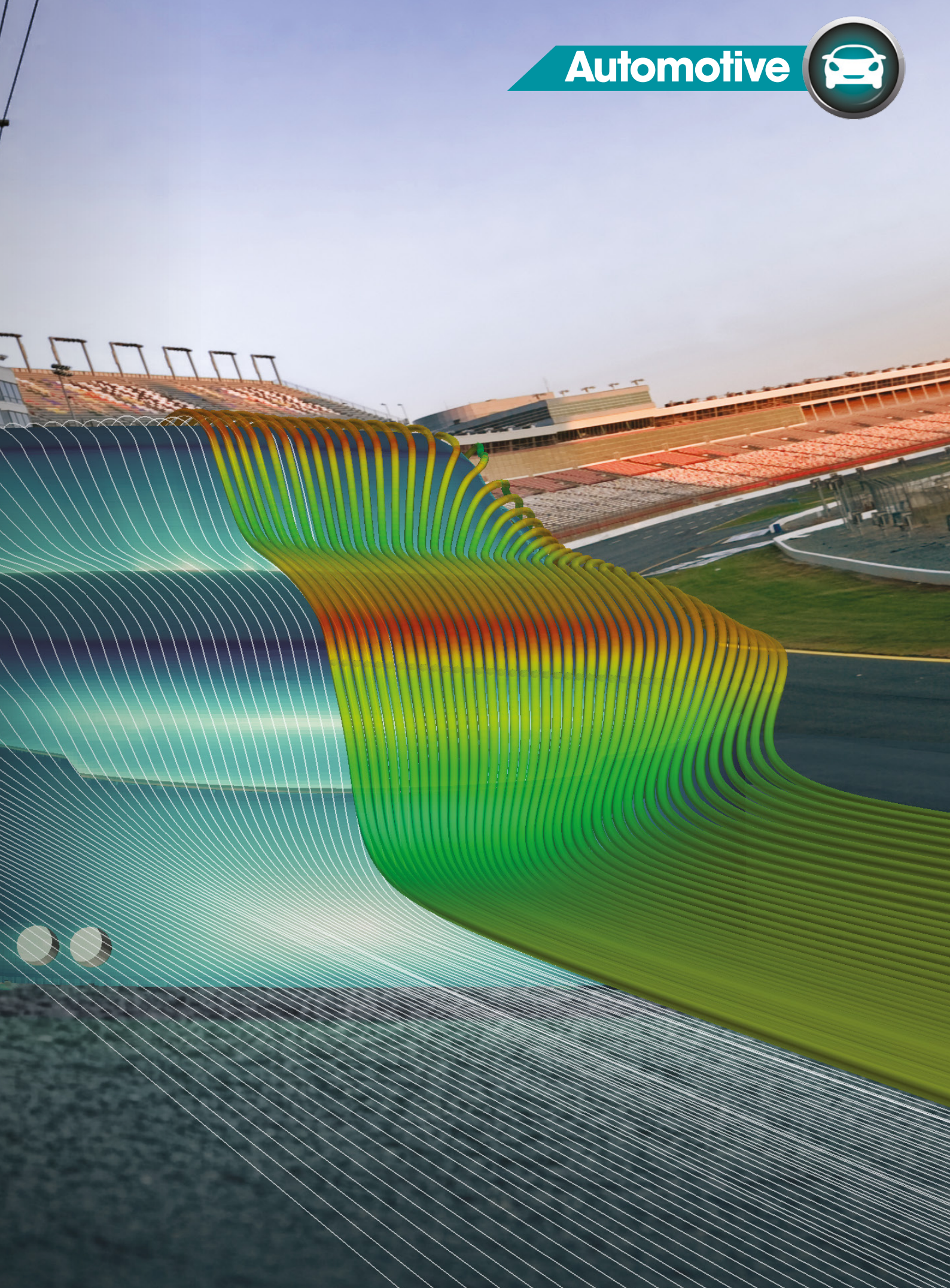
Voxdale collaborate to engineer a champion car using FloEFD

By Mike Gruetzmacher, Technical Marketing Engineer, Mentor Graphics

NASCAR is the most popular motorsport competition in the USA. The three largest racing-series are the Sprint Cup Series, the Xfinity Series, and the Camping World Truck Series. NASCAR sanctions over 1,500 races at over 100 tracks in 39 of the 50 US states, as well as in Canada, and its races are broadcast in over 150 countries.

Initially only modified large scale series vehicles were used for NASCAR. Today's NASCAR vehicles are racing cars with a V8 engine and up to 800 horsepower, but restricted in compliance to the applicable regulations. Only the car body silhouette resembles a series car. The cars are subjected to strict regulations, for example a limited size for the rear spoiler, the chassis material thickness or allowed production processes for the engine cylinders. It is normal practice that winning team cars are dismantled by NASCAR officials after a race to check for any irregularities. The car performances are almost equivalent. There are only a few rare opportunities to gain any technical advantage. This leads to the teams needing to find ways of making small gains wherever they can to improve their performance.





The popularity of NASCAR racing is increasing in Europe, with the NASCAR Whelen Euro Season. NASCAR rules and standards are adopted in the series but the cars are built specifically for European tracks and the horsepower is restricted to 450 hp. One of the most successful European race drivers is Anthony Kumpen from Belgium. He is the overall winner of the 2014 NASCAR Whelen Euro Series season. His huge success in Europe qualified Anthony to compete in the US NASCAR K&N Pro Series East. Today he combines the NASCAR championship in Europe with races in the USA.

We met Anthony Kumpen together with Koen Beyers, CEO of Voxdale BVBA, a successful CFD engineering consultancy, to see what CFD could do to improve their car. Voxdale collaborate to engineer Anthony's team cars using Mentor Graphics' FloEFD.

Anthony explains that there are many aspects to be considered for a racing driver, "There is the driving aspect which is one of the real interesting parts but there are also all the technical details to be optimized. I'm working with engineers and mechanics. There is a lot more than just driving fast in a car. That's what racing is all about. Being a racing driver everybody thinks I spend all the time in the car but actually I spend 80% of my time in meetings with my engineers, with my chief mechanics. Engineering is something we have to study every day in order to be a good driver."

One field Anthony and his team are particularly interested in, is aerodynamics. Since the team does not own or have access to a wind tunnel, like an F1 team would have, they had to find another way to analyze their car's performance. So they teamed up with Koen and the Voxdale team, who are experienced in racing aerodynamics. Voxdale Engineers began working on this NASCAR project by conducting CFD simulations in Mentor Graphics' FloEFD 3D Simulation software.

"The main goal of the partnership was to get insights in the behavior of the car. So when we got involved in the NASCAR project with Anthony the first thing we had to do was to look into what was actually possible to do," Koen Beyers, Voxdale CEO explains.

The NASCAR series is a closed racing series with a very tight rulebook and strict regulations. For instance, the body work could be changed nor could the manifolds or engine parts. Anthony's team and Voxdale decided to analyze the car's aero-mapping and overall behavior. They also investigated the internal flows, the flows underneath the body, and

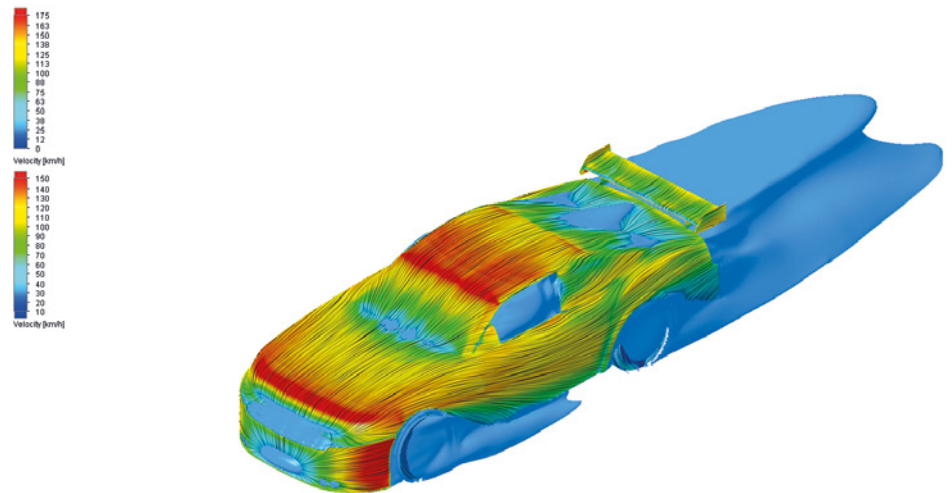


Figure 1. Velocity Streamlines on Body Surface and Isosurface around the Car Body



Figure 2. Anthony Kumpen (left) and Koen Beyers (right)

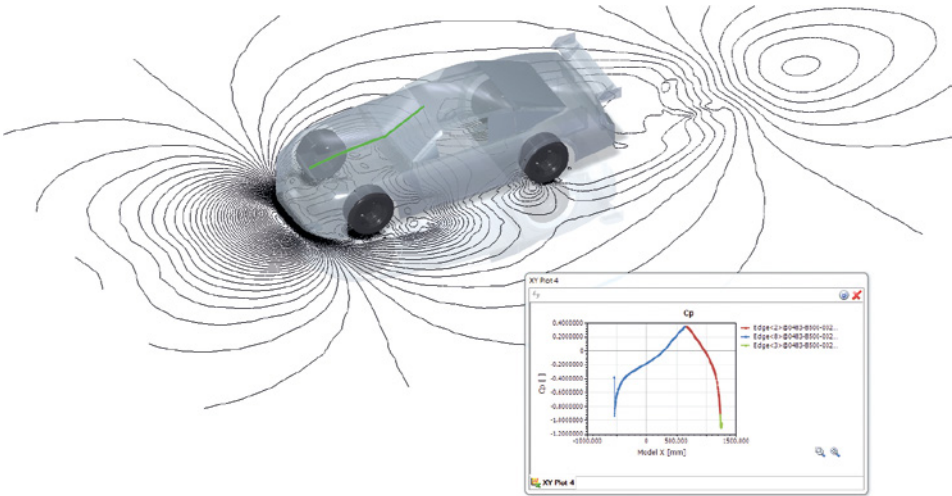


Figure 3. Pressure Coefficient Cp



the hood. Furthermore they optimized the cooling of the brakes and the exhausts. As preparation for the simulations the car model was set up in FloEFD for PTC Creo. The modeling of the geometry took around three days, the FloEFD simulation setup took about a day. The engineers conducted around ten simulations directly within the PTC Creo environment which took about two weeks including post processing. The results of these quickly prepared and evaluated simulations were used for rapid optimizations as the regulations and schedules disallow long predevelopment phases.

“At one point, we saw the effect of a specific riding height combined with an explicit rake angle resulting in a drag reduction of 0.8%. Over one lap at Brands Hatch, with this car with this power, this buys you 0.2 second. An important leap in a closed racing series”, Koen illustrates.

“It is very cool to see the car racing on track, that you analyzed the car and helped the team to give an even better performance” says Patrick Vlieger, Engineer at Voxdale.

“There are a lot of different aspects on aerodynamics that are important for racing. Sometimes you want to have the maximum downforce, sometimes you want to have as little as possible downforce and make the car run really smooth. With all the data the Voxdale engineers gained Anthony's team and his engineers tried to improve the cars on the track and so far it's working really well.” as Anthony confirms.

Anthony Kumpen, “With FloEFD we could do a lot of tests and improvements of the car which helped us a lot. We are winning a lot of races. It's all about the details of racing and finding the right partners and we are really happy to do this with Voxdale.”

References

<http://www.nascar.com>
https://en.wikipedia.org/wiki/K%26N_Pro_Series_East
<https://en.wikipedia.org/wiki/NASCAR>
http://www.formula1-dictionary.net/map_aero.html
<http://www.f1buzz.net/2009/02/17/what-is-aero-mapping/>
<https://www.reference.com/sports-active-lifestyle/much-horsepower-nascar-stock-car-eb5f6a334398b967#>
<http://auto.howstuffworks.com/auto-racing/nascar/nascar-basics/nascar-engines1.htm>
<http://www.racingblog.de/nascar-faq/>

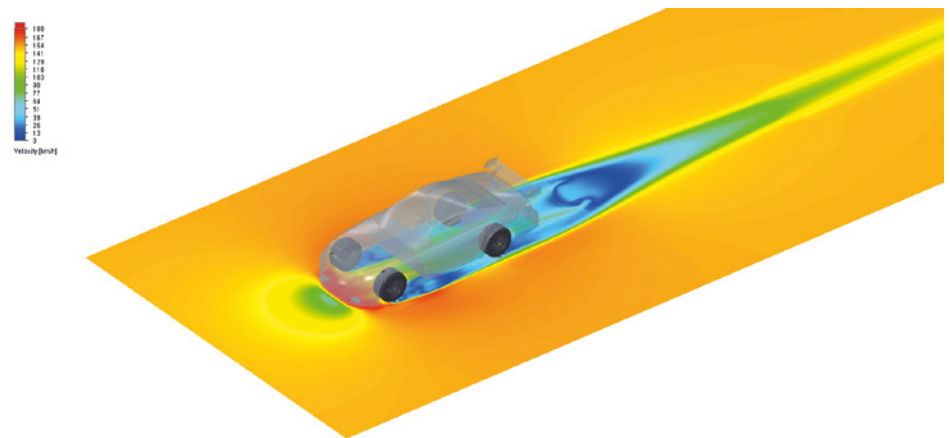


Figure 4. : Velocity Profile underneath the vehicle

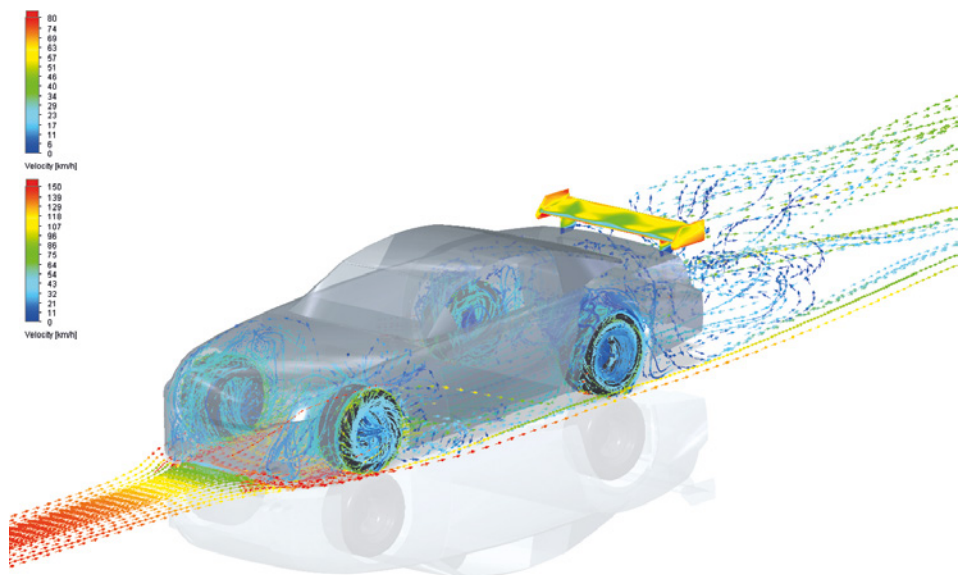


Figure 5. Velocity Profile underneath the Car Body and Wheelhouses

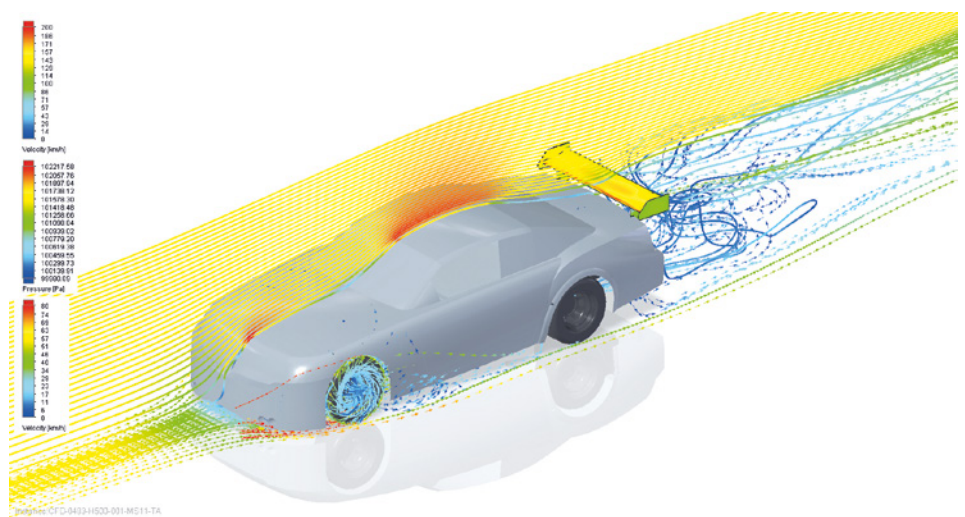


Figure 6. Velocity Profile underneath Car Body and Pressure Distribution the Spoiler

Air Dynamics Simulation of the Tamturbo Oil-Free Air Turbo Compressor

By Timo Pulkki, Mihail Lopatin, Tamturbo Oy, Tampere, Finland & Alexandr Nikulin, Axis Engineering (Mentor Graphics distributor), Saint Petersburg, Russia & Tatiana Trebunskikh, Mentor Graphics, Moscow, Russia

Nowadays to be competitive in the air turbo compressor industry, the company must provide high performing hardware with the lowest life cycle cost. In most cases to achieve such characteristics the company has to use a range of innovative technologies. Tamturbo Oy, was founded in 2010 in the Tampere region, the birthplace of several compressor innovations, has achieved their goal of transforming their view of oil free technology into a worldwide success story. They are fully committed to delivering solutions that bring the highest life cycle value to their customers.

Performance prediction of the prototypes of air turbo compressors is one of critical questions during the design process. As soon as such predictions are available, the design engineers are able to optimize the device, taking into account a number of factors like the cooling of the compressor stages or cooling of the electrical engine driving the compressor. Moreover all issues with new design should be discovered as soon as possible before hardware testing, to reduce development time and cost. The required changes can be minor or major for larger parts. Without dependency on the scale of the changes, a deeper understanding is required into processes inside the particular parts as well as the whole device. This is the reason Computer-Aided Engineering (CAE) software and Computational Fluid Dynamics (CFD) software in particular are so popular in the modern industrial world. CFD in particular is



Figure 1. The Tamturbo compressor

more effective in investigating directly, during the product design process as an integral part of the product lifecycle management (PLM) in the early development stages. There are several approaches in CFD including traditional and frontloading. In addition to relying on the vast knowledge and experience in CFD, the traditional

approach usually requires transferring geometry from a CAD system to CFD software, via different exchange formats, where some issues with geometry can occur. Issues such as cleaning and healing geometry to make it suitable for mesh creation and manual mesh generation with focus on boundary layers. Investigations



of a wide range of designs using such an approach is very time-consuming and as a result only a few particular cases are examined by CFD experts after all changes are made by the design engineer.

The frontloading approach presented in Mentor Graphics' FloEFD™ tool, is intended for use in the early design development stages by design engineers. There are two main principals in FloEFD: direct use of native CAD as the source of geometry information, and a combination of full three-dimensional CFD modeling solving Favre-averaged Navier-Stokes equations with simpler engineering methods in the cases where the mesh resolution is insufficient for direct simulation.

To overcome a traditional CFD code restriction of having a very fine mesh density near walls in a calculation domain, FloEFD describes boundary layer, with the "Two-Scale Wall Functions" method including the near wall functions and the sub-grid model of the boundary layer.

For the simulation of the compressor, the rotation model should be used. There are two local rotation models in FloEFD – circumferential averaging and sliding. The circumferential averaging approach is employed for calculating transient or steady-state flows in regions surrounding rotating solids, which are not bodies of revolution (e.g. impellers, mixers, propellers, etc). To connect solutions obtained within the rotating regions and in the non-rotating part of the computational domain, special internal boundary conditions are set automatically at the fluid boundaries of the rotating regions. The rotating region's boundaries are sliced into rings of equal width and the values of flow parameters, transferred as boundary conditions from the adjacent fluid regions are averaged circumferentially over each of these rings.

The sliding rotation model produces a time-accurate unsteady solution of the flow fields, where the rotor-stator interaction is strong. The sliding technique takes into account the relative motion between stationary and rotating regions. Rotor and stator control volume (CV) zones are connected with each other through "sliding interface". During the calculation, zones linked through "sliding interface" remain in contact with each other. The sliding interface has CVs on both sides and as a consequence each face of the sliding interface has two sides belonging to both rotor and stator zones. All these techniques allow FloEFD to be used for the calculation of air turbo compressors.

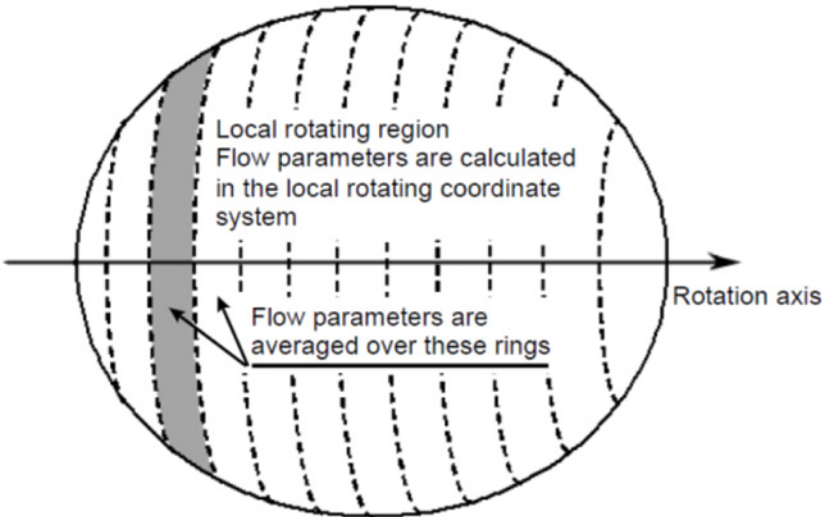


Figure 2. Ring creation in the Circumferential Averaging Rotation Approach

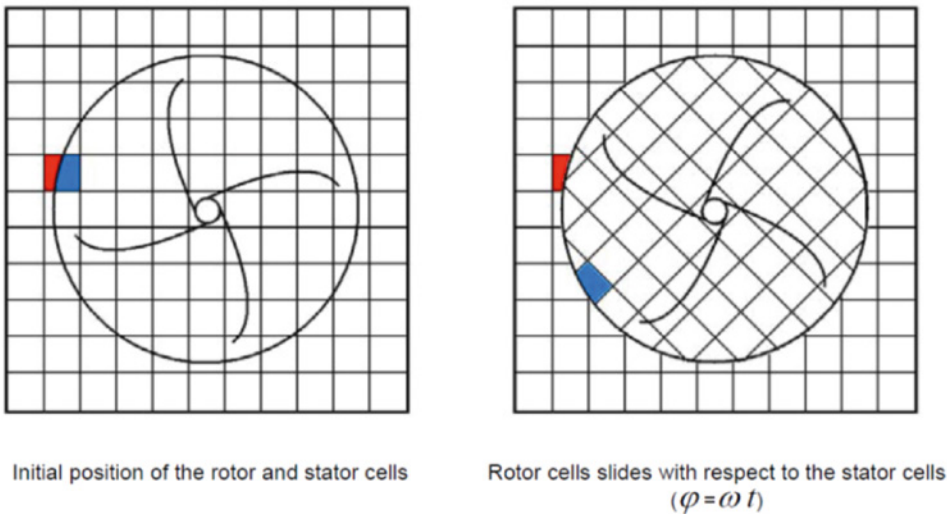


Figure 3. Sliding Rotation Approach

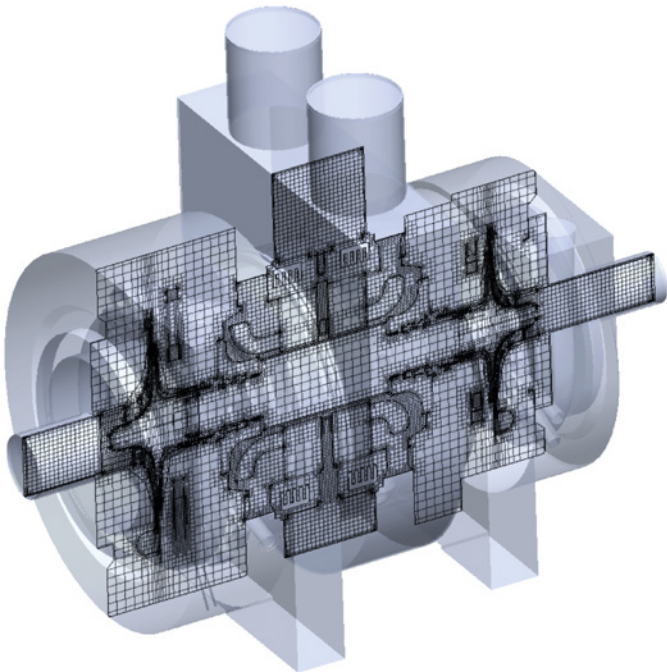


Figure 4. The Mesh of the Compressor Model

This article shows a great example of the two stages of oil free compressor investigation, completed by Tamturbo Oy with support from Axis Engineering.

For analysis, the full assembly of the compressor was used, the construction of which includes several contours: compressor flow area, and several cooling contours. Each contour includes components manufactured from different materials, such as titanium steel or aluminum, which were chosen based on the results of the preliminary calculations of thermal loads and strengths of the various parts of the compressor.

The geometry of flow area has been determined by required compressor characteristics and has a very complex internal structure. The CFD analysis of the compressor, where final pressure rise ratio was calculated, allows for the assessment of air temperature rise. To decrease the temperature of the compressor's body, Tamturbo engineers added the cooling system for the compressor with a complex internal structure.

All geometry features of the compressor, presence of the rotating parts and special requirements for temperature in some critical places like bearings, volutes, shaft and so on, predetermined mathematical models which were needed for the analysis.

The turbulence model used in the analysis can detect a flow regime and switch the mode between laminar and turbulent automatically. This solver is unique and allows an engineer to obtain a solution inside narrow channels even on a coarse grid. The calculation was made taking into account conjugated heat transfer, where heat transfer equations were solved in solid bodies. The radiation model has been disabled due to relatively low temperatures.

In the analysis of the flow, to consider the rotation of the impellers, special rotating model "sliding" was used, which helps to predict characteristics of any type of turbomachines with better quality.

As boundary conditions for the airflow inside the compressor were specified so were the conditions for pressure at the volutes outlets, mass flow rate at their inlets, and shaft rotating speed. For cooling paths, pressure difference between inlet and outlet boundaries was determined. To simplify the thermal analysis of the engine and the shaft, a heat emission process was simulated by adding heat sources with constant power

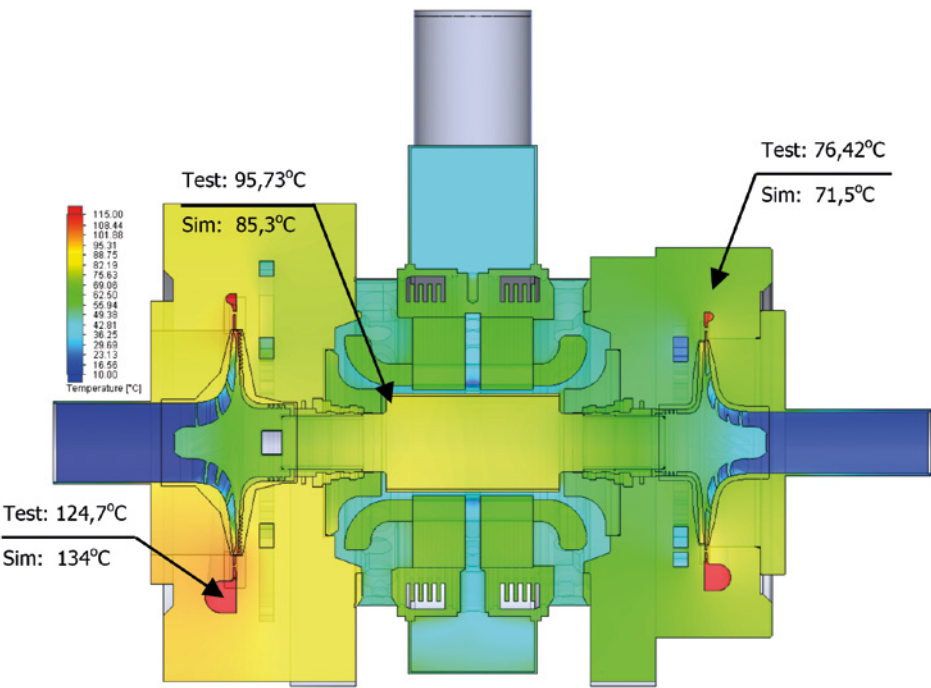


Figure 5. Temperature Distribution in the Longitudinal Section of the Compressor

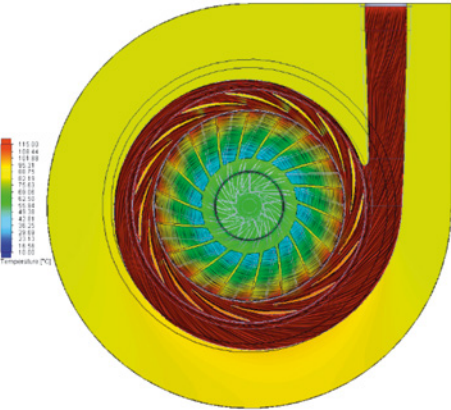


Figure 6. Stage 1. Temperature Distribution in the Cross Section of the Compressor with Streamlines

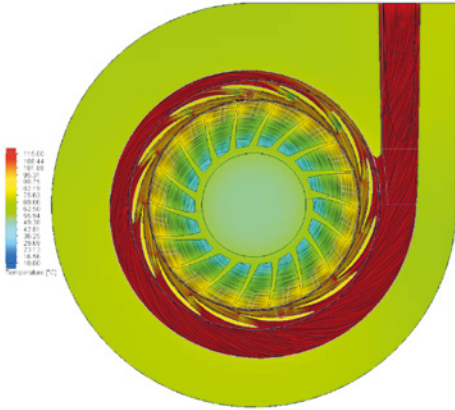


Figure 7. Stage 2. Temperature Distribution in the Cross Section of the Compressor with Streamlines

values instead of using the FloEFD feature emulating a real Joule heating process.

Simulation of conjugate heat transfer process for all zones and units of the compressor, allowed for the investigation of their mutual influence and predicting the thermal state of the compressor components.

The most important parameters under investigation were air temperature before the bearings the volute and the shaft temperature. Mainly bearings work properly when their temperature is lower than 100-120°C, but on the other hand the temperature of the compressed air can be higher than 200°C. And of course every calculation has to predict the compressor pressure rise ratio for the required mass flow rate range.

Initially homogeneous structured mesh was created on the entire geometry, where the number of cells along the main axis of the compressor did not exceed 90. The number of cells for the other axis was chosen in the way that the final size of the basic cells was similar in all three dimensions. After creating the basic mesh, some local regions for better mesh resolution around compressor impellers and in the bearing's area were added. Additionally mesh generator settings were specified to allow for automatic detection of the narrow channels and further splitting mesh in these areas. As a result the total number of cells in the entire two-stage machine was approximately 4.9 million.

The analysis was run in the transient regime on the usual workstation for CFD calculation:



two CPU with frequency 3.1 GHz and only 8GB RAM were used for the task. As a result the simulation of 30 seconds of physical time took only 1.5 days of computer time.

According to the calculation results, the additional seals have been designed and the optimal mass flow rate of the cooling agents were chosen. The temperature in the bearings, was in the range of 60-80 degrees in the calculation results. Tests showed the temperature rise in the nodes close to the bearings up 7-12 degrees.

The difference between pressure values of simulation results and natural tests of the real equipment was not more than 3-5%.

Tamturbo Oy uses FloEFD for a wide range of other tasks, from the turbo compressors developing area, closing all questions of aero and thermal calculations. The quality of the results was proved by the series of experiments which were provided by Tamturbo Oy and a number of completed projects. The software has several direct interfaces with other codes which are used in the company, and as a result of this fact and due to the unique solver technology as well as all other features mentioned above, the development product lifecycle and its costs were significantly reduced without compromising the quality of the results.

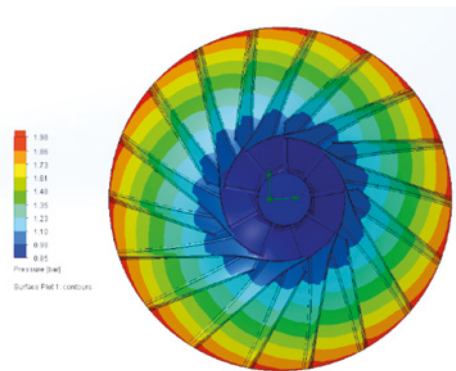


Figure 8. Stage1 impeller. Static pressure distribution on the surfaces at normalized mass flow rate 0.8, normalized rotational speed 0.943. Pressure rise ratio - from simulation 1,9718/ from test 1,9723

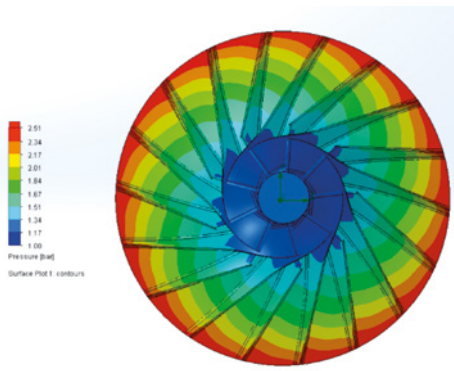


Figure 9. Stage1 impeller. Static pressure distribution on the surfaces at normalized mass flow rate 1.5, normalized rotational speed 0.943. Pressure rise ratio - from simulation 1,9585/ from test 1,9589

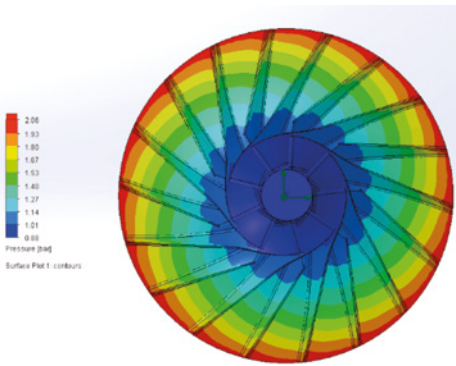


Figure 10. Stage1 impeller. Static pressure distribution on the surfaces at normalized mass flow rate 0.9, normalized rotational speed 0.97. Pressure rise ratio - from simulation 2,0391/ from test 2,0302

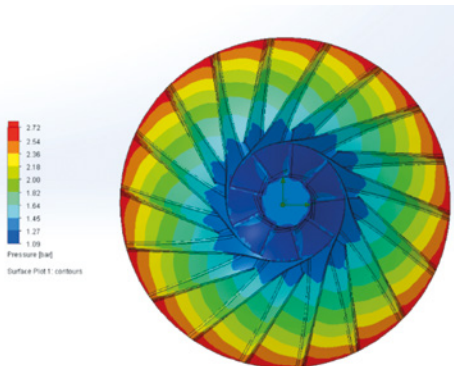


Figure 11. Stage1 impeller. Static pressure distribution on the surfaces at normalized mass flow rate 1.6, normalized rotational speed 0.97. Pressure rise ratio - from simulation 2,0083/ from test 2,0057

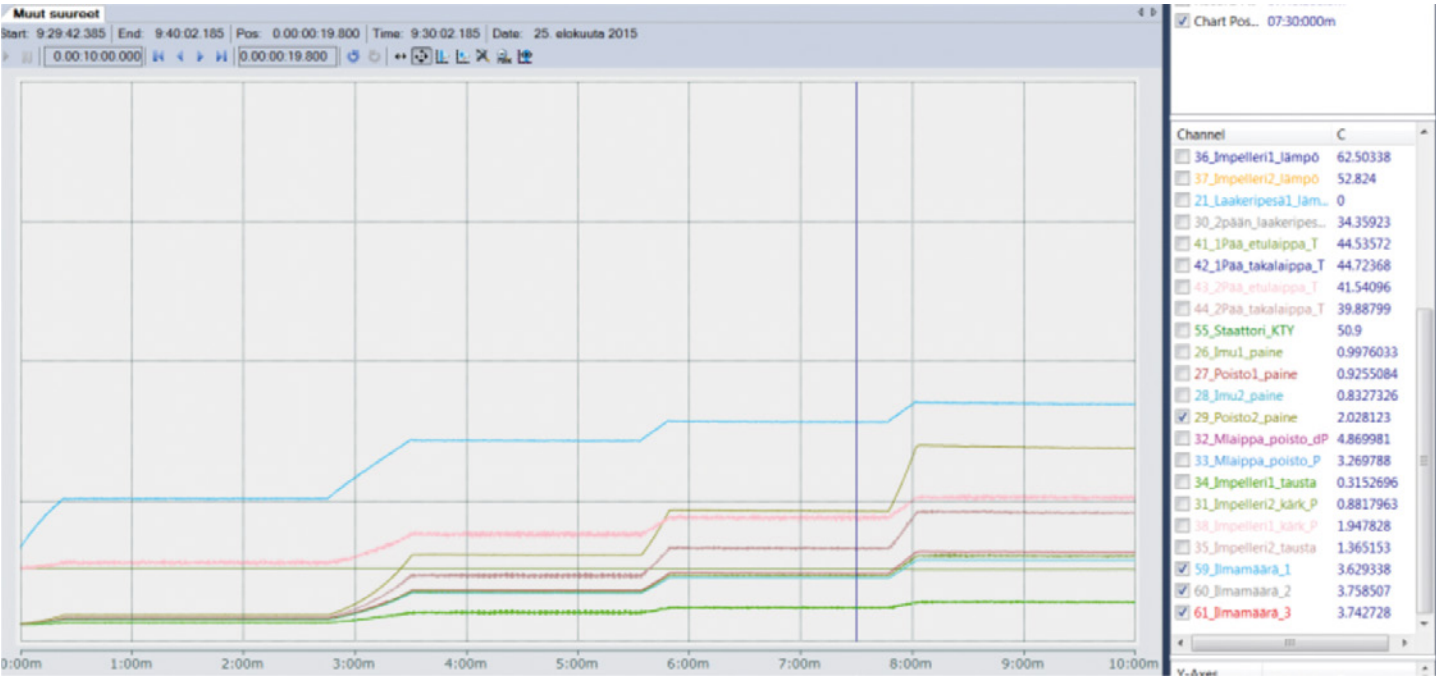


Figure 12. Dynamics of different parameters from the final compressor test.



Dr. Uwe Lautenschlager
Senior Technical Expert - Simulation

Q. Tell us about Continental AG

A. Continental can look back on a successful history for 145 years, founded in 1871, when the company started manufacturing soft rubber and rubberized fabrics. Although most consumers recognize Continental for its tire division, we are a leading diversified German automotive manufacturing company specialized in brake systems, automotive safety, powertrain and chassis components, as well as instrumentation or driver HMI, connectivity, infotainment, access systems and many more. Today, Continental has sales above €39 Billion with around 215000 employees worldwide. My place is inside the "Infotainment & Connectivity" Business Unit's Mechanical Engineering team within the Interior Division. We are located here in Wetzlar, Germany, a town known for optical and fine-mechanics industry.

Q. Tell us about what you do in your role at Continental?

A. I started my career at our Wetzlar site in 1999 as a structural analysis specialist. However, the task quickly extended into the electronics cooling and thermal simulation area. Today I manage our BU's mechanical simulation team which is based at several sites around the world. It covers optical, structural, EMC, molding and thermal simulation of our products. My team role is to innovate the simulation processes by setting the simulation methodology, tools and knowledge sharing and targeting the same level at all sites. Nevertheless, I'm always passionate about developing models and doing simulations by myself. Besides my work in the simulation team, I'm also fortunate because Continental supports me to be an "ambassador" at the nearby University of Siegen where I have been giving lectures on "Modeling and Simulation" since 2009. The students love the close connection to Industry they can get from my hands-on course.

Q. What are the products that you and your team are involved with?

A. Speaking about our Business Unit, our product portfolio includes radios, which have evolved from simple tuners and amplifiers to proper entertainment hubs, multimedia systems, and telematics modules. Connectivity

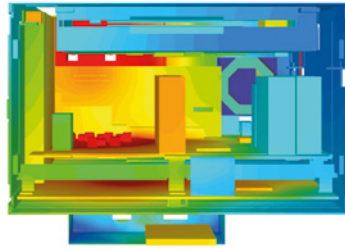


Figure 1. Thermal analysis of an infotainment system with multiple components and devices.

devices allow the communication between the vehicle and the internet and, in future, increasingly to other peers as part of the Vehicle-to-X (V2X) trend. A permanent exchange of data from the vehicle is aimed in our "Always On" vision. Infotainment is a fast growing part of the automotive industry and is rapidly changing from year to year in both car connectivity and car communications. Our products have to deliver new answers for future mobility and intelligent technologies, they are networked together by taking on more driving tasks.

Q. Do you work mostly within your Business Unit or does your work stretch to other Continental Business Units in Germany or even Worldwide?

A. We have two aspects here, one being the integration of products across our division in the future. The second aspect is our simulation network. Not only do we have our experienced and agile simulation team, we have established a close simulation network and User and Working Groups across Continental for several disciplines. For example, I'm the speaker and organizer of our FloTHERM® User Group. We meet regularly with all international users in varying locations and support each other across all divisions if necessary and possible. Our BU's simulation team itself is positioned worldwide like in Singapore, France, Germany, Romania etc. so it really is a worldwide working group. Our team has the desire to serve our customer's, (internal and external) needs quickly and reliably; we have a high documentation standard in order to provide the same high quality in all our simulation results.

Q. How different are the requirements or thermal limits of your products and how different are the environmental boundary conditions for them?

A. Thermal limits become increasingly obvious as package dimensions shrink,

power dissipation increases locally or globally and packages have lower temperature specifications, e.g. from consumer electronics. Boundary conditions as part of the requirements are given by the OEM and can therefore vary according to the standards they specify. The ambient temperatures vary, the requirements on housing temperatures and the thermal management options differ and are dependent on the location of where the product is installed (roof, dashboard etc.). Since our infotainment systems can be found in trucks, we have to fulfil a higher lifetime expectation (25,000 hours) for them compared to cars (with around 10,000 hours being more normal). Hence, the overall variation is more between the OEM or vehicle type and we try to re-use the platforms across OEMs to keep the costs for development to a minimum. There are many parallel thermal challenges nowadays, not "only" designing a good amplifier heatsink as maybe in the past.

Q. When you use FloTHERM in your work, how many simulations do you run on one product on average until the design has matured?

A. In 2000 we chose FloTHERM as our thermal simulation tool, convinced primarily by its quality and robust solution capabilities. We use FloTHERM to run thermal simulation very quickly and it is deeply integrated into our design process. It allows us to do lots of variant simulations very fast. If my boss says "we need something today", I can get a satisfactory answer quickly. Productivity is important but it depends on what type of answer is needed, or how much detail and data to include. In the very early phase of a product's design, such as the quotation phase, the simulation detail is secondary as the product cannot be defined as accurate as compared to the final product development stages. So it is not a number, it is a level of confidence that can be achieved rather quickly.

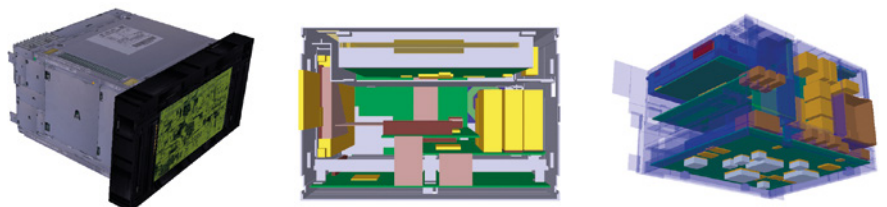


Figure 2. A FloTHERM model with texture map and the internal view of an assembly with its components and modules.

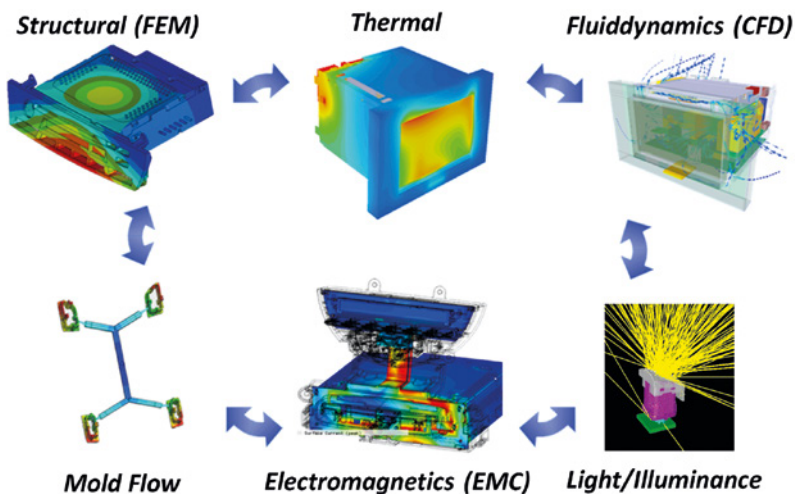


Figure 3. The overall connectivity of various simulation disciplines in multimedia system simulations.

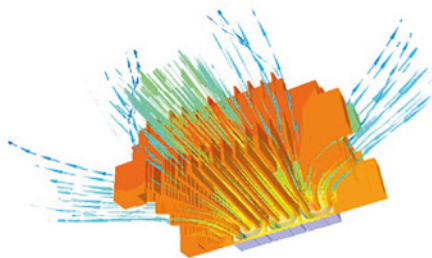


Figure 4. Thermal analysis of an infotainment system with multiple components and devices.

Q. Do you think the products you develop today would be realizable without simulations?

A. We always need to understand our products - that's where simulation tools come in. Of course, developing a product on time and to cost was a goal when there was not much virtual analysis done 20 years ago. Often the products were overdesigned and we had many prototypes and samples created. Today, however, we can design the products closer to their limits as we understand the physics behind them better through simulation. The development cycle we have today could not be done without simulation. Our first shot has to be correct. A good simulation is also not only about being correct, but it also helps to understand the product. The design of our automotive multimedia systems has to fulfill requirements from mechanical stability and thermal management to electromagnetic compliance, hence a multi-disciplinary design and optimization problem. Conflicting objectives among these disciplines require a concurrent design approach with different modeling levels, parameter variation (e.g. DOE techniques), optimization techniques and the consideration of uncertainties and changes within the design process. Such up-front simulations enable us to test and modify system and components as virtual prototypes before performing physical tests and building real prototypes.

Q. How important is it to interact with the other simulation groups from electrical and circuitry design teams and how often do you need to communicate the changes and the results?

A. Extremely important! Every change with a thermal benefit can greatly impact the structural behavior or Electromagnetic Compatibility (EMC) and electrical circuitry aspects. A larger heat sink in the back of the system could increase the vibration and cause rattling for instance; or moving a processor closer to a colder zone for better cooling, but also closer to a high frequency zone near an antenna for example can cause EMI issues. As said before, we have a multi-disciplinary design problem.

Q. Where do you see electronics thermal simulation in the future? Will there still be physical testing or will it be all virtual testing through simulation?

A. We typically skip the A-Sample that we had in the past and almost directly go into the tools as we expect already a good sample from the simulation. Potential design risks are typically identified by simulation early enough and eliminated. This is besides the many tests we

put our devices under with physical laboratory stress tests from long term use of buttons, shock and random vibration to environmental tests in climate chambers. For us the testing will not be replaced in any foreseeable future; final qualification testing will always be done on the matured design in a laboratory. However, the number of prototypes is reduced and the risk of failure should be at a minimum.

Q. When thinking about the future, where do you see the biggest challenges in your work with the future technology developments that will go into your products?

A. Several years back CPUs generated 1-2 W of heat in a car; now they are more in the range of 10W. We are also seeing the trend towards bigger touch-screen displays and multimedia systems are getting more and more condensed into smaller spaces of non-rectangular shape. Those are some of the technical challenges we face, additionally we must put a big focus on developing the skills of our simulation team to be able to understand and handle new technologies and simulation tool features accordingly. I always see the resource aspect as we will never have enough simulation people to do everything that could be done, but we do everything that's necessary.

Q. Do you have any goals over the coming years to increase your simulation productivity?

A. Our daily work is changing faster than ever. Improving the post processing and documentation of simulation tools and results will help us to communicate answers more efficiently to our customers. We try to reduce the time for modeling and documentation and spend more time for creativity and solutions. We want to implement highly efficient workflows with the right tool landscape. Continental is on the way to being a digital company for sure.

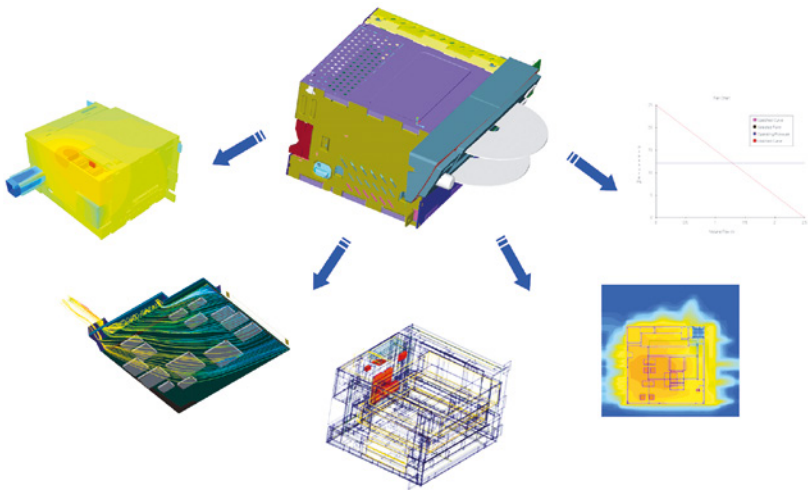


Figure 5. Showing a range of simulation tasks and result evaluations in an infotainment thermal simulation.

Using FloEFD™ to design Liquid-Cooled Nozzles for Cutting Tools



By Hidebumi Takahashi, Mitsubishi Materials Corporation, Advanced Materials & Tools Company, Machining Technology Center

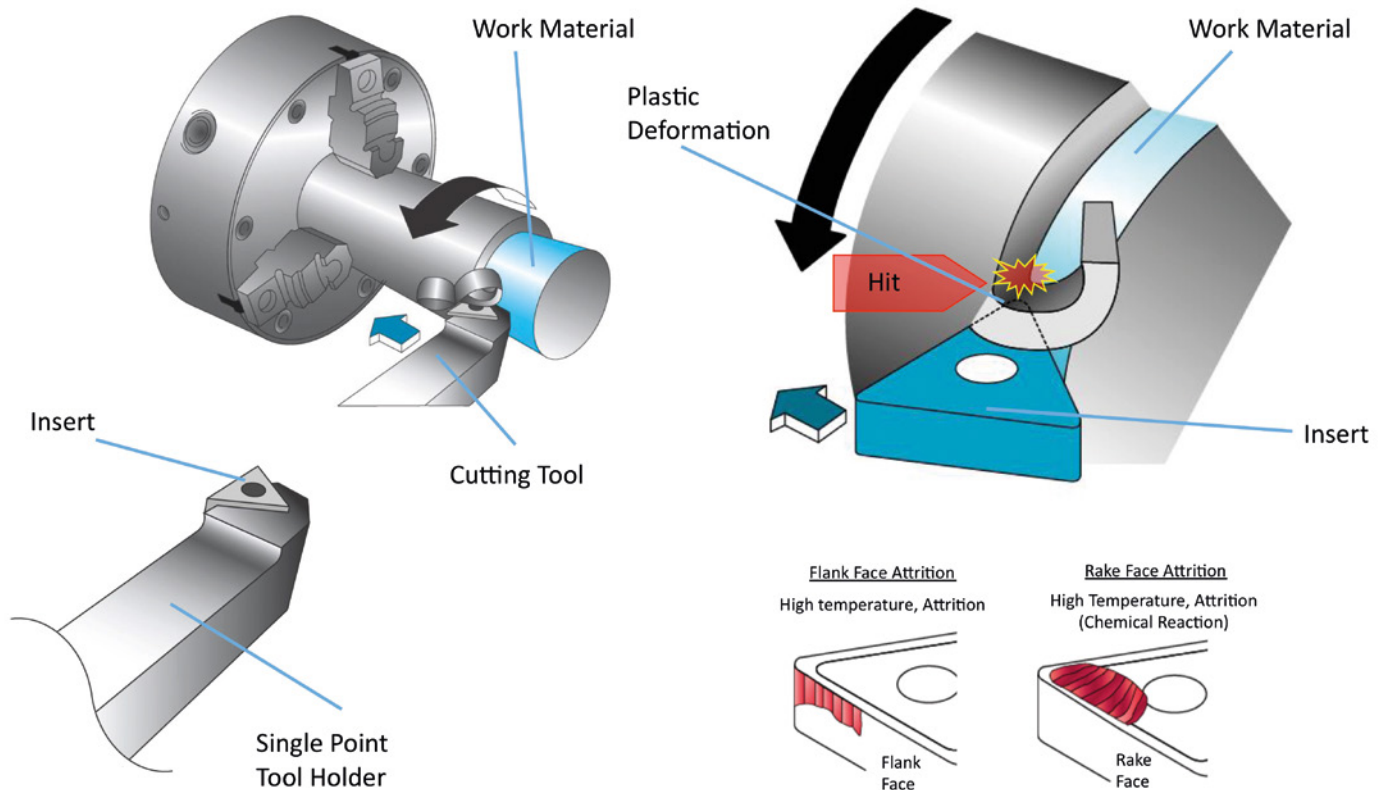


Figure 1. Typical Cutting Bits used in Lathe Turning and the wear issues they face

The Mitsubishi Group is a huge Japanese industrial conglomerate and Mitsubishi Materials Corporation is one of the subsidiary companies of Mitsubishi Mining Company Ltd. and has been in existence for approximately 100 years. Its Advanced Materials & Tools Company and its consolidated subsidiary companies employ approximately 6,800 people worldwide, making and delivering a wide range of machine

cutting tools based on tungsten carbide. A subset of these tools is in rotating lathe applications (Figure 1) that tend to generate surface temperatures of 600 – 700 degrees at the contact cutting point (at the rake and flank faces) and the cutting tool's lifespan can consequently be low. Tungsten Carbide triangular tool inserts are typically used on all six of their corners before they are disposed. They therefore experience several thermo-mechanical effects that

damages them and affect their lifetime – attritional wear on the rake and flank faces of the tool, frictional heating effects, mechanical separation due to the extreme forces involved in the cutting, and even chemical reactions.

Traditional cooling systems for such cutting tools have used a single circular nozzle cooling hole near the insert. The tungsten carbide insert can last for 20 minutes per corner edge whereas better cooling could

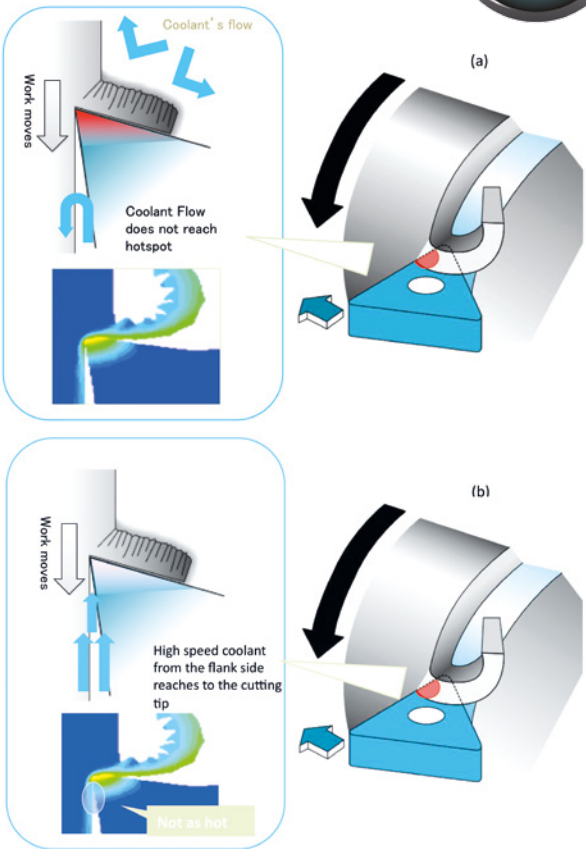


Figure 2. Typical Cutting Bits Coolant Spray and good hot spot cooling (b) versus bad (a)

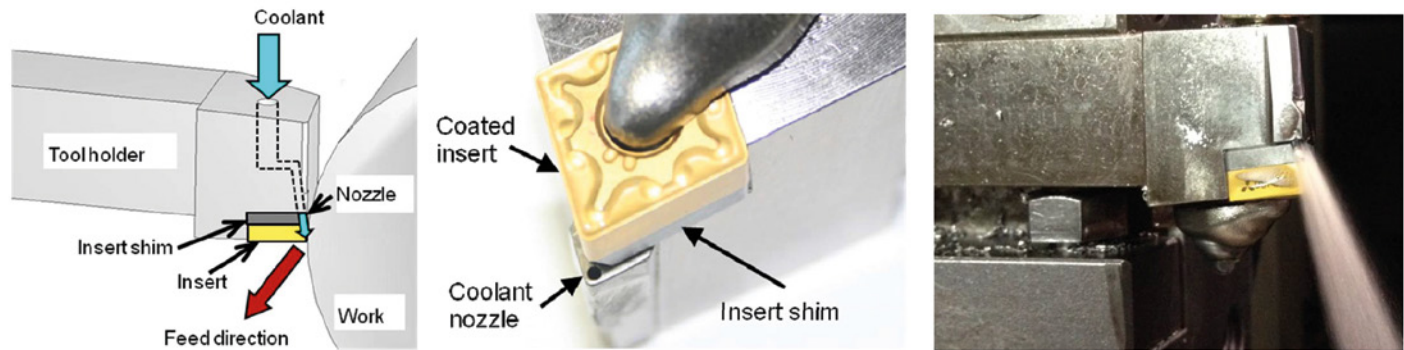


Figure 3. JC Technology's laboratory concept for a Tool Bit Cooling Jet (with circular nozzle)

increase the insert's lifetime by 40%, to 28-30 minutes per corner edge. Such well-cooled tool holder's lifetime performance is an advantage to productivity for cutting tool users.

Mitsubishi turned to Prof Obikawa of the Institute of Industrial Science at Tokyo University and established an academic-industrial partnership to extend the life of their tools. He came up with ideas for new cooling technology for the Mitsubishi tool holder that needed to be tested. The goal of the new cooling technology was to reduce extreme frictional heat generated while cutting (Figure 2), which in turn has the adverse effect of reducing product lifetimes. Prof Obikawa's "Jet Coolant Tech" (JC Technology) came out of the collaboration.

SUS304
 $V_c : 220\text{m/min}$
 $a_p : 1\text{mm}$
 $f_r : 0.2\text{mm/rev}$

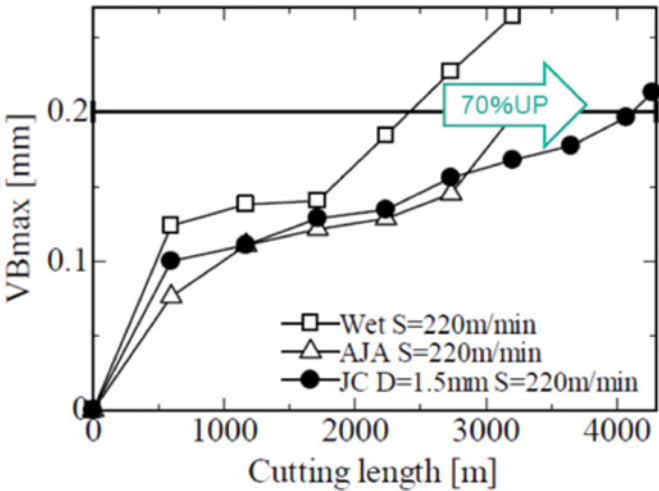


Figure 4. JC Technology's results in a Cutting test - Jet Coolant effect is proved by the basic lab study

Usually it is hard to make the nozzle coolant liquid reach the hottest point on the tool, thereby cooling is not working effectively, (Figure 2a), versus the ideal scenario of coolant getting to the hot spot (Figure 2b). Making the coolant spray reach the heat source by applying high speed targeted jets from the flank face in particular is key.

The crucial idea from JC Technology was to apply the liquid coolant as a “high speed jet” spray from the bottom part of the insert sheet, cooling it down directly, and thus extending the insert’s lifetime (Figure 3). At SUS304 laboratory test, JC Technology was able to show significant improvements (70%) in the laboratory, in cutting length for the coolant jet configuration employed (Figure 4).

Mitsubishi worked with JC Technology to come up with an “L” Shaped nozzle that they believed would perform better than a circular nozzle in terms of jet performance in cooling (Figure 5) within their laboratory tests.

Mitsubishi needed a methodology to simulate the cooling and mechanical effects of its new nozzle. Would it produce enough cooling? Would the nozzle component be durable enough? As such engineers and designers assembled an array of computer-aided engineering tools to virtually test the new design (Figure 6). With regard to fluid flow and heat transfer analysis, they decided to use FloEFD™ from Mentor Graphics and Particleworks™ from Prometech Inc. They only used the standard functions of FloEFD (Figure 7) and Particleworks (Figure 8) software in their coupled simulations with no user subroutines required.

The coolant used in the holder itself was 5-10% diluted water but regular water was used in the CFD simulations. The main goal of the simulations was to optimize the liquid cooling channel opening geometry for enhanced cooling purposes with as few prototypes as possible. Hence, the best cooling geometry was sought for the system. FloEFD showed that for the same pressure drop, the “L” shaped nozzle allowed 11% more liquid flowrate and produced 57% higher peak velocities than the round nozzle. Liquid flow rates and pressures were extracted from the FloEFD CFD simulation as inputs into the Particleworks simulation tool. It simulated the way droplets emerged from the nozzles and where they ended up on the Holder for cooling purposes (Figure 8). Commenting on how Mitsubishi used FloEFD, Hidebumi Takahashi said, “We like

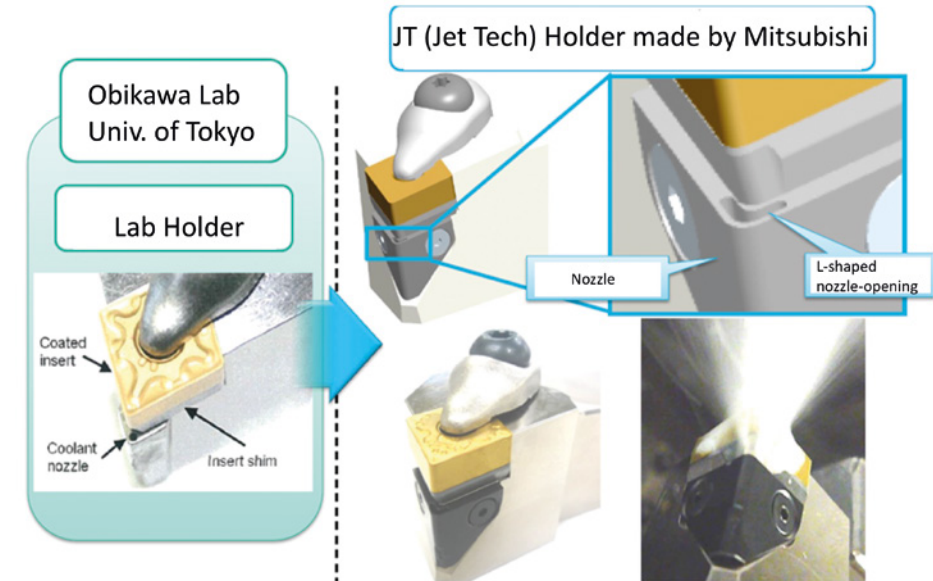


Figure 5. Mitsubishi's Jet Tech Holder configuration and associated CAD model

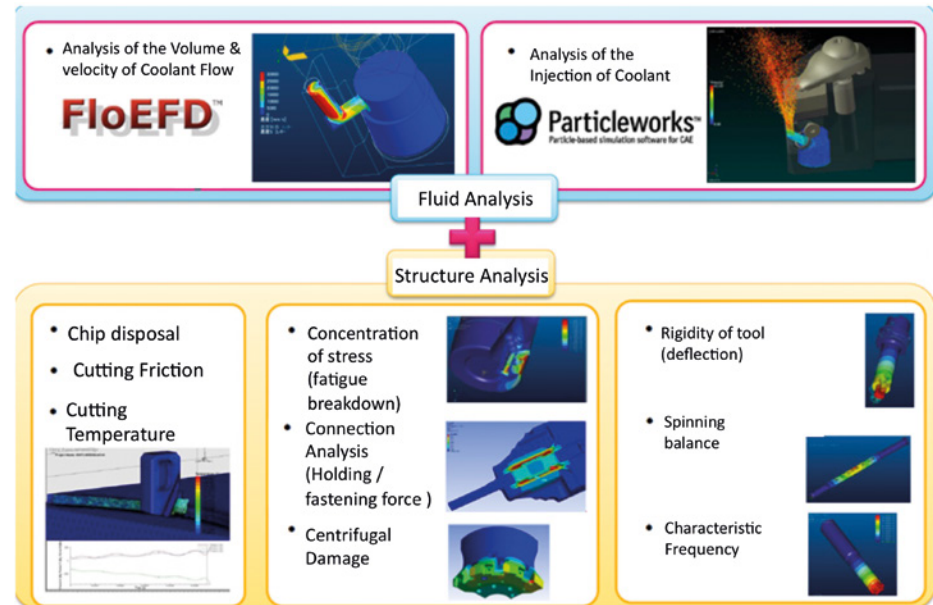


Figure 6. Mitsubishi's Coolant Nozzle Computer Aided Engineering Design Process Methodology

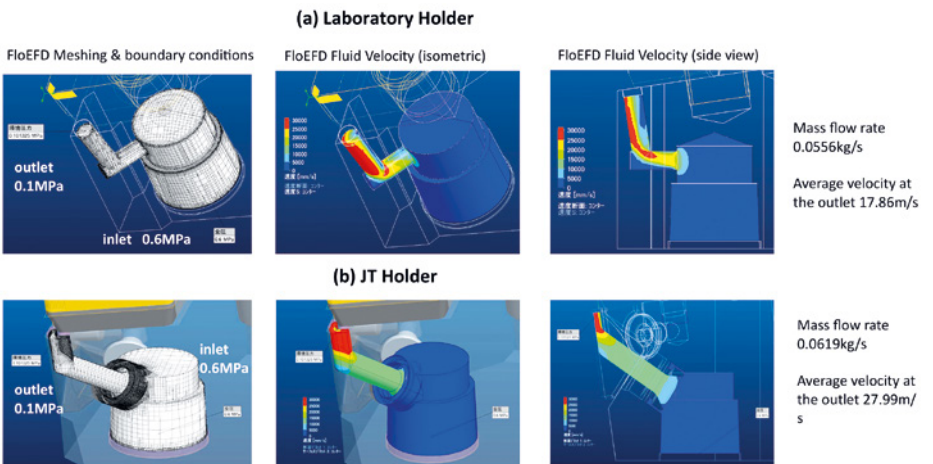


Figure 7. CFD Analysis inside FloEFD of the Laboratory Holder (a) & JT Holder (b) Volume Flow Rate and Velocity of Coolant Flow

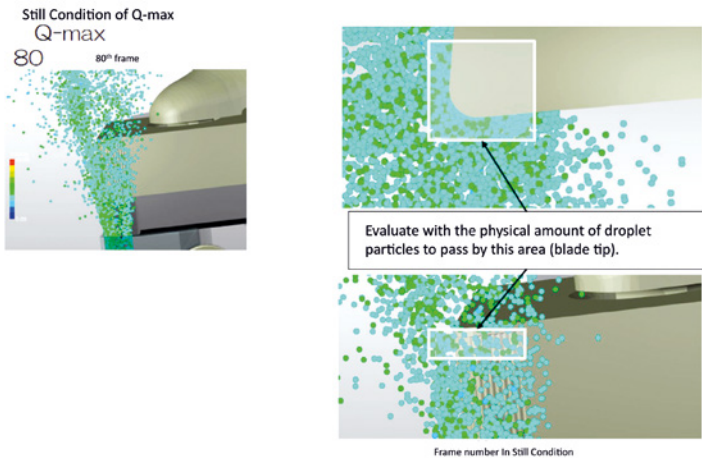


Figure 8. Spray Analysis of the JT Holder in Particleworks™



Figure 9. Final JT Holder Nozzle Spray Configuration

FloEFD because it is fast in calculation for steady analysis. Since we have no specialist CFD experts, our designers take care of simulation analysis. FloEFD is the best for CFD because of its simplified auto-meshing setting inside our preferred CAD package, PTC Creo. We found the cut cell CFD function to be very valuable.”

Subsequent experimental test measurements of the JT Holder system prototype created by this approach proved to be very satisfactory in thermal performance as was structural simulation analysis of the rigidity and durability of the nozzle. The methodology devised by Mitsubishi allowed them to patent the JT Tech nozzle (Figure 9) they devised and can be used to create other Holder nozzle configurations relatively quickly. In future Mitsubishi would like to see a closer coupling of the two fluid simulation software tools for similar analyses.

Cutting Test Results

Figure 10 shows the damage of the wear after cutting test and figure 11 shows the line graph of frank wear. In figure 10, the level of wear describes the wear distance from the cutting edge, and the end of the life time is based on when the amount of frank wear reaches to 0.2mm. As seen in figures 10 and 11, with conventional coolant, the edge is worn out with 0.5mm of the frank wear in 14 minutes of cutting, when the remarkable attrition can be seen on the cutting edge, in the meanwhile, with JT holder, the frank wear is only 0.15mm at the time of 14 minutes and it finally became worn out with 0.2 mm of frank wear, in 20 minutes of cutting time. The JT holder performs 40% better in lifetime extension compared with the case of conventional coolant.

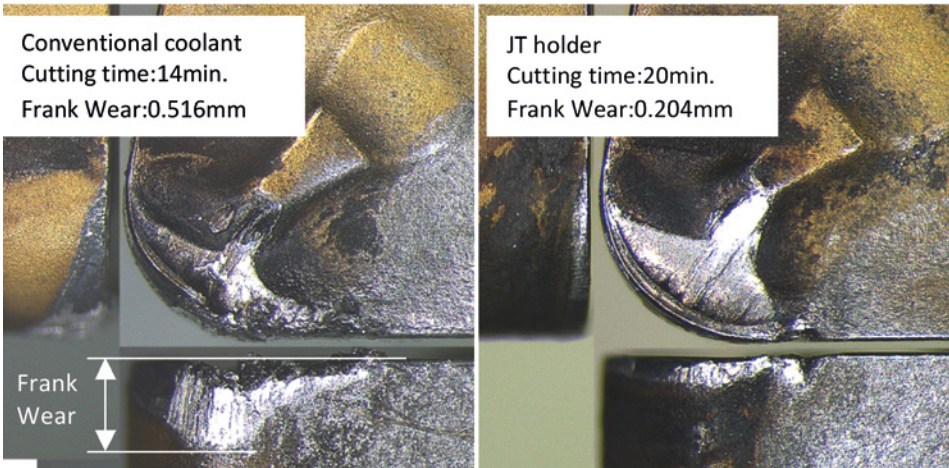


Figure 10. Wear apparatus after cutting test.

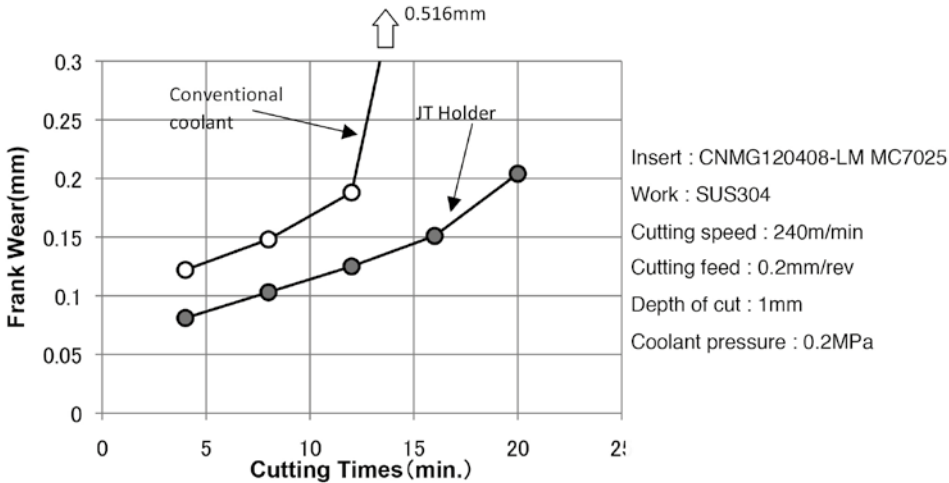


Figure 11. Frank wear of JT holder compared with Conventional coolant.

Mitsubishi Material succeeded in applying the lab testing result to the design process and achieved their target of extending the lifetime of the cutting tools, with an efficient

cooling method. The fluid analysis tool, FloEFD, is an extremely efficient tool for product development.

Voxdale and Flanders' Bike Valley build a Wind Tunnel using FloEFD™

By Mike Gruetzmacher, Technical Marketing Engineer, Mentor Graphics

In April 2016, the Flanders' Bike Valley wind tunnel in Beringen, Belgium was unveiled. The eye-catching structure attracted more than 400 spectators to the opening event. The wind tunnel, with a surface area of around 600 square meters, is the latest project co-created by Voxdale BVBA, and Flanders' Bike Valley. The purpose of the wind tunnel is to provide cyclists, the growing cycling industry and its manufacturers, product developers and athletes with accurate test data to improve product and athlete performance. The tunnel will also be used for additional low speed aerodynamic testing like sports equipment, clothing, drones etc.

The open circuit wind tunnel, also known as an "Eiffel" or NPL Tunnel, is constructed in such a way that air is sucked from the ambient into the test section. The Flanders' Bike Valley wind tunnel is housed in a purpose built hanger measuring 50m x 16m x 10m. The tunnel itself has a length of approximately 50m.

The tunnel comprises several sections: the contraction section, the test section, and the diffuser section. The test section is 2.5m x 2.5m x 6.5m and the maximum wind speed is 108 km/h. The wind tunnel design enables a high level of laminar flow, which leads to very accurate and repeatable results. The test

section is equipped with a balance measuring system to determine weight and drag forces and a PIV (Particle Image Velocimetry) system to visualize velocity and the direction of the air.

Marc Hufkens, Chairman Board of Directors of Bike Valley Innovation Center said, "The first idea for a common wind tunnel facility came in Spring of 2012 and we took a few years of preparation to find the right partners, Voxdale is one of them. We started with the construction of the infrastructure in April 2015

and were happy to celebrate the inauguration in April 2016. The wind tunnel is unique, because we have a very exact measurement system. This is unique for cyclist and also for ski and alpine sports applications to determine the exact gain in cm or seconds with the optimized aerodynamics"

Koen Beyers, CEO of Voxdale said, "One of the main challenges we have in our work is the validation of our results and that is the reason why we participated in the Flanders'



Figure 1. Test Section

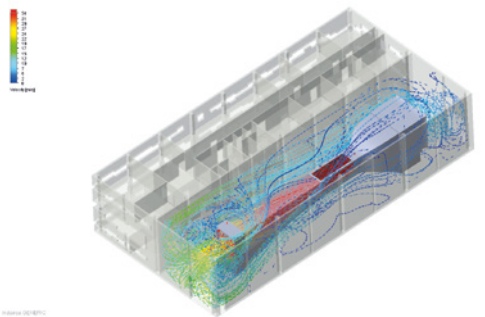
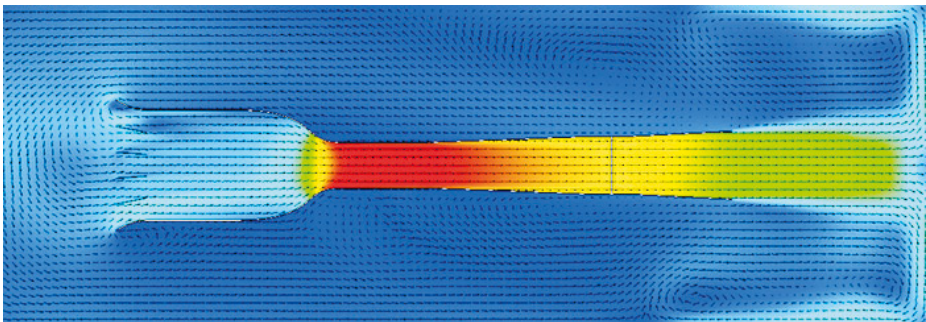


Figure 2 a+b. Wind tunnel simulation set up inside the building

Bike Valley Wind Tunnel project". Additional founding companies include BioRacer, Flanders Make, Lazer Helmets and Ridley with the support of Agentschap Ondernemen, Province Limburg and the European Regional Development Fund.

Voxdale built a very early mockup of the Flanders' Bike Valley Wind Tunnel and building. Many aspects have to be considered during the conceptual phase, for example, the type and size of wind tunnel, performance, velocity and naturally the budget. Voxdale was involved from the beginning in the conceptual design of the wind tunnel as well as in the aerodynamics. Mentor Graphics' FloEFD 3D Simulation Tool was used in the very early design phase. The contraction section, the test section and the diffuser section were modeled, simulated and designed directly in PTC Creo embedded FloEFD. Furthermore the entire hall around the wind tunnel was simulated because it is an open return wind tunnel.

One of the main challenges was the positioning of the wind tunnel inside the brand new building. The flow back from the fans to the contraction section was simulated and visualized. At the same time the laminar flow in the test section and the wind tunnel design were simulated.

Patrick Vlieger, Engineer at Voxdale commented, "At first we did a concept design of the Flanders' Bike Valley wind tunnel. We simulated inside the building to analyze the backflow inside the building and then we could also see the laminar flow in the test section. So we positioned the wind tunnel a little bit higher, a little bit more to the back or to the front of the building. We checked how this influences the laminar flow inside the test section and inside the building itself".

The height and the distances to the walls were optimized taking into consideration the effect on the flow conditions inside the wind tunnel. Hence, the FloEFD simulations ensured a good detailed engineering of the wind tunnel as well as a reliable and efficient design of the hall because an overdesign would lead to unnecessary expenses for the building.

The next stage is to create a digital replica of the test section in FloEFD to prepare the tests virtually. "With that we will be able to facilitate the preparation of the wind tunnel use. We can decide how many runs and which configuration we will do", says Koen Beyers. The correlated results can then be used also for further development in FloEFD. By doing this the time spent in the wind tunnel can be reduced noticeably.

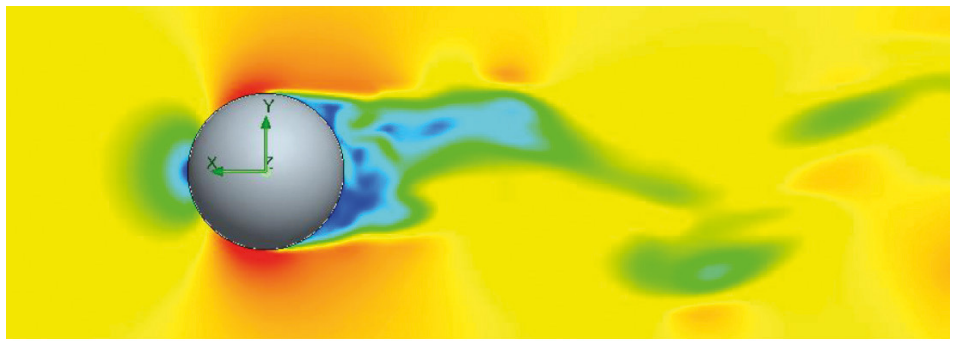


Figure 3. Sphere calibration picture and corresponding FloEFD simulation



Figure 4. The "Aerobar"

Besides all the strictly technically focused solutions the engineers elaborated an additional idea, they found a way to install a bar below the wind tunnel contraction section, which is called the "Aerobar".

Koen Beyers sums up, "You have to imagine, this is a multi-million Euro project. You have to come up with the design and then you have to step-by-step really build it. And that might be a risk, imagine that it does not perform as expected or it does not work very well. That's why we stepped in with FloEFD. That gave us enough confidence to validate the design of the tunnel itself and to have the correct

dimensions of the hall. We are really proud of this project and it's almost unbelievable what we have materialized in this short period of time to end up with this F1-like facility".

References

<https://issuu.com/mtss5/docs/201604fbv>
<http://www.flandersbikevalley.be/windtunnel/>
<https://www.grc.nasa.gov/www/k-12/airplane/tuncret.html>
<https://www.grc.nasa.gov/www/k-12/airplane/tunor>
<http://bit.ly/2dtwazF>

Cleared for Landing

Numerical Methods for the Definition of the Hinge Moments of the Nose Landing Gear Doors of the Commercial Aircraft

By O.V. Pavlenko, TsAGI, A.V. Makhankov, A.V. Chuban, Irkut Corporation

To investigate the impact of the fluid flow on the aircraft's units CFD (Computational Fluid Dynamics) methods based on the numerical calculation of the hydrodynamic equations becomes widely used along with the conventional analytical approaches and experimental tests. Continuously developed and improved CFD methods can serve as a good alternative of the natural experiments in solving many practical problems [1].

Thus, at the design stage of the landing gear doors production often without being able to carry out the natural experiment, designers need to have level of aerodynamic loads acting on the

closed doors at high speed of aircraft as well as during aircraft's maneuvers with the opened doors and gear release/retraction. The aerodynamic loads data obtained from CFD analysis gives the possibility to estimate the doors strength and define characteristics of the opening actuator, run the optimization of the kinematic connection between small rear doors with the landing gear strut. For instance, for the considered aircraft the initial variant of the small landing gear door rod mounting to the landing gear main fitting has been replaced



by the mounting to the landing gear strut to reduce the loads on the rod. The calculation results obtained for the selected variant of the doors were confirmed experimentally that indicates good accuracy of the modern software.

The results of the numerical study of aerodynamic loads on the nose landing gear doors demonstrated in this paper were obtained in ANSYS® Fluent and Mentor Graphics FloEFD™ software, based on the solution of the Reynolds averaged and Favre averaged Navier-Stokes equations accordingly.

The calculation in ANSYS Fluent software (license number 501024) was done using the structured computational mesh (about 6 million cells) with « $\kappa - \epsilon$ realizable » turbulence model ($\kappa - \epsilon$ method based on a simultaneous solution of the momentum transport equations, the kinetic energy and the dissipation rate equations) with the enhanced modeling of turbulence parameters near the wall and with taking into account the influence of the pressure gradient. The solved equations were approximated with a finite-volume scheme of the second order.

The numerical study in FloEFD software was performed using rectangular computational mesh adapted to the surface (about 2.5 million cells) [3]. To speed up the calculations the local meshes with the increased mesh resolution around the nose of the fuselage and landing gear doors

were used. The automatically adapting computational mesh with concentration in the areas of high gradients of velocity was applied. It should be noted that FloEFD uses a relatively small number of cells of the computational mesh as far as in case of a low resolution of the boundary layer the theory based on the Prandtl boundary layer

hypothesis is applied. Turbulence model used in FloEFD bases on the modified model with damping functions proposed by Lam and Bremhorstom [4].

The calculations of the hinge moments of the nose landing gear doors were performed for the three-dimensional model of the part

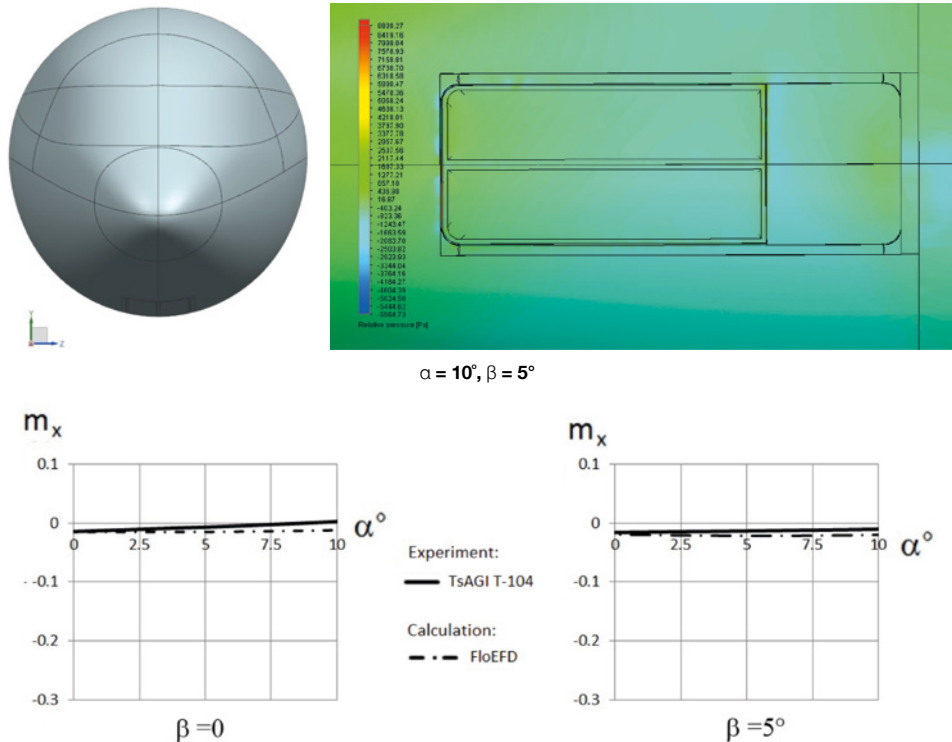


Figure 1. The model with the closed landing gear doors and hinge moments of the large left nose landing gear doors at $\delta_{door1} = 0^\circ$, $\delta_{door2} = 0^\circ$, $\delta_{strut} = 0^\circ$, $\beta = 0^\circ$ and $\beta = 5^\circ$.

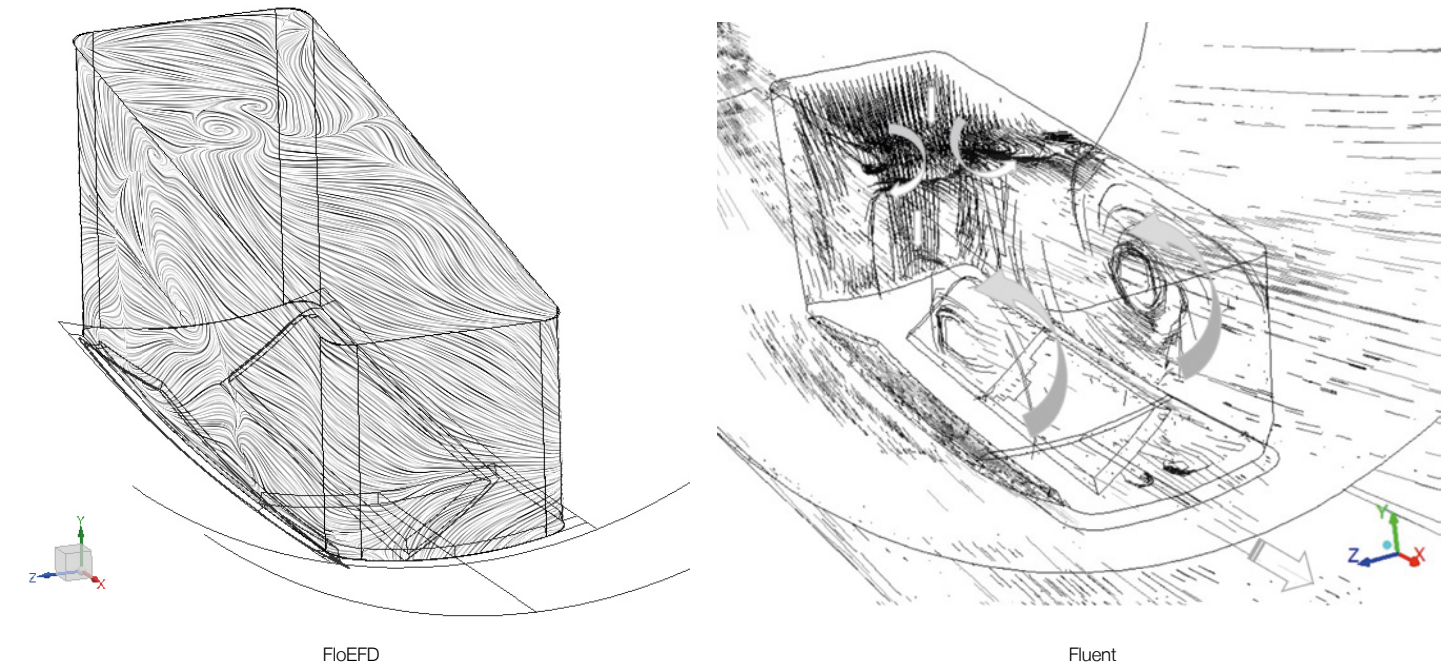


Figure 2. Streamlines on the doors and in the niche at $\delta_{door1} = 30^\circ$, $\delta_{door2} = 0^\circ$.



of the commercial aircraft in the scale of 1:1 which includes the fuselage, large front and small rear nose landing gear doors as well as the nose gear and the wheel well. The calculation results were obtained for the stage of release – retraction of the landing gear at Mach number $M = 0.34$ and impact air pressure $q = 771 \text{ kg/m}^2$. Experimental data was obtained by Andreev G.T. in the TsAGI wind tunnel T-104 for the full aircraft model in the scale of 1:8.16 at Mach number $M = 0.2$. All of the graphs below are related to the left landing gear doors, hinge moments of the right (windward) landing gear doors are less usually.

1. Flow around the large nose landing gear doors at their opening

The calculations and the experimental investigations have shown that in the closed position ($\delta_{\text{door1}} = 0^\circ$, $\delta_{\text{door2}} = 0^\circ$, $\delta_{\text{strut}} = 0^\circ$) hinge moments of the nose landing gear doors are minimal (Figure 1).

This fact is due to the presence of gaps along the doors which balance the static pressure on the outer surfaces of them near their edges and in the landing gear niche. A calculation of the loads without taking into account these gaps leads to an overestimation of normal forces acting on the detachment of the doors because nose gear of the considered aircraft are located in the flow acceleration zone from the nose of the fuselage to the regular part. Since at the sideslip angle of 5° nature of the flow around the fuselage nose does not change much the hinge moments of the closed doors are practically independent on the sideslip angle within a specified range.

During opening of the large doors ($\delta_{\text{door1}} = 30^\circ$, $\delta_{\text{door2}} = 30^\circ$, $\delta_{\text{strut}} = 0^\circ$ - experiment, $\delta_{\text{door1}} = 30^\circ$, $\delta_{\text{door2}} = 0^\circ$, $\delta_{\text{strut}} = 0^\circ$ - calculation) airflow circulation occurs in the niche of the landing gear (Figure 2), which leads to slow down the flow over the doors and increase the pressure on the inner surfaces of them.

As a result, the hinge moments of the opened doors are significantly higher than of the closed ones even in the absence of the sideslip angle, which is confirmed by the results of calculations as well as experiments (Figure 3). The right chart in figure 3 shows the influence of the sideslip angle on the loads. It is seen that even at the initial stage of opening of the doors the presence of sideslip angle of 5° leads to the drastic (up to 4 times) growth of the hinge moments.

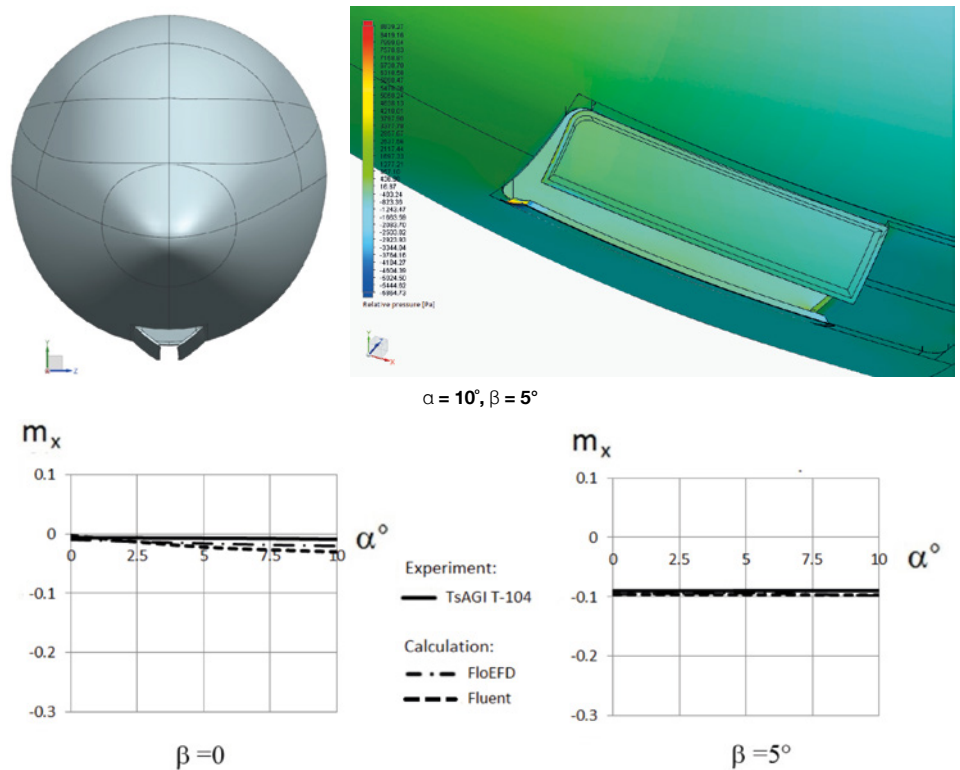


Figure 3. The model with the opened large landing gear doors and the hinge moments of the large nose landing gear doors at $\delta_{\text{door1}} = 30^\circ$, $\delta_{\text{door2}} = 30^\circ$, $\delta_{\text{strut}} = 0^\circ$ for the experiment, $\delta_{\text{door1}} = 30^\circ$, $\delta_{\text{door2}} = 0^\circ$, $\delta_{\text{strut}} = 0^\circ$ for the calculation, $\beta = 0^\circ$ and $\beta = 5^\circ$.

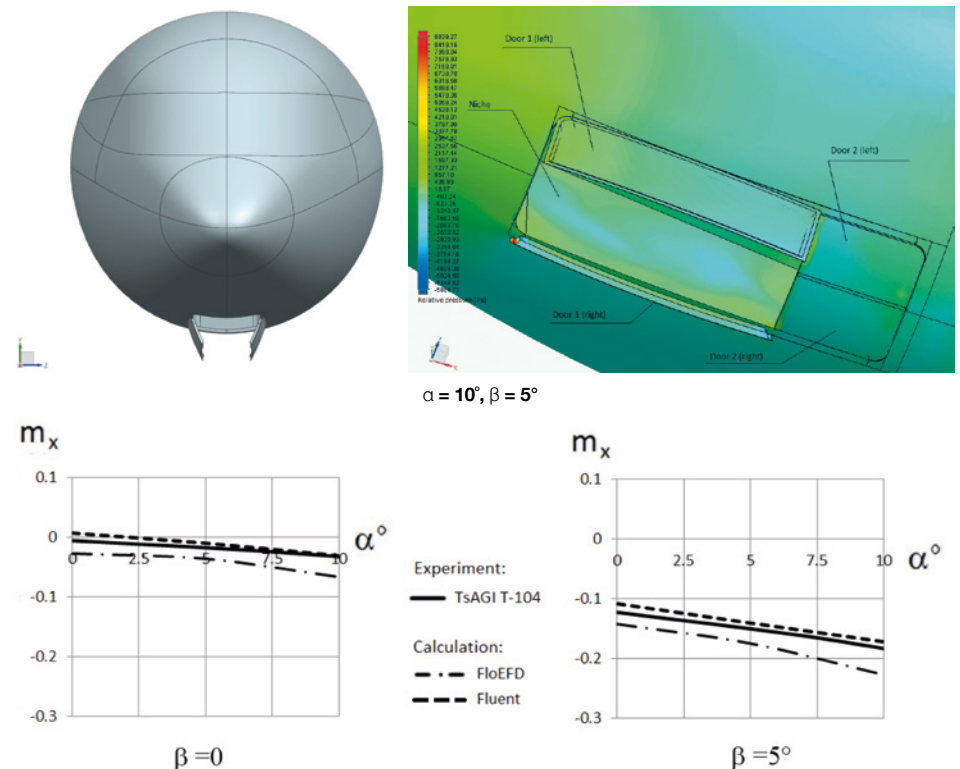


Figure 4. The model with opened large landing gear doors and the hinge moments of the large nose landing gear doors at $\delta_{\text{door1}} = 60^\circ$, $\delta_{\text{door2}} = 60^\circ$, $\delta_{\text{strut}} = 0^\circ$ for the experiment, $\delta_{\text{door1}} = 60^\circ$, $\delta_{\text{door2}} = 0^\circ$, $\delta_{\text{strut}} = 0^\circ$ for calculation, $\beta = 0^\circ$ and $\beta = 5^\circ$.

From the calculations and the experiments it was obtained that the greatest values of the hinge moments of the doors are observed in their open position in a range of angles $\delta_{door1} = 60^\circ \div 90^\circ$ (Figures 4 and 5).

Increasing of the sideslip angle up to 5° leads to increase values of the hinge moments approximately in four times. It can be concluded about the constancy of the relative increase of the aerodynamic loads on the doors in the presence of the sideslip angle at all stages of their opening. This pattern can be observed on the charts of the hinge moment coefficients of the nose landing gear doors depending on the angle of their opening as shown on Figure 6. Presented dependencies relate to the angle of attack of 12° in the experiment and 10° in the calculations. The chart below for the sideslip angle of 5° shows nearly linear dependence of growth of hinge moments on the deflecting angle of the doors (with a slight dip in the region of $\delta = 60^\circ$ in FloEFD).

2. Flow around the small landing gear doors during the release of the nose landing gear

The computational models of the small rear doors at the release of nose landing gear are shown on figure 7.

The models are made in strict accordance with the kinematics of the connection between the strut and the small door. The hinge moment coefficients of the small door depending on its angle of deflection are shown on figure 8.

Since the left door considered in the article is in the "shadow" of the landing gear by having a kinematic connection with the strut at all stages of the opening, the dependence of the hinge moment on the opening angle of the door is not obvious. The increase of the sideslip angle up to 5° leads to increase of loads only in two times. There is no experimental data of wind tunnel tests for

the small doors considering simultaneous release of the landing gear strut.

Conclusions

Computational study of flow around the large and small nose landing gear doors of the commercial aircraft showed that the effect of increasing of the sideslip angle and the opening angle is the most noticeable

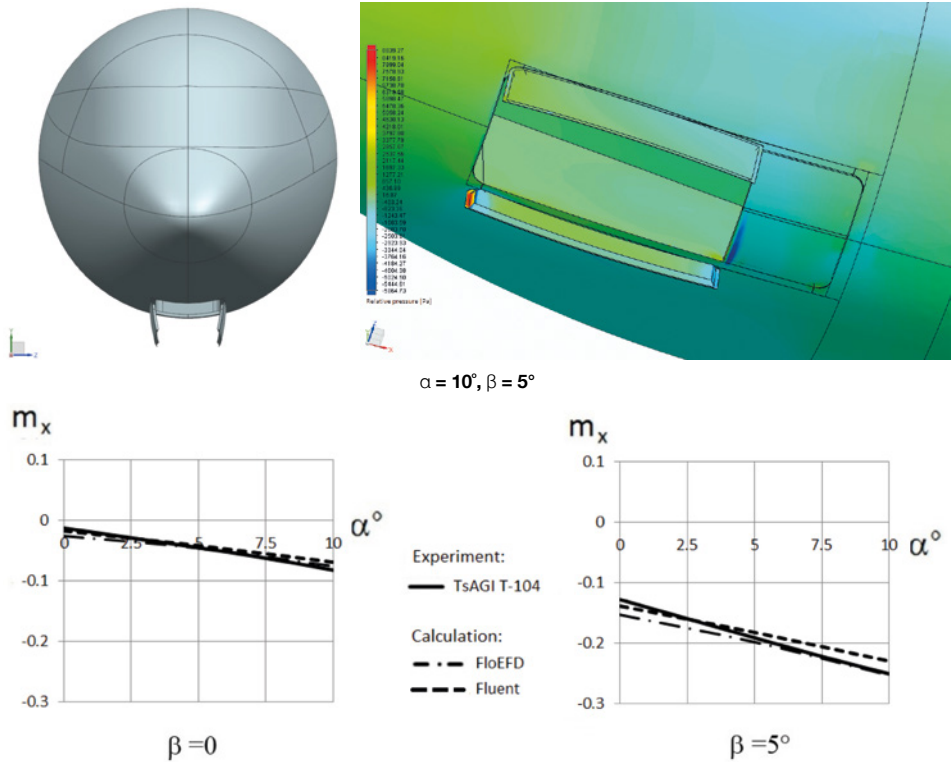


Figure 5. The model with opened large landing gear doors and the hinge moments of the large nose landing gear doors at $\delta_{door1} = 90^\circ$, $\delta_{door2} = 90^\circ$, $\delta_{strut} = 0^\circ$ for experiment, $\delta_{door1} = 74^\circ$, $\delta_{door2} = 0^\circ$, $\delta_{strut} = 0^\circ$ for calculation, $\beta = 0^\circ$ and $\beta = 5^\circ$.

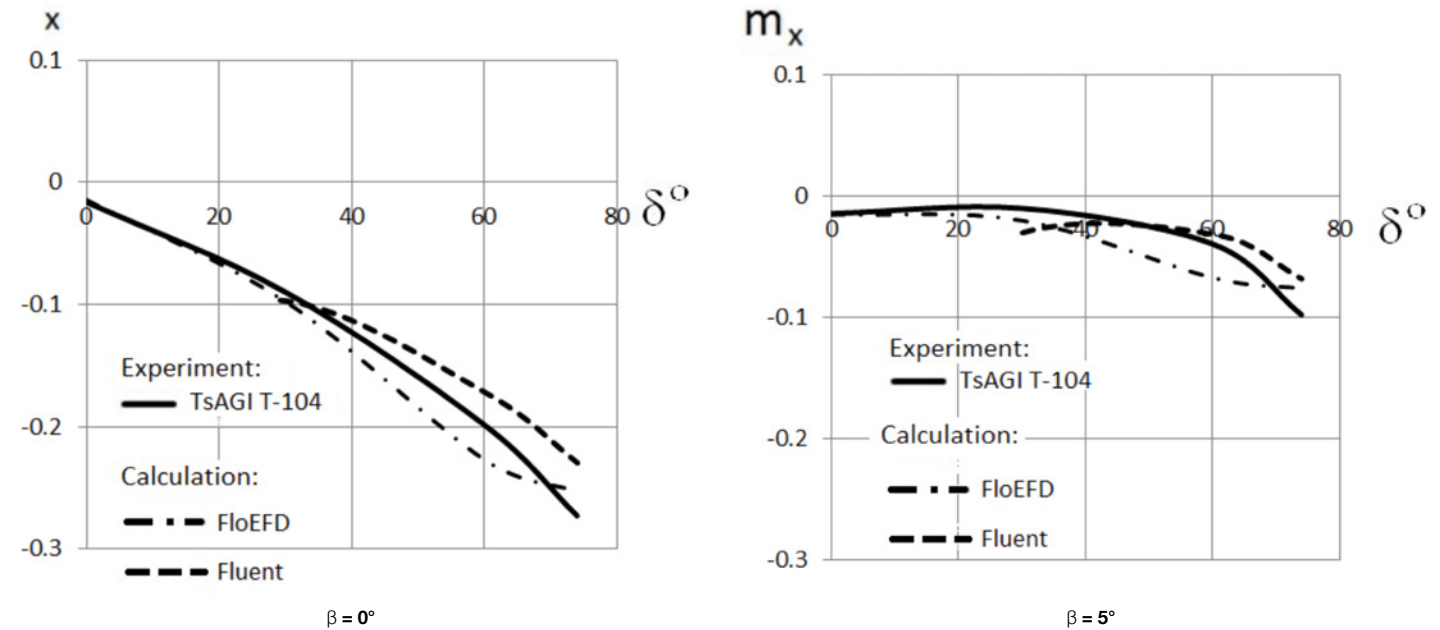
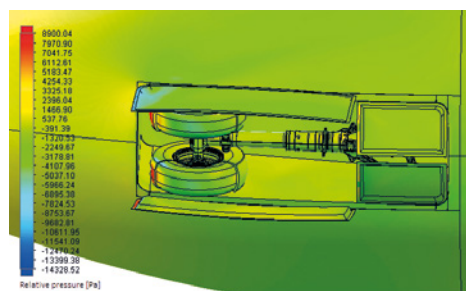
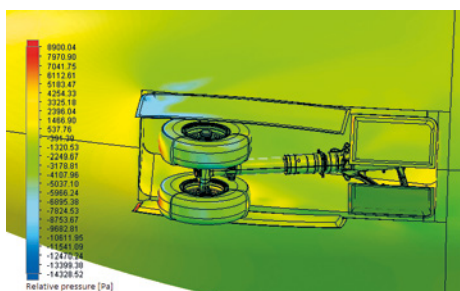


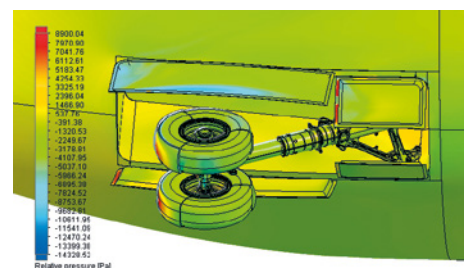
Figure 6. The hinge moment coefficients of large left nose landing gear doors depending on their deflecting angle.



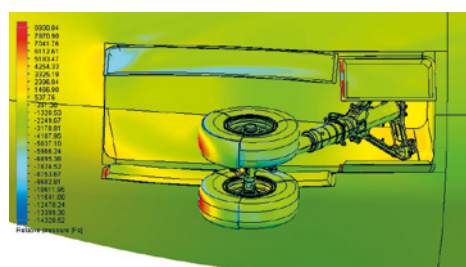
$$\delta_{\text{strut}} = 15^\circ, \delta_{\text{large door}} = 74^\circ, \\ \delta_{\text{small door}} = 14.304^\circ$$



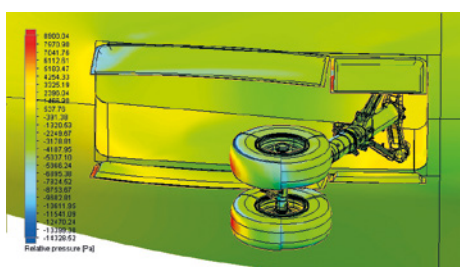
$$\delta_{\text{strut}} = 30^\circ, \delta_{\text{large door}} = 74^\circ, \\ \delta_{\text{small door}} = 27.846^\circ$$



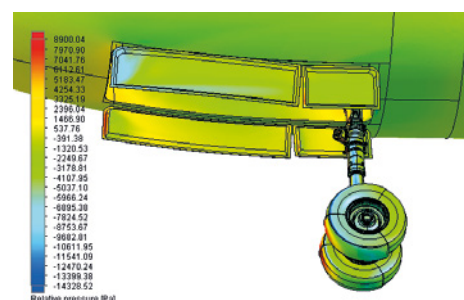
$$\delta_{\text{strut}} = 45^\circ, \delta_{\text{large door}} = 74^\circ, \\ \delta_{\text{small door}} = 41.498^\circ$$



$$\delta_{\text{strut}} = 60^\circ, \delta_{\text{large door}} = 74^\circ, \\ \delta_{\text{small door}} = 55.378^\circ$$

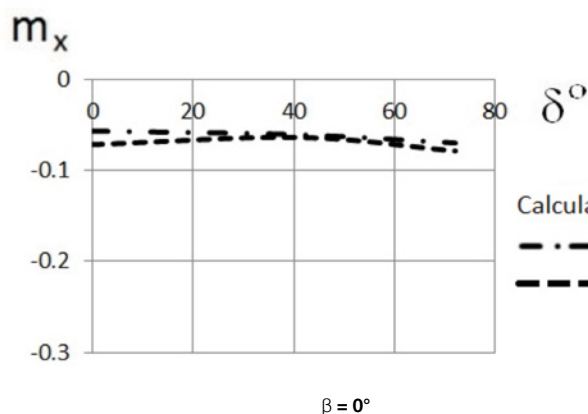


$$\delta_{\text{strut}} = 75^\circ, \delta_{\text{large door}} = 74^\circ, \\ \delta_{\text{small door}} = 68.125^\circ$$

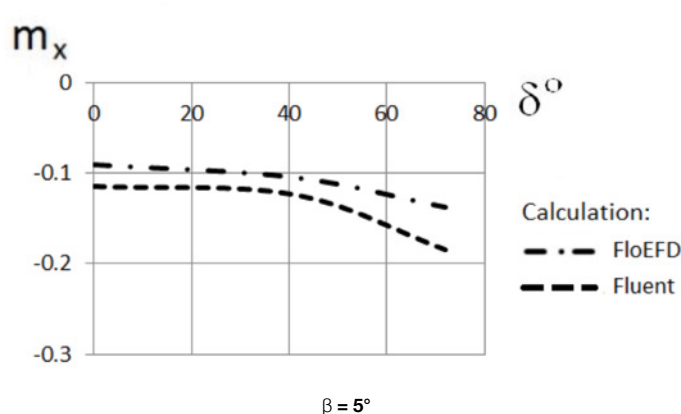


$$\delta_{\text{strut}} = 100^\circ, \delta_{\text{large door}} = 74^\circ, \\ \delta_{\text{small door}} = 72.232^\circ$$

Figure 7. The computational models with different angles of the strut, large and small doors.



$$\beta = 0^\circ$$



$$\beta = 5^\circ$$

Figure 8. The hinge moment coefficients of small left nose landing gear doors depending on their deflecting angle.

for the large doors with a big aerodynamic surface.

Loads acting on the small doors kinematically connected with the landing gear strut depend on the sideslip angle much less. The dependence of the loads on the small doors on their opening angle occurs only in the presence of sideslip angle.

The results of calculations performed in Fluent and FloEFD presented in this article show good agreement with the experimental data and demonstrate the ability to use these software for the calculation of the loads on the landing gear doors during the design stages.

The use of FloEFD software does not require thorough preparation of the computational model as far as this tool uses an automatic meshing and it is embedded in all modern CAD-software. On the contrary the use of Fluent software with structured mesh requires long preparation of the computational model but allows to perform a fast calculation.

References

- [1] Platonov D.V., Minakov A.V., Dekterev A.A., Kharlamov E.B., Comparative Analysis of CFD-packages SigmaFlow and Ansys Fluent on the solution of the laminar problems // Bulletin of the Tomsk State University, 2013, №1 (21)
- [2] Pavlenko O.V., Determination of loads on

the nose landing gear doors and strut of a commercial aircraft based on the numerical solution of the Navier-Stokes equations // TVF. 2011, Volume LXXXV, №2 (703), p. 19-25

[3] Dr. A. Sobachkin, Dr. G. Dumnov Numerical Basis of CAD-embedded CFD, NAFEMS World Congress 2013

[4] Lam, C.K.G. and Bremhorst, K.A. (1981) Modified Form of Model for Predicting Wall Turbulence, ASME Journal of Fluids Engineering, Vol.103, pp. 456-46

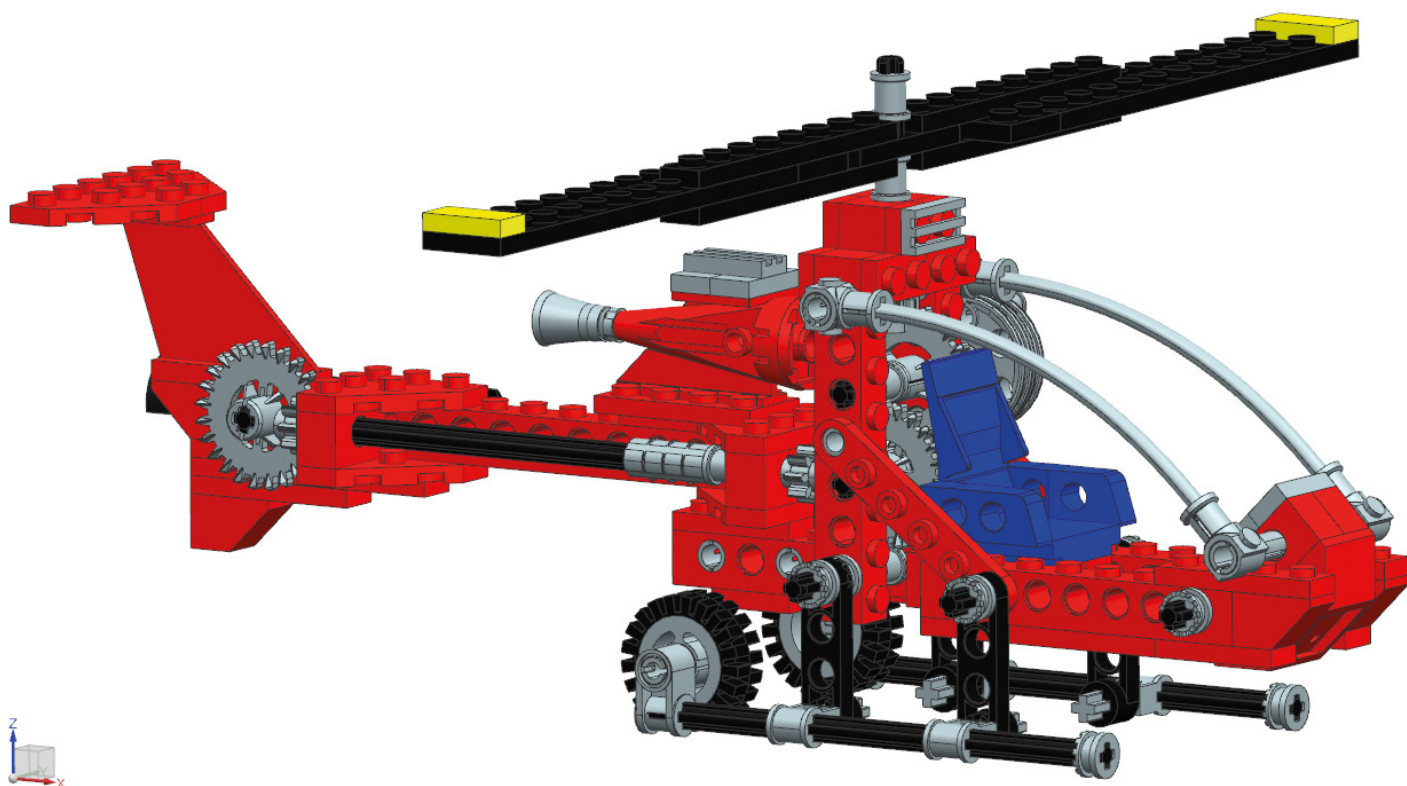


Figure 1. LEGO Technic Aero Hawk. The CAD model of the Aero Hawk was obtained from <http://www.GrabCAD.com>.

Ever wondered if a
LEGO Aero Hawk
Helicopter could
actually fly?

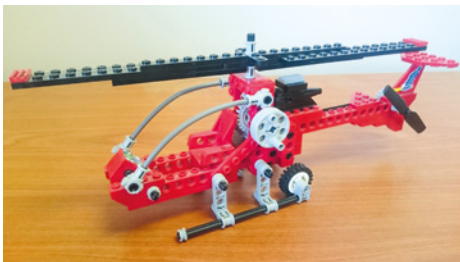
By Karl du Plessis,
Technical Specialist
Esteq



Remember that LEGO Aero Hawk from your seventh birthday? Remember how it did loops, flew upside down and even reached warp speed? In the imagination of a seven-year-old anything is possible. But being all grown-up, combined with harsh reality and a degree in engineering, you know that anything is indeed possible, but sadly everything isn't. So you set out to apply your engineering knowledge to determine if there is even the slightest possibility of a LEGO Aero Hawk managing some form of flight. You dive into your vast engineering toolbox and pull out your traditional Computational Fluid Dynamics (CFD) tool.

At first glance, the geometry is quite complex. The LEGO parts being modeled in meticulous detail, which the designer in you can definitely appreciate, but knowing what you know about CFD simulation, immediately

you start to think "How on earth am I going to build the mesh for this model?" You consider doing some serious CAD clean-up to reduce the complexity but consequently realise that you would lose too much of the authenticity of the LEGO model when simplifying the geometry down to the level typically required to perform CFD simulations. You are faced with a conundrum. It is time to revive and even stretch a little further that imagination that is long lost due to the doctrine of what is and what isn't possible in the world of CFD... Imagine a world in which one can open up a



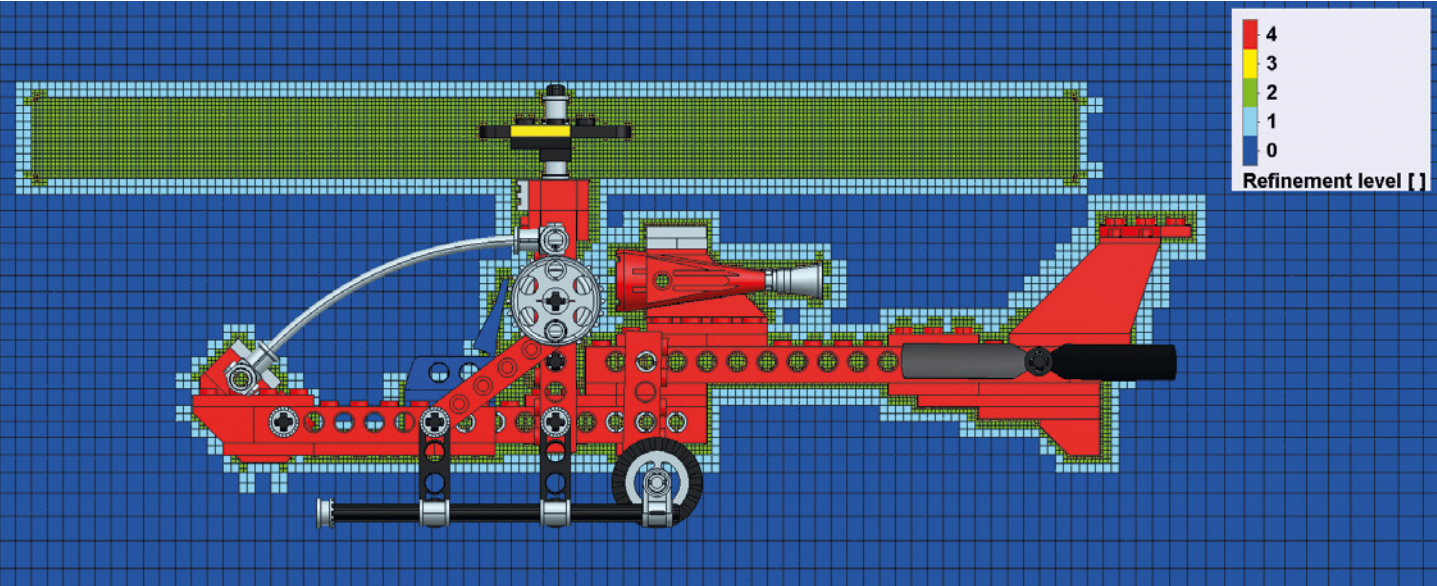


Figure 2. FloEFD Immersed Boundary Cartesian Mesh Cut-plot showing Level of Refinement

CAD model, specify the mesh settings, apply boundary conditions and start solving within a matter of minutes. Sounds like a bit of a stretch of the imagination, doesn't it? Enter FloEFD™!

FloEFD as integrated in Siemens NX was selected to analyse the LEGO Aero Hawk helicopter, making use of the new Sliding Mesh technology in FloEFD to simulate the rotation of the main rotor. This serves as a good test to see how FloEFD would handle the rotation of more complex geometry. You load the model into NX as-is, with only an additional rotating region part (simple cylindrical component) modeled to represent the rotation region that encapsulates the main rotor. You apply a rotor speed of 300rpm. You set the computational domain size and make use of a relatively coarse base mesh as a start with local mesh refinements to control the level of mesh resolution in the rotating region and on the helicopter. You are satisfied with the resulting mesh resolution as in the image below, with approximately one million cells being generated. You are completely amazed at the fact that FloEFD had no trouble creating the mesh even with all of the small geometric features and unnecessary narrow channels between the stacked LEGO blocks. This is obviously wasteful and one would spend some time cleaning up the CAD model in this regard. Nonetheless, you are curious as to how FloEFD will cope with this and proceed, leaving the model as-is in order to test the solver stability. When you are ready to solve you notice that you have access to all of

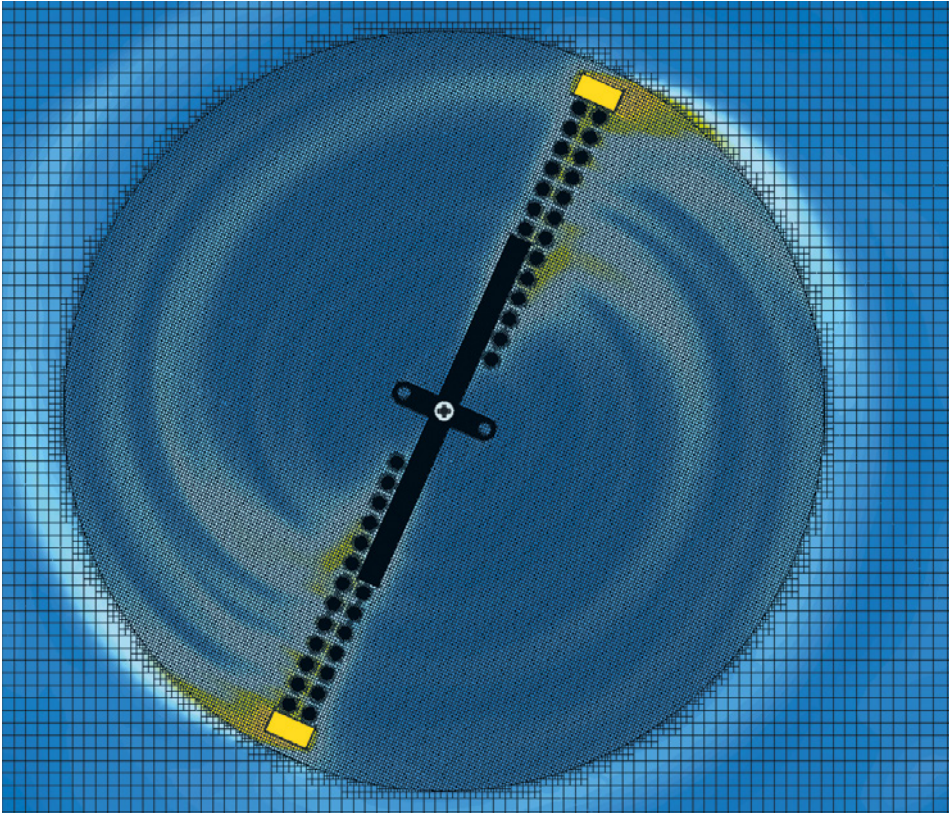


Figure 3. FloEFD Sliding Mesh Rotation

your CPU cores. You select all 16 cores to your availability (or four if you don't have that luxury) and press the "Solve" button and leave the simulation to run overnight. The sliding rotation option requires a transient analysis to be conducted and of course you do have to sleep at some point...

Come morning, the simulation has finished

solving without error or divergence. Again you find yourself quite impressed. You play around with the animations post-processing feature and record videos of the velocity field in the plane of the propeller rotation as shown in figure 3, shows the rotation of the mesh within the rotating region just moments after the initial start-

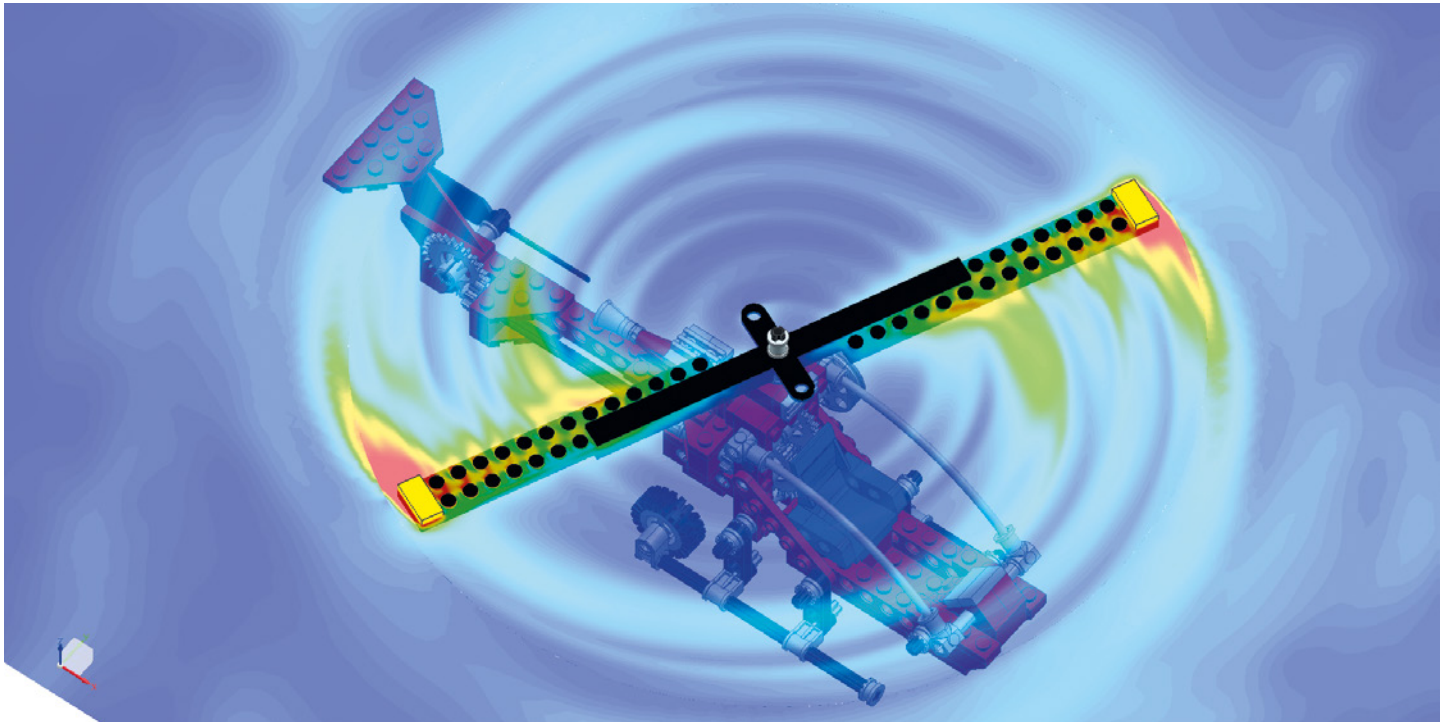


Figure 4. Velocity contour plot with rotor blade rotation

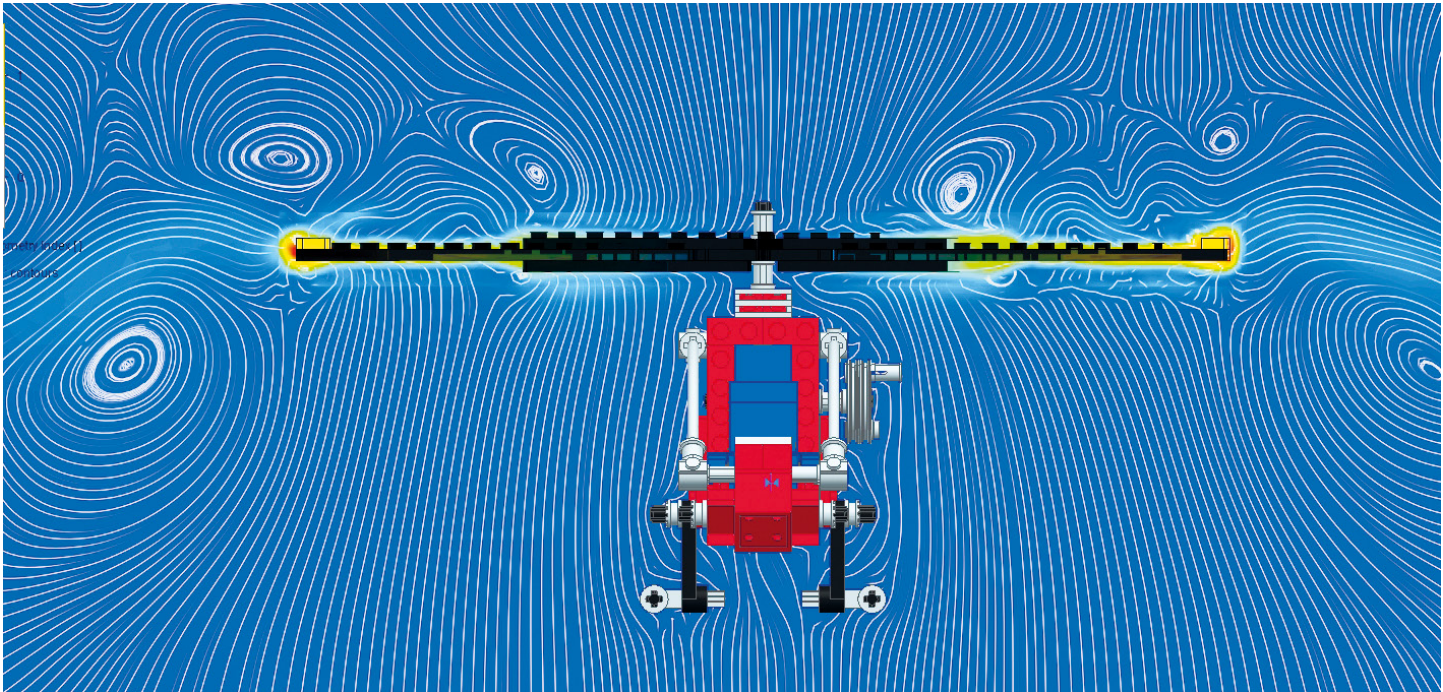


Figure 4. Velocity contour plot with rotor blade rotation

up. Figure 4 shows the velocity field as developed after a few rotations. You make cut-plots of the velocity over the propeller blades and you note in these images the development of the boundary layer at the propeller surfaces, one of the key technologies within FloEFD that make it possible to perform simulations with such complex geometry. There is still the question – Can this LEGO

Aero Hawk actually fly? You make a time-history plot of the propeller lift force. After close inspection you can see a definite positive offset in the average lift force, albeit fairly small, definitely not enough to lift the helicopter off the ground in the real world, but still a positive lift force nonetheless, enough to revive that youthful imagination that knows no bounds. You start to think like the seven-year-old you once were, thinking

“if I can develop a strong lightweight material, lighter than anything known to man...or if I can spin the propeller at 3,000,000 rpm, then this LEGO Aero Hawk from my childhood just might actually be able to fly”! Thanks to FloEFD this whole new world of CFD has been unlocked. A world not confined to simplified geometry or constrained by meshes and convergence issues. What seemed hard to imagine in the past has

become a reality, giving the engineer in you free reign to imagine more... (It goes without saying that the very low lift force is due to the fact that the LEGO propeller does not represent an airfoil very well)

FloEFD (Engineering Fluid Dynamics) is a highly sophisticated CFD tool aimed at Engineers. The main objective of FloEFD is to enable engineers to make design decisions as quickly and simply as possible, without having to ask the resident CFD specialist (if one should be so lucky to employ one of these very rare specimens) to perform the thermal-fluid analyses that traditionally required a lot of expertise and patience. FloEFD transcends almost all of the inherent obstacles of traditional CFD through innovative and ingenious technologies that truly stretch the imagination. Some of these technologies include,

- CAD Embedded
- Immersed Boundary Adaptive Cartesian Mesh
- Two-scale Modified Wall Functions
- Enhanced $k-\epsilon$ Turbulence Model.

These technologies are what make FloEFD the efficient and productive engineering tool that it is. Now hopefully the engineer in you is starting to imagine again a world of possibilities that seemed lost in translation and that it is easy to imagine a CFD tool that is easy to use, makes meshing a breeze, is highly tolerant of complex geometry and provides quick, stable, accurate and converged solutions. So in closing, if I may borrow the theme song from The LEGO Movie...

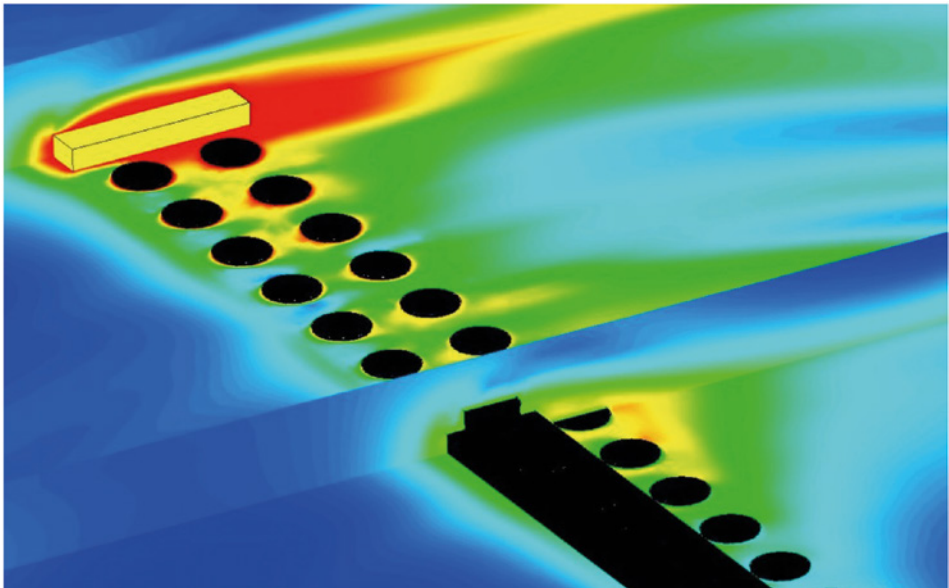


Figure 5. Velocity Cut-plots around rotor blade detail

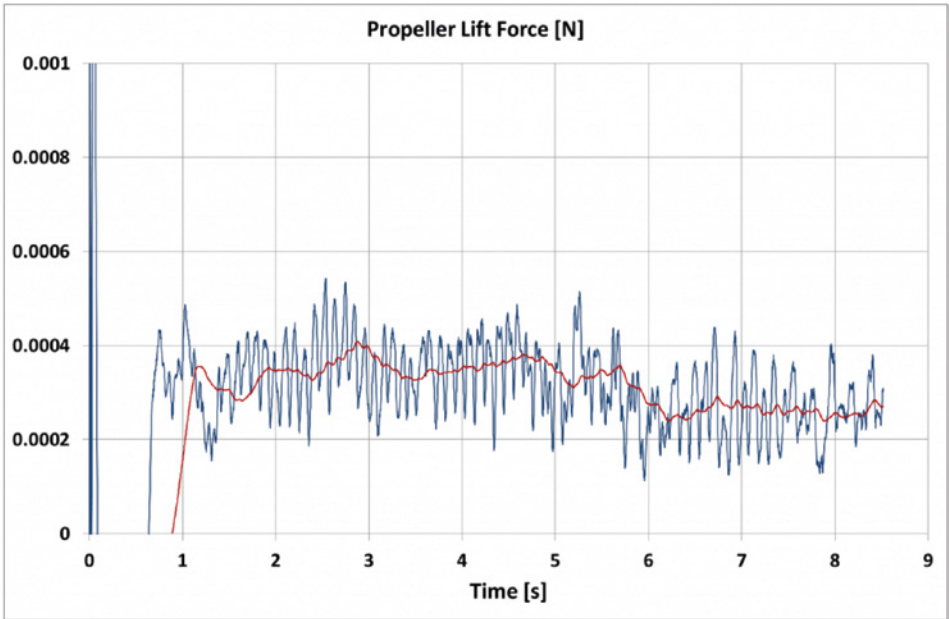




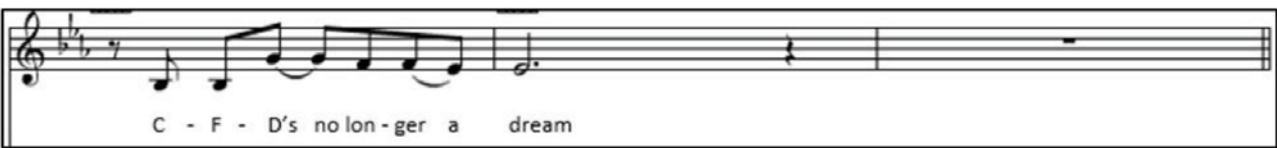
Figure 6. Time-history graph of rotor blade lift force



Flo - E - F - D's awe - some E - F - D's the



tool for your En - gi - neer - ing team Flo - E - F - D's awe - some



C - F - D's no lon - ger a dream

Aces High for Team Velarde

FloEFD® explores external aerodynamics for Team Velarde in the Red Bull Air Race World Championship

By Matt Milne, Application Engineer, Mentor Graphics

I don't know about you but I'm partial to a bit of Iron Maiden now and then. And if there's a more fitting, more intense, higher energy soundtrack than "Aces High" to accompany the Red Bull Air Races then I want to know about it! Established in 2003, the Red Bull Air Race World Championship sees pilots from around the world compete against the clock as they navigate their aircraft through a challenging obstacle course in a breathtaking combination of high-speed low-level flying.

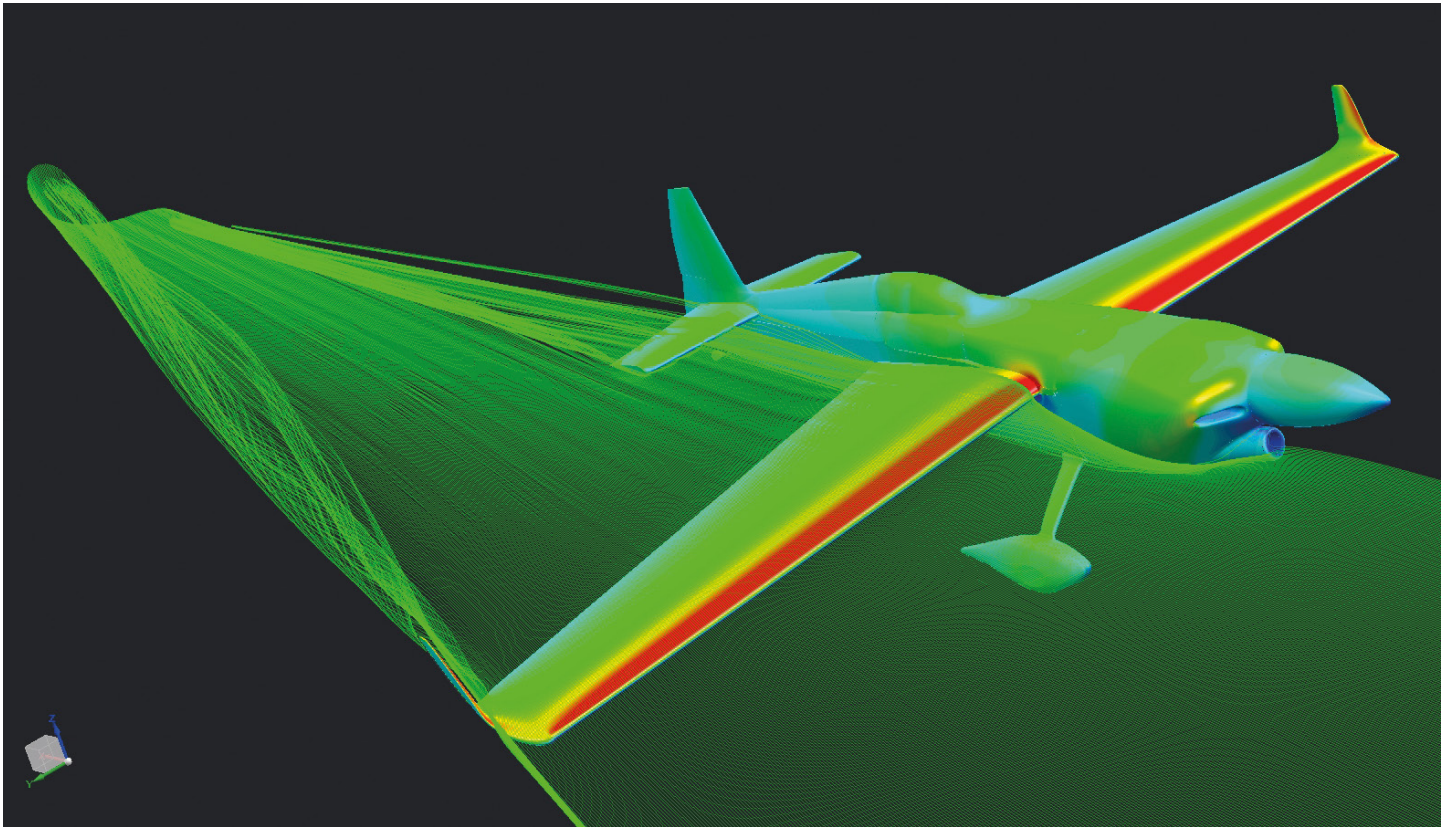
2017 sees Team Velarde begin their third year in the championship. Pilot Juan Velarde is looking to build upon his impressive 2016 record where he took the top spot in qualifying in one round and proved he could be

competitive against the other more experienced pilots.

It is often said in racing that to stand still is to go backwards. With this in mind, Team Velarde continued working hard through the off-season to make their goal a reality. "Regarding the race plane, we are







aiming to have a new set of winglets and a few other aerodynamic improvements ready by the second race of the season," explained Velarde. "We are working with a team of engineers to optimize the performance of the plane," he added.

Team Velarde approached Mentor Graphics for help investigating the aerodynamics of the race plane. Specifically they wanted to use CFD to investigate the performance benefits of the new winglets. Working with CAEsoft in Madrid, Team Velarde used 3D scanning technology to create a 3D CAD model of the aircraft which was then provided to Mentor Graphics for CFD analysis.

While modern 3D scanning techniques are without question impressive, it turns out that the technology does a rather better job than some might desire for CFD analysis. Close inspection of the CAD model revealed a number of excrescences and other lumps and bumps. For traditional CFD, such features might be the cause of considerable pain, requiring time and effort to modify the CAD geometry to a state where it is suitable for meshing. However, with FloEFD these features are simply not a problem.

During my time in aerospace research, a lot of effort was spent working on the CAD geometry to get it into a suitable state for meshing - the process was well developed

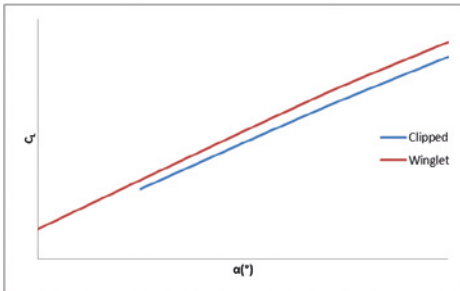


Figure 1. C_L vs. α (Full span model)

but it still had to be done manually. And then came meshing. For conceptual models with a relatively clean shape some degree of automation was possible, but for more complex models meshing had to be completed manually. I remember clearly some cases where meshing alone took more than a month.

This is all in stark contrast to the situation today with FloEFD. Put simply, the SmartCell™ meshing technology employed by FloEFD addresses meshing challenges with minimal user effort. Regardless of whether the geometry is a clean conceptual model, or dirty with lumps, bumps and excrescences, FloEFD can mesh it. With less time spent on geometry preparation and meshing, the user has more time to think about the results, what they mean and how to improve performance.

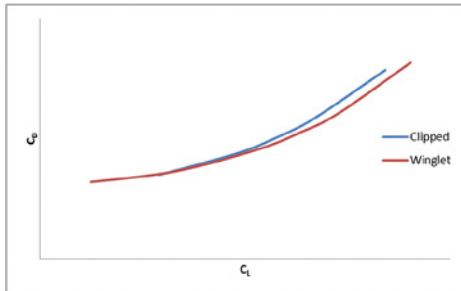


Figure 2. C_D vs. C_L (Full span model)

A new simulation was set up using the CAD geometry supplied by Team Velarde. The time taken to prepare the model, generate the mesh and begin the first flow calculation was less than one hour. Furthermore, our previous work on a wide range of well-known external aerodynamics test-cases meant we could follow a set of well documented best practices for this class of simulation and be confident of obtaining consistent and reliable results.

Initial calculations were run at low-medium angle of attack (AoA) at $M=0.25$, comparing the original clipped wing and revised "winglet" designs. These calculations were run using the complete aircraft span (i.e. port and starboard sides) but omitting the propeller blades. It was assumed that the propeller wash has only an incremental effect on the overall wing performance and



that since the wing leading edge is unswept any interaction between the propeller and wingtip flows is negligible. Each calculation used approximately 1.9 million cells and took around two hours to run using 12 cores (Intel Xeon E5-2643 v3).

It can be seen from Figure 1 that the "Winglet" design yields a slight increase in lift curve slope ($dC_L/d\alpha$). Figure 2 shows that there is also a reduction in drag. These predictions are expected from basic aerodynamic theory, since both designs effectively increase wing aspect ratio.

Further simulations were run to quantify performance of the "Winglet" design at medium-high AoA at $M=0.25$. It is noted that this area of the flight envelope (i.e. accurate prediction of onset and development of flow separation and associated effects) continues to be a challenge for all CFD methods today. While validation against well-established aerospace test-cases has shown FloEFD to perform acceptably in this regard, caution is nevertheless advised when interpreting computed predictions in this part of the flight envelope - the ability to obtain plausible looking solutions is no guarantee of accuracy.

To increase computational efficiency, only the starboard half of the aircraft was simulated. The effects of asymmetry in the model were assumed to be negligible and the propeller blades were again omitted. Appropriate revisions were made to the aircraft reference

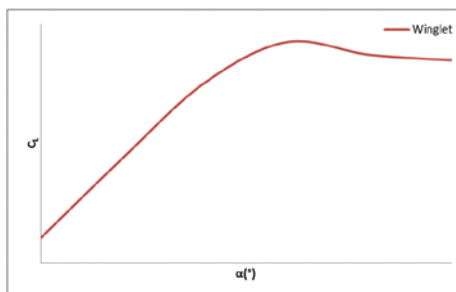


Figure 4. C_L vs. α (Half span model)

dimensions used to non-dimensionalize the integrated forces and moments. Each calculation used approximately 5.6 million cells and took around seven hours to run using 12 cores (Intel Xeon E5-2643 v3).

Predictions of integrated forces are shown in Figures 4 and 5. As expected the lift curve slope remains linear at low-medium AoA before becoming non-linear as flow separations develop. A thorough investigation of the predictions obtained using FloEFD is ongoing. This will give more insight into the development of the flow topology, and hence ways in which the "Winglet" design might be optimized to improve performance.

The improvement from the original clipped wing to the "Winglet" design is expected and indeed is predicted by basic aerodynamic theory. Performance of the "Winglet" design has been quantified for a wider range of AoA. Further improvement of the "Winglet" design may be possible through the use of

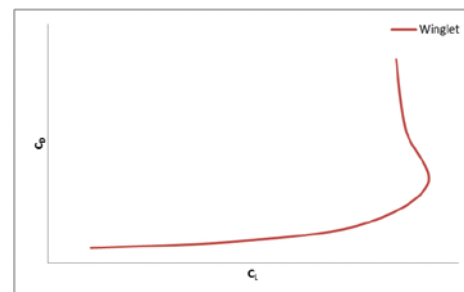


Figure 5. C_D vs. C_L (Half span model)

optimization and further work in this regard is recommended for the future. Based on these findings, the team are currently working on modifications to the race plane.

The first race of the 2017 Red Bull Air Race World Championship took place in Abu Dhabi on 10-11 February. After setting an impressive fifth fastest time in qualifying, Team Velarde took a sensational second place finish in the race, a best ever result for the team. The second race takes place in San Diego on 15-16 April. With luck, FloEFD will prove to be the ace in Team Velarde's hand and help them on their way to success in the 2017 Red Bull Air Race World Championship.

More information:

www.juanvelarde26.es
www.redbullairrace.com



E-Cooling: Cooling Power Electronics at Room Level

By Karim Segond, Consulting Engineer, E-Cooling GmbH and John Wilson, Technical Marketing Engineer, Mentor Graphics

The conversion of electrical power with power electronics has become a key technology that enables many of today's innovations for electric vehicles as well as electricity production. Though the applications vary greatly there are two features they have in common: the electric components generate a significant amount of heat, and are trusted to operate reliably. A key factor in the reliability of electronics is the operating temperature. To maintain the operating temperature within specifications with a high heat dissipation, a proper thermal design must be developed.

Challenges

The market of inverter solutions for photovoltaic is growing. The Middle East, Africa and India are expected to massively invest in photovoltaic. In these regions, an average summer's day temperature of 50°C is usual. The customers require reliable inverters integrated in enclosures or containers without air conditioning. As the cooling air takes away the electrical losses, its temperature usually exceeds the environment temperature. Dust or sand entering the electric enclosures must also be avoided. Therefore, filters are necessary, despite large pressure losses.

E-Cooling, an engineering consultancy firm based in Germany, has expertise in the thermal design of Power Electronics, Transformers and Chokes at the component level or at room level where the computational domain enhances a complete enclosure, container or room. At room level, it must be ensured that the cooling path provides adequate airflow to all critical components.

Solution

E-Cooling performs thermal and airflow design with FloEFD® from Mentor Graphics. One of their recent designs involved the overall cooling of a 2.2 MW frequency converter enclosure. Such a frequency converter could be used for a wind power station to provide the grid with the correct

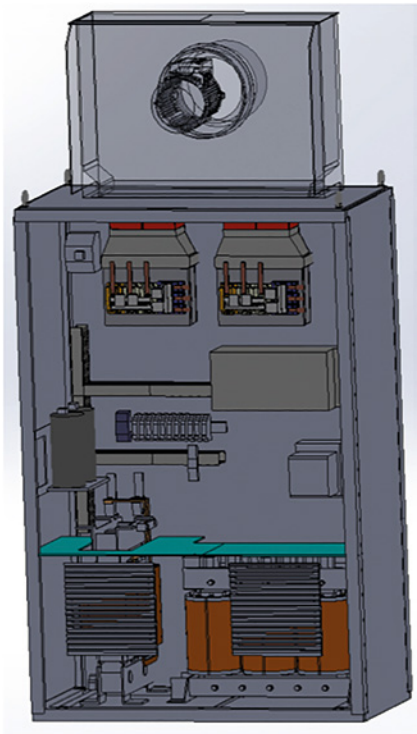


Figure 2. The enclosure with its electric components and fan

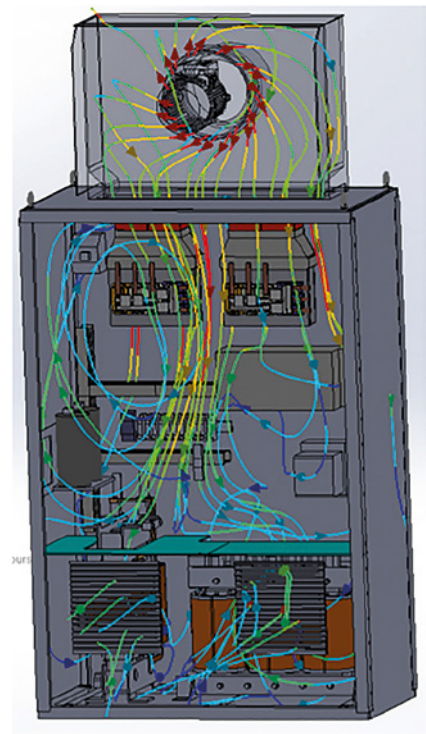


Figure 3. Streamlines starting from fan colored with the velocity

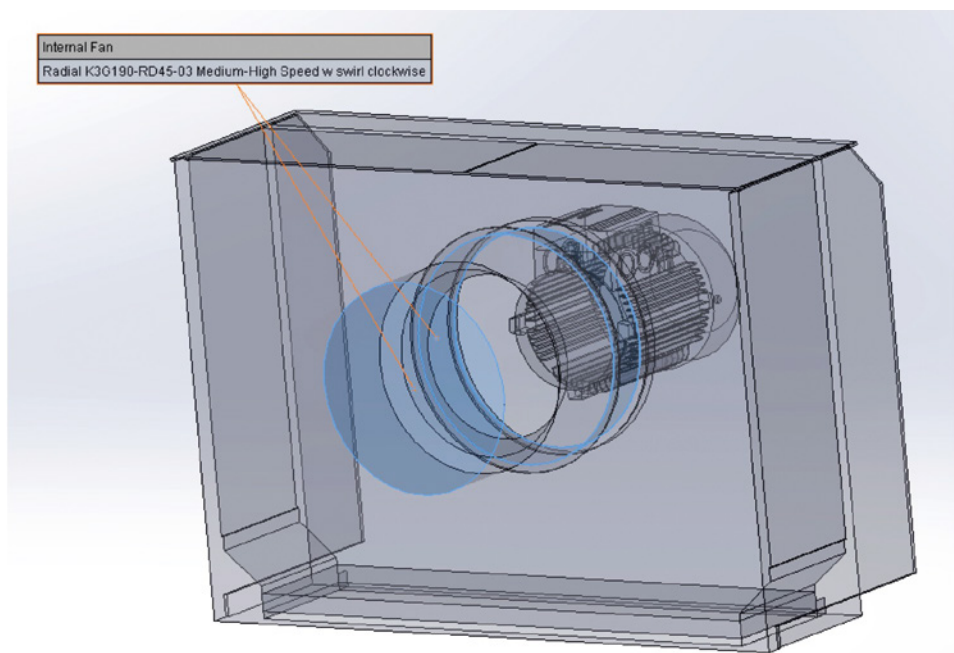


Figure 4. Frequency Converter Fans



frequency or for an electrical drive in order to control the rotation speed. This power is reached by two frequency converter boards, each has three IGBT power modules and two dedicated axial fans. Each board dissipates 1,350 Watts.

When integrating electronic systems into an enclosure, it is important to determine if there is enough airflow through all critical components. This requires the accurate representation of all the significant flow obstructions as well as the fans. Here each fan as well as the dust filter were modeled with characteristic performance curves (pressure vs. volume flow) provided by the manufacturers. With the analysis, E-Cooling is able to determine the flow distribution within the enclosure and make any design modifications to allow the necessary airflow for each component, including the use of alternative fans.

In the lower portion of the enclosure the model detail was not compromised. A detailed representation of the choke and auxiliary transformer was included as well as the flow diaphragm flow upwards and the exhaust grid flow downwards. A critical aspect of the design is to ensure that a large amount of the flow is going through the tiny passages between the windings. This can only be realized by obstructing the flow with a diaphragm or inner walls.

Benefits

Designing airflow and cooling solutions at the room level for power electronics is essential for providing reliable products to the market. During a development project the electrical requirements and losses usually change and components are likely to be replaced. With FloEFD embedded in the MCAD program, the automatic Cartesian meshing, and the possibility to start a calculation with an initial field, E-Cooling can update the thermal and flow model very quickly to meet project datelines.

“The most viable method of airflow design prior to testing is with CFD simulation based design software such as FloEFD. FloEFD allows E-Cooling to quickly build and assess the viability of an airflow and thermal design.” Karim Segond, Consulting Engineer, E-Cooling.

E-Cooling in Berlin is an engineering consultancy founded by Karim Segond. Their expertise lies in providing 3D thermal and flow analysis, enhancement and development supporting electronics, electric engines, and power electronics.

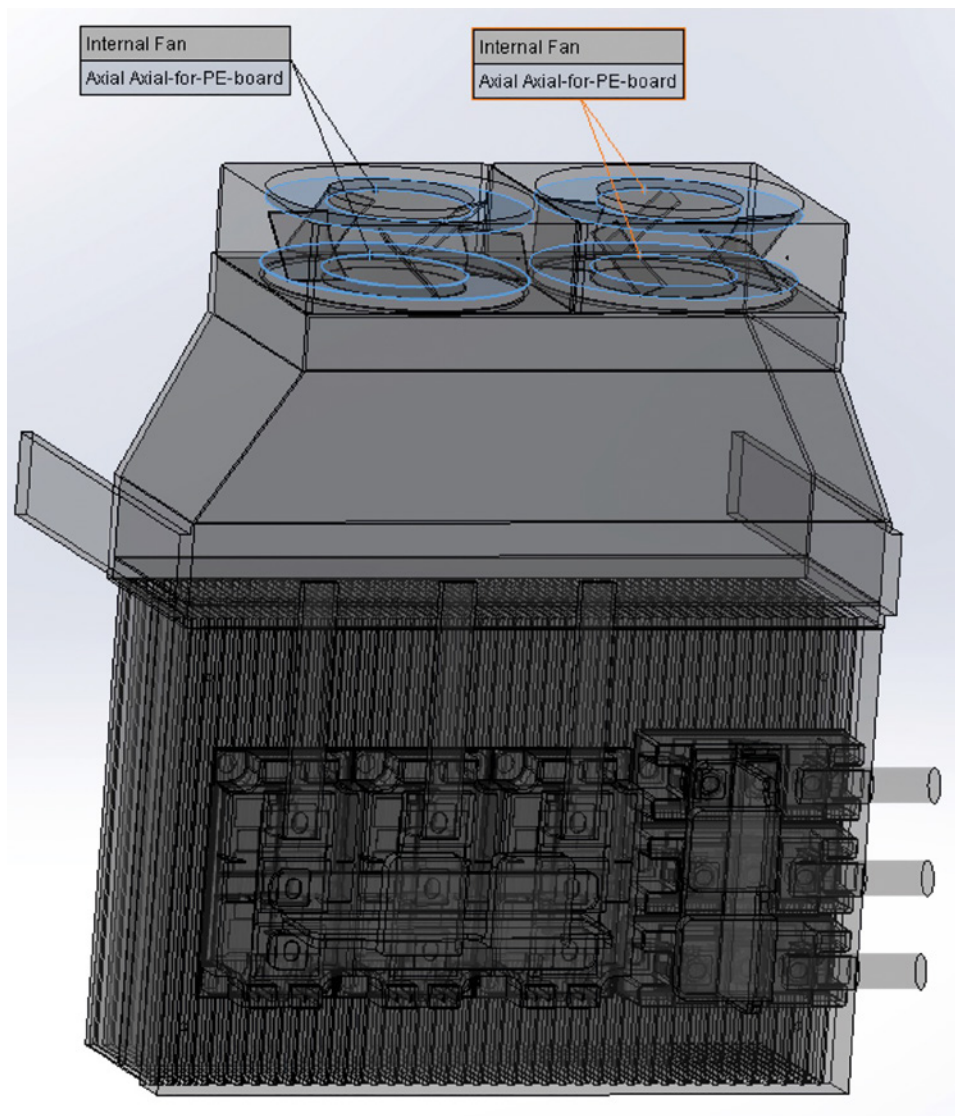


Figure 5. Enclosure Fan

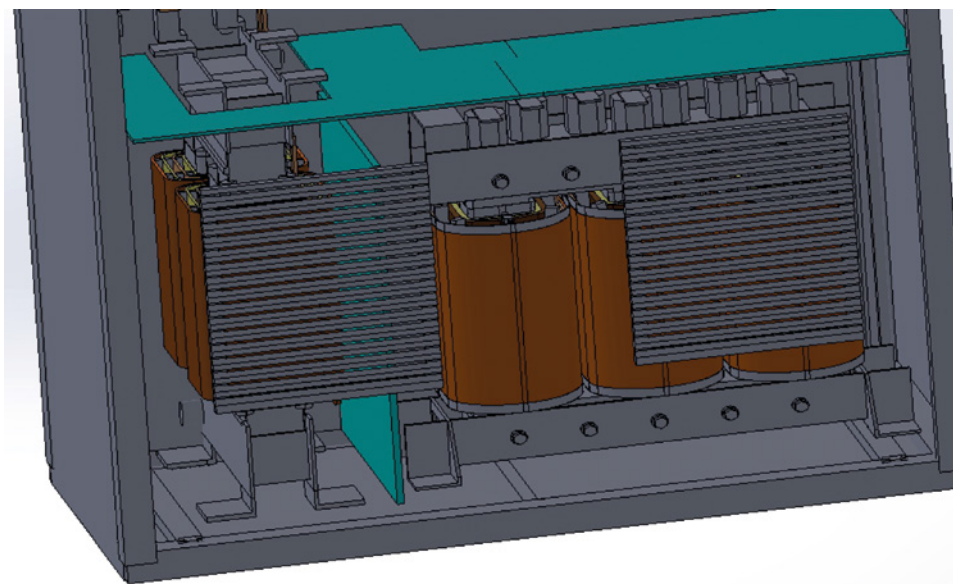
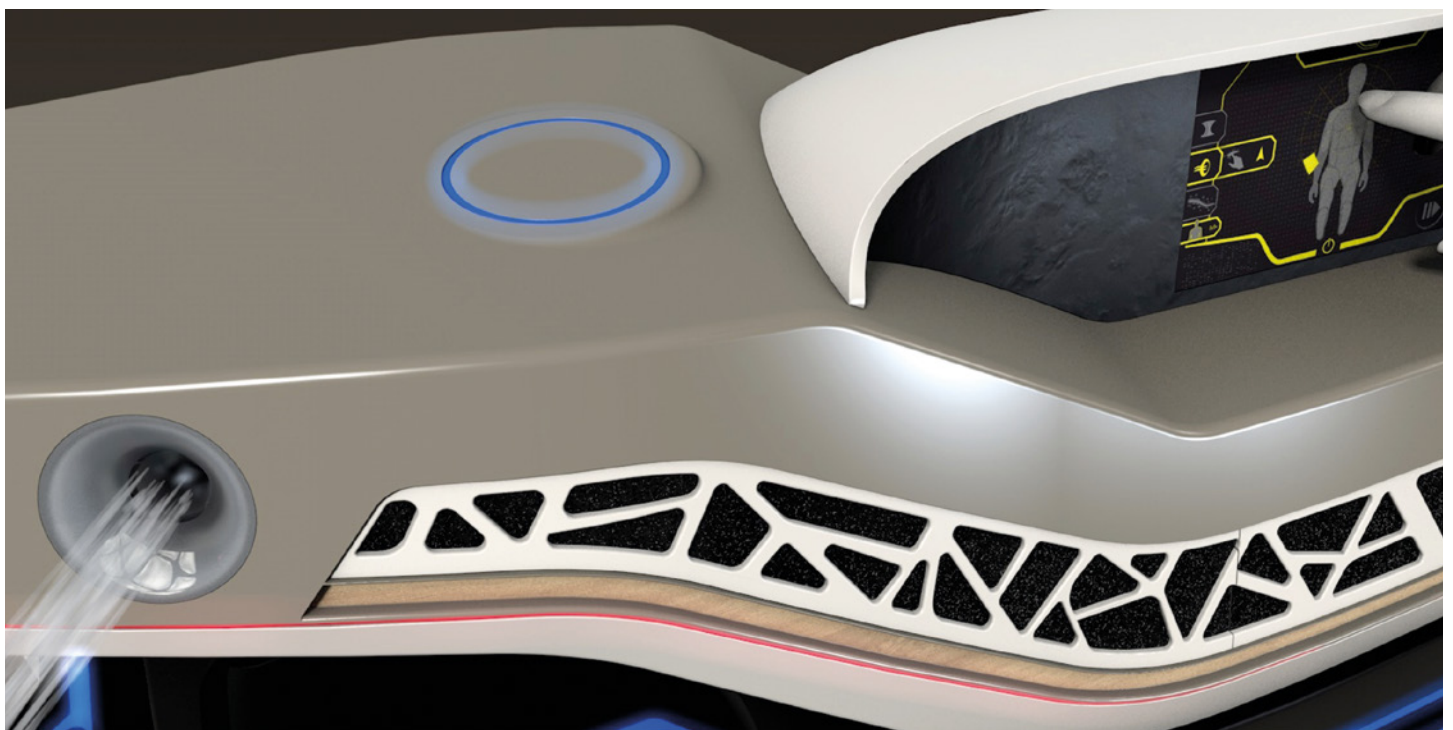


Figure 6. Lower portion of the enclosure

FloEFD helps Dr. Schneider's mission: To make the Car the Best Place in the World

By Enrico Lorenz, Research & Development, Dr. Schneider Unternehmensgruppe GmbH



Dr. Schneider, a successful family-run business, located in Kronach-Neuses in Germany, supplies and develops vehicle plastics components and systems for renowned automotive producers all over the world. The entire process chain is handled within the group, from research and design to prototype construction. (Figure 2) Dr. Schneider has more than 3,900 employees and 90 years of experience in the plastics field, 60 of which are in the automotive industry.

Dr. Schneider's primary products are visible parts for the car interior: air vents (figure 1), stowage boxes, kinematic components,

bezels, covers and trims, grills and window frames.

As the automotive market expands and grows, product development times are dramatically reduced. For many projects even the use of prototyping is no longer an option, making the need for reliable, fast and accurate simulation tools essential to overcome these challenges. Furthermore, frontloading the Computational Fluid Dynamics (CFD) simulation into the product development phase is crucial to the success at Dr. Schneider. Mentor Graphics' FloEFD tool is used mainly for the simulation of the air vents, one of Dr. Schneider's core products.





Figure 1. Extract of Dr. Schneider's products: air vents

"With FloEFD we can shorten product development time, quickly find appropriate design variants, save costs and explain and present the flow behavior of our products to our colleagues and customers."

Enrico Lorenz, Research & Development, Dr. Schneider Unternehmensgruppe GmbH

As FloEFD can be directly embedded into Catia V5, CAD models were used directly in the program with no need for additional geometrical preparations. Airflow distribution is investigated at a very early stage and must adhere to strict customer targets and specifications. For the example shown in figure 4, the influence of a bezel was investigated. The two variants of this broadband vent, with and without bezel, were simulated. The broadband vent variant including the bezel shows a better distribution of the airflow. The flow angle into the lower area is enlarged. Additional experiments in the lab using fog to visualize the air flow confirmed the FloEFD predictions. (Figure 5)

Enrico Lorenz, Simulation Engineer, explains: "We make up to 100 FloEFD simulations per month per license. We need fast, robust and accurate simulation results. In addition we need an efficient way to create the result reports and presentations". In combination with the batch run functionality which allows automatically runs of many variations, the pictures for comparing the defined

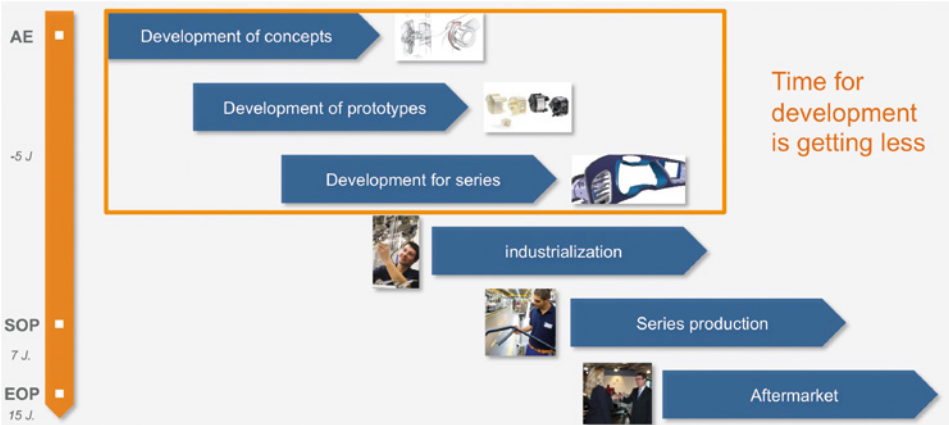


Figure 2. Today's product development process



Figure 3. Driver, broadband and rear vent

"FloEFD predicts what we need, so it helps us to make the car the best place in the world."

Enrico Lorenz, Research & Development, Dr. Schneider Unternehmensgruppe GmbH

results items are created automatically. The influence of design changes on the fluid flow behavior can immediately be identified. (Figure 6)

One of the major tasks is creating MS PowerPoint presentations for internal purposes and for customer presentations. This might take more time than the simulation itself. For this reason, a VBA code is generated by the Dr. Schneider engineers which automates this work in MS PowerPoint.

With FloEFD embedded in Catia V5, Dr. Schneiders' engineers are able to meet today's requirements of short development times and fulfill the strict targets of automotive manufacturers.



Figure 4. Broadband vent and airflow

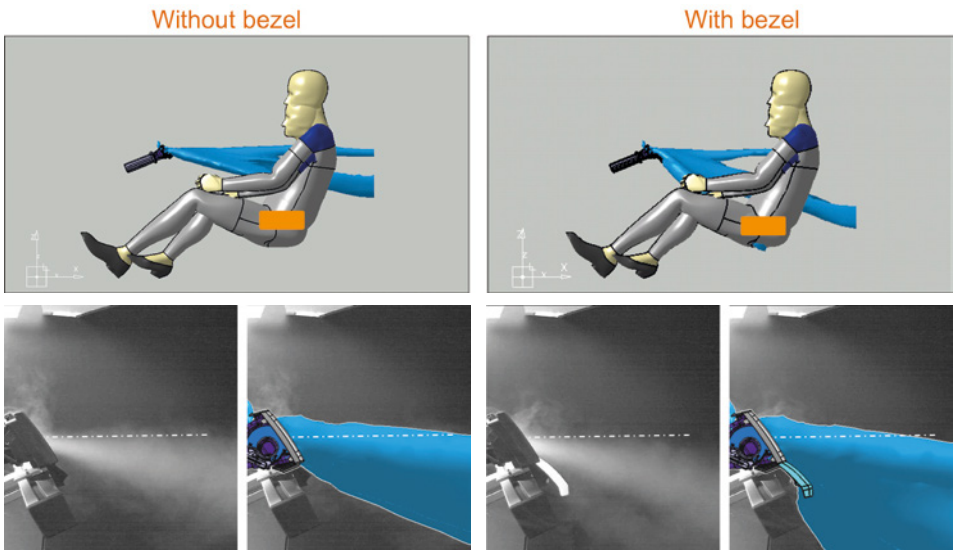


Figure 5. Comparison of the broadband vent without and with bezel

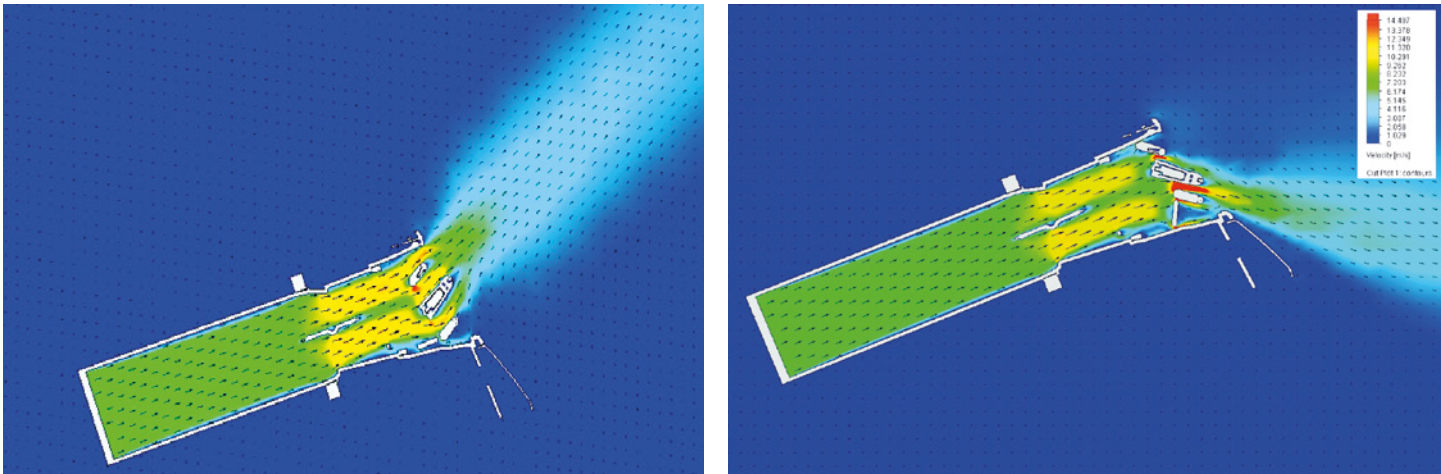


Figure 6. Cut plots showing the velocity for different variations

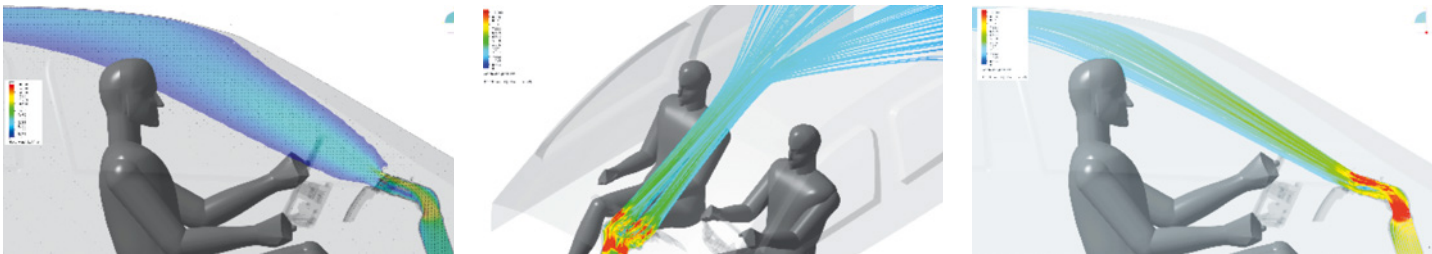


Figure 7. Airflow distribution in the car interior



**Paul-Henri Matha, Lighting Expert,
Groupe Renault**

Q. Tell our readers a bit about Groupe Renault?

A. Groupe Renault is a long established €45bn/yr French multinational automobile manufacturer that makes a wide range of cars, and vans (no trucks). It is a top ten OEM supplier and an international alliance with Nissan in Japan that makes us number three in the world, with subsidiaries that include Dacia and Renault Samsung Motors. We are strongest in B and C category segments cars like the Renault Clio, Megane, Scenic, Espace and Kadjar. We have been a pioneer in automotive styling over the years and our 'C' shaped headlight assemblies based on Light Emitting Diodes (LEDs) are a signature part of our marque these days.

Q. What is your background and your current role as a Lighting Expert in Renault?

A. I actually trained as a Mining Engineer before I joined Renault in 2000 to become part of their, then, small lighting group where I have risen to become the resident Lighting Expert in 2015. My role includes technologies and processes associated with our global lighting design activities with a primary focus on optimizing our simulation and test workflows thereby reducing costs in manufacturing. My work has a real impact on the financial bottomline at Renault. I also constantly try to think 'out of the box' and seek technology innovations that helps keep us ahead of the competition in a very competitive sector.

Q. Tell us about the Automotive Lighting Design Group in Renault-Nissan?

A. We have a large dispersed group around the world with most based in Paris but other significant groups in Korea, Romania, Brazil and India. We are closely linked to the Electronics Design Group inside Renault. We cover both simulation and test and deal with suppliers which Renault holds to very high specifications for incoming components and assemblies.

Q. How does your role influence the bottom-line at Renault?

A. A big part of my role is to understand the supply chain for lighting inside and outside Renault to manage and reduce costs. To do this properly, especially with suppliers, you have to have pre-development technical knowledge of all components and things like their thermal performance. With the advent of LED lights we can save on CO₂ emissions versus the old halogen lamps we used to employ. But also in

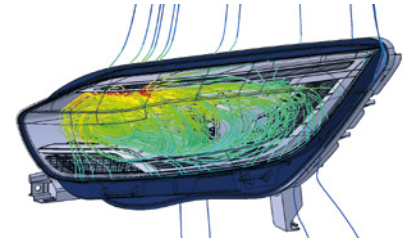
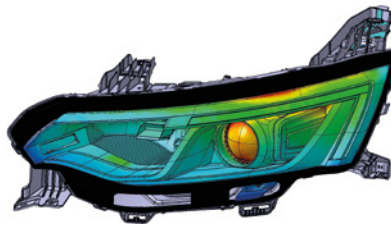


Figure 1. Renault Laguna Headlight assembly thermal analysis (left) in FloEFD and airflow pathline details (right)

the size of the headlight assembly package, such that it can be several centimeters shorter than before, for instance. It is essential to manage costs early in the design cycle with preferably multiple loops to optimize designs. Questions we might want to ask include 'If you change the temperature of a bulb will it fail?', 'Can we design for a smaller heatsink with less weight?' etc. Designing our headlamp LED arrays so we can go down from five to three LEDs yet maintain lighting quality and thermal levels can save several Euros per headlight in costs. That soon mounts up over large production runs. At Renault we have reduced our headlamp costs by 50% between 2014 and 2016 and we are aiming for a further 50% reduction in costs for our Generation 3 LED headlamps by 2018-2020.

Q. Why did you select FloEFD® as your headlight thermal analysis tool?

A. Well, first we correlated FloEFD with experimental measurements and it was very good. The big advantage with FloEFD we found is that you don't have to do meshing and you can save a lot of time at this stage of CFD. Because it is embedded and highly integrated into CATIA, our preferred MCAD tool, one thermal engineer can be over twice as productive. It also moves the analysis tool further up the design sequence. Invariably, we can do many more design loops of increasingly more complicated designs with FloEFD. We shoot for hundreds of simulations versus two or three in the past in our design optimization. With FloEFD's vapor absorption, deicing and condensation capabilities it is very well suited to our head and tail lighting applications in future.

Q. How does thermal modeling of headlights fit into the other physics simulations Renault does?

A. Of course we have to do EMC (electromagnetic confirmation), structural analysis, vibration and optical modeling (using Lucidshape) associated with each headlight design. And, naturally, a headlight is close to the engine underhood cavity which can produce surface temperatures of 70 – 80 °C which we have to take into account. Hence, we have to devise simulation workflows that accommodate all our different tools to make sure the boundary conditions for each tool is correct. Managing our software and the transition between them is becoming ever more important.

Interview

Q. There are a lot of new technologies coming to automotive lighting – what do you see as the most significant?

A. If I look to the horizon we all see electric vehicles and autonomous driving coming to the industry plus laser lighting and OLEDs (Organic LEDs). All of these will pose different lighting challenges I think. Laser lighting is being used in high-end automobiles, but we are not sure how much it will impact the market. At the moment it is only used for high beam headlights and there are questions over the efficiency of light emission in terms of lumens/watt. Mood lighting is being used today throughout all car ranges and in terms of thermal impact, it is not that significant due to it being low power. However, if they get hot the driver needs to turn them off and driving in tunnels may require them on automatically for instance. In terms of OLEDs, there is talk of V2X (vehicle to exterior) applications, but there are questions over OLED thermal reliability and the quality of the light source degrading over time, plus they are relatively expensive. In terms of electric vehicles they are easier to design in terms of lighting compared to conventional internal combustion engines as there is no hot engine cavity nearby plus condensation tends to be less of a problem. Finally, autonomous vehicles will pose a whole new set of regulatory lighting challenges. With no driver in such a vehicle, how do you light up a vehicle so that it is apparent to other drivers that it is autonomous? Do you have external red and green lights for instance? How do you determine standards between countries? All these need to be determined internationally still.

Q. Where do you see Thermal Analysis going in future at Renault Automotive Lighting?

A. We are in the business of managing headlight thermal and optical reliability. A good example of this is a Matrix Beam headlight with ten LEDs for instance. What if some LEDs are on and some are off during a normal drive cycle? At the moment we deal with steady state CFD simulations but in reality transient behavior will become more and more important in determining headlight lifetimes of up to 10 -15 years. Ultimately my dream is to push CFD down to the design engineer such that they would have a specification for a headlight and they could figure out for a given junction temperature at the LEDs, what size of heatsink, the overall size of assembly, and the number of LEDs that will be necessary to perform the specification well.

Driving down Automotive Headlamp costs at Renault



By Paul-Henri Matha, Lighting Expert, Groupe Renault

Automotive headlight design is an important part of the Renault brand these days and our ‘C shape’ headlights are a signature part of the appeal of our cars. About 30% of the cost of automotive headlight assemblies can be found in the mechanics and 70% in the electronics. Hence, any savings that can be made on the electronic side will have a profound influence on the overall cost of these units. This article will outline how we have broken down our headlamp costs and used thermal analysis tools to incrementally optimize headlight designs to achieve a 50% cost reduction in the two years from 2014 – 2016 and how we intend to halve it again in the next few years.

In Generation 1 of our full LED headlight assemblies we looked at six of our C and D-segment vehicles from the Espace to the Koleos. (Figure 1) We first standardized all platforms to one common height sensor, one common static leveller, one common DRL/low beam/high beam driver, one common central connector, and common low and high beam modules with two suppliers for each. We did this in one year by examining the partition of costs and standardized about 60% of the components of our headlights. (Figure 2) It can be seen that the plastics we used only made up about 30% of the overall assembly price. The volume effect is the main cost factor for a headlamp’s part price as is its supply entry ticket. However, by moving from Halogen headlights in 2012 (see figure 3) to LED based headlights in 2014 the overall costs went up four-fold. This in itself gave us the impetus to see if we could cut costs in Generation 2 of our headlight evolution.

We focused our Generation 2 headlamp effort on our popular Segment B car, the Renault Clio, which was going through a facelift and stylistically we wanted to move it to our LED based C-shape DRL lighting. (Figure 3) There were four pillars to our Generation 2 strategy:



1. Be the first generalist automotive OEM with full LED headlights in this B-Segment car,
2. To reduce by a factor of two the headlight part price between Generations 1 and 2,
3. To have a better LED lighting performance than the Clio Initiale (which had Xenon 25W lights), and
4. To reduce overall headlight assembly depth by 50mm.

We standardized the Clio on a common LED Electronic Control Unit (ECU), a common height sensor, and a common leveller. We then focused on the LED Low Beam light and reduced its price to 30% by reducing the number of LEDs, the size of the heatsink by 30%, and improved the optical system. By doing all these things (see Table 1) we improved the LED light flux by 33%, and

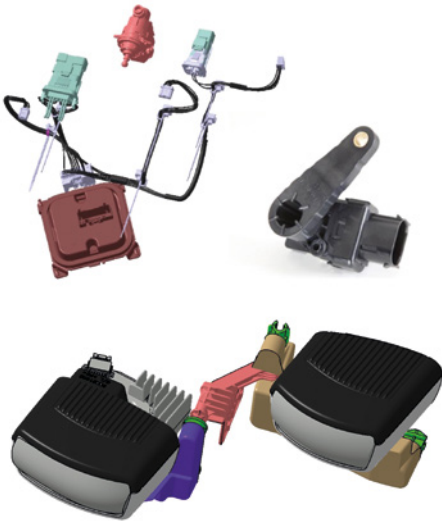


Figure 1. C and D-segment vehicle headlighting in this study

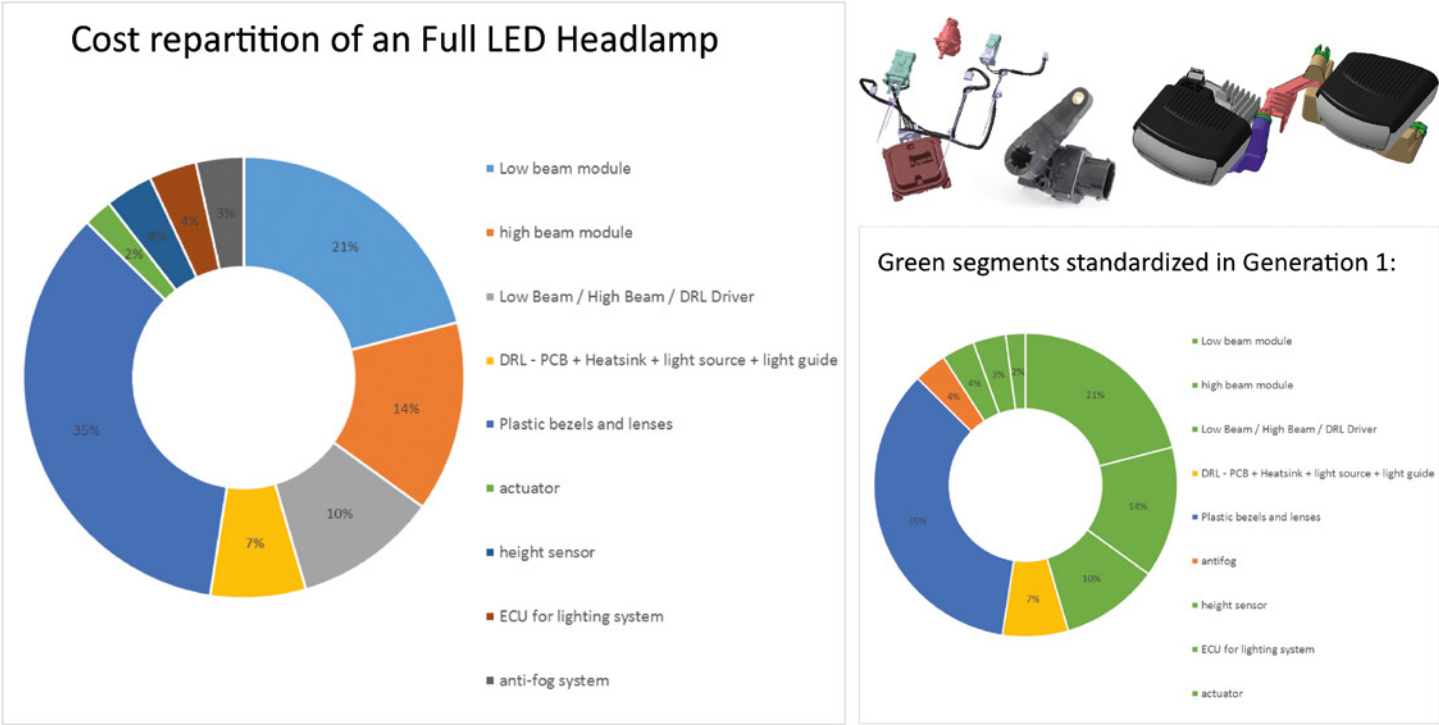


Figure 2. Headlight components standardized in Generation 1 versus overall cost partition of a Headlight Assembly

reduced the assembly from eight to five LEDs. We also increased optical efficiency by 25% and produced an overall assembly size reduction of 50mm. With the thermal improvements to the LEDs we were able to increase the LED current, increase the maximum junction temperature usage and the flux derating at a lower ambient temperature (Table 1). Similarly, with the associated heatsink design, we were able to get better junction temperature management and better derating management through our detailed thermal simulations. (Figure 4)

With respect to the overall headlamp package size, figure 5 shows the 50mm depth saving we were able to achieve between Generation 1 with a halogen headlamp and Generation 2 with a LED headlamp due to a better designed assembly. Figure 6 shows typical CFD simulations for a halogen headlamp in Mentor Graphics’ CAD-embedded software, FloEFD®, illustrating the complex air flows and thermal effects to be found on the surfaces in the assembly.

Looking deeper at our general CFD-based thermal analysis approach to headlamp design that typically is used to optimize designs, we would normally be interested in predicting lighting performance at 23°C outside the headlamp in ambient air and up to a maximum of 70°C for the outside temperature for the outer boundary of LED reliability. To validate our simulations, we therefore carried out some experimental tests where we fixed the ambient

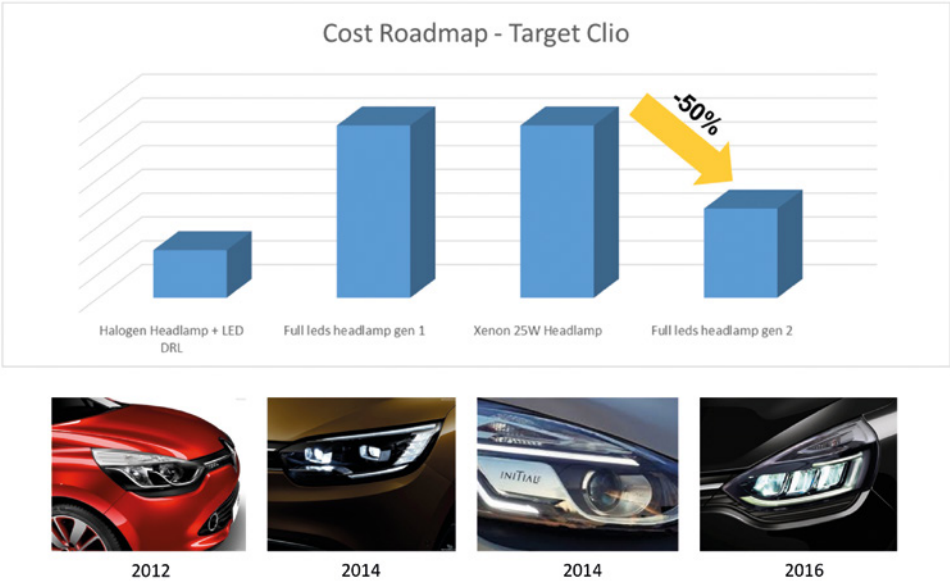


Figure 3. Renault Clio Headlamp changes and cost reductions from 2012 – 2016: Generations 0 to 2

Solution	Current (mA)	flux / LED	Number of LEDs	Tj @ 23°C T° ambient	Start of derating
LED Low beam Gen1	800 mA	200lm	8	120°C	T° ambient 60°C
LED Low beam Gen2	1A	270lm	5	130°C	T° ambient 50°C
LED High beam Gen1	800 mA	200lm	4	120°C	T° ambient 60°C
LED High beam Gen2	1A	270lm	4	130°C	T° ambient 50°C

Table 1: LED solution evolution from Generation 1 to 2 for the Renault Clio Headlamp





	Gen 1		Gen2	
Low Beam		309 gr -30%		198 gr
High Beam		186 gr -20%		154 gr

Figure 4: Renault Clio Headlamp heatsink weight evolution Generations 1 to 2

temperature outside the headlamp at 23°C and installed eight thermocouples outside the assembly (see figure 7) for a car with its engine on and off.

Figure 8 shows thermocouple time traces for both the engine on and car stationary for 3hr 30mins; then lights switched on for 1hr 30mins with the engine on and stationary, and then the lights on and engine driving for 1hr 30 minutes. It is clear that the temperatures can reach over 50°C inside the headlamp when the engine is idling and the lighting is on for a prolonged period. In addition, headlamp surface temperatures can rise to 65°C in certain idling conditions. With other tests we were able to show that with just a low beam on for an hour, the temperature inside the headlight went to 20°C and with both low and high beam on for an hour an extra 5°C in temperature was measured.

We also carried out a series of tests where we evaluated the effects of engine idling and lights either on or off by looking at Rjth of an Altiron LED with 3K/W and 3 chips @ 1A and for a Delta (Tjunction – Tcase) of 20°C. We were able to show that for ambient temperatures of 70°C and with both low beam and high beam lights on, together with the engine on that the junction temperature of the LEDs comes very close to the worst case scenario of 150°C. We concluded that it was not possible to design a LED system if we were to take into account all the use cases. The OEM must therefore define the best compromise. For example, at 23°C, after one hour engine idling, lighting performance was shown to be at 100%, but if the ambient temperature rose to 50°C for the same situation the lighting performance would go down to 80%. In order to respect this specification we concluded that a thermal sensor had to be added to the PCB so that the current could be reduced if

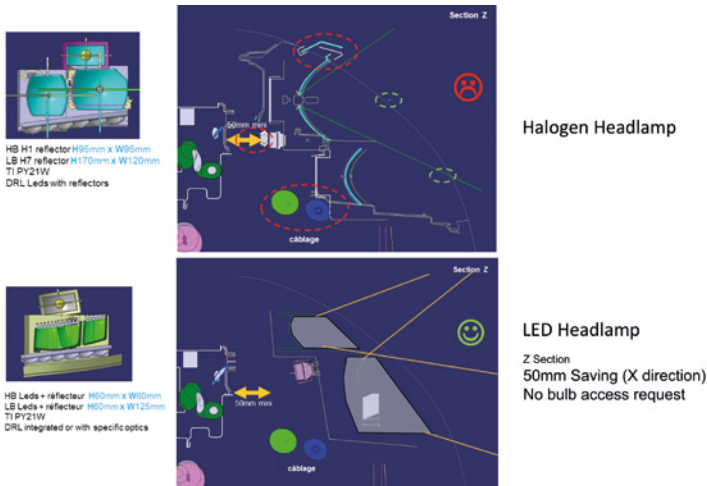


Figure 5: 50mm Headlamp Package saving between Generation 1 (halogen) and Generation 2 (LED)

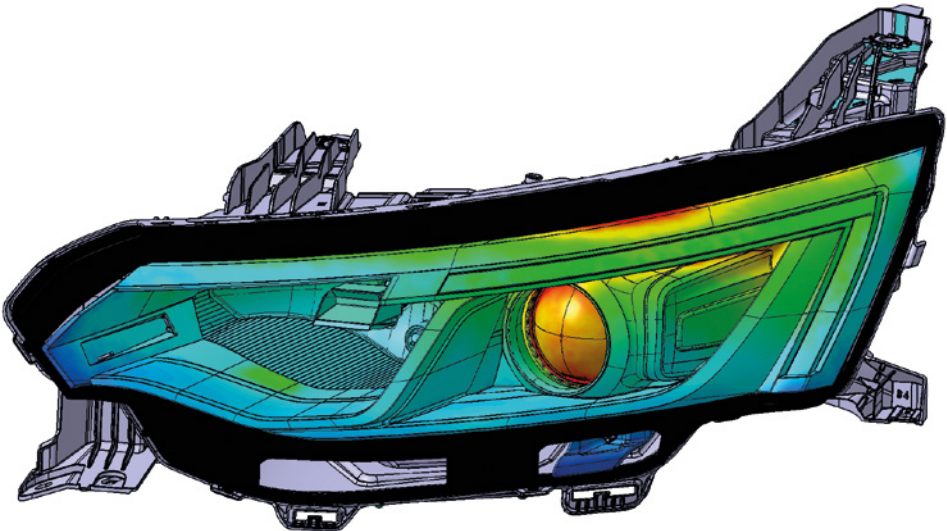


Figure 6: FloEFD Thermal Predictions for a Renault Halogen Headlamp Assembly



Figure 7: Location of the eight thermocouples for the Ambient Temperature Headlamp Engine Tests

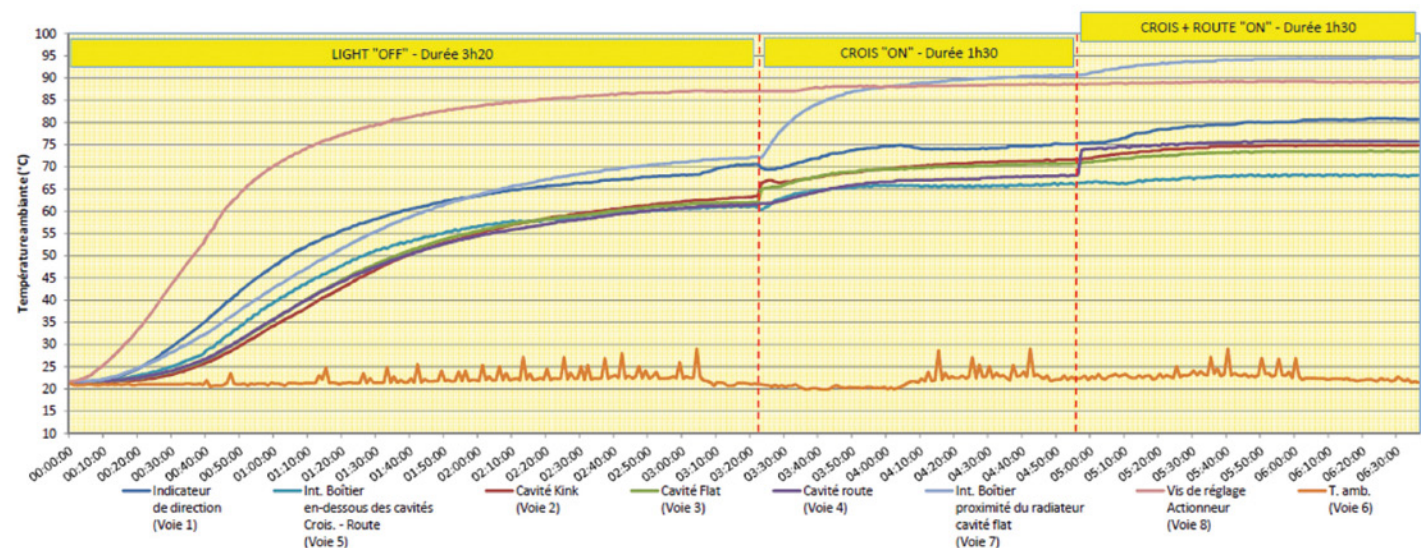


Figure 8: Thermocouple Temperatures outside the Headlamp Assembly for Various Engine on and light on/off scenarios

the temperature at the LED was greater than a threshold we would define. We could then do a thermal derating and a flux derating of the full LED headlamp.

Going forward, we are putting in place an action plan to deal with simulation and testing of lighting in transient drive cycle modes. (Figure 9) As an OEM we want to be able to simulate the impact of car speed on its lighting's thermal performance, and in particular the thermal variation due to speed of each of our engines. This will make thermal CFD software key for lighting engineers in future.

We also need to be able to model the nearby engine bay's thermal behavior in parallel with the headlight simulation as they affect each other. And we also see the need for thermal management inside the headlamp when thermal inductors will be present. In short, Renault believes that the OEM should be responsible for the complete thermal system associated with headlamp design. To do so will make the OEM a market system leader.

Our immediate goal in the Renault Lighting Team with Generation 3 of our project is to increase the LED flux of headlamps from 270lm to 320lm by 2018 – 2020 and introduce new LED Drivers to deal with higher power, plus we are aiming for the introduction of Turn Indicators and AFS functionalities, as well as overall assembly size reduction. Finally, we are aiming for a Height Sensor regulation evolution. Our eventual target is to get our full headlamp assembly to reduce in price by another 50% bringing it to the levels we saw with halogen headlamps five years ago. (Figure 10)

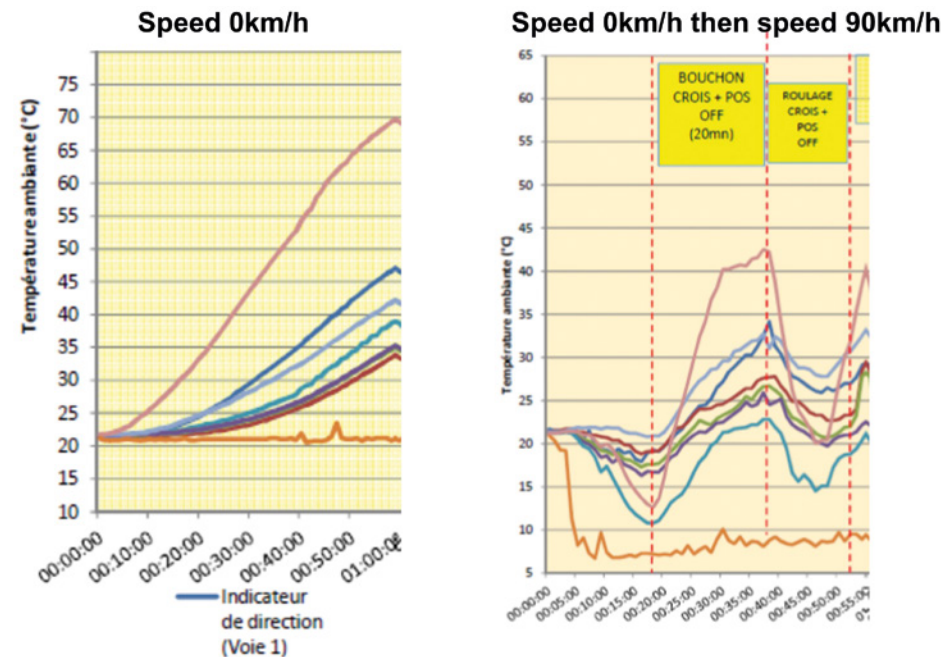


Figure 9: Headlamp Temperature Measurements for Engine Idling and during a Car Drive Cycle

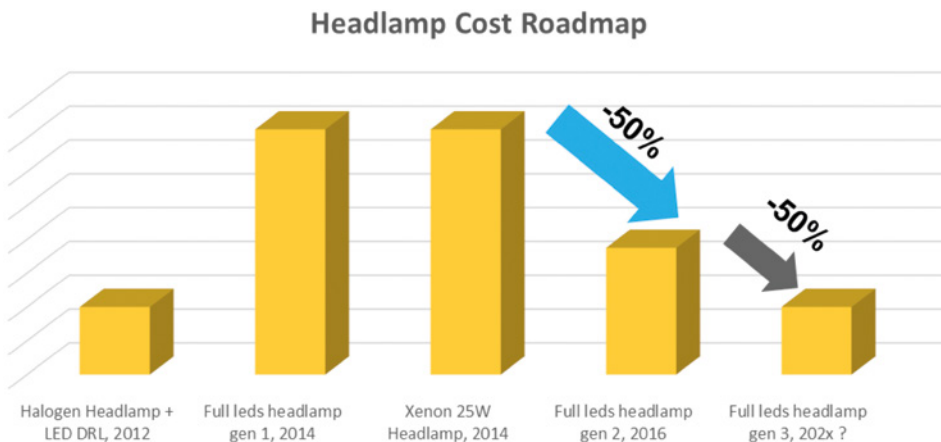


Figure 10: Renault Headlamp Cost Reduction Roadmap to Generation 3 Headlighting

"With FloEFD, the configuration of the simulation is made from within the CAD software, which eliminates the need for exporting/importing geometry. The software also has features such as automatic meshing, a case configuration wizard and integrated post processing, all from within the CAD software."

Arne Lindgren, Halmstad University, Sweden



Image Credit: Koenigsegg Automotive AB



Sports Car Brake Cooling Simulation with CAD-embedded CFD

By Arne Lindgren, Halmstad University, Sweden



Brake cooling is a crucial area in motorsport and sports car engineering. A recent thesis project by Arne Lindgren of Halmstad University in Sweden considered different cooling solutions for the extreme conditions of super cars. The project, conducted for super car manufacturer Koenigsegg Automotive AB, had the objective to design an efficient brake cooling solution for their latest model, the Regera. (Figure 1)

Regera, which means "to reign" in Swedish, is the first Koenigsegg car with hybrid-technology, the combined power of its internal combustion engine and its electric motors exceeds 1,500 horsepower. Such a powerful car needs effective and reliable brakes. During a braking event from 300 to 0 km/h, the average brake power is over 1 MW in the Regera.

Koenigsegg Automotive AB is a Swedish company founded in 1994 by Christian von Koenigsegg. The first prototype was completed in 1996 and the series production of their CC8S model started in 2002 [2]. The Koenigsegg CCR became the fastest production car in 2005 and the CCX model took the Top Gear lap record in 2006 with a time that wasn't beaten for over two years. In 2014 the One:1 model was introduced, the world's first production car with a hp-to-kg curb weight ratio of 1:1. The company employs approximately 120 staff including an engineering department which consists of about 25 engineers.

Lindgren evaluated several brake cooling designs for the Regera in his thesis. For

his CFD simulations he used FloEFD™ embedded in CATIA V5 from Mentor Graphics – experimental testing being deemed too expensive and lacking in acquisition of certain flow data [1].

While dedicated brake cooling is not necessary for ordinary passenger vehicles, it is a huge challenge for sports cars that must tolerate racing conditions. The cooling effect of the ambient air is normally sufficient for ordinary car brakes during normal driving conditions. Modern road vehicles are equipped with internally vented brake discs (at least at the front axle, and usually also at the rear). The internal vanes help to pump air through the disc, internal channels are where the biggest heat dissipation takes place [1].

Over-heating of brakes can lead to a number of problems:

- Friction material degradation;
- Thermal stress in the brake disc, which can lead to distortion and stress cracks; and
- Brake fluid vaporization in the brake caliper.

These failures can lead to partial or complete loss of braking, which is very serious.

With regard to racing cars and cars for track driving, this issue becomes more complex. Special cooling ducts which direct ambient airflow to the brakes are used to ensure sufficient cooling performance taking into account the more frequent braking intervals that occur during track driving.

Brakes are mainly cooled through the heat transfer method called convection, where a fluid absorbs heat and transports it away from the hot object. Lindgren focused his work on improving the convective air cooling of the brakes, and limited his studies to the front axle brakes as this is where heat generation is at its greatest. The brake cooling solution that was used on the previous generation of Koenigsegg cars was used as a baseline for the cooling simulations.

The baseline design consists of inlet ducts in the front bumper of the car (that captures ambient airflow) and flexible hoses that channel the air to ducts (or nozzles), which are mounted on the wheel bearing carriers and direct the cooling air towards the center of the brake discs. (Figure 3) For the simulations, CAD models of the relevant geometry were provided by Koenigsegg which were used for the embedded CFD simulations.



Figure 1. Koenigsegg Regera

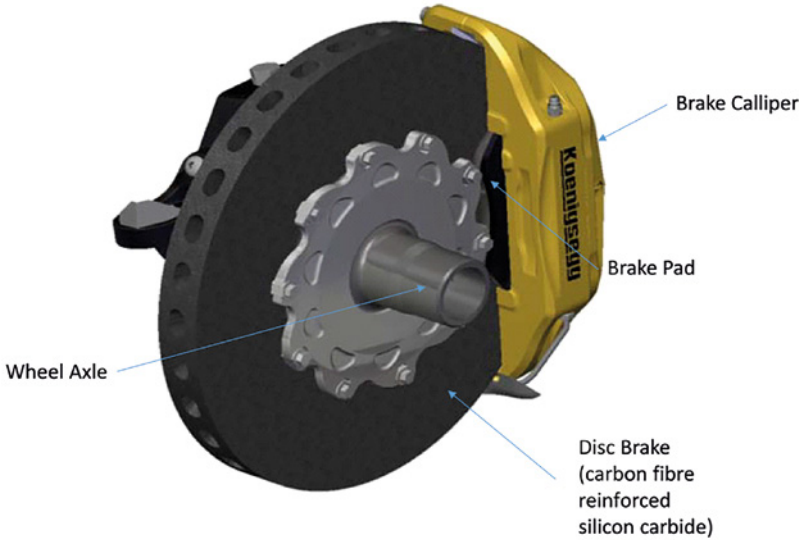


Figure 2. Koenigsegg Regera front brake.



Figure 3. Brake cooling duct mounted on a Koenigsegg Regera upright (the baseline design). (Klingelhofer, 2013, Ref 3)

The main geometries used in the simulations were:

- The brake discs made of Carbon fibre-reinforced silicon carbide (C/SiC), diameter 396 mm and thickness 38 mm, equipped with radial ventilation channels;
- The brake pads;
- The brake caliper;
- The upright (or wheel bearing carrier);
- The hollow wheel axle;
- The 19" wheel rim with tire; and
- The wheelhouse geometry.

After simulating the baseline configuration, different brake duct concepts were generated and their cooling effect was simulated. The same computational model was used for both baseline and concept simulations, only the brake duct geometry and, naturally, the position of the duct inlet boundary conditions were changed. The simulations were conducted directly within the 3D geometry models in the CATIA V5 embedded FloEFD™ CFD software. This allowed for efficient simulation of complex geometries. An efficient and productive workflow was found as a result of the automatic meshing function, the case configuration wizard, the post processing features, and because geometry could be modified directly within the CAD environment [1].

As to the objective of the project was to investigate many concepts, a reasonable calculation time was required. Therefore, a complete simulation of the entire vehicle was not expedient. A partial car body with wheelhouse was used as well as wheel and the brake as assemblies (figure 4) with similar dimensions and ground clearance as the Regera.

The ambient velocity was defined as 150 km/h, which is a typical average speed on a race track. An additional airflow from the radiator was applied on the inboard side of the wheelhouse (figure 4, red arrows). The

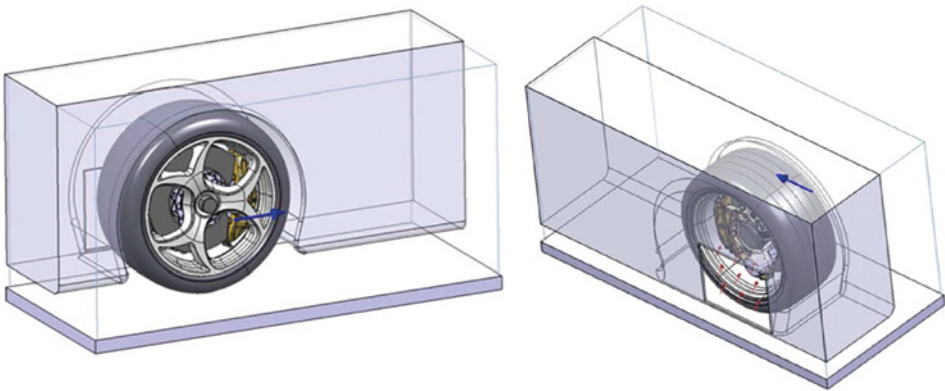


Figure 4. The geometrical wheelarch model (blue arrow indicates ambient airflow direction)

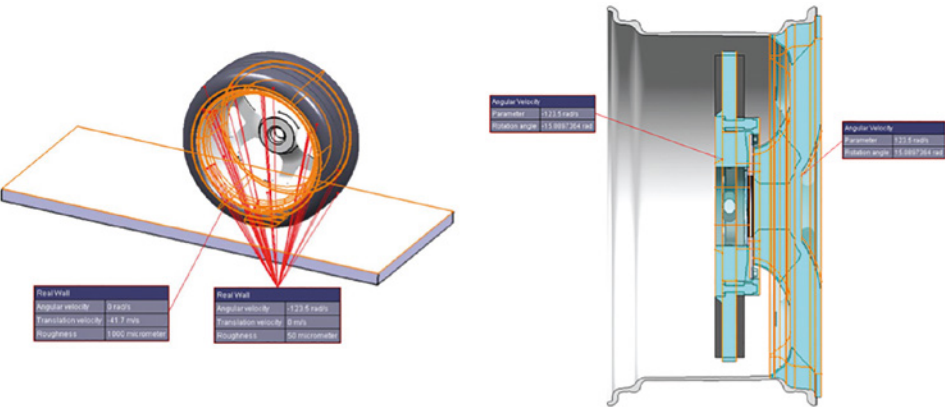


Figure 5. Wheel and ground boundary conditions. Rotating regions highlighted in turquoise

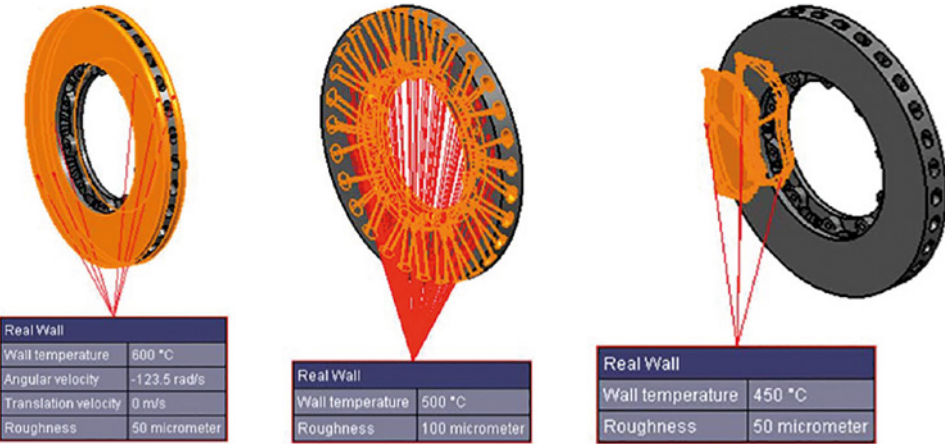


Figure 6. Disc and pad with FloEFD wall boundary conditions

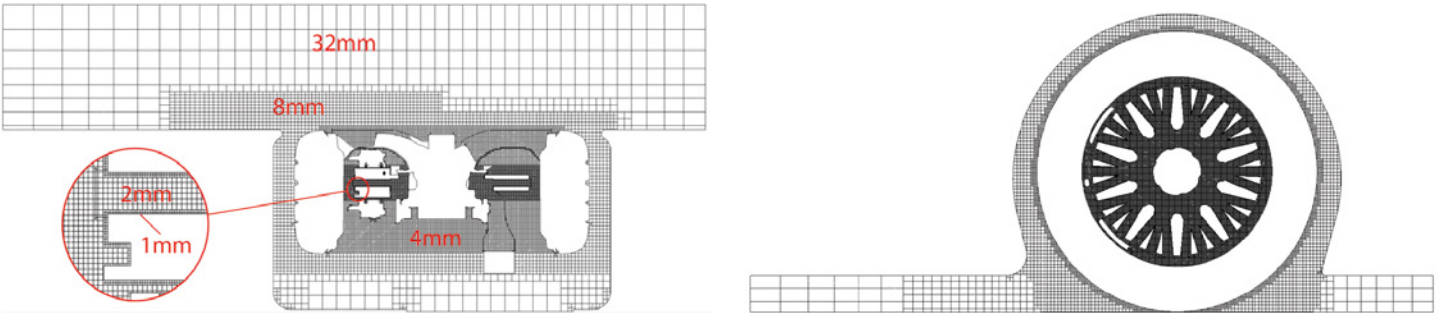


Figure 7. FloEFD Computational mesh of the Wheel, Brake Disc and Wheel Housing

airflow through the flexible hose from the inlet ducts in the front bumper was modeled as a pressure to get a realistic flow rate for all possible brake duct designs. The rotation of rotationally symmetric geometries, such as the tires and brake disc friction surfaces, were defined with wall conditions. The FloEFD sliding mesh approach was applied to the non-rotationally symmetric parts. A 3D body (rotating region) is used to define which geometries should rotate, in this case the rim spokes and brake disc channels. A translation velocity of 150 km/h was applied to the ground (figure 5) to include ground effects. Only convection was considered for the CFD simulations as this is the easiest heat transfer process to influence and has a proportion of about 60 – 90 % of the total heat dissipation. The surface temperatures applied on the surfaces of the parts (figure 6) were based on values recorded by Koenigsegg during track testing. The simulation was conducted with approximately 3.5 million cells (figure 7) using the FloEFD two-scale wall function technique, which enables the use of a coarser mesh than would be otherwise necessary in traditional CFD codes.

The concepts were based on Lindgren’s own ideas, observed brake cooling designs, and observations in other applications while taking into account only concepts that are possible to manufacture. 12 different concepts were investigated using the described FloEFD boundary conditions. With the given settings, the simulation time was approximately 24 hours on a computer with a six-core Intel Xeon E5 CPU at 3.5 GHz and 32 GB RAM.

The baseline simulation results are shown in figure 8.

Each concept was compared with the baseline concept. The investigations

focused on the cooling of the brake discs as most of the braking energy goes into the discs. The approach was to increase the convective cooling by breaking up the temperature boundary layer, which can be done by using high air velocity or by introducing turbulence. In addition, other design criteria were considered to ensure that the solution withstands forces, vibrations, and temperatures etc., that occur in driving conditions.

The investigations showed that a local improvement of the airflow often led to worse heat dissipation in other areas simultaneously. The airflow rate was simply not sufficient to improve the cooling over larger surfaces.

Another early discovery was that the design of the cooling channels in the brake discs could be improved. But the brake disc design was outside the scope of this project so it was not studied further. The breakthrough was the idea of putting the brake duct inlet in the center of a wheel axle that has radial channels. This resulted in higher hose flow rate because the radial channels in the axle and the brake disc work together as a centrifugal fan. Finally, this concept was supplemented by a “passive” cooling design (not relying on airflow from the hose), realized by two ring-shaped plates perforated with slots. (Figure 10) The simulations showed that these plates improved the cooling of the discs friction faces, but Lindgren expresses

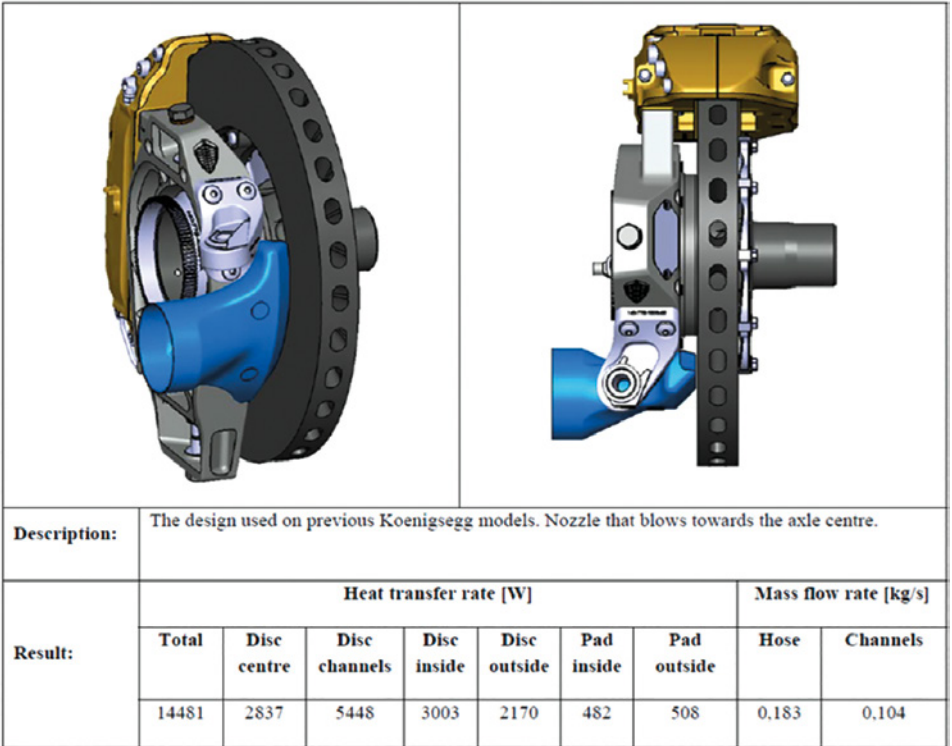


Figure 8. Baseline brake duct highlighted in blue and table with the numerical results from FloEFD

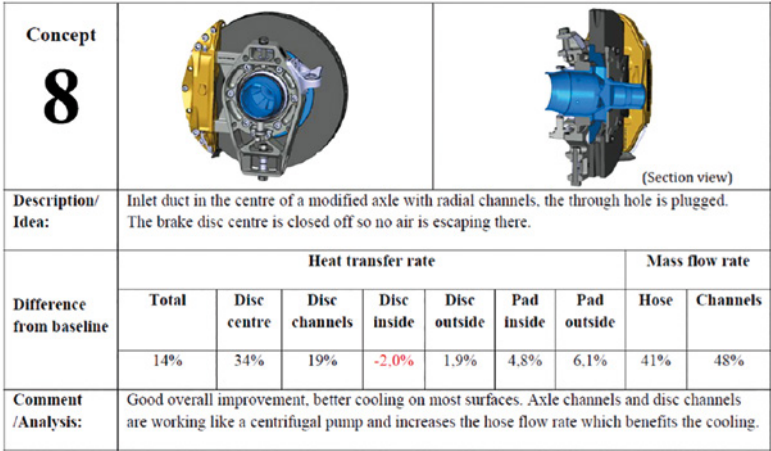


Figure 9. Overall view and FloEFD results for concept No. 8

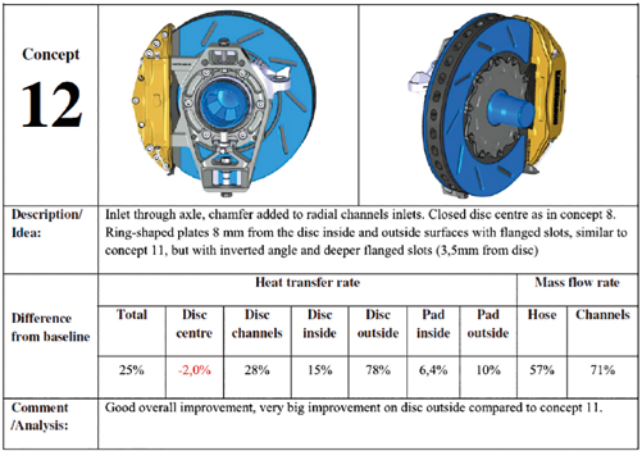


Figure 10. Overall view and FloEFD results for concept No.12



skepticism to these results as the simulations didn't include radiation (in reality the plates would reflect heat back to the disc). Concepts 8 and 12 were the most promising, although concept 12 needs further analysis or testing to see the effect of radiation. The designs of the concepts and the results given as the difference in percent from the baseline values are shown in figures 9 and 10. Concept 8 has the advantage that only a few relatively simple additional parts are needed.

From the almost infinite number of possible cooling solutions, 12 concepts were analyzed (figures 11 - 13) and compared with the baseline design from Koenigsegg. The two most promising solutions lead to an overall thermal improvement of 14% and 25%. Concept 8 was proposed as an enhancement, which had the hose inlet in the center of the wheel axle thus directing the cooling air through radial channels to the brake disc. FloEFD simulations indicated that the proposed design should result in 14% higher heat transfer rate compared to the previously used cooling solution. In addition to these cooling ducts, some passive cooling devices could also be considered in future.

In this study FloEFD was able to provide trend predictions within engineering timescales for a wide range of concepts although it was recommended that finer meshes and radiation effects be examined more in the future which require more computational resources. However, the CFD results described here indicate that when compared to brake cooling with the previous Koenigsegg ducts analyzed as a baseline, new concepts could be created, analyzed and developed in an easy iterative process. The simulations with the CATIA V5 embedded version of FloEFD made these investigations possible because creating a real prototype of each concept would lead to high cost and time requirements. The most promising solutions can now be investigated deeper in terms of structural analysis, manufacturing processes, and finally produced as a prototype.

References

[1] "Development of Brake Cooling", Arne Lindgren, Bachelor Thesis in Mechanical Engineering, 15 credits, Halmstad 2016-05-20:

<http://www.diva-portal.se/smash/get/diva2:938489/FULLTEXT01.pdf>

[2] Koenigsegg website: <http://koenigsegg.com/>

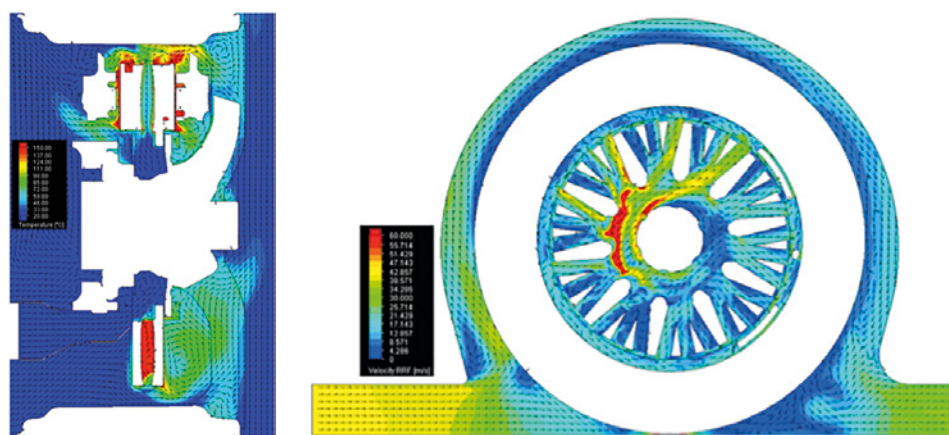


Figure 11. Baseline Case (a) temperature cut-plot on a horizontal plane through the wheel, and, (b) vector velocity on a vertical plane through the disc channels.

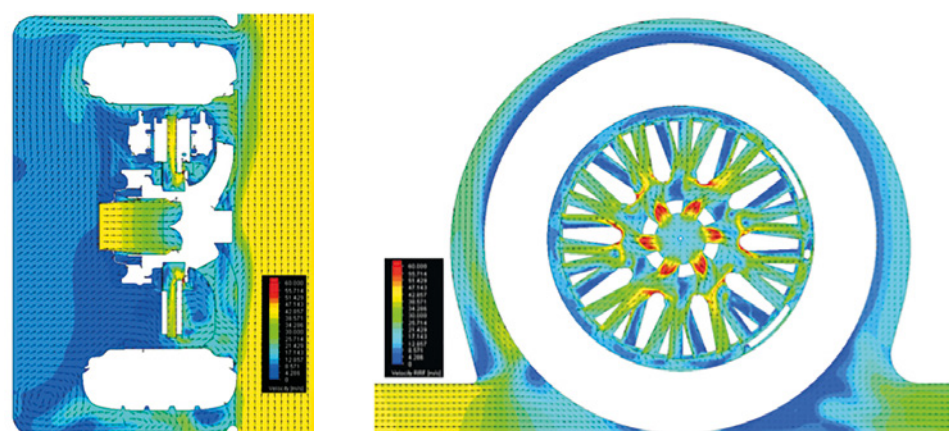
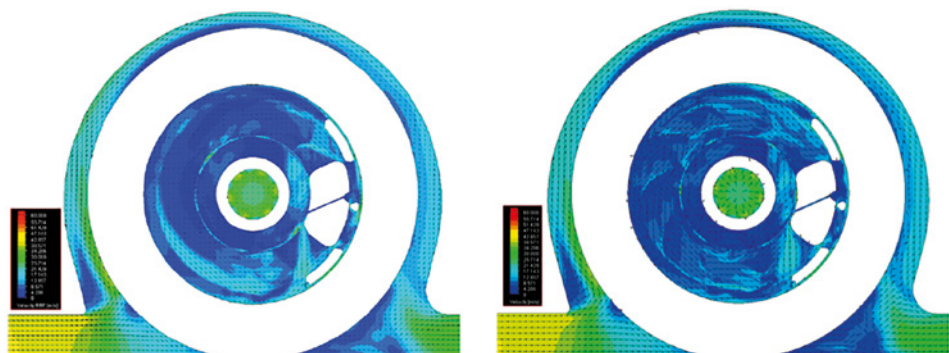
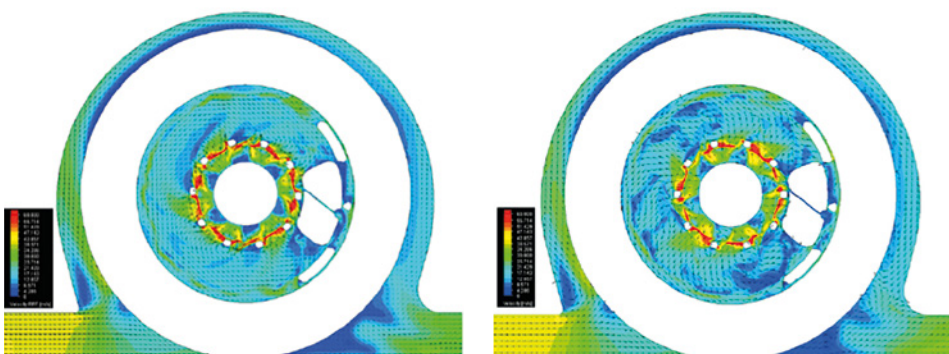


Figure 12. Concept 8 velocity cut-plot horizontal plane (a) through the wheel, and, cut-plot vertical plane through disc channels (b).



Concept 8, velocity 1 mm inside disc

Concept 12, velocity 1 mm inside disc



Concept 8, velocity 1 mm outside disc

Concept 12, velocity 1 mm outside disc

Figure 13. Comparison of Concept 8 and 12

Winging It!

FloEFD® provides Accurate and Fast Flight Load Data for Aircraft Wing High Lift Devices at Irkut

By Andrey Chuban, Lead Design Engineer, Irkut Corporation

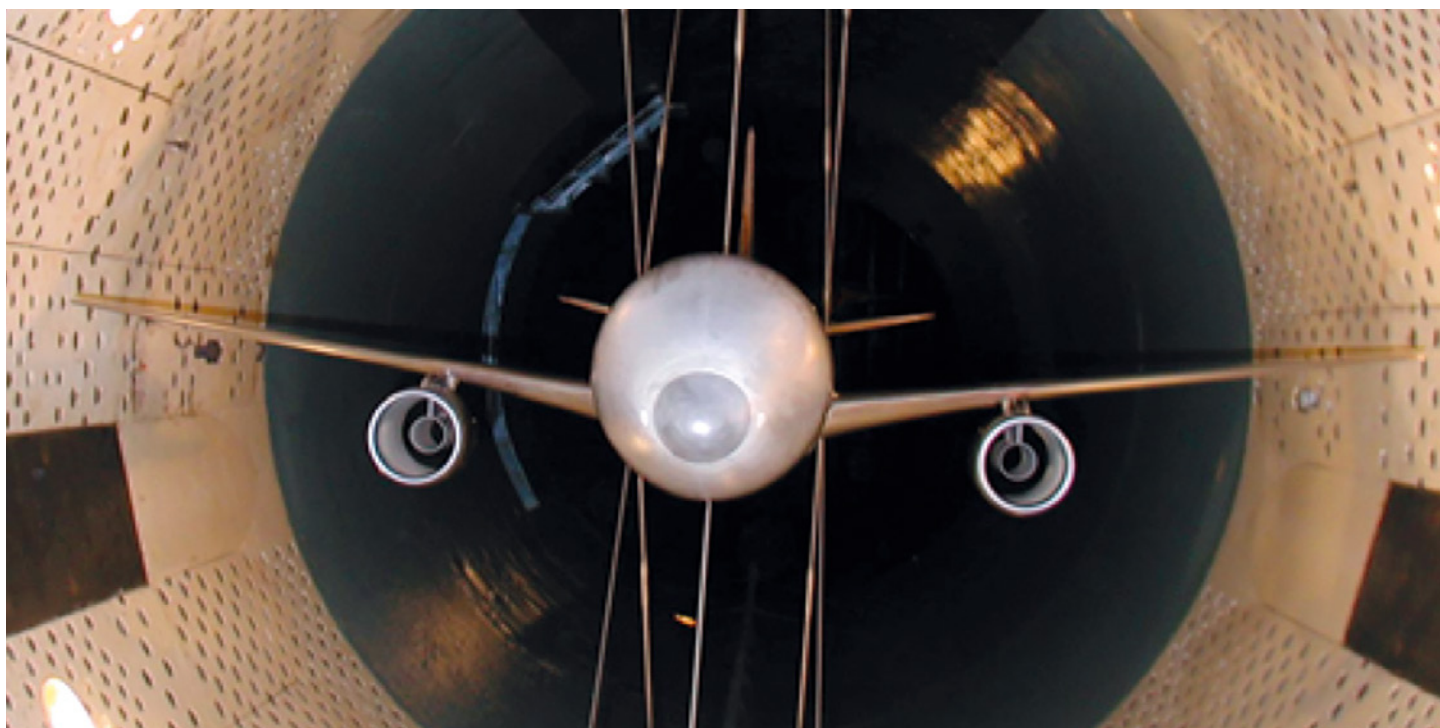


Figure 1. Typical tube experiment for a scale model aircraft

Engineers at Irkut Corporation were looking for a way to get better external aerodynamics data than what they were currently able to get from tube experiments. Tube experiments consist of building scale models of the aircraft and measuring values in a wind tunnel. This approach is expensive and has some inherent disadvantages. These include low Reynolds numbers and higher airflow turbulence intensity for scale models vs. full size aircraft. There are also inaccuracies due to the scaled geometry such as radii and points where different structures such as the wings and fuselage meet. Finally, tests run in different wind tunnels can produce varied results. To solve these issues Irkut turned to CFD as

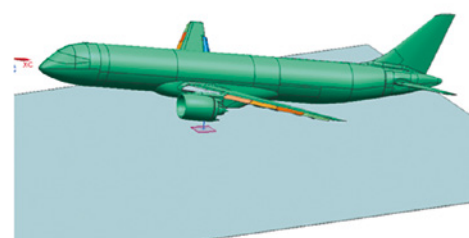


Figure 2. 3D CAD model of aircraft

an alternative approach. As part of this the CFD tools needed to be validated for this use, the tools tested included Mentor Graphics' FloEFD and Ansys' CFX.

The criteria for validating the tools were:

- Obtain the computational results close



to those of the tube experiment,

- Provide loads for the flight modes and configurations, that were not tested during experiments,
- Compare solutions with or without ground effect simulation screen, and
- Compare the FloEFD results with the load data obtained with CFX.

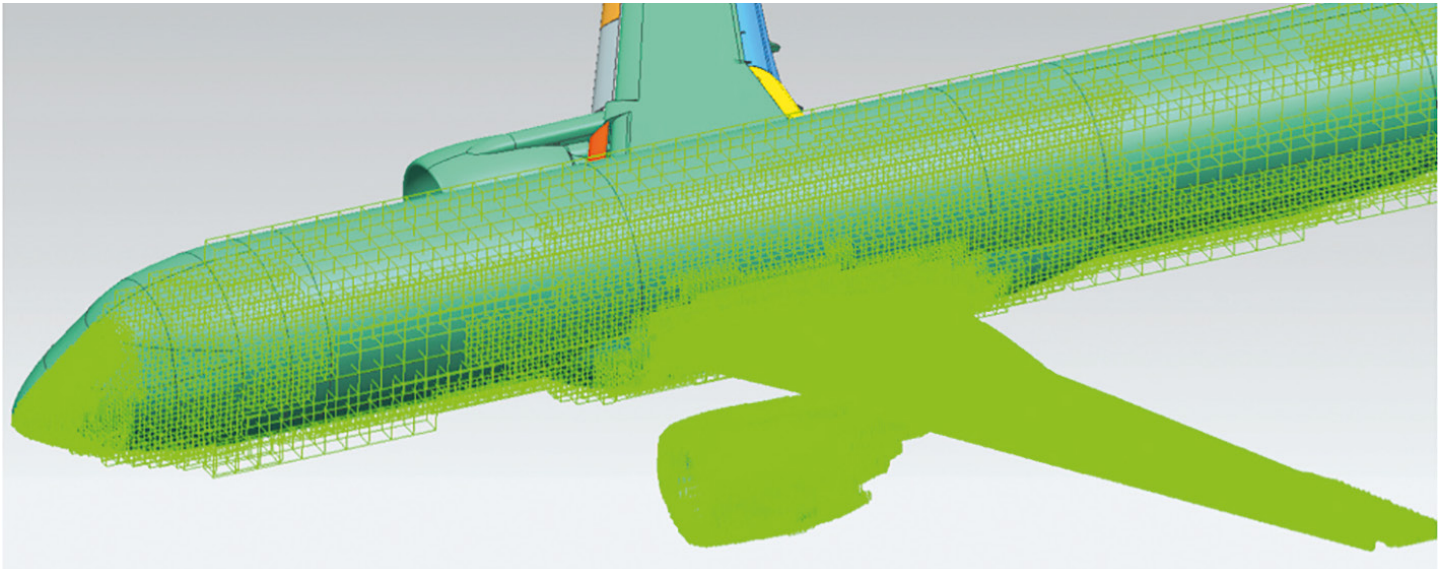


Figure 3. Final Mesh after a single adaption

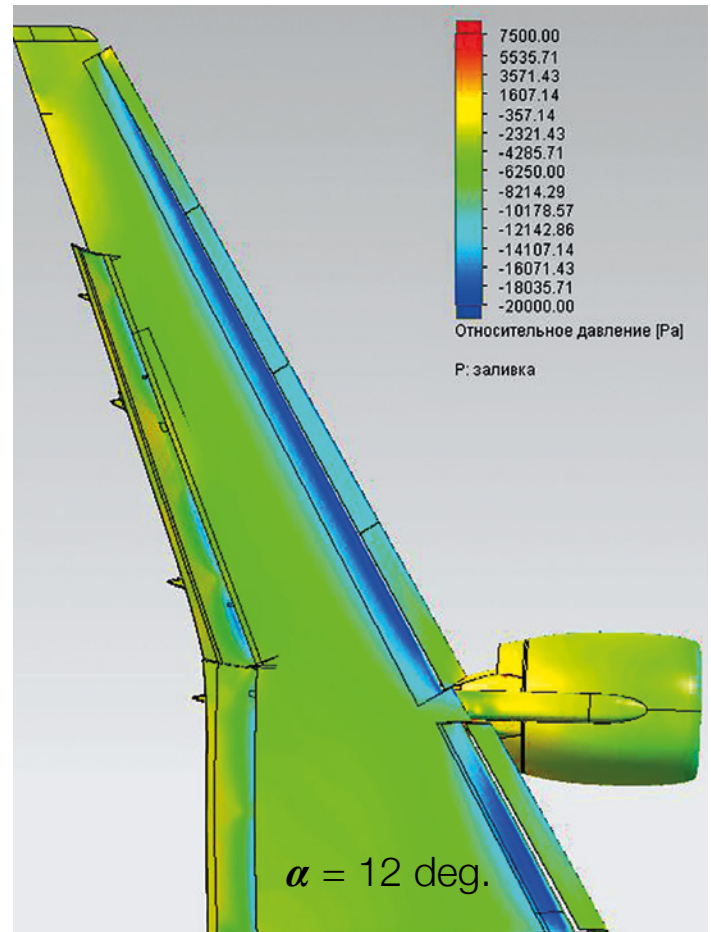


Figure 4. Computation Results: ΔP on Wing Surface

The FloEFD software was installed on a double Xenon powered computer with 48 Gb RAM. The mesh size was limited to 4 million cells (about 1.4 million before mesh adaptation process). The density of the mesh was organized with the help of volumetric zones to meet the basic rule: very dense mesh in areas with large airflow

speed gradients.

After construction of volumetric zones around the nose of fuselage, high lift devices, wing with engine and whole aircraft a basic mesh was refined automatically. The picture in figure 3 presents the final mesh after a single adaptation.

The simulation was then run for two angles of attack, 7 degrees and 12 degrees and several computational results were examined. The first result studied was the ΔP on the wing surface. This showed an increase of pitch angle leading to the growth of negative relative pressure along the wing leading edge surface and upper surface of

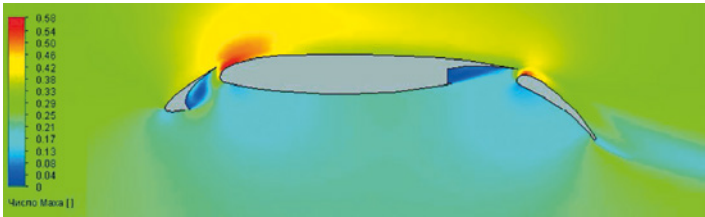


Figure 5. Computation Results: Mach Number Distribution along Wing Airfoil

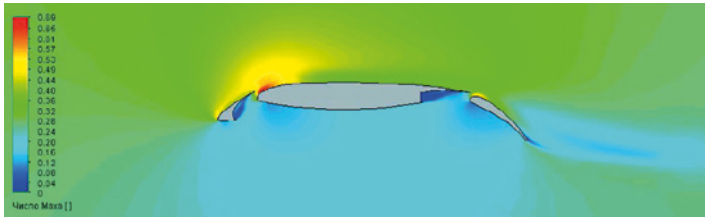


Figure 6. Results Comparison: Slat Drag Coefficient



Figure 7. Results Comparison: Slat Lift Coefficient

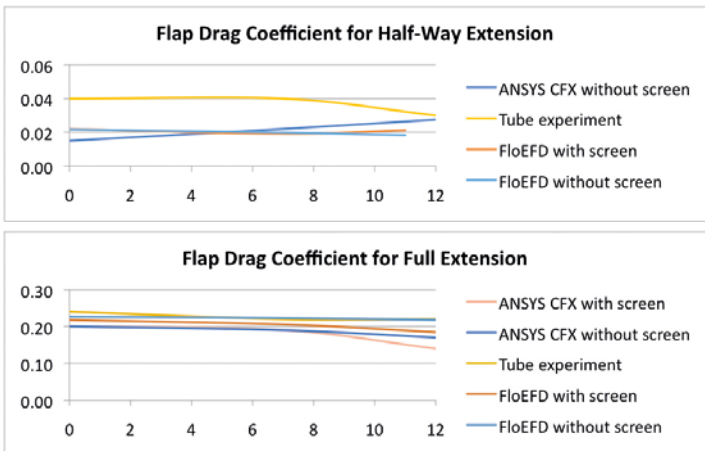


Figure 8. Results Comparison: Flap Drag Coefficient

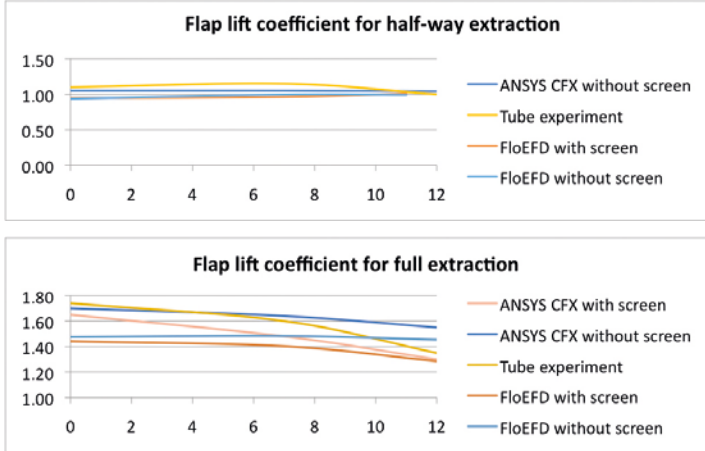


Figure 9. Results Comparison: Flap Lift Coefficient

the slats. So slat loads are the function of an angle of attack.

The relative pressure on a bottom wing surface doesn't really depend on the angle of attack; flap loads are almost independent of the angle of attack.

Next they examined the Mach number distribution along the wing airfoil. In case of a full flap extension, a high pitch angle may provoke flow separation on the flap's upper surface. The relative pressure growth on the upper surface led to flap loads decrease.

Since the experiment was run with the

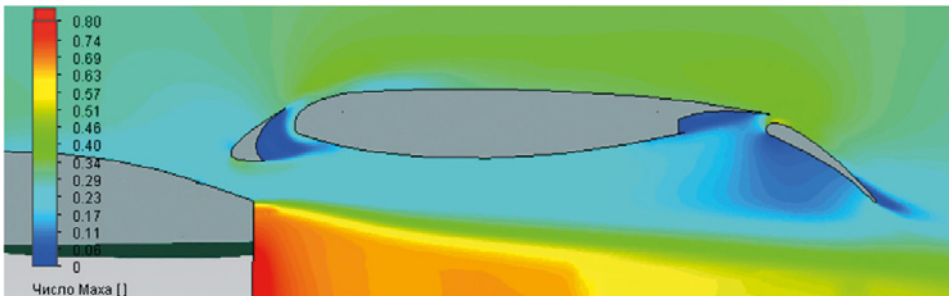


Figure 10. Engine Thrust Effect: Flow Stagnation on the Flap Bottom Surface

ground effect simulation screen, a plate was added to the FloEFD model to capture the screen effect. This resulted in an almost doubling of drag load level with

screen presence.

The drag and lift coefficient plots illustrate that qualitatively identical airflow around



the slat in the half-way and fully extended positions.

The addition of the screen also greatly raised the slat loading, but for flap, the opposite is true.

The flap lift coefficient is especially affected by screen, they observed a 15% load decrease at high angles of attack.

The next stage of the validation was to consider the engine thrust effect. The tube experiment was also done with the engine simulator which demonstrated a 10% increase of flap lift at high angles of attack. To investigate the engine thrust, effect the boundary conditions at the inlet and outlet of the engine were added to the model. This led to flow stagnation on the flap bottom surface.

FloEFD also shows a flap load increase during computation with the engine thrust taken into account, but the gap between the results with and without thrust tends to decrease with the angle of attack growth.

The spoilers, release effect at a small angle, (within 10 degrees) results in a substantial increase of outward flap loading. Wherein large spoiler release angles greatly disrupt the flow around the flap, causing a reduction of flap loading. The main problem for the flap release kinematics designer is a huge tangent load increase after spoiler release.

10 degree spoiler release causes flow separation on the flap aft edge and flow acceleration on the leading edge.

The tube experiment and FloEFD calculations show large increase (four times for FloEFD) of flap drag load for half-way extraction configuration and about 20% increase of lift load. For the outward flap tube experiment, results differs from CFD calculations due to slightly different flap release angles of a tube model and real aircraft.

The final criteria studied was the Reynolds number effect. The tube model's small scale leads to a difference in Reynolds number of a flow around the model and the aircraft. To determine the effect of the Reynolds number, the scale model was calculated in FloEFD. The results of the calculation of the aircraft and a scale model were almost identical.

Conclusions

- The FloEFD results satisfactorily correlate with the experimental data which are very close to the results of ANSYS CFX calculations. The size of the CFX mesh used for calculations was about 18 M cells, so these flow computations took too much time and required a very high-capacity equipment. Each FloEFD calculation took about six to eight hours on a standard workstation.
- The ground effect simulation screen greatly affects the drag coefficient of the slat and must be accounted for during calculation. Outward flap loading is highly dependent on spoilers release. The inner flap load growth due to the

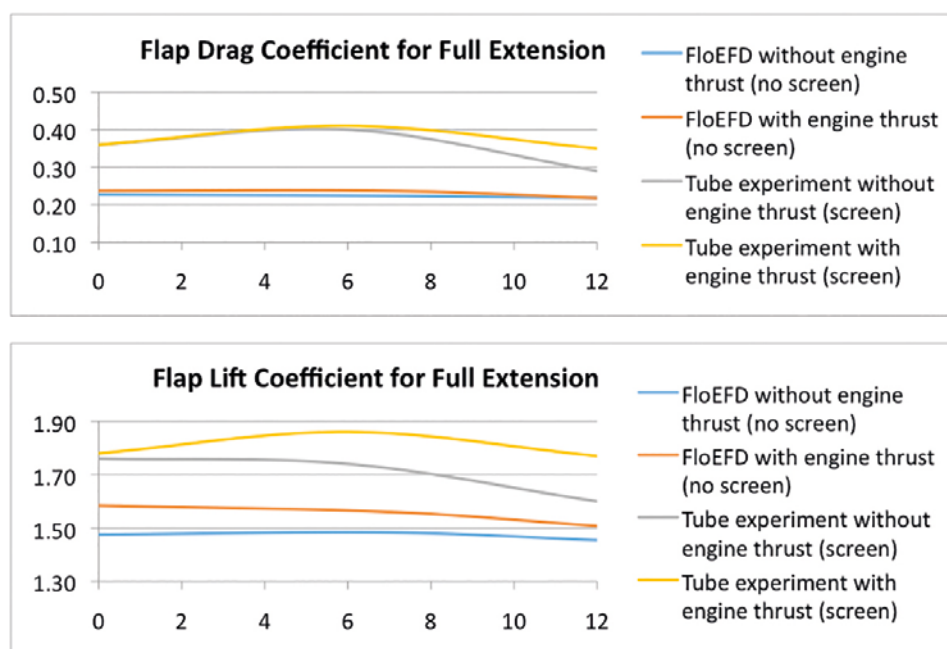


Figure 11. Engine Thrust Effect: Flap Drag Coefficient

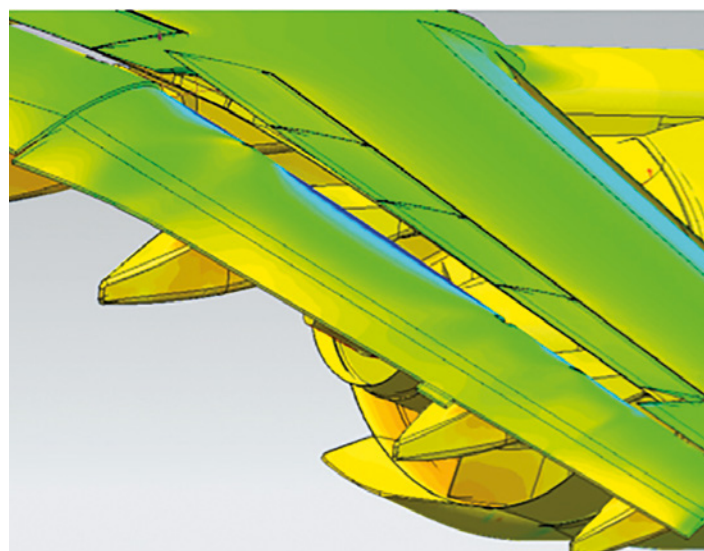
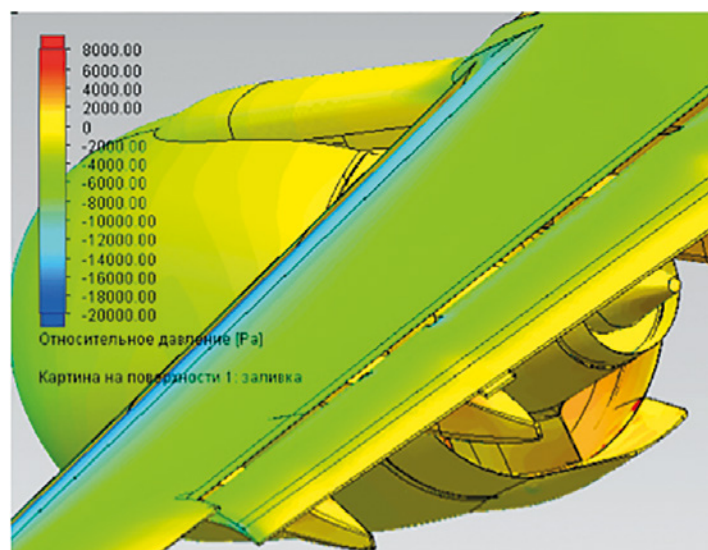


Figure 12. Spoilers Release Effect: Negative relative pressure growth on flap leading edge after spoilers release

- engine thrust increase must also be considered.
- The difference between the experimentally defined and FloEFD and ANSYS CFX computed loads raises the

question about the load data source at the aircraft design stage. On the one side there is a traditional distrust in CFD results and on the other side there is a difference in Reynolds numbers and

geometry between the tube model and the real aircraft.

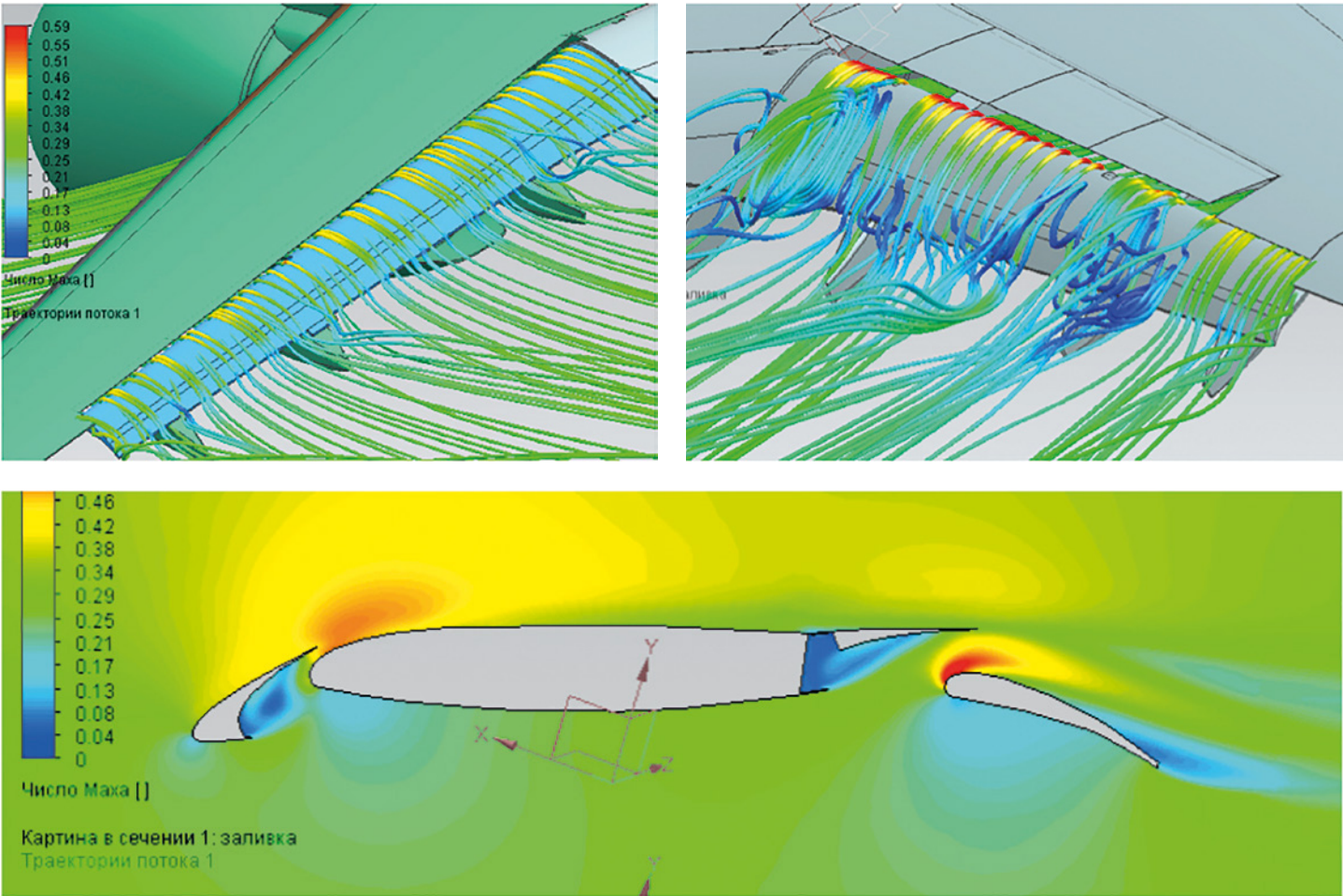


Figure 13. Spoilers Release Effect: Flow separation on the flap aft edge and flow acceleration on the leading edge

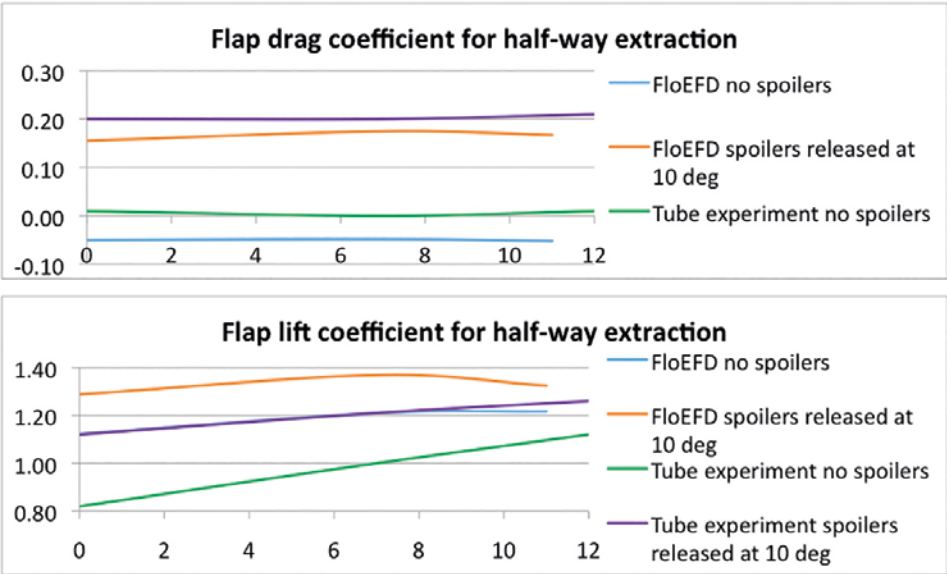


Figure 14. Spoilers Release Effect: Flap Drag Coefficient

	Scale model	True model	Δ
Slat drag coefficient	-0,11	-0,08	37%
Slat lift coefficient	0,91	0,96	5%
Flap drag coefficient	0,02	0,02	0%
Flap lift coefficient	0,89	0,96	7%

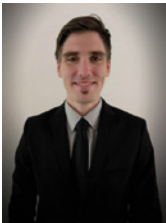
Figure 15. Reynolds Number Effect: Comparison of scale model to True Model

Electrothermal Simulation Study

by ZFW

Successfully carried out with MicReD[®] Power Tester and FloEFD[™]

By Christian Rommelfanger, ZFW



ZFW, Zentrum für Wärmemanagement (Center for heat management) based in Stuttgart, specializes in comprehensive services in heat management and lifetime testing of components and systems. No matter the industry, our clients all basically want the same thing: a fast and simple solution for a specific thermal problem. We rely on a fast and easy to use CFD system that is capable of handling different applications as our consulting projects are spread through almost every industry sector, from automotive to production systems, and usually our clients give us a call when a project is time critical. That's why we use congruent CFD software to give our customers a fast and reliable answer to their questions. Besides simulation we offer our clients a wide range of measurement techniques and test benches. We think, in a modern engineering department, simulation and measurement needs to fit closely together to work effectively.

In power electronics, it is critical to have a tight fit between simulation and measurement. Even small differences in the simulation can have a big difference in predicting the lifetime of a component. Within an industrial project, ZFW conducted a detailed electrothermal simulation study of a bridge rectifier as an example for the use of coupled simulations to get more

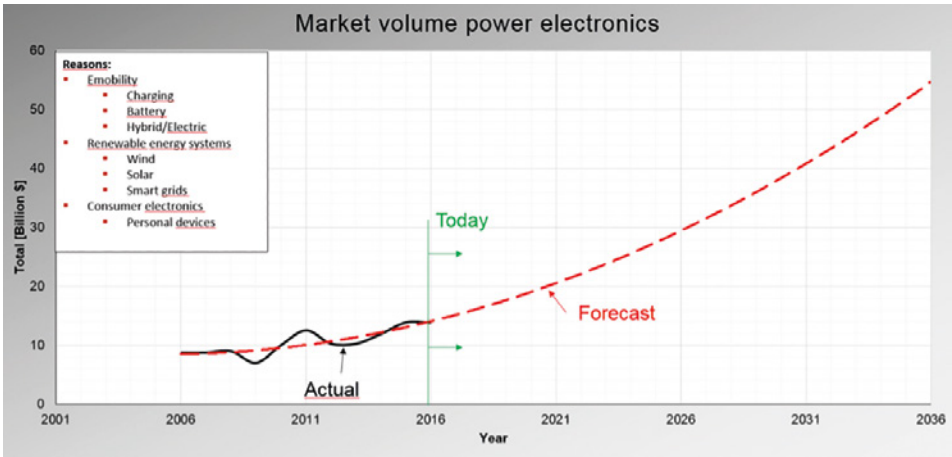


Figure 1. Forecast of the power electronics market

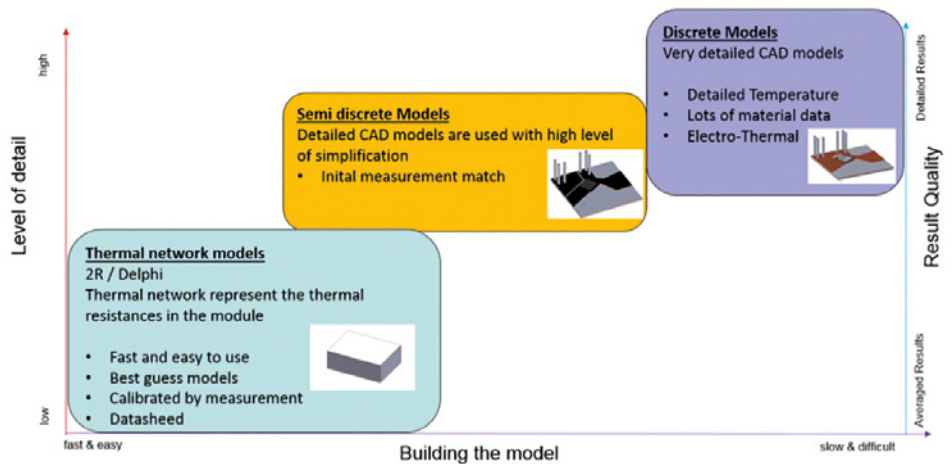


Figure 2. Level of Detail – Model building – Result quality



Types of power electronics			
Input	Output	Name	Application Example
AC	DC	Rectifier	E-mobility, renewable energy systems or industrial applications. Exchange between AC and DC electricity (socket <-> battery)
DC	AC	Inverter	
DC	DC	Converter	In mobile phones to maintain the voltage at a fixed value independent from the state of charge
AC	AC	Converter	Change of frequency or voltage, for example in power distribution network for change utility frequency 50 Hz to 60 Hz power grids

Table 1.

accurate results for reliability prediction of power electronics.

The forecast of the power electronics market predicts a rise of 200% in the next ten years. (Figure 1) There are several reasons for the increased demand in power electronics, such as the rapidly increasing market for e-mobility, the strong demand for renewable energy, and the uprising market for personal devices – just to mention a few. In most of these applications clients have high requirements on the sustainability of the device.

Keeping in mind that the rule of thumb of a 10 K change in temperature leads to almost 50% change in lifetime, it becomes clear that even with typical errors from thermal simulations, the error in the lifetime prediction can be worse. A 5% error in power losses within the device can have a serious impact in lifetime prediction. Usually our customers have +/- 10% error in their power loss prediction.

That’s why it is very important for engineers to have accurate models for reliability prediction in early stages of development. Furthermore, it is crucial to have good and accurate boundary conditions that match the application.

In a nutshell, power electronics means the application of solid-state electronics to control electric power. In modern industry, there are plenty of applications where power electronics helps to control power. AC/DC rectifiers are used to change the alternating current of the electricity grid network to direct current for loading the battery of an e-car. In personal devices like mobile phones, DC/DC converters are used to maintain the voltage at a fixed value independent from the state of charge of the battery.



Figure 3. MicReD Power Tester

Most companies use the basic empirical based Coffin-Manson model (Equation 1) and add specific influences in the equation that they observed in experiments.

$$N_f=a*\Delta T^n$$

N_f : Cycles to Failure
 a,n : Empirical Parameter
 T : Temperature

Equation 1

A typical addition to the Coffin-Manson

law is an Arrhenius approach (Equation 2) to implement the influence of the average junction temperature to the lifetime prediction.

$$N_f=a*\Delta T_j^{-n}*e^{\frac{E_a}{K*T_m}}$$

E_a : Activation Energy
 K : Empirical Parameter
 T_m : Average Temperature
 T_j : Junction Temperature

Equation 2

The MicReD® Power Tester was used to determine the empirical coefficients in the Coffin-Manson equation. As well as for many additional parameters for various types of customer based lifetime laws. There are many different strategies to determine the constants in the lifetime laws for components, such as constant temperature change or constant current

and so on. Which tactic is the right one always depends on the specific application. Assuming the following constants for a given application, that fit the basic Coffin-Manson law, we arrive at the results that a change of the Junction Temperature of around 10 K leads to about 44% change in lifetime (Equation 3).

Coffin-Manson: $N_f = a * \Delta T^n$

$a = 10000000000$

$n = 2,7$

$N_f(80\text{ }^{\circ}\text{C}) = 72720$

$N_f(70\text{ }^{\circ}\text{C}) = 104288$

Equation 3

Electric Boundaries

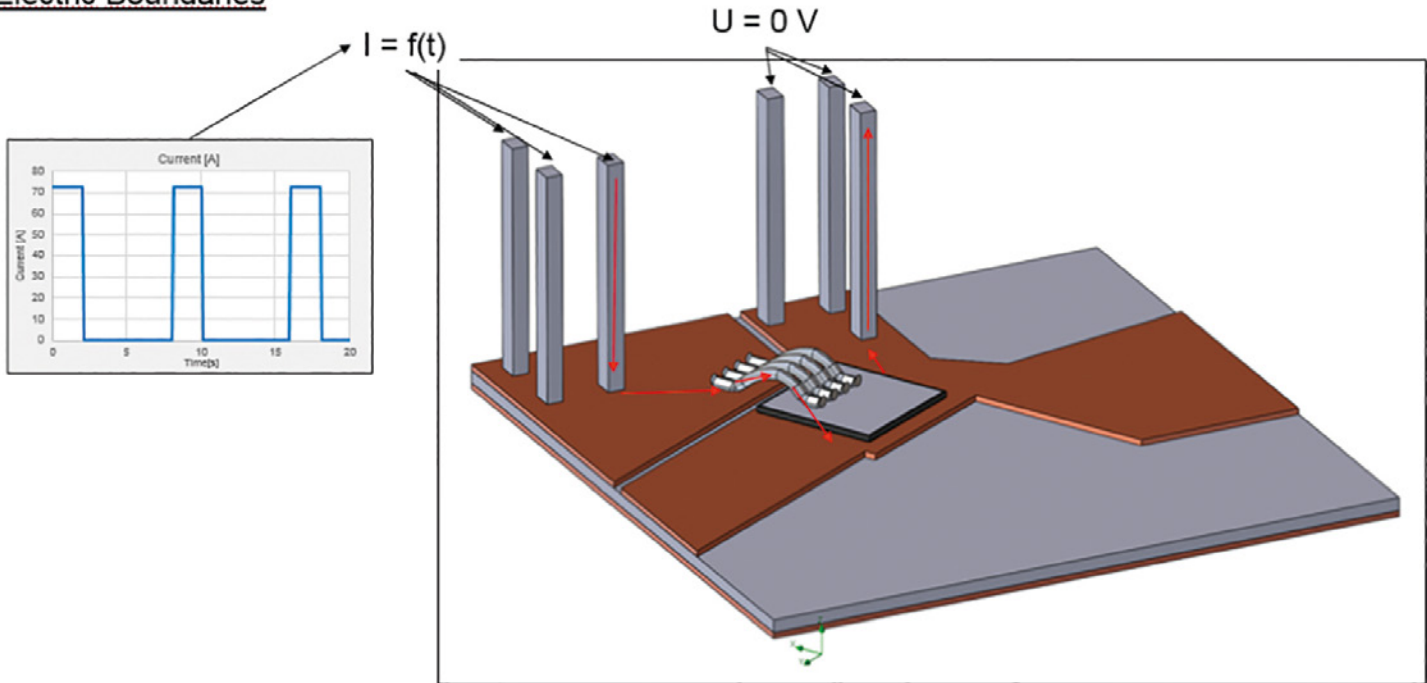


Figure 4. Electro-thermal simulations in FloEFD

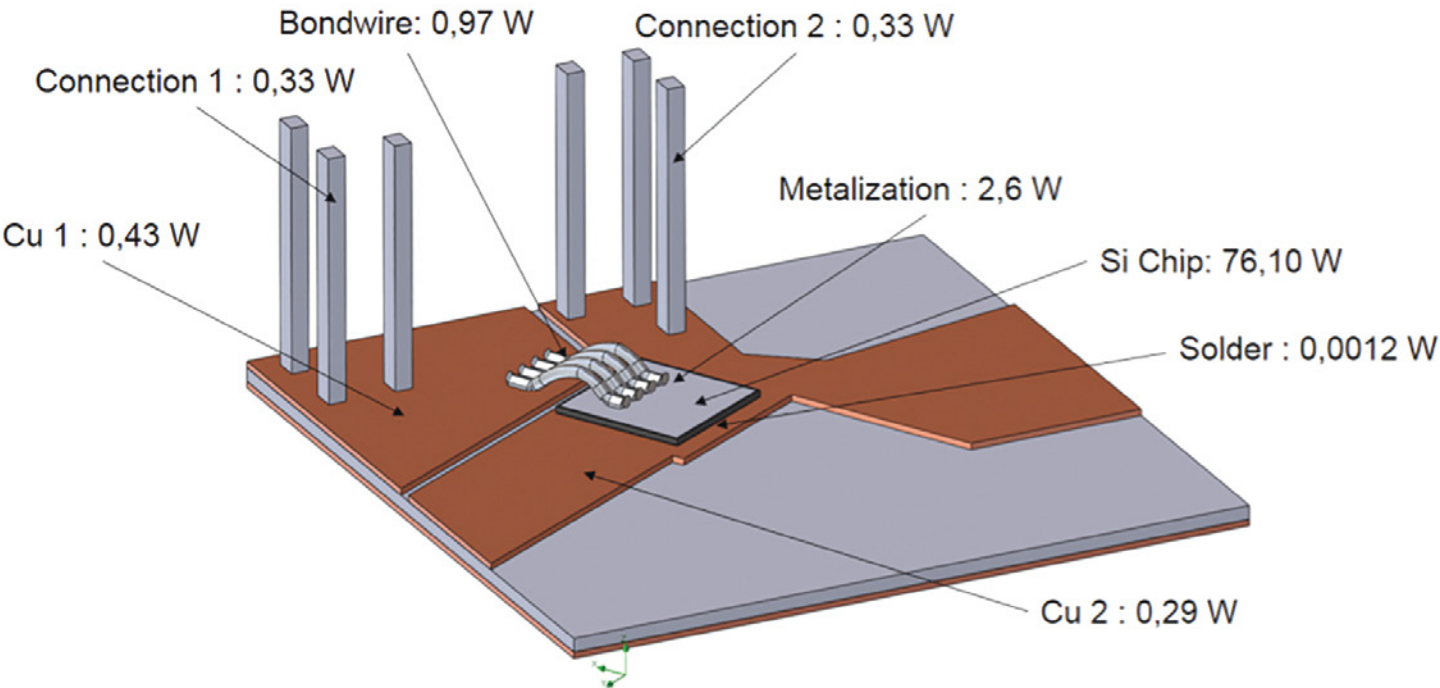


Figure 5. Detailed Power loss distribution increases design accuracy



"With these findings from the study, using the combination of the MicReD Power Tester and FloEFD, reliable simulation models can be created and used in the future."

Christian Rommelfanger, ZFW

As mentioned before, a 10 K change in temperature leads to almost 50% change in lifetime. Because of this relationship between temperature and lifetime, it is critical to have accurate models for electronics. The results of thermal models can be improved by coupling the thermal simulation with an electric one.

Figure 4 shows an overview of how electro-thermal simulations works with FloEFD™. The geometry is based on a single diode of a bridge rectifier. The electric boundaries are three power steps in 20 seconds with a length for each power step of two seconds. The thermal boundary is a fixed temperature at the bottom of the device.

The 3D electric simulation can predict the actual Joule heating in every part of the system. Two-way coupling between electric and thermal simulation works in two directions. It enables the direct transfer from the power losses due to Joule heating into the thermal simulation (figure 5) and the temperature for predicting the temperature dependent electric resistance into the electric simulation.

In the Si-chip itself power loss is 76,1 W. A stand-alone thermal model that would use the overall power loss of 81,6 W, as a volume source in the silicon would lead to an error of 7%. This leads to a temperature error of 8,4 K, assuming a junction temperature of 120°C. Calculating the lifetime with the error of 8,4 K would result in a 50% error in lifetime prediction.

The temperature dependent electric resistance of the silicon chip is calibrated through a parameter study of the measured $R_{SD, on}$ in the MicReD Power Tester for a given current. In the post process of the electric simulation the voltage drop in the Si-chip can clearly be seen.

In the thermal simulation, the distribution of the temperature through the diode is shown. Notice that the bond wire works in this transient load chase, due their thermal capacity as a heatsink. Comparing this simulation with measurement results in the MicReD Power Tester the error in temperature at the junction is less than 1K.

it is important to have accurate temperature field prediction in the Si-Chip. Ordinary thermal models give a good insight in the temperature distribution in an electronic system, but when it comes to component reliability detailed electric/thermal studies need to be done due to their sensitivity to temperature. To simulate the thermal chip behavior, it is very important to have reliable material data. A parameter study that compares a measured voltage drop to a simulated voltage drop can help to characterize the material value. The error with a calibrated electro/thermal model can be less than 1K if the baseplate temperature is fixed (coolplate) and the heat losses occurs due Joule heating. The methodology used in this example isn't just for diodes it can transferred to MOSFETs and similar devices as well.

With these findings from the study, using the combination of the MicReD Power Tester and FloEFD, reliable simulation models can be created and used in the future.

References
<https://www.zfw-stuttgart.de/>

Conclusion
In reliability investigations of power electronics,

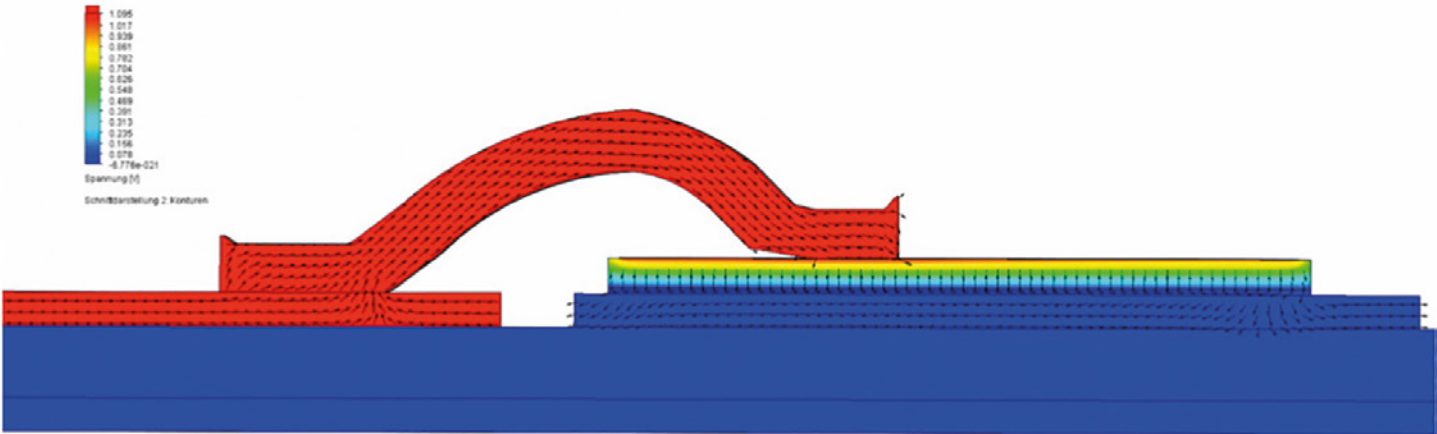


Figure 6. Voltage drop

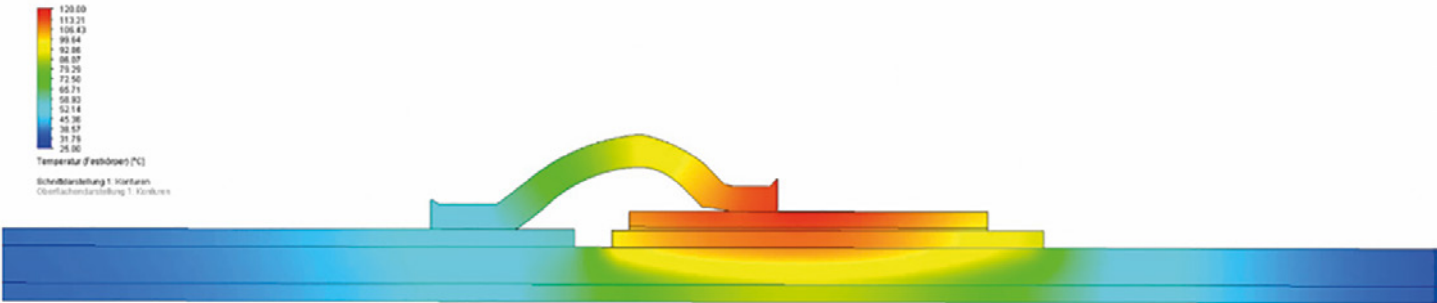


Figure 7. Temperature distribution



Figure 1. Industrial example of two stacks

Spiralled Skyline

By Mike Gruetzmacher,
Technical Marketing
Engineer, Mentor Graphics

Ever wondered why some industrial stacks have spiral structures snaking skyward? Well, since these are industrial plants, designer or artistic reasons can be eliminated. So it must be scientific.

The spirally arranged extensions are called Scruton strakes, named after the British engineer, Christopher Scruton. Working together with D. E. J. Walshe at the National Physics Laboratory in Great Britain, he invented the helical strake and first published the results in 1957[1]. These helical strakes are used to prevent vibrations caused by alternating vortices caused by the wind.

Vortex-induced vibrations (VIV), are caused by vortex shedding and can occur when long slender structures such as chimneys or car antennas are exposed to a flowing fluid. The repeated pattern of wind causes alternating eddies or vortices, also known as a Kármán vortex street. But what do those helical strakes actually do and why are they needed?

For the purposes of this investigation, I used Mentor Graphics' FloEFD 3D CFD Analysis Software, to better understand these structures.

For low Re numbers the vortices downstream the cylinder are steady (figure 2), for higher Re numbers >100, the vortices begin to oscillate (figure 3). The Strouhal number describes the frequency of the vortex shedding:

$$St = \frac{fd}{U}$$

f =frequency of vortex shedding
 d =hydraulic diameter
 U =flow velocity

These alternating shedding of vortices produce periodic forces across to the flow direction. Each elastic component, including industrial stacks, has a natural frequency. If the excitation frequency generated by the vortex shedding approaches the natural frequency of the stack, resonance and vibrations can occur. This can, at worst, cause damage to the structure.

According to Scruton, another dimensionless quantity was named, the Scruton number:

$$Sc = \frac{2\delta_s m_e}{pb_{ref}^2}$$

δ_s =structural damping by the logarithmic decrement
 m_e =effective mass per unit length
 p =density of the fluid
 b_{ref} =characteristic width of the structure

The Scruton number is an indicator for the design engineer to assess whether further measures must be taken to avoid the effects of vibration damage. Constructive measures may include, for example, damping or other structural engineering measures. Massive, stable stacks seem to be more resistant against these effects, as seen in figure 1. The stack with the larger diameter on the left side is not equipped with the Scruton spirals.

Focusing on the fluid dynamics, the aim of the helical strakes is to interrupt the alternating shedding of the vortices and thus a suppression of the oscillating lateral forces. I was able to quickly set up a simple FloEFD model with the following boundary conditions: Stack diameter: 1.5m, ambient air velocity: 2 m/s (wind velocity 7.2 km/h), as seen in figure 4.

Figure 5 shows a cut plot for velocity and at the top left a curve of the lateral forces depending on the time. We can see the oscillating force in y-direction caused by the alternating vortices.

In comparison, a further variant, which is equipped with exemplary helical strakes. This is demonstrated in figure 6. As we can see in the velocity plot, the alternating vortices don't occur anymore and the curve does not show the oscillating course.

The example in figure 6, has three helices, each 120 degrees apart around the cylinder with a pitch of 7m and 1.2 revolutions each. The helices are not constructed all the way to the top, since in the upper region the vortices are already interrupted by the flow above the stack.

Comparison of the lateral force, time dependent can be seen in figure 7.

As we can see in the graph in figure 7, the stack that is equipped with the helical strakes shows much lower lateral forces and does not oscillate around the x-axis. These are, of course, exemplary results for a slice of the stack, but the qualitative difference is clearly visible.

Thus, the Scruton strakes seem to present an economical solution as opposed to a structural reinforcement of the stack, while at the same time minimizing additional load. Increasing mass often provides remedies, but clever solutions are often the most efficient and here we could explain and present the clever solution using FloEFD with its SmartCells technology.

Additional applications of the described Scruton strakes can be found in measurement

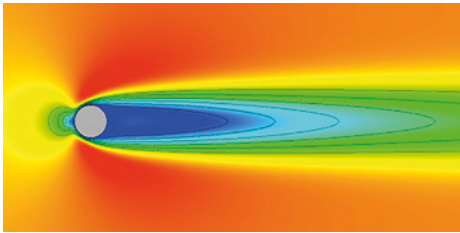


Figure 2. Steady flow at low Re number

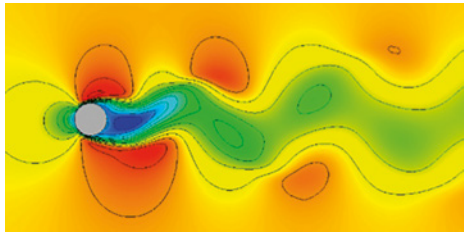


Figure 3. Oscillating at Re>100

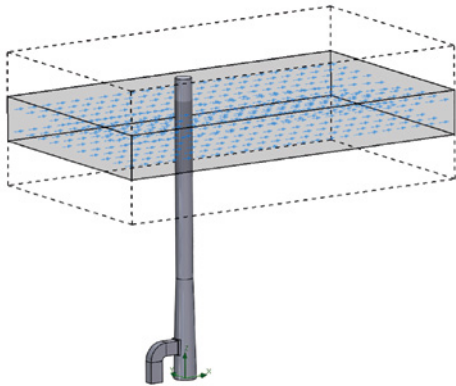


Figure 4. FloEFD simulation for one slice

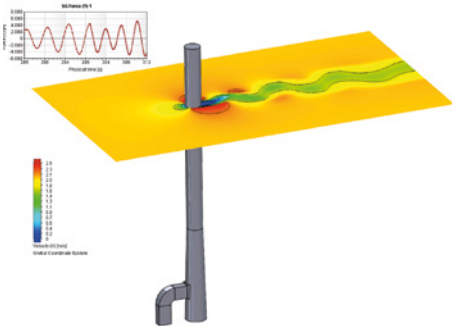


Figure 5. Stack without strakes

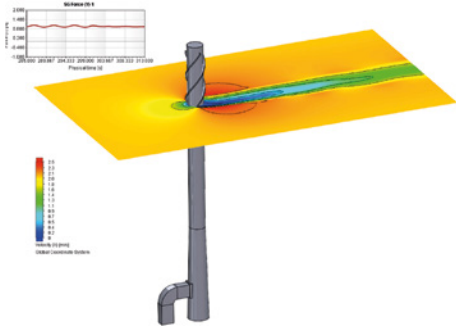


Figure 6. Stack equipped with helical strakes

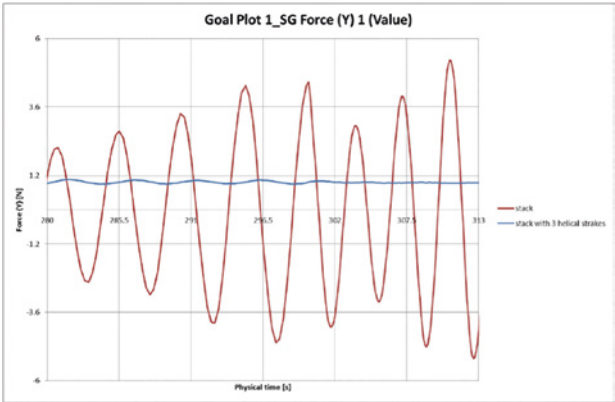


Figure 7. Time dependent lateral forces

technology to avoid the damage of protection tubes, in oil rigs, car antennas and electrical transmission towers.

References

[1] C. Scruton and D.E.J. Walshe, A Means for Avoiding Wind-excited Oscillations of Structures with Circular Or Nearly Circular Cross-section, National Physics Laboratory

(Great Britain), 1957.

<https://www.youtube.com/watch?v=ripUhgfEZPU>

<http://www.helicalstrakes.com/>

https://en.wikipedia.org/wiki/Scruton_number

https://en.wikipedia.org/wiki/Strouhal_number